UNIVERSITÀ
DEGLI STUDI
DI PADOVA

Sede Amministrativa: Università degli Studi di Padova

Dipartimento di Scienze Chimiche

CORSO DI DOTTORATO DI RICERCA IN: SCIENZE MOLECOLARI

CURRICOLO: SCIENZE CHIMICHE

CICLO XXIX

QUANTUM MOLECULAR TRAJECTORY AND STOCHASTIC THEORIES OF QUANTUM FLUCTUATIONS

Coordinatore: Ch.mo. Prof. Antonino Polimeno

Supervisore: Ch.mo. Prof. Giorgio Moro

Dottorando: Francesco Avanzini

Contents

Abstract

Bohm theory is a formulation of Quantum Mechanics that characterises the state of a quantum system according to both the wave function, as in the conventional formulation, and the coordinates (positions) of all the particles that evolve in time drawing quantum continuous trajectories. Furthermore, a statistical ensemble of all the possible trajectories, raising from the impossibility to know the initial position of all the particles, establishes the exact correspondence with the traditional Quantum Mechanics. From a computational point of view, Bohm theory has found many applications in Chemical Physics especially to develop new methodologies for solving the Schrödinger equation and to address semi-classical approximations of Quantum Mechanics.

From a theoretical point of view, the most appealing feature of Bohm theory is its capability to supply a conceptual map between the quantum formalism and our representation of what a chemical system is. Chemical systems are composed of molecules, but the same idea of molecule requires a specific arrangement in the space of particles, i.e., the nuclei of the atoms. The statistical description of conventional Quantum Mechanics on the basis of wave function alone is insufficient to establish a clear correspondence with such a picture of molecules. Indeed, chemists employ usually Classical Mechanics in order to overcome this drawback of the standard quantum theory. On the other hand, if the particles position is included in the quantum formalism, as Bohm theory does, the map can be defined in a self-consistent way. In other words, Bohm theory appears to be the suitable quantum framework to represent molecules and their motion.

The chemical representation of molecular systems finds a natural correspondence with a single Bohm trajectory, since it is always implicitly assumed that molecular components have specific spatial position independently of our knowledge about it. Consequently, we develop a quantum method whose fundamental assumption is that a single Bohm trajectory, i.e., a *quantum molecular trajectory*, describes the

molecular systems and the molecular motion correctly.

First of all, we examine the correspondence between a single Bohm trajectory and the conventional Quantum Mechanics, without using the ensemble of trajectories. We verify that such a correspondence exists through numerical simulations and we prove formally that the statistical properties of a single Bohm trajectory explain the probabilistic description of Quantum Mechanics. Once the consistency of this original approach has been established, we investigate the predicted properties. For instance, we take into account the constants of motion (such as the energy) corresponding to the time evolution of the coordinates and the behaviour of simple chemical systems, e.g., the vibrational motion of single molecules interacting with a resonant field. In this way, unexpected features of the molecular motion are found.

Secondly, we tackle the challenge of describing many components systems (like the chemical systems in ordinary conditions). As a matter of fact, the computation of the Bohm trajectory and of the wave function is extremely demanding. However, the statistical properties of the Bohm trajectory allow the derivation of *stochastic theories* for examining the dynamics of open quantum systems, i.e., few molecules (or few degrees of freedom) interacting with their environment (the other molecules). One of the developed stochastic methods correlates the dynamics of the reduced density matrix, for the degrees of freedom of interest, to the evolution of the corresponding Bohm coordinates. In other words, the Bohm equation, determining the set of all the particles velocities according to the full wave function, is replaced with a stochastic one that approximates the velocity of a subset of coordinates according to the reduced density matrix. In such a way, the *quantum fluctuations* induced by the environment are taken into account.

The advantage of this method concerns its capability of describing quantum systems, including open quantum systems, in terms of a quantum trajectory. This could allow the understanding of the molecular motion during a spectroscopical experiment. The possibility of investigating reactive systems, such as conformational changes, is particularly interesting. As a matter of fact, chemical reactions can be completely characterised only through the particles motion and we define the suitable quantum methodology providing a self-consistent description of the molecular motion.

Sommario

La teoria di Bohm è una formulazione della Meccanica Quantistica che caratterizza lo stato di un sistema quantistico attraverso sia la funzione d'onda, come la teoria standard, sia le coordinate (le posizioni) di tutte le particelle che evolvono nel tempo secondo traiettorie quantistiche continue. Inoltre, un ensemble statistico di tutte le possibile traiettorie, che deriva dall'impossibilità di conoscere la posizione iniziale di tutte le particelle, stabilisce l'esatta corrispondenza con la Meccanica Quantistica tradizionale. Da un punto di vista computazionale, la teoria di Bohm è stata impiegata in Chimica Fisica principalmente per sviluppare nuove strategie risolutive dell'equazione di Schrödinger o nuove approssimazioni semi-classiche della Meccanica Quantistica.

Da un punto di vista teorico, la caratteristica più attraente della teoria di Bohm è quella di essere il contesto naturale per definire un mappa concettuale tra il formalismo quantistico e la nostra rappresentazione dei sistemi chimici. I sistemi chimici sono composti di molecole, ma l'idea stessa di molecola è associata ad una specifica posizione spaziale delle particelle, i.e., i nuclei degli atomi. La descrizione statistica della Meccanica Quantistica convenzionale, sulla base della sola funzione d'onda, è insufficiente per definire una chiara corrispondenza con questa immagine delle molecole. Infatti, i chimici fanno spesso affidamento alla Meccanica Classica per aggirare questa difficoltà della teoria quantistica standard. Tuttavia, se la posizione delle particelle è inclusa nel formalismo quantistico, così come fa la teoria di Bohm, la corrispondenza può essere definita in modo autoconsistente. In altre parole, la teoria di Bohm sembra essere il contesto formale idoneo per rappresentare quantisticamente le molecole e il loro moto.

Comunque, la raffigurazione chimica dei sistemi molecolari corrisponde ad una singola traiettoria di Bohm dato che si assume implicitamente che i componenti delle molecole abbiano una specifica posizione spaziale indipendentemente dal fatto che essa sia nota o meno. Di conseguenza, si è sviluppata una metodologia quantistica

che si basa sull'assunzione che una singola traiettoria di Bohm, cioè una *traiettoria molecolare quantistica*, descrive correttamente i sistemi molecolari e il moto molecolare.

In primo luogo, viene esaminata la corrispondenza tra una singola traiettoria di Bohm e la Meccanica Quantistica convenzionale dato che si rinuncia all'ensemble di traiettorie. Si verifica che tale corrispondenza esiste attraverso un esperimento numerico e si dimostra formalmente che le proprietà statistiche di una singola traiettoria spiegano la descrizione probabilistica della Meccanica Quantistica. Una volta che la coerenza di questa metodologia è stata verificata, vengono esaminate accuratamente le sue previsioni. Per esempio, si prendono in considerazione le costanti del moto (come l'energia) associate all'evoluzione temporale delle particelle e il comportamento di semplici sistemi chimici, e.g., il moto vibrazionale di singole molecole che interagiscono con un campo esterno risonante. In questo modo, proprietà inaspettate del moto molecolare emergono naturalmente.

In secondo luogo, si considera la sfida di descrivere sistemi a molti componenti (quali sono i sistemi chimici in condizioni ordinarie). È ben noto che il calcolo della traiettoria di Bohm e della funzione d'onda è molto costoso computazionalmente. Comunque, le proprietà statistiche della traiettoria di Bohm permettono di derivare *teorie stocastiche* per esaminare la dinamica di sistemi quantistici aperti, come qualche molecola (o qualche grado di libertà) interagente con l'ambiente (le altre molecole). Uno dei metodi stocastici sviluppati correla la dinamica della matrice densità ridotta, per i gradi di libertà di interesse, all'evoluzione delle corrispondenti coordinate di Bohm. In altre parole, l'equazione di Bohm, che determina la velocità delle particelle attraverso la funzione d'onda, è sostituita da un'equazione stocastica che approssima la veclocità di un sott'insieme di coordinate attraverso la matrice densità ridotta. In questo modo, le *fluttuazioni quantistiche* indotte dall'ambiente sono prese in considerazione.

Il vantaggio del metodo riguarda la sua capacità di descrivere i sistemi quantistici, compresi quelli aperti, in termini di una traiettoria quantistica. Questo potrebbe permettere la comprensione del moto molecolare durante un esperimento spettroscopico. Di particolare interesse è la possibilità di esaminare sistemi reattivi, come quelli in cui avvengono cambi conformazionali. Come è ben noto, le reazioni chimiche possono essere totalmente caratterizzate solo attraverso il moto delle particelle e in questa tesi viene definita esattamente una metodologia quantistica che fornisce una descrizione autoconsistente del moto molecolare.

CHAPTER 1

Introduction

"At the heart of chemistry, let there be no doubt, is the molecule!"
— Hoffmann (1987)

1.1 Molecules and Quantum Mechanics

It might be said that Chemistry is the science that studies the laws that rule the properties and the behaviour (including the reactivity) of molecular systems. A major objective is that of explaining the features of macroscopic systems in terms of molecular properties. In this regard, the focus is on the single molecular constituents that are at the origin of the observed properties. However, an important issue arises from these well known considerations: what is a molecule? Despite the answer to this question appears obvious to chemists, it is not straightforward from a theoretical point of view.

Consider a macroscopic volume of water. The idea that it is composed of water molecules is strictly related to specific reciprocal spatial positions of the particles, and in particular of the nuclei. Broadly speaking, two nuclei of hydrogens and one nucleus of oxygen must be closer each others than to the rest of the nuclei of the system. In this way, and only in this way, a water molecule can be recognised. This representation is so much natural and deep-rooted in Chemistry that the above issue might sound absurd. Therefore, we correct our question: can a molecule be well defined within a theoretical framework? Obviously, it can be. Within Classical Mechanics. Indeed Classical Mechanics takes for granted the cartesian positions of

all the particles (nuclei).

One could reasonably expect that a more deeply rooted answer should be provided by Quantum Mechanics. Indeed, it is implicitly considered the best theory at our disposal for interpreting and understanding the properties of molecular systems, e.g., spectroscopic properties, reactivity and reaction rates. Furthermore, it is well known that the classification of atoms in the Periodic Table is explainable by employing Quantum Mechanics. In other words, Quantum Mechanics succeeded in predicting the experimental observations regarding the molecular systems since it has been developed. Nevertheless, it does not supply the suitable theoretical framework for establishing a conceptual map between our imagination of what a chemical system is and the theory itself. The motivation lies on its probabilistic predictions. Consequently, one can consider either the average position of the particles or the position corresponding to a certain probability of observing a particle in the framework of Quantum Mechanics. However, the idea of molecule is related to a specific spatial position of the particles in order to distinguish one from another in molecular systems. This specific position is undefined in Quantum Mechanics: the actual position of a particle, including nuclei, has no meaning if a measure process is not taken into account. Therefore, one relies on Classical Mechanics in order to represent molecules. The same sketch of a molecule, or its representation with 3D computer model, links the nuclei to specific positions independently of the fact that this operation is unjustifiable according to Quantum Mechanics.

For these reasons, it seems that the behaviour of molecular systems has to be described by using both Classical and Quantum Mechanics. It seems that a complete understanding of the chemical phenomenology can be reached only through the concerted use of both these two theories. This has impacted significantly the development of theoretical and computational methods. Indeed, Classical Mechanics is necessary to represent some aspects of the molecular behaviour even if Quantum Mechanics is considered the correct theory for the appropriate description of molecules.

Consider, for instance, the dynamics of a cluster composed of six water molecules within a quantum framework [Clary (2016)]. Such kind of systems are studied in order to understand how the hydrogen bond network evolves in time: which hydrogen bonds are broken, which are formed and at which time. Indeed, the dynamics of this network influences the properties of liquid water that are correlated for example to the conformation of proteins and the dissolution of ions. Furthermore, experimental evidences from rotational spectroscopy suggest that the cluster is characterised

by different conformers and the interconversion happens according to a tunnelling mechanism [Richardson et al. (2016)]. Each conformer is characterised by a different hydrogen bond network. In order to understand this kind of phenomena and to interpreted the experimental observations, quantum methods have been recently developed [Craig and Manolopoulos (2005); Richardson and Althorpe (2011); Richardson et al. (2011)]. In particular they focus on the characterisation of the tunnelling process. However, the dynamics of the hydrogen bond network can be investigated only by examining the time evolution of the nuclear distance (oxygen-hydrogen distance). For this purpose, the actual positions of the nuclei have to be established and consequently one has to rely on Classical Molecular Dynamics [Clary (2016)]. Actually, the use of Classical Molecular Dynamics is not a reasonable approximation of the quantum methodologies, but it is necessary representation due to the simple fact that precise nuclear distances at a given time are undefined in Quantum Mechanics. In other words, one has to identify the nuclear positions for describing the molecular motion and this appears that can be done only in the framework of Classical Mechanics.

Therefore, a wide set of methods have been developed in order to represent the molecular motion with Classical Molecular Dynamics and to take into account the quantum effects. This class of methods is known in literature as *ab initio* Molecular Dynamics [Grotendorst (2000); Helgaker et al. (1990); Millam et al. (1999)]. Broadly speaking, the nuclear motion is described according to classical equations of motion, i.e., Newton equation, but including also the quantum effects due to electrons. One of the first work in this field is of Car and Parrinello (1985). Recently, the development of advanced experimental techniques, that allows the efficient examination of photochemical processes [Fang et al. (2009); Liu et al. (2012)], has revived the interest for these theoretical tools. In particular the focus concerns the correlation between the dynamics of the molecular scaffold and the photochemical/photophysical properties. Some efforts in this direction has been done by Raucci et al. (2015), Petrone et al. (2014), Wohlgemuth et al. (2011).

An accurate representation of the molecular motion is perhaps even more important when the interesting phenomena are reaction paths, such as conformational changes. A prototype of these processes is the photoisomerization of azobenzene. In order to establish the conformation of an azobenzene, the actual positions of the atoms have to be known during the photoinduced dynamics because the probability corresponding to each conformer is insufficient to completely characterise the molecular geometry. To this aim, one can use mixed methods, such as the one of Tully

(1990), that describes the photoexcitation according to Quantum Mechanics and the molecular motion according to Classical Molecular Dynamics. The classical potential energy surface is determined by the electronic state. Recently, it has been investigated the dynamics of self-assembled monolayer of azobenzenes during the photoexcitation [Benassi et al. (2015); Titov et al. (2016); Cantatore et al. (2016)]. The final aim is the understanding of the role of packing in the isomerisation dynamics.

All these examples are quite common in the theoretical chemistry literature. They point out the importance of Classical Mechanics also in the framework of pure quantum processes, e.g., photoinduced reactions and photoinduced conformational changes. However, some doubts can raise even if the results of these methodologies are in agreement with experimental observations. First of all, these methods are limited because of the impossibility of absolutely classifying which degrees of freedom are "classical" and which are "quantum". For example, electrons are usually considered quantum particles, whereas the nuclei are described with Classical Mechanics. The common justification of this choice relies on the different magnitude of their masses. Despite this justification is reasonable, it does not ensure that the nuclear behaviour satisfies Classical Mechanics. In principle, the whole system should be characterised according to Quantum Mechanics. Secondly, it has been implicitly assumed the validity of classical equations of motion. However, if the Classical Mechanics has failed to explain the molecular properties, why should its dynamical equations be suitable for representing the molecular motion? Thirdly, Quantum Mechanics and Classical Mechanics are defined with respect to different formal framework and their concerted use is never obvious. These uncertainties leave open several conceptual issues and the comparison between the theoretical predictions and the experimental seems the only way for verifying the validity of a procedure.

Consequently, an interesting challenge arises: can molecular systems be described according to a single theoretical framework? In other words, the problem is of identifying a theory that is in agreement with the prediction of Quantum Mechanics, but at the same time allows the representation of molecules as sets of nuclei with specific positions in space like in Classical Mechanics. This is exactly the issue investigated in this Ph.D. thesis.

On the one hand, one can suppose that if such a theoretical framework exists, then it should be a re-elaborated version of Quantum Mechanics since it is considered more general than Classical Mechanics. On the other hand, as already stated,

the conventional Quantum Mechanics is not suitable to this purpose because of the impossibility of defining precisely particle positions. However, it has to be mentioned that there are some attempts of representing the molecular motion with conventional Quantum Mechanics. The idea consists in exploiting localised wave functions, such as wave packets, that represent localised particles approximately [Balakrishnan et al. (1997); Althorpe and Clary (2003)]. These approaches are employed in the studies of a wide range of phenomena in Chemical Physics, such as reactive collisions, photodissociation of molecules and ions, gas molecule-solid surface scattering, tunnelling of atoms and electrons in solids and on solid surfaces [Zhang (1999); Wyatt and Zhang (1996)]. In particular, wave packet scattering has be used for examining both simple chemical reactions, e.g., $Cl + H_2$ [Skouteris et al. (2004)] and $^{18}O+^{32}O_2$ [Xie et al. (2015)], and more complex processes such as the cyclohexadiene/hexatriene photoisomerization [Tamura et al. (2006)]. However, they are characterised by a practical disadvantage: their computational cost increases rapidly with the number of degrees of freedom (exact solutions are available for 5/6 degrees of freedom [Skouteris (2016)]). Moreover, as a matter of fact there are neither theoretical nor experimental reasons for assuming that the system wave function is a particular wave packet. From our point of view, this second reason represents a methodological drawback that asks for more general approaches.

Therefore, are there other ways to describe the molecular motion within a quantum framework? Even if the task seems to be impossible, there is a formulation of Quantum Mechanics that potentially represents the suitable theoretical framework for finding a solution. We borrow the words of John S. Bell that embodies the scientific enthusiasm in front a discovery,

> *"But in 1952 I saw the impossible done. It was in papers by David Bohm."*
>
> — Bell (1982)

Bohm theory represents a suitable quantum framework for describing the molecular motion without breaking the laws of Quantum Mechanics.

1.2 Another Quantum Mechanics

Bohm theory is a formulation of Quantum Mechanics that characterises the state of a quantum system according to both the wave function, as in the conventional formulation, and the coordinates (positions) of all the particles composing the whole

quantum system [Bohm (1952a,b)]. On the one hand, the wave function evolves in time according to Schrödinger equation; on the other hand, the coordinates evolution is determined by the Bohm equation according to a deterministic dynamics. The result is that the particle coordinates draw quantum continuous trajectories. Once the initial position of all the particles is known, then their position at a generic time is determined by solving the Bohm equation. Furthermore, there is no relation between the Bohm trajectories and those supplied by Classical Mechanics. The Bohm trajectories are quantum trajectories because of the pilot role of the wave function in driving the particles through the Bohm equation. The original formulation of Bohm theory is described in detail in Chap. 2, but here we would like to emphasise two fundamental aspects.

First of all, Bohm theory is the natural context to establish a conceptual map between the quantum formalism and our imagination of what a molecular system is. Since the same idea of molecule requires a specific arrangement of the particles in space, only if the particles position is included in the quantum formalism, as Bohm theory does, the correspondence is given without ambiguities. Consequently, also the molecular motion can be described without using Classical Mechanics in order to identify the particles position.

Secondly, Bohm theory gives the same predictions as the standard Quantum Mechanics for all the phenomena. Despite the particles dynamics is described by a deterministic trajectory, the probabilistic predictions can be recovered. A statistical ensemble of all the possible trajectories, arising from the impossibility to characterise completely the initial position of all the particles, establishes the exact correspondence with the conventional Quantum Mechanics: by examining the evolution of a suitable swarm of trajectories the results of Bohm theory become equivalent to the statistical distribution provided by the wave function. For this reason, it can be considered just a mathematical re-elaboration of the conventional approach. However, the univocal identification of the particles position is the unquestionable advantage of Bohm theory, and this is especially relevant to Chemistry.

Besides the exact correspondence between the Bohm approach and the Quantum Mechanics, there are no evident reasons for supporting a description based on an ensemble of trajectories. In Chemistry, it is always implicitly assumed that the molecular systems are characterised by a precise spatial position of their components. This representation corresponds to a single Bohm trajectory in opposition to the statistical ensemble of different realisations of the system. In other words, the chemical idea of molecular systems can be mapped to Bohm theory only if the

reference to the swarm of trajectories is avoided.

In this Ph.D. thesis, a quantum theory, based on a single Bohm trajectory, is developed. The aim is that of representing the molecular behaviour and the molecular motion accurately by employing a quantum methodology. In this regard, molecular systems are characterised completely according to a *single* "Quantum Molecular Trajectory".

1.3 Quantum Molecular Trajectory

By supposing that the molecular behaviour is described by a single Bohm trajectory, then a major issue arises: does a formal connection to the standard Quantum Mechanics exist? If it is possible to establish such a formal connection, then chemists could employ a theory that is coherent with Quantum Mechanics, and which is able to describe formally molecules as objects composed of particles as in the chemical intuition. Consequently, the answer to the question posed at the beginning of this chapter is that molecules can be well defined within a quantum theory, i.e., a single Bohm trajectory.

In Part I of this thesis, the properties of a single Bohm trajectory are examined in detail. The purpose is to investigate the consequences of assuming that a single Bohm trajectory is the "correct" theoretical framework for characterising the molecular properties.

In Chapter 3, it is shown that a correspondence exists between the statistical distribution of coordinates along the single Bohm trajectory and the quantum distribution for a subsystem interacting with the environment in a multicomponent system. To this aim, we present the numerical results of the single Bohm trajectory description of a model system composed of six confined planar rotors with random interactions. We find a rather close correspondence between the coordinate distribution of one rotor, the others representing the environment, along its trajectory and the time averaged marginal quantum distribution for the same rotor. Furthermore, a strongly fluctuating behaviour with a fast loss of correlation is found for the evolution of each rotor coordinate. This suggests that a Markov process might well approximate the evolution of the Bohm coordinate of a single rotor (the subsystem) and, under this condition, it is shown that the correspondence between the coordinate distribution and the quantum distribution of the rotor is exactly verified.

In Chapter 4, the dynamics along a single Bohm trajectory is analysed in order to determine the constants of motion. By drawing inspiration from Classical Mechan-

ics, we define an action functional such that the time evolution of the wave function and of the Bohm coordinates can be determined by solving a variational problem. Furthermore, we generalise the Noether's theorem for correlating the symmetries of the action functional to the constants of motion. In this way, it can be proven that the time independent expectation values are still conserved quantities also in the framework of a single Bohm trajectory. On the other hand, no further constants of motion are derived for the coordinates dynamics through the Noether symmetries.

In Chapter 5, the nuclear motion during a vibrational transition is analysed. We propose a straightforward perturbative procedure for computing the Bohm trajectory of a single molecule interacting with a resonant external field. We focus on the transition between the ground and one excited state for both diatomic and polyatomic molecules. When the wave function is a stationary state (such as the ground or the excited state) the vibrational degrees of freedom are at rest: the stationary states are mechanical equilibria of the Bohm trajectory (a feature that has no correspondence with Classical Mechanics). Conversely, when the system is in resonance between two eigenstates, the resulting vibrational motion is an oscillation at the resonance frequency with a modulated amplitude. The modulation is related to the time dependence of the populations of the states involved in the transition.

The statistical properties of the single Bohm trajectory and the correspondence with the conventional Quantum Mechanics are investigated more in detail in Part II.

In Chapter 6, we examine the statistical properties of a single Bohm trajectory. In particular, we formulate the counterpart of the Liouville's theorem in the framework of Bohm theory. To this end, we use an appropriate representation of the quantum state, that is the set of the particles position and the wave function. We establish a correspondence between the wave function and a set of variables called phases. This is essential in order to avoid the complications arising from the task of defining a probability density on a space of functions (Hilbert space). Furthermore, the statistical characterisation allows us to prove formally that the predictions of standard Quantum Mechanics can be interpreted as statistical properties of an underlying deterministic dynamics determined according to a single Bohm trajectory.

Finally, in Chapter 7, we tackle the challenge of describing the molecular motion of a many components system (that is the most common chemical system). As a matter of fact, the computation of the Bohm trajectory is as demanding as for solving the Schrödinger equation and consequently the trajectory can be determined only for small systems. However, the statistical properties of a single Bohm trajectory (see Chap. 6) are particularly suitable to infer approximate methods for

describing open quantum systems, for instance a single molecule interacting with its environment (the other molecules). In particular, quantum stochastic equations, through projection operator techniques, are derived. The Bohm equation is replaced by a stochastic equation that approximates the velocity of a subset of coordinates according to the reduced density matrix. The method allows an extension of the conventional quantum description for a single molecule by including both the coordinate trajectories and the fluctuating effects due to the environment.

CHAPTER 2

Bohm Theory

Quantum Mechanics, there is no doubt, is the best theory at our disposal to rationalise the behaviour of molecular systems. However, alternative approaches were proposed in the last century in order to overcome some methodological issues concerning the quantum formalism and particularly its interpretation.

Bohm theory [Holland (1995)], or pilot wave theory, is perhaps the most debated of these alternatives in literature. The definition of the spatial position for all the particles of a quantum system, through their coordinates, is its most appealing feature and the main difference with respect to Quantum Mechanics. The coordinates evolve drawing continuous trajectories similarly to Classical Mechanics: if the initial position of the particles is known, then their position at a generic time is precisely determined by the equations of motion. As A. Figalli and coworkers stated [Figalli et al. (2014)], despite Bohm theory "as particle trajectories remains controversial from the physics point of view, its mathematical foundation is solid": the Bohmian trajectories are well defined for all times [Berndl et al. (1995); Teufel and Tumulka (2005)].

Bohm theory was firstly proposed by Louis de Broglie at the Solvay conference [de Broglie (1928)], for this reason called also de Broglie-Bohm theory, and then independently rediscovered in 1952 by David Bohm [Bohm (1952a,b)]: through an analysis of the Schrödinger equation, David Bohm suggested a formal definition of the velocity for all the particles and consequently of their evolving positions. Since Bohm theory supplies the same statistical predictions of Quantum Mechanics under suitable hypotheses, it can be considered just a mathematical re-elaborated ver-

sion of the standard approach. However, the univocal identification of the particles position is an unquestionable advantage of the Bohm approach compared to the standard one, especially in the chemical framework.

Indeed Bohm theory is the natural context to establish a conceptual map between the quantum formalism and our imagination of what a chemical system is. The chemical systems are quantum systems whose properties can be predicted by Quantum Mechanics. At the same time, chemists imagine those kind of systems as composed of molecules. However, the same idea of molecule requires a specific arrangement in space of particles, i.e., the nuclei of the atoms. For instance, in a macroscopic volume of water, two precise nuclei of hydrogen have to be adjacent to one particular nucleus of oxygen in order to identify a water molecule. Such a water molecule can interact with the environment (the other water molecules), for instance by exchanging a proton, but the chemical idea of molecule requires a specific reciprocal spatial positions of nuclei. It is obvious that the statistical description of conventional Quantum Mechanics on the basis of the wave function alone is insufficient to establish a clear correspondence with such a picture of molecules. If and only if the particles position is included in the quantum formalism, as Bohm theory does, the map can be defined in a self-consistent way. Generally, computational chemists assign a position to nuclei in order to compute the electronic structure of molecules by employing the Born-Oppenheimer approximation. After a geometry optimisation, the electronic structure is precisely determined. Despite this approach has found many experimental confirmations, it has no theoretical justification: according to Quantum Mechanics the precise spatial position of the particles, including nuclei, is undefined. For this reasons, Bohm theory should be considered the suitable formal framework to describe molecular systems.

In this chapter, the original formulation of the de Broglie-Bohm theory is summarised by emphasising both the mathematical structure (Sec. 2.1) and some of its applications reported in literature (Sec. 2.2). In order to avoid misunderstandings, the particular terminology and notation adopted in all the thesis will be specified throughout this chapter. In Sec. 2.3, emphasis will be given to a critical issue of the theory that can be considered one of the main motivations of the study reported in this thesis.

2.1 From Quantum Mechanics to Bohm theory

Molecular systems are systems of particles. The position of all the particles can be identified by the generalised coordinates q, called also coordinates for the sake convenience, that belongs to the appropriate manifold (called also configuration space $\mathcal{C}$ in the following) [Dubrovin et al. (1991a,b,c)]. In the absence of constraints, q corresponds to the set of the cartesian coordinates of all the particles, otherwise it is the set of n variables, $q \equiv (q_1, q_2, \ldots, q_n)$, that are derived from the cartesian coordinates through an appropriate isomorphism. We will refer to each variable q_k (with $k = 1, \ldots, n$) as a degree of freedom and to n as the number of degrees of freedom. In the framework of Quantum Mechanics [Cohen-Tannoudji et al. (1977a,b)] the state of an isolated quantum system is completely specified in the coordinate representation by the wave function $\Psi(q,t) = \langle q|\Psi(t)\rangle$ that is a function of the generalised coordinates q. Broadly speaking, the square modulus of the wave function $|\Psi(q,t)|^2$ is interpreted as the probability density that the particles can be found in positions close to those identified by the coordinates q. Notice that the term "wave function" will be used to tag both the quantum state $|\Psi(t)\rangle$ and its coordinate representation $\Psi(q,t) = \langle q|\Psi(t)\rangle$ without distinction. The wave function evolves in time according to Schrödinger equation,

$$\frac{\partial}{\partial t}|\Psi(t)\rangle = -\frac{\imath}{\hbar}\hat{H}|\Psi(t)\rangle\,, \tag{2.1}$$

where $\hat{H}$ is the time independent Hamiltonian operator of the system supposed to be isolated. In the coordinate representation, for a system of particles under the action of the potential $V(q)$ and without constraints, the Hamiltonian operator can be represented as follows,

$$\hat{H} = -\frac{\hbar^2}{2}\nabla \cdot m^{-1}\nabla + V(\hat{q}), \tag{2.2}$$

where $\nabla = (\partial/\partial q_1, \partial/\partial q_2, \ldots, \partial/\partial q_n)$, and m^{-1} is a diagonal matrix with elements the reciprocal of the masses corresponding to each degree of freedom. It has to be emphasised that the kinetic operator can be different with respect to the previous one $\nabla \cdot m^{-1}\nabla$: for example, if the coordinates for one particle are the spherical ones $q = (r, \theta, \phi)$, the Laplacian operator in spherical coordinates has to be employed. For simplicity, unless otherwise indicated, we will adopt the kinetic operator in cartesian coordinates like the one reported in Eq. (2.2).

Through a simple analysis of the structure of the Schrödinger equation, in the

1952 David Bohm developed his alternative approach, i.e., his alternative formulation of Quantum Mechanics [Bohm (1952a,b)]. For simplicity, we summarise the Bohm derivation for a single degree of freedom, i.e., with $m^{-1} = 1/m$ and $\nabla = \partial/\partial q$ in Eq. (2.2). For example, one can think to a single particle in one dimensional space. By converting the wave function to the polar representation $\Psi(q,t) = R(q,t)e^{\imath S(q,t)/\hbar}$ where $R(q,t) \geq 0$ and $S(q,t)$ are real functions for its amplitude and its phase, the Schrödinger equation is separated in a system of two differential equations,

$$\begin{cases} \dfrac{\partial}{\partial t}S(q,t) + \dfrac{\left|\nabla S(q,t)\right|^2}{2m} + V(q) - \dfrac{\hbar^2}{2m}\dfrac{\nabla^2 R(q,t)}{R(q,t)} = 0 \\ \dfrac{\partial}{\partial t}R^2(q,t) + \nabla \cdot \left(\dfrac{\nabla S(q,t)}{m}R^2(q,t)\right) = 0 \end{cases} \tag{2.3}$$

The second equation in Eq. (2.3) is the well known continuity equation corresponding to the Schrödinger equation and it represents the local conservation of the probability density $R^2(q,t) = |\Psi(q,t)|^2$, while the first equation is the essential ingredient in the Bohm derivation. Indeed, it converges to the classical equation of motion known as Hamilton-Jacobi equation [Landau and Lifshitz (1976)] in the limit $\hbar \to 0$. Within this limit, the term $\nabla S(q,t)/m$ is the particle velocity for the classical formalism. Such an interpretation can be extended also for the more general case with $\hbar \neq 0$ by identifying the last contribution $\left(-\frac{\hbar^2}{2m}\frac{\nabla^2 R(q,t)}{R(q,t)}\right)$ as an additional potential, often called the quantum potential $U(q,t)$:

$$U(q,t) := -\frac{\hbar^2}{2m}\frac{\nabla^2 R(q,t)}{R(q,t)}. \tag{2.4}$$

Therefore the mathematical equivalence between the first equation in Eq. (2.3) and the Hamilton-Jacobi equation still holds and $\nabla S(q,t)/m$ can be interpreted as the particle velocity. In order to distinguish the classical case from the quantum case, the first equation in (2.3) will be called quantum Hamilton-Jacobi equation according to R. E. Wyatt and coworkers [Lopreore and Wyatt (1999)].

By assuming that initially $Q(0)$ is the coordinate of the system at $t = 0$, i.e., $Q(0)$ identifies the initial position of the particle, then the value of the coordinate at generic time $Q(t)$ can be obtained by solving the quantum Hamilton-Jacobi equation tantamount to calculate the particle trajectory according to the so-called Bohm equation,

$$\frac{\mathrm{d}}{\mathrm{d}t}Q(t) = \left.\frac{\nabla S(q,t)}{m}\right|_{q=Q(t)} = \left.\frac{\hbar}{m}\mathrm{Im}\left\{\frac{\Psi^*(q,t)\nabla\Psi(q,t)}{|\Psi(q,t)|^2}\right\}\right|_{q=Q(t)}, \tag{2.5}$$

where in the second relation the phase $S(q,t)$ is expressed in terms of the wave function $\Psi(q,t)$ and $\mathrm{Im}\{\dots\}$ supplies the imaginary part of the argument. Once the wave function and the initial coordinate $Q(0)$ are known, the solution of the Bohm equation is the trajectory $Q(t)$ drawn by the coordinate associated to the particle. The trajectory allows the identification of the particle position at any time exactly as in Classical Mechanics. Notice the substantial difference between the two types of coordinate q and $Q(t)$ previously introduced. Despite the fact that both are coordinates of the system and they correspond to the cartesian coordinate through the same isomorphism, they have a substantial different meaning. While q is the wave function variable, $Q(t)$ defines the cartesian coordinate of the particle at time t. In other words, $Q(t)$ attributes a numerical value to the actual position of the particle at time t in the one dimensional space.

The generalisation to the case with n degrees of freedom is straightforward. A set of coordinates $Q(t) = \big(Q_1(t), Q_2(t), \dots, Q_n(t)\big)$ corresponds to the coordinates $q = (q_1, q_2, \dots, q_n)$ and it attributes the position at time t to all the particles. For this reason we will call $Q(t)$ the configuration of the system at time t and $Q_k(t)$ the coordinate of the k-th degree of freedom at time t. The function that maps the initial configuration $Q(0) = q_0$ to the configuration at a generic time $Q(t)$ will be termed trajectory and labeled with the same symbol of the configuration itself $Q(t)$ or $Q(t; q_0)$ if the initial configuration has to be specified. By substituting the arguments of Eq. (2.5) with the coloum vector $Q(t)$, the matrix m^{-1} and the gradient operator $\nabla = (\partial/\partial q_1, \partial/\partial q_2, \dots, \partial/\partial q_n)$, one obtains the Bohm equation for the general case with n degrees of freedom. The velocity $\dot{Q}_k(t) \equiv \mathrm{d}Q_k(t)/\mathrm{d}t$ of the k-th degree of freedom with mass m_k is defined by

$$\frac{\mathrm{d}}{\mathrm{d}t} Q_k(t) = \left. \frac{\nabla_k S(q_1, q_2, \dots, q_n, t)}{m_k} \right|_{q=Q(t)}, \tag{2.6}$$

with $\nabla_k = \partial/\partial q_k$. It is important to emphasise that the term "trajectory" will be used to tag the curve drawn by the configuration $Q(t)$ and not by the k-th coordinate $Q_k(t)$. In this way, a single trajectory $Q(t)$ defines the spatial position of all the the particles in a quantum system, like in molecular systems.

The Bohm equation for the k-th coordinate can be also written with a structure similar to the Newton law. Indeed, by considering the second time derivative of the trajectory $Q(t)$ and the quantum Hamilton-Jacobi equation, the particle acceleration

can be directly related to the total potential acting on the particle:

$$\frac{\mathrm{d}^2}{\mathrm{d}t^2}Q_k(t) = -\frac{1}{m_k}\nabla_k\big(V(q) + U(q,t)\big)\big|_{q=Q(t)}. \tag{2.7}$$

In this way one can easily understand that the motion is influenced by both the classical and the quantum potential that have a different origin. The potential $V(q)$ is the same for both the classical and the quantum system, while the wave function is the source, through its amplitude $R(q,t)$, of the quantum potential $U(q,t)$ that is responsible for the differences between the Bohm trajectory and that expected for the corresponding classical system. For this reason the Bohm trajectory has not to be confused with the classical one: by definition it is a quantum trajectory that shares only the physical meaning with the classical trajectory. Moreover, the two formulations of the Bohm equation, Eq. (2.6) and Eq. (2.7), are equivalent even if two initial conditions $Q(0)$ and $\dot{Q}(0)$ have to be specified to solve Eq. (2.7). The second condition is not independent from the first one, but correlated by Eq. (2.6).

The great benefit of the Bohm analysis is the definition of the system configuration $Q(t)$. It has to be emphasised that his definition is strictly based on the formal equivalence between the classical Hamilton-Jacobi equation and the first equation in (2.3) and, therefore, it is an intrinsic feature of the Schrödinger equation. Furthermore, the evolution of the configuration $Q(t)$ and of the wave function $\Psi(q,t)$ is completely deterministic: known the initial condition $\big(Q(0), \Psi(q,0)\big)$, one can determine $\big(Q(t), \Psi(q,t)\big)$ by solving respectively the Bohm and the Schrödinger equation. As previously anticipated, Bohm theory is the natural approach to support the intuitive picture of molecular systems within the formal quantum theory. In this framework the systems are composed of particles, where "particle" has the same meaning as in Classical Mechanics: a body whose dimensions may be neglected in describing its motion [Landau and Lifshitz (1976)]. The wave function is the field that pilots the particles: all the quantum features of the motion derive from the wave function role as pilot agent. For instance the tunnelling of a proton, forbidden in Classical Mechanics, can be predicted by Bohm theory since the quantum potential can reduce the classical barrier and the particle can reach classically forbidden regions. For the fundamental contribution of the wave function to determine the particles motion, Bohm theory is also called "pilot wave theory".

From this point of view, the wave function can be compared to the electromagnetic field: as the electromagnetic field influences the motion of charges, the wave function drives the motion of the quantum particles. However, in classical electro-

magnetism the charges are themselves source of electromagnetic field. Thus the field and the particles are mutually interacting. In Bohm theory the trajectory is strictly determined by the wave function (Eq. (2.5)), but the wave function evolution is completely independent of Bohm coordinates $Q(t)$ as it can be verified by observing that the Schrödinger equation (Eq. (2.1)) has no reference to these coordinates $Q(t)$. The absence of a backreaction from the particles to the field is a peculiarity of Bohm theory that has no equivalent in the classical world and that preserves the validity of the Schrödinger equation also in this alternative formulation of Quantum Mechanics.

The pilot role of the wave function correlates the motion of different particles independently of the magnitude of their interaction through the classical potential $V(q)$: the motion of classically non-interacting particles can be reciprocally influenced. In other words, Bohm theory maintains the non locality nature of the conventional Quantum Mechanics, as it is also been experimentally verified for two entangled photons [Mahler et al. (2016)]. For example, one can consider two non interacting systems (A, B) characterised respectively by the Hamiltonian operators $\hat{H}_A$, $\hat{H}_B$ and by the coordinates $Q_A(t)$, $Q_B(t)$. Assuming that the total Hamiltonian operator is separated as $\hat{H} = \hat{H}_A \otimes \hat{\mathbb{1}}_B + \hat{\mathbb{1}}_A \otimes \hat{H}_B$, the time evolution of the coordinates $Q_A(t)$ and $Q_B(t)$ could be mutually related. Indeed if and only if the wave function is factorised $|\Psi(t)\rangle = |\Psi_A(t)\rangle \otimes |\Psi_B(t)\rangle$ then $Q_A(t)$ and $Q_B(t)$ are independent. On the contrary, if the wave function is entangled $|\Psi(t)\rangle \neq |\Psi_A(t)\rangle \otimes |\Psi_B(t)\rangle$ then the motion of $Q_A(t)$ affects strongly the evolution of $Q_B(t)$ and *vice versa*. This can be verified simply for the entangled wave function as the one reported below:

$$\Psi(q_A, q_B, t) = c(t)\varphi_A(q_A)\varphi_B(q_B) + d(t)\chi_A(q_A)\chi_B(q_B), \tag{2.8}$$

where $\varphi_A(q_A)$ and $\chi_A(q_A)$ ($\varphi_B(q_B)$ and $\chi_B(q_B)$) are generic eigenfunctions of the Hamiltonian operator $\hat{H}_A$ ($\hat{H}_B$); the coefficients satisfy $|c(t)|^2 + |d(t)|^2 = 1$. By inserting this peculiar wave function in Eq. (2.6), one can check that the velocity $\dot{Q}_A(t)$ is dependent on both the coordinates $Q_A(t)$ and $Q_B(t)$. The entangled wave function is responsible for non local phenomena also for the dynamics of the Bohm coordinates.

In this framework, the dynamical state of the system is specified by the coordinates and the wave function. The set of configuration and wave function $\big(Q(t), \Psi(q,t)\big)$ defines fully the system state in Bohm theory [Dürr et al. (2012)] as the wave function alone describes the system state in Quantum Mechanics. The state evolves

according to the Bohm equation and the Schrödinger equation,

$$\begin{cases} \dfrac{\mathrm{d}}{\mathrm{d}t}Q_k(t) = \left.\dfrac{\nabla_k S(q_1, q_2, \ldots, q_n, t)}{m_k}\right|_{q=Q(t)} & \forall k = 1, \ldots, n \\ \dfrac{\partial}{\partial t}\Psi(q,t) = -\dfrac{\imath}{\hbar}\hat{H}\Psi(q,t) \end{cases} \tag{2.9}$$

in a full deterministic way: known the initial state, the state at a generic time t is completely determined by the above dynamical equations.

At first sight, Bohm theory seems to be incompatible with the standard Quantum Mechanics: the deterministic evolution of the $Q(t)$ can not be directly compared with the statistical predictions of the Quantum Mechanics. The square modulus of the wave function $|\Psi(q,t)|^2$ is interpreted as the probability density that the system particles can be found about the positions identified by the coordinates q, while, on the other hand, $Q(t)$ identifies the actual positions. However, a complete deterministic prediction about the position of the system components is conditioned upon the knowledge of the initial configuration $Q(0)$. This means the knowledge of the position of all the components of a molecular system. Any chemist can easily understand that this piece of information is unattainable. For this reason, a statistical approach has been proposed by Bohm himself in order to overcome the issue of the incomplete characterisation of the initial state [Bohm (1952a)]. Assuming that at least the initial wave function is known $\Psi(q,0)$, similarly to Quantum Mechanics, then an ensemble of different system realisations, characterised by different initial configurations $Q(0)$, has to be considered. By ensemble, we mean the set of all possible configurations and a probability density for the statistical sampling of the elements belonging to such a set. Chosen the density distribution $\rho(q,0)$ on the set of initial configurations, the natural evolution of each configuration of the ensemble through its own trajectory modifies the distribution. The overall result can be imagined as a swarm of evolving trajectories each corresponding to a different initial configuration. The distribution $\rho(q,t)$ at the generic time can be determined by solving the continuity equation for a given initial distribution $\rho(q,0)$:

$$\frac{\partial}{\partial t}\rho(q,t) + \nabla \cdot \left(m^{-1}\nabla S(q,t)\rho(q,t) \right) = 0. \tag{2.10}$$

Broadly speaking, $\rho(q,0)$ is the probability that the initial configuration $Q(0)$ of the system is q, whereas $\rho(q,t)$ is the probability that system configuration $Q(t)$ at time t is q. In this way, the average of an observable on the statistical ensemble can be compared with the corresponding expectation value at any time. Notice that

Eq. (2.10) is equivalent to the continuity equation satisfied by the square modulus of the wave function (the second relation in Eq. (2.3)): the same velocity field accounts for the evolution of the configuration in Eq. (2.5), of the ensemble density distribution in Eq. (2.10) as well, and of the square modulus of the wave function (second relation in Eq. (2.3)). Therefore, if the initial density distribution on the configuration space is set equal to the square modulus of the initial wave function, $\rho(q,0) = |\Psi(q,0)|^2$, then this equivalence holds at any time,

$$\rho(q,t) = |\Psi(q,t)|^2, \tag{2.11}$$

since both the functions are solution of the same differential equation with the same initial condition. Consequently the expectation value of an observable $B(q)$, specified as a function of the coordinates only, is equivalent to its ensemble average at any time:

$$\langle \Psi(t)|B(\hat{q})|\Psi(t)\rangle = \int \mathrm{d}q \; B(q)\rho(q,t). \tag{2.12}$$

Therefore, the equivalence between the predictions of Bohm theory and of Quantum Mechanics is ensured by the swarm of trajectories. Notice that the statistical nature of the predictions in the framework of Bohm theory originates from the impossibility of a complete knowledge of the initial position of all the particles. It is not an intrinsic feature of the theory as in Quantum Mechanics. This correspondence between the Quantum Mechanics predictions and the statistical predictions of Bohm theory holds also for a generic observables (that do not depend on the coordinates only), but a less intuitive proof has to be adopted, which requires the description of the measure process [Bohm (1952b)], and which is not reported here. However, it has to be emphasised that the predictions of the two quantum theories are always in agreement if the Bohm statistical ensemble is employed.

Moreover, the statistical formulation of Bohm theory is equivalent to another alternative quantum theory proposed by E. Madelung in the 1927 [Madelung (1927)]. This approach was inspired by the mathematical equivalence between the second equation in (2.3) and the classical continuity equation. Madelung suggested that the square modulus of the wave function has to be considered formally as the density of a hyperdimensional continuous fluid. Similarly to Classical Mechanics, each fluid element of volume evolves in time along a trajectory whose velocity field is related to the wave function phase. Furthermore, the instantaneous expectation values of the Quantum Mechanics can be interpreted as the instantaneous average properties of the fluid. For these reasons, Madelung's approach is called Quantum

Hydrodynamics. Using the square modulus of the wave function as the statistical distribution on the configurations ensemble, the Bohm method becomes structurally equivalent to Quantum Hydrodynamics: the Bohm configurations ensemble is the Madelung fluid. Therefore, the average of a general observable on the ensemble is equivalent to the corresponding average property of the fluid. For this reason, in the literature Quantum Hydrodynamics is usually considered equivalent to Bohm theory, although the idea of a specific configuration $Q(t)$ and the evolution along a single trajectory suggested by the Hamilton-Jacobi structure of the phase equation, represents the audacity of the Bohm interpretation that has no counterpart on Madelung's approach: the statistical ensemble is merely a methods to overcome the absence of the complete knowledge about the initial configuration.

At this stage Bohm theory can be summarised in the following three postulates [Bohm (1952a)]:

(i) the wave function $\Psi(q,t) = \langle q|\Psi(t)\rangle$ is a field that evolves in time by satisfying the Schrödinger equation, Eq. (2.1);

(ii) the system configuration is $Q(t)$ and the corresponding velocity $\dot{Q}(t)$ is supplied by the Bohm equation, Eq. (2.5);

(iii) a density distribution $\rho(q,0)$ has to be employed in order to sample the possible initial configurations which are unpredictable. Furthermore, the initial density distribution is identified with the square modulus of the wave function, $\rho(q,0) = |\Psi(q,0)|^2$.

These assumptions ensure the exact equivalence between the predictions of Quantum Mechanics and of Bohm theory. Furthermore, Bohm theory supplies a suitable framework to describe molecular systems since it is able to characterise molecules as a set of particles with precise positions.

In order to provide an example of the use of Bohm theory, a simple experiment will be described qualitatively in the following. In particular, the focus will be on the difference between the Quantum Mechanics and the Bohm theory explanations. The case under examination is the well known double-slit experiment, which highlights the wave-particle duality of the matter [Feynman et al. (1964)]. It is so fundamental that is mentioned in almost all the textbooks about Quantum Mechanics. The Figure 2.1 shows a simplified sketch of the experimental setup. During the experiment, the source S emits objects, e.g., classical particles, classical waves or quantum particles, that pass the central separation (wall) through the two slits and they are revealed by the detector on the right side of the setup. The experimental results are

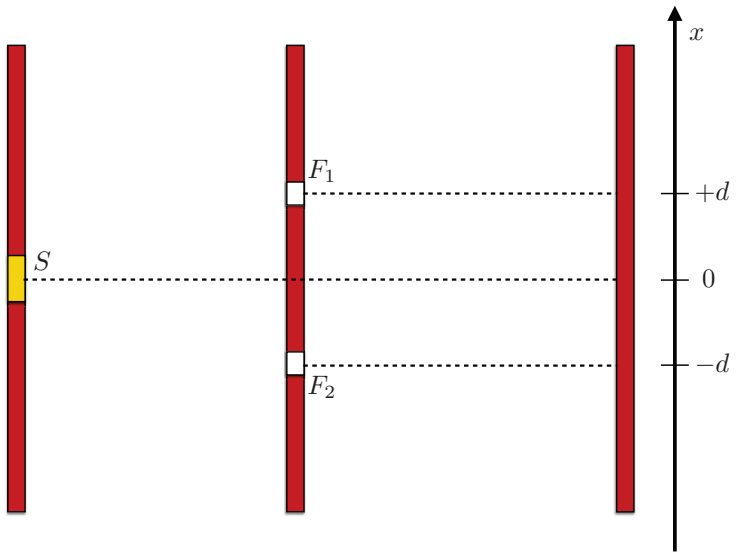

Figure 2.1: Sketch of experimental setup employed in the double slit experiment, where S is the source, F_1 and F_2 are the two slits (or holes), x is the coordinate on the detector, $\pm d$ are the coordinates of the slits projection on the measuring apparatus. Notice that the origin of the x coordinate is the middle point between the slits projection.

strictly dependent on the the type of objects emitted by the source. For instance, by employing a source of classical particles, as bullets, one can observe that:

(i) the particles are emitted one at a time;

(ii) each particles can pass through either one slit or the other;

(iii) the particles that pass through the hole F_1 reach with higher probability the points close to the coordinate $x = d$. On the other hand, the particles that pass through the hole F_2 reach with higher probability the points close to the coordinate $x = -d$. The overall density distribution that a particle reaches a point with coordinate x on the measuring apparatus is defined as the ratio between the number of particles that arrive in x and the total number of particles that pass through the slits and it is equal to an unimodal distribution with maximum at $x = 0$. Notice that the interaction between the holes and the particles is fundamental to address the particles towards either the point $x = d$ or $x = -d$, otherwise the particles move along a straight trajectories from the source to the detector passing through one of the slits.

Instead, if one use a source of classical waves (e.g., a source of circular waves in water), then the results are deeply different as it is well known:

(i) a single wave is diffracted at the holes;

(ii) each slit becomes a source of circular waves that interfere;

(iii) the measuring apparatus records the magnitude of the wave at all the coordinates x on the detector, which is proportional to the square modulus of its amplitude. By drawing the intensity of the wave versus the coordinate x, one obtains the interference pattern.

Finally, by employing a source of quantum particles (e.g., a tungsten filament as a source of electrons), properties of both the classical particles and the classical waves can be observed during the experiment:

(i) the particles are emitted one at a time. With an appropriate voltage on the tungsten filament in vacuum, the measuring apparatus can detect each single electron;

(ii) by defining the density distribution that a particle reaches a point with coordinate x on the detector similarly to the case with classical particles, one obtains the same profile of the interference pattern expected for the classical waves. This, however, is no the result of the interaction between different particles, but it is an intrinsic feature of each quantum particle since it can be obtained also by collecting measures of one emitted particle at a time. Furthermore, if one of the holes is covered, the particles can pass only through the other slit and the observed density distribution is unimodal with the maximum in either $x = +d$ or $x = -d$ position depending on which slit has been left open. In other words, one observes a behaviour identical to that of classical bullets with one only open slit.

These last observations, concerning the behaviour of the quantum particles, can be explained by both the standard Quantum Mechanics and Bohm theory, although the interpretation of the underlying phenomenon is deeply different. In the standard framework the observation of the particle on the detector corresponds to the wave function collapse. The probability of the collapse around the detector coordinate x is proportional to the wave function amplitude in x that is the result of the wave interference if and only if both holes are open. If one slit is covered, then the square modulus of the wave function is an unimodal distribution, so recovering the classical result. Bohm theory does not employ the wave function collapse, but it exploits the pilot character of the wave function. Indeed, the wave function is still subjected to the interference phenomenon and consequently its amplitude along the coordinate x on the detector is in agreement with the interference pattern. According to the Bohm

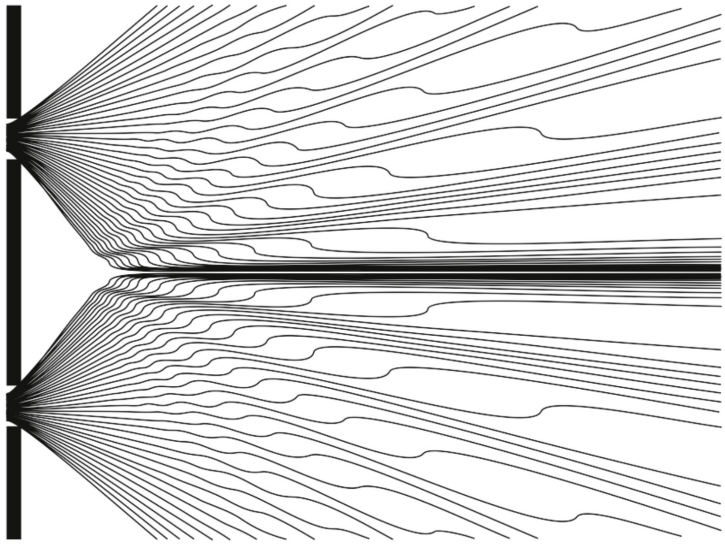

Figure 2.2: Trajectories predicted by Bohm theory for the double slit experiment and characterised by different initial configurations (figure adapted from Philippidis et al. (1979)) and Dürr et al. (2012)).

equation, it pilots the particles mainly to the detector positions where its amplitude is large enough. Therefore, the majority of the trajectories reach the regions of the measuring apparatus characterised by a high value of the wave function amplitude, as shown in Figure 2.2 for the case with no covered holes. The specific path of each single trajectory depends on the initial position and different particles with different initial conditions reach different regions of the detector. However, the pilot role of the wave function selects the trajectories that carry the particles to the regions of the detector where the maxima of the interference pattern are observed. In other words, Bohm theory is able to explain in a rather straightforward way the double slit experiment using continuous trajectories and the pilot role of the wave function. To the question "are the quantum systems composed of particles or waves?" Bohm theory replies that they are composed of both particles and wave. This consideration can be extended to a general quantum system including the molecular systems: Bohm theory can explain any quantum experiment in terms of continuous trajectories. In the following we summarise some works available in the literature that employ exactly this important feature of the Bohm approach. The uses of Bohm theory range from the description of the underlying quantum dynamics to the development of new computational methods.

2.2 Applications of Bohm theory

Bohm theory has found many application in Chemical Physics for both its capability to supply an intuitive image of quantum dynamics and for the exact correspondence between the evolution of a swarm of trajectories and the wave function dynamics. As we mentioned before, Bohm theory and Quantum Hydrodynamics are often not distinguished in literature and they are considered as realisations of the same approach.

Recently, T. Norsen used Bohm theory in order to illustrate the dynamics of two "elementary textbook examples" in terms of quantum trajectories [Norsen (2013)]. In particular, he considered the one dimensional scattering at a potential step and the tunnelling through a rectangular barrier. In both cases the evolution of a wave packet gives rise to a bifurcation of the swarm of trajectories. In the scattering example some trajectories are reflected by the barrier, whereas others are transmitted. Thereafter, only a subset of the whole swarm of trajectories can tunnel the barrier. The transmission probability is related to the number of trajectories that can pass through the classical forbidden region and it depends strictly on the wave function. Once the initial wave function is chosen, a single trajectory will overcome the classical forbidden region depending on its initial configuration.

Besides this simple example, Bohm theory has been adopted to describe molecular behaviour. For example, R. Sawada and coworkers investigated the ionization process of a two electrons molecule, i.e., an hydrogen molecule [Sawada et al. (2014)]. The trajectories allowed the visualisation of the probability density flow from a computational point of view and in parallel they illustrate how the ionization proceeds. Furthermore, Z. S. Wang and coworkers examined the dissociation of an hydrogen molecule at the metal surface by modelling the nuclear wave function with a suitable wave packet [Wang et al. (2001)].

In 2013 Braverman and coworkers suggested how to test the non local features of the Bohm trajectories by employing a double-slit setup and a week-measurement technique [Braverman and Simon (2013)]. This idea inspired a recent experimental study that verified the mutual correlation between two entangled photons [Mahler et al. (2016)]. The authors observed that the evolution of two distinct photons is inseparable: they mapped out the trajectories of one photon and how a week-measurement on the second photon influences the motion of the first one.

With a totally different purpose, the exact equivalence between the evolution of the swarm of trajectories and the standard Quantum Mechanics has been em-

ployed to develop new computational tools in place to the numerical solution of the Schrödinger equation. The first pioneering studies in this field can be ascribed to Weiner and coworkers who were mainly interested in the examination of the tunnelling probabilities between different sites in a solid lattice [Weiner and Partom (1969); Weiner and Askar (1971); Askar and Weiner (1971)]. Afterwards, Wyatt and coworkers elaborated a self-consistent computational method based on the Quantum Hydrodynamics formulation [Lopreore and Wyatt (1999); Wyatt (1999b, 2005)]. They were inspired by the numerical difficulties for the calculation of the wave packet evolution that are employed in the studies of a wide range of phenomena in Chemical Physics, such as reactive collisions, photodissociation of molecules and ions, gas molecule-solid surface scattering, tunnelling of atoms and electrons in solids and on solid surfaces [Zhang (1999); Wyatt and Zhang (1996)]. Their method allows the calculation of the wave function at any time through the integration of a swarm of quantum trajectories. In this way the algorithms usually employed in the study of Classical Hydrodynamics can be adopted also in this framework by adding the contribution of the quantum potential to the classical equation. In this way the difficulties of solving the Schrödinger equation, e.g., the choice of the basis set and the exponential growth of the computational cost with the number of degrees of freedom, are avoided [Rassolov and Garashchuk (2008)]. It has to be emphasised that the only limitation in the Wyatt approach is the number of the trajectories employed in the calculation. Formally, the evolution of the Madelung fluid is determined by an infinite set of trajectories that is computationally unmanageable. Nevertheless, a good agreement between the Wyatt method and the standard predictions can be achieved with a restricted number of trajectories. From a Chemical Physics point of view, the study of the reaction scattering $\mathrm{A} + \mathrm{BC} \rightarrow \mathrm{AB} + \mathrm{C}$ is particularly interesting [Wyatt (1999a)]. It should be stressed that the work of Wyatt exploits Bohm theory in order to achieve computational advantages for the study of the quantum dynamics.

In parallel to the development of the Wyatt approach for the computation of the exact quantum dynamics, similar methods have been proposed with the aim of incorporating some quantum effects in the framework of a classical dynamics. The underlying reasons come from the possibility to compute the dynamics of very large systems, like liquids and biomolecules, with algorithms based on Classical Mechanics. On the other hand, it is well known that the quantum effects can not be neglected for light particles, as protons, and some kind of quantum correction is essential to combine the computational efficiency of Classical Mechanics with the

intrinsic quantum nature of some phenomena. Bohm theory is the suitable framework to develop these kind of methodologies since its equations of motion are like the classical ones with all the quantum effects included into the quantum potential. Therefore, in 2002 S. Garashchuk and coworkers simplified the Wyatt approach by employing an approximate quantum potential [Garashchuk and Rassolov (2002, 2004); Rassolov and Garashchuk (2004)]. One of the proposals consists of fitting the square modulus of the wave function in terms of gaussian functions in order to derive the corresponding quantum potential. Increasing the accuracy of the fitting, also the accuracy of the dynamics improves. A limited number of fitting functions should be sufficient to well describe the dynamics of systems with an almost classical behaviour. With the same main motivations, approximations of the quantum potential can be used to incorporate quantum effects into a reduced number of degrees of freedom, like the positions of light nuclei, while describing the remaining ones, heavy nuclei, with standard Classical Mechanics [Garashchuk and Volkov (2012)]. For this kind of procedures, called in general multiscale methods, the description of the backreaction from the quantum degrees of freedom to the classical degrees of freedom is still an open issue. Again the quantum potential has been adopted to introduce a non arbitrary correlation between the classical and the quantum degrees of feedom [Garashchuk et al. (2014); Prezhdo and Brooksby (2001)].

It has to be emphasised that in the majority of the recent uses of Bohm theory, as the few examples reported above, the Bohm approach is employed exactly as it was defined by Bohm himself in the 1952 [Bohm (1952a,b)]. One of the main motivation to its use is undoubtedly related to the exact correspondence with the standard and widely accepted Quantum Mechanics ensured by the Bohm ensemble. However, from a different point of view the configurations ensemble is a critical issue of the theory as it will be clarified in the next section.

2.3 Beyond the configurations ensemble

As stressed previously, the most appealing feature of Bohm theory is the definition of system configuration $Q(t)$ that allows the identification of the particles position in space. Furthermore, an ensemble of possible initial configurations has been postulated in order to ensure a complete equivalence between the expectation values and Bohm theory predictions. It has to be emphasised that the perfect agreement between the two quantum theories is conditioned by the initial constraint

$$\rho(q,0) = |\Psi(q,0)|^2, \tag{2.13}$$

between the ensemble distribution and the square modulus of the wave function.

On the other hand there are no evident reasons for supporting on a physical ground the equivalence between the square modulus of the wave function and the density of system's configurations at the initial time. Bohm himself recognised the critical role of this assumption and argued that if this is not the case, then the randomness deriving from particle's interactions would enforce such a correspondence during the time evolution [Bohm (1953)]. Such a point of view has been further developed by Valentini and coworkers with the objective of demonstrating that an arbitrary initial distribution on the configuration space relaxes in the time to the square modulus of the wave function [Valentini (1991a,b)]. In particular Valentini proved that the natural dynamics of Bohm theory, that means the natural dynamics of the configurations ensemble, assures the convergence of a generic coarse-grained distribution to the corse-grained approximation of the square modulus of the wave function. Furthermore, numerical simulations have been performed to confirm the Valentini analysis [Towler et al. (2012)]. A different procedures have been proposed by Struyve and coworkers modifying the velocity field of Bohm coordinates [Colin and Struyve (2010)] and by Dürr and coworkers by introducing an effective wave function representative of a system interacting with the environment [Dürr et al. (1992)].

However, from our point of view the same idea of the statistical ensemble represent a critical point of Bohm theory. In Chemistry, it is always implicitly assumed that molecular systems at a given time are characterised by a precise spatial position of their components or at least of their nuclei. This representation corresponds to a single configuration $Q(t)$ in the theoretical framework of Bohm theory, so removing any possibility of a physical meaning to the abstract statistical ensemble. In other words, the chemical representation of molecular systems can be mapped in Bohm theory if and only if we overcome the idea of an ensemble of configurations. By assuming that the molecular behaviour is described by a single Bohm trajectory, then a major issue remains open: does still a formal connection to the standard Quantum Mechanics exist? If it does, then it is available to chemists a quantum theory whose predictions are in agreement with the standard Quantum Mechanics, but which, at the same time, is able to describe formally molecules as objects composed of particles with well defined positions as in the chemical intuition.

A quantum approach based on a single Bohm trajectory is defined and develop in this thesis. In particular in Part I, we investigate the implications of assuming that the behaviour of quantum systems, such as molecular systems, is fully defined

according to a single Bohm trajectory. In Part II the statistical properties of a single Bohm trajectory will be examined formally. It should be anticipated that we prove the equivalence between the predictions of a single Bohm trajectory and conventional Quantum Mechanics under reasonable hypotheses.

Part I

Dynamics of a single Bohm trajectory

CHAPTER 3

Single Bohm trajectory approach

From a methodological point of view, the single Bohm trajectory approach is apparently the best chance to reconcile the chemical representation of molecular systems and a formal theory that accounts for the quantum behaviour of molecules. Besides, form an experimental point of view, the recent investigations on single-molecule or single-spin observables [Berezovsky et al. (2008); Neumann et al. (2008)] together with the efforts towards the realisation of quantum computers based on nanostructures [Biercuk et al. (2009); Suter and Mahesh (2008); Nielsen and Chuang (2010)], calls for a representation of molecular systems according to a single quantum state that is incompatible with an ensemble of quantum states.

The formal structure of the Bohm theory is well defined and self-consistent also when an unique wave function and an unique system configuration are used to describe a particular realisation of the quantum system. This point of view might be considered as the most natural way of interpreting Bohm theory without requiring any particular constraint on the distribution of initial configurations.

As mentioned in advance, however, a major issue remains open: what is the connection with standard Quantum Mechanics? More specifically, how to define from a single trajectory of the system configuration a probability density on the configuration space, which is a prerequisite before establishing a relation with the wave function? One can exploit the analogy with Classical Statistical Mechanics which introduces the equilibrium distribution by considering the density of phase space points along a single time dependent realisation of the isolated system [Khinchin (1949)]. Also in the case of Bohm theory with a single trajectory, one can define

in an analogous way the equilibrium probability density on the configuration space. But then, how to compare such an equilibrium distribution, which is time independent by definition, with the quantum distribution given as the square modulus of the wave function, which is intrinsically a time dependent distribution? As a matter of fact the comparison becomes meaningful when the marginal distributions are considered for a subsystem interacting with a larger environment acting as thermal bath. Indeed, by employing the methods developed in a previous work [Fresch and Moro (2013)], one can show that in such a case the fluctuations of the marginal quantum distribution become negligible. In this particular situation the marginal distributions obtained from the configuration distribution along a single Bohm trajectory and from the wave function tend to coincide as it is explained in this chapter and in a work of us [Avanzini et al. (2016)]. In order to provide evidences of this behaviour, we present some computational results for a model system of several confined, randomly coupled, planar rotors. Such a numerical observation evidences that a correspondence between a single Bohm trajectory and the standard Quantum Mechanics exists and that it plays the same role of the Bohm statistical ensemble.

We would like to mention that only few previous attempts has been done to connect the standard Quantum Mechanics with a single Bohm trajectory. Yu V. Shtanov [Shtanov (1997)] investigated the problem from the point of view of ergodicity. Very recently, T. Philbin [Philbin (2015)] considered a simple one dimensional system (an harmonic oscillator) in the presence of an external time dependent potential which mimics the position measurement. From a temporal sequence of these position measurements he obtains the same distribution given by the square modulus of the wave function. In spite of the differences on the employed model systems and on the type of dynamical regime, we share the same objective of developing Bohm theory for a single realisation of the quantum system.

In the following we report the detail of the numerical methods employed to verify the existence of the previously invoked correspondence. Since the model system is composed of several interacting components, statistical tools are required to analyse the quantum pure state represented by the wave function. In Sec. 3.1 we introduce the Random Pure State Ensemble (RPSE) employed for the sampling of the wave function, and we summarise its fundamental properties [Fresch and Moro (2009, 2010a, 2011, 2013)]. Such a statistical ensemble allows one to evaluate the amplitude of fluctuations of the quantum observables (expectation values) with respect to their equilibrium values defined by time averages, and to estimate the behaviour of fluctuation amplitudes in the thermodynamic limit for an increasing

size of the system. By recalling the results of Fresch and Moro (2013), it is shown that the marginal distribution on a subsystem, as obtained from integration of the square modulus of the wave function on the environmental degrees of freedom, is characterised by fluctuations of vanishing amplitude for an increasing size of the environment. Correspondingly the subsystem can be described by a nearly stationary marginal quantum distribution if the environment is large enough, which can be well approximated by its time average. In Sec. 3.2 the model system of six interacting and confined planar rotors is used to verify the approximate equivalence between the quantum marginal distribution and the distribution obtained by sampling a single Bohm trajectory. First the model system is described in detail together with the numerical procedures employed for the calculation of time dependent properties. Then the main results are illustrated in relation to: i) the nearly stationarity of the marginal quantum distribution of one rotor, the other five rotors constituting the environment, ii) the randomly fluctuating behaviour displayed by the evolution of the Bohm coordinate of one rotor with the corresponding loss of correlation with the time, iii) the close correspondence between the marginal quantum distribution and the distribution of Bohm coordinate of the subsystem, which provides the computational evidence of the correspondence between a single Bohm trajectory and the Quantum Mechanics of the wave function. In Sec. 3.3 we show that the correspondence is exactly verified if the Bohm coordinate of the subsystem behaves like an independent Markov stochastic variable, as partially suggested by the numerical results. Finally, in Sec. 3.4 the general considerations are drawn by focusing on their implications.

3.1 Statistics of quantum pure states

In this section we present the statistical description of quantum pure states to be employed in the analysis of single Bohm trajectory. The need of a statistics of pure states, that is of a wave function belonging to the proper Hilbert space for an isolated (closed) system, arose mainly from the efforts of demonstrating the typicality of quantum observables [Popescu et al. (2006); Goldstein et al. (2006)]. On the other hand, well defined statistical rules are required for sampling the initial wave function whenever the quantum dynamics is examined without particular *a priori* choices of the initial state. We stress that in Quantum Mechanics the condition of isolated system is more stringent than in Classical Mechanics: entanglement would keep the system connected to his environment even though there is no energy exchange

between them.

Given the Hamiltonian $\hat{H}$ of the system, the wave function $|\Psi(t)\rangle$, an Hilbert $\mathcal{H}$ space's element, evolves in time through the Schrödinger equation from a given initial state $|\Psi(0)\rangle$,

$$|\Psi(t)\rangle = e^{-\imath\hat{H}t/\hbar}\,|\Psi(0)\rangle\,, \tag{3.1}$$

$\exp(-\imath\hat{H}t/\hbar)$ is the propagator of the system. The time evolution of a generic physical property described by self-adjoint operator $\hat{B}$ is determined by the expectation value $B(t)$,

$$B(t) = \langle\Psi(t)|\hat{B}|\Psi(t)\rangle = \mathrm{Tr}\Big\{\hat{B}\hat{\varrho}(t)\Big\}, \tag{3.2}$$

where $\hat{\varrho}(t)$ is the density matrix operator for the pure state

$$\hat{\varrho}(t) = |\Psi(t)\rangle\,\langle\Psi(t)|\,. \tag{3.3}$$

The expectation value $B(t)$ is usually interpreted as the mean value of a infinite number of measures of the observable at time t. By considering in all generality an operator $\hat{B}$ which does not commute with the Hamiltonian $\hat{H}$, the corresponding expectation value $B(t)$ displays an explicit time dependence. The nature of such a time dependence is determined by the physical structure of the system and the particular operating conditions, in practice its initial conditions. The elaboration of well defined theoretical tools for the statistical characterisation of the time dependence of quantum pure states has been an important objective of the recent research in relation to the issues of equilibration and thermalisation, see for instance Reimann (2008), Linden et al. (2009), Goldstein et al. (2010). Here we consider sufficiently complex quantum systems with a randomly chosen initial state. Then for the typical observable $B(t)$ one expects a purely fluctuating evolution about the time average, very much like the fluctuating dynamics of classical observables in equilibrium conditions. The observation of non-equilibrium dynamics would require the selection of particular initial conditions within a set of vanishing measure on the unitary Bloch sphere, choice which is excluded when random initial conditions are considered. Thus, like in Classical Statistical Mechanics [Khinchin (1949)], we identify the equilibrium value of observable B with the asymptotic time average of the expectation value:

$$\overline{B(t)} := \lim_{T\to+\infty}\frac{1}{T}\int_0^T \mathrm{d}t\; B(t) = \mathrm{Tr}\Big\{\hat{B}\overline{\hat{\varrho}(t)}\Big\}, \tag{3.4}$$

where $\overline{\hat{\varrho}(t)}$ is the time average of the density matrix.

If we are interested in properties of a subsystem, we can imagine to partition the isolated system: the subsystem S and the environment E for the remaining part of the isolated system. Correspondingly the overall Hilbert space $\mathcal{H}$ is factorised into the Hilbert spaces $\mathcal{H}_S$ of the system and $\mathcal{H}_E$ of the environment, $\mathcal{H} = \mathcal{H}_S \otimes \mathcal{H}_E$. In this situation the observable of interest $b(t)$, i.e., a property of the subsystem, is represented by the expectation value of an operator $\hat{b} \otimes \hat{\mathbb{1}}_E$. The reduced density matrix operator $\hat{\sigma}(t)$, as obtained by partial trace Tr_E over the environment states of the pure state density operator,

$$\hat{\sigma}(t) := \mathrm{Tr}_E\big\{\hat{\varrho}(t)\big\}, \tag{3.5}$$

allows the calculation of this expectation value within the subsystem Hilbert space

$$b(t) = \mathrm{Tr}\Big\{\big(\hat{b} \otimes \hat{\mathbb{1}}_E\big)\hat{\varrho}(t)\Big\} = \mathrm{Tr}_S\Big\{\hat{b}\ \hat{\sigma}(t)\Big\}. \tag{3.6}$$

Its equilibrium value $\overline{b(t)}$ is defined again by time averaging and it can be evaluated like in Eq. (3.4) by means of the time average $\overline{\hat{\sigma}(t)}$ of the reduced density matrix.

In order to formulate a statistical description of quantum pure states, a finite set of parameters identifying the instantaneous wave function has to be selected, very much like for the phase space of Classical Statistical Mechanics. This requires the confinement of the wave function to a finite dimensional subspace of $\mathcal{H}$, say a N-dimensional subspace $\mathcal{H}_N$ in the following called active space. To select the active space, it is convenient to resort to the orthonormal eigenstates $|E_k\rangle$ of the Hamiltonian:

$$\hat{H}\,|E_k\rangle = E_k\,|E_k\rangle\,. \tag{3.7}$$

Like in previous works [Fresch and Moro (2009, 2010a,b, 2011)], we shall employ the following type of active space

$$\mathcal{H}_N := \left\{\bigoplus_{k=1}^{N} |E_k\rangle \ \text{ with } E_N < E_{max} < E_{N+1}\right\}, \tag{3.8}$$

that is the subspace due to eigenstates with eigenvalues smaller than E_{max}. The energy cutoff E_{max} is the only parameter required for the identification of this active space, and it has been shown that in the limit of macroscopic systems E_{max} represents the internal energy [Fresch and Moro (2011)].

It should be mentioned that one can employ an alternative active space by introducing also a low energy cutoff E_{min}, like in the definition of microcanonical

density matrix of standard Quantum Statistical Mechanics [Huang (1987)]. In this way, however, one has to manage two different cutoff parameters and, furthermore, no direct relation exists between the lower energy cutoff E_{min} and thermodynamic properties [Fresch and Moro (2011)].

The wave function $|\Psi(t)\rangle$ at a given time is then conveniently specified as a linear combination of the basis elements $|E_k\rangle$ of the active space through its expansion coefficients $c_k(t)$ or, equivalently, through the sets of populations $(P_1, P_2, \ldots, P_N)$ and of phases $A(t) = (A_1(t), A_2(t), \ldots, A_N(t))$ obtained from the polar representation of the expansion coefficients

$$c_k(t) := \langle E_k|\Psi(t)\rangle = \sqrt{P_k}e^{-\imath A_k(t)}, \tag{3.9}$$

with a linear time dependence of the phases: $A_k(t) = A_k(0) + E_k t/\hbar$. Because of the normalisation condition,

$$\langle\Psi(t)|\Psi(t)\rangle = \sum_{k=1}^{N} P_k = 1, \tag{3.10}$$

only $(N-1)$ populations are independent, say the set $P = (P_1, P_2, \ldots, P_{N-1})$. Therefore a bijection exists between the normalised wave function and a particular set of these $(2N-1)$ real parameters, that is the set of populations P and of phases $A(t)$. In other words, all the pure states of the active space can be imagined like unit vectors drawing an unit sphere in a $2N$-dimensional Euclidean space [Fresch and Moro (2009)].

Because of the choice of expanding the wave function along the Hamiltonian eigenstates, the phases are the only dynamic variables of the system, while the populations represent the constants of motion. Correspondingly it is easily shown that equilibrium properties $\overline{B(t)}$ of Eq. (3.4) depend on populations only. Indeed, under the condition of rational independence of Hamiltonian eigenvalues, meaning that equation $\sum_{k=1}^{N} n_k E_k = 0$ for integer n_k has only the trivial solution $n_k = 0$ $\forall k$, the equilibrium density matrix is diagonal with the populations as diagonal elements [Fresch and Moro (2009)],

$$\overline{\hat{\varrho}(t)} = \sum_{k=1}^{N} |E_k\rangle\, P_k\, \langle E_k| \equiv \overline{\hat{\varrho}}^{P}, \tag{3.11}$$

where we have introduced the symbol $\overline{\hat{\varrho}}^{P}$ to highlight the dependence of equilibrium density matrix on populations only. We emphasise that the condition of rational

independence is not too restrictive because of the contribution of random interactions, typical of molecular systems, leading to energy eigenvalue distribution having, at least partially, a random character [Wigner (1967)]. Therefore, according to Eq. (3.4), also the equilibrium value of a generic observable depends on populations only,

$$\overline{B(t)} = \mathrm{Tr}\Big\{\hat{B}\overline{\hat{\varrho}}^{P}\Big\} \equiv \overline{B}^{P}, \tag{3.12}$$

as stressed by the symbol $\overline{B}^{P}$.

In this way, the parametric dependence of the equilibrium properties on the populations is evident. On the other hand, there are no empirical methods leading to a complete characterisation of the initial state $|\Psi(0)\rangle$ and, therefore, also of the populations. This implies that populations can be characterised only on statistical grounds by selecting the ensemble for their probability distribution. The absence of privileged directions for $|\Psi(0)\rangle$ within the unit sphere, leads quite naturally to a purely random choice for the ensemble of pure states. The Random Pure State Ensemble (RPSE) for populations has been characterised from the geometrical analysis of the measure on the unit sphere, so deriving the probability density on the $(N-1)$ independent populations P [Fresch and Moro (2009)],

$$p_{\mathrm{RPSE}}(P) = (N-1)!. \tag{3.13}$$

Such a probability density allows the explicit calculation of the ensemble average of equilibrium properties,

$$\Big\langle \overline{B}^{P} \Big\rangle := \int \mathrm{d}P_1 \ldots \mathrm{d}P_{N-1} \;\; \overline{B}^{P} \; p_{\mathrm{RPSE}}(P_1, \ldots, P_{N-1}), \tag{3.14}$$

which can be interpreted as the average of $\overline{B}^{P}$ amongst random realisations of the initial pure state $|\Psi(0)\rangle$. Notice that integration domain on populations is bounded by constraints $0 \leq P_k \leq 1$, $\forall k = 1, 2, \ldots N$. In the following we shall employ the bracket $\Big\langle \ldots \Big\rangle$ to denote the RPSE average of a function of populations. It should be stressed out that in Eq. (3.14), as well as in following ones, two different types of averages are involved: the ensemble average on the populations P and the time average which is equivalent to the averages on the phases A [Fresch and Moro (2010a)]. Both these averages might be recast as integral operators acting, however, on different kinds of variables. On the other hand these averages play a completely different role in the methodological framework of single Bohm trajectory. As long as we are looking to a single realisation of the system, therefore for a given set of

populations, only the time average is relevant to evaluate equilibrium properties. The ensemble average on the set of populations is required for the analysis of the dependences on the populations of the equilibrium properties in relation to the typicality (see Eq. (3.19) below) and to characterise the time dependence of the marginal quantum distribution.

In order to recover also the macroscopic description of the system, one should consider the equilibrium energy, $\overline{H}^P = \sum_{k=1}^N P_k E_k$, and Shannon's entropy [Shannon and Weaver (1949)] with respect to the populations, $S^P = -k_B \sum_{k=1}^N P_k \ln P_k$. Their RPSE average are associated respectively to the thermodynamical internal energy, $U := \langle \overline{H}^P \rangle$, and to the thermodynamical entropy, $S := \langle S^P \rangle$, both being functions of E_{max}. By eliminating the E_{max} dependence between functions $U(E_{max})$ and $S(E_{max})$, one recovers the thermodynamical state function $S(U)$ and the temperature as well from its derivative $1/T = dS/dU$. In this framework, by considering the system as a set of n distinct components, like molecules in material systems, one can define the thermodynamic limit for $n \to \infty$ at a given temperature [Fresch and Moro (2011)]. The thermodynamic limit requires the tensorial product of the Hilbert spaces of all the distinct components, and this implies an exponential growth of the dimension N of the active space $\mathcal{H}_N$ with the number n of components [Fresch and Moro (2013)]. Finally, in the same limit, the RPSE average of the equilibrium reduced density matrix $\left\langle \overline{\hat{\sigma}}^P \right\rangle$ of a subsystem having weak enough interactions with the environment, takes the canonical form

$$\left\langle \overline{\hat{\sigma}}^P \right\rangle = \frac{e^{-\hat{H}_S/k_B T}}{\mathrm{Tr}_S\left\{ e^{-\hat{H}_S/k_B T} \right\}}, \tag{3.15}$$

where $\hat{H}_S$ is the Hamiltonian of the subsystem [Fresch and Moro (2011)].

The RPSE statistics allows the quantitative analysis of typicality [Fresch and Moro (2011)] of an equilibrium property $\overline{B}^P$ by evaluating the thermodynamic limit of its square variance within the ensemble,

$$\lim_{n\to\infty} \left\langle \left(\overline{B}^P - \left\langle \overline{B}^P \right\rangle \right)^2 \right\rangle. \tag{3.16}$$

Typicality of property $\overline{B}^P$ is assured if this limit vanishes, this implying that the value of $\overline{B}^P$ in a realisation of the pure state is independent of the set of populations, as long as its deviation from the ensemble average $\left\langle \overline{B}^P \right\rangle$ tends to vanish. In other words, property $\overline{B}^P$ is typical in the meaning that it is nearly independent of the

particular realisation of the pure state.

Furthermore, RPSE ensemble allows the quantitative analysis not only of typicality of an observable, but also of its time fluctuations which are of primary importance for the objectives of proving the existence of a correspondence between the single Bohm trajectory and the standard Quantum Mechanics. In order to characterise the amplitude of fluctuations of $B(t)$ during its time evolution, we consider the equilibrium value, i.e., the time average, of the squared deviation $\Delta B(t) := B(t) - \overline{B}^P$ from the time average

$$\overline{(\Delta B)^2}^P := \overline{\left(B(t) - \overline{B}^P\right)^2}^P \tag{3.17}$$

that, like all the equilibrium properties, depends on the population set. The population average within RPSE provides an estimate $\left\langle \overline{(\Delta B)^2}^P \right\rangle$ of squared fluctuations which is independent of the particular realisation of the pure state [Bartsch and Gemmer (2009); Fresch and Moro (2013)] and reads

$$\left\langle \overline{(\Delta B)^2}^P \right\rangle + \left\langle \left(\overline{B}^P - \left\langle \overline{B}^P \right\rangle \right)^2 \right\rangle = \frac{D_2(\hat{B})}{N+1}, \tag{3.18}$$

where the second term at the left hand side describes the typicality of equilibrium property $\overline{B}^P$ as previously discussed. At the right hand side, N is the dimension of the active space $\mathcal{H}_N$, while $D_2(\hat{B})$ represents the squared spectral variance of the operator $\hat{B}$, $D_2(\hat{B}) = \sum_{k=1}^{N} (\lambda_k - D_1(\hat{B}))^2$, where $\{\lambda_k\}$ is the set of eigenvalues of $\hat{B}$ in $\mathcal{H}_N$ and $D_1(\hat{B}) = \sum_{k=1}^{N} \lambda_k / N$ is the eigenvalue average. Such a relation connects the statistical properties of the expectation value $B(t)$, at the left hand side of the equation, to the spectral properties of the operator $\hat{B}$, on the right hand side of equation. If operator $\hat{B}$ has a bounded spectrum, then $D_2(\hat{B})$ is finite and in the thermodynamic limit, $n \to +\infty$, the right hand side of Eq. (3.18) vanishes because of the exponential growth with n of the active space dimension N. Correspondingly also both terms at the left hand side of Eq. (3.18) vanish since they are non negative

$$\lim_{n \to +\infty} \left\langle \left(\overline{B}^P - \left\langle \overline{B}^P \right\rangle \right)^2 \right\rangle = 0, \qquad \lim_{n \to +\infty} \left\langle \overline{(\Delta B)^2}^P \right\rangle = 0. \tag{3.19}$$

Thus, in the thermodynamic limit, both typicality and the vanishing of fluctuations are assured for bounded operators. The second equation in (3.19) ensures that $\overline{(\Delta B)^2}^P$ vanishes on average by sampling the populations according to RPSE. The condition holds also for a single set of populations because of typicality (first equation in (3.19)). Outside the thermodynamic limit, for finite but large enough isolated

quantum systems a nearly stationarity $B(t) \simeq \overline{B}^P$ is predicted. Furthermore, we note that in these conditions the expectation value $B(t)$ is nearly equal to the thermodynamic value $\left\langle \overline{B}^P \right\rangle$ always because of typicality: $B(t) \simeq \left\langle \overline{B}^P \right\rangle$.

These results for typicality and fluctuation amplitude of bounded operators can be applied to the reduced density matrix of a subsystem of an isolated system. In particular, as shown in detail by Fresch and Moro (2013), the following condition for the expectation value $b(t)$ of subsystem operator $\hat{b}$ derives from Eq. (3.18),

$$\begin{aligned} &\left\langle \left(\overline{b}^P - \langle \overline{b}^P \rangle \right)^2 \right\rangle + \left\langle \overline{(\Delta b)^2}^P \right\rangle \\ &\qquad \leq \frac{\mathrm{Tr}_S\left\{ \hat{b}^2 \left\langle \overline{\hat{\sigma}}^P \right\rangle \right\} - \mathrm{Tr}_S\left\{ \hat{b} \left\langle \overline{\hat{\sigma}}^P \right\rangle \right\}^2}{N+1}. \end{aligned} \tag{3.20}$$

In the thermodynamic limit the ensemble average of the reduced density matrix tends to the canonical form Eq. (3.15) and, therefore, the right hand side vanishes because of the active space dimension N of at the denominator. Then both typicality and the vanishing of fluctuations are recovered like in Eq. (3.18) for bounded operators, but now for a generic operator $\hat{b}$ of the subsystem. For finite but large enough isolated systems this implies that subsystem observables are nearly stationary,

$$b(t) \simeq \overline{b}^P \tag{3.21}$$

that is, their time dependent deviations from the equilibrium values are negligible.

As an application of the previous analysis, we examine the statistical distribution on the coordinates q_S for the subsystem degrees of freedom. In standard Quantum Mechanics the wave function allows the calculation of the time dependent distribution on the generalised coordinates $q = (q_1, q_2, \ldots q_n)$ of the isolated system with n degrees of freedom through the probability density

$$p(q,t) = \left| \Psi(q,t) \right|^2 \tag{3.22}$$

with a parametric dependence on the initial pure state determining the time dependent wave function. Once the subsystem S, and the environment E as well, has been selected, the isolated system generalised coordinate can be identified with the set $q = (q_S, q_E)$ of subsystem coordinates q_S and of coordinates q_E for the environment degrees of freedom. Then, by integration on the environment coordinates, the

marginal distribution on the subsystem degrees of freedom is recovered

$$p^S(q_S,t) := \int \mathrm{d}q_E \; p(q_S,q_E,t). \tag{3.23}$$

As for any time dependent observable, the time average defines the corresponding equilibrium property, in this case the equilibrium distribution

$$p^S_{eq}(q_S) := \overline{p^S(q_S,t)}, \tag{3.24}$$

where the reference to the parametric dependence on population set P has been omitted for the sake of a compact notation.

Let us consider now an orthonormal basis $\{|\varphi_m\rangle\}$ for the subsystem Hilbert space $\mathcal{H}_S$, and its coordinate representation $\{\varphi_m(q_S)\}$ as explicit functions of subsystem coordinates q_S. For any set of q_S values, we can define the following operator

$$\hat{b}(q_S) := \sum_{m,m'} |\varphi_m\rangle \, \varphi^*_m(q_S)\varphi_{m'}(q_S) \, \langle\varphi_{m'}| \,, \tag{3.25}$$

where its operator nature is determined by the kets $|\varphi_m\rangle$ and bras $\langle\varphi_{m'}|$ on the r.h.s.. One can easily verify that its q_S-dependent expectation value supplies the subsystem marginal probability density calculated at q_S

$$p^S(q_S,t) = \mathrm{Tr}_S\Big\{\hat{b}(q_S)\hat{\sigma}(t)\Big\}. \tag{3.26}$$

In this way, the marginal distribution can be interpreted as expectation value of a subsystem operator, which is characterised by typicality and absence of fluctuations in the thermodynamic limit in agreement with the previous conclusions. Outside the thermodynamic limit, but for large enough isolated systems, negligible contributions of fluctuations about the time average Eq. (3.24) are expected like in Eq. (3.21),

$$p^S(q_S,t) \simeq p^S_{eq}(q_S), \tag{3.27}$$

so that the subsystem is characterised by a nearly time independent marginal distribution.

As long as expectation values or, equivalently, marginal distributions derived from the wave function are employed to describe a subsystem which is part of a much larger isolated system, the time evolution of the subsystem appears to be secondary. As a matter of fact the environment quenches the dynamics of these subsystem properties. In a classical world this would correspond to a picture of

motionless subsystems, like molecules in material systems, without fluctuations in the thermodynamic limit. Such a stationarity derives from the fact that the expectation value is not a directly observed physical property, but an average of infinite measures of the physical property. Nonetheless, the expectation value is the standard tool supplied by Quantum Mechanics for the description of the time evolution of physical properties, tool which displays stationarity in the thermodynamic limit. It should then be useful to explore Bohm theory by looking for alternative tools able to capture the fluctuation dynamics of parts, like molecules, of a larger isolated system.

In parallel, the nearly stationarity of $p^S(q_S, t)$ allows a meaningful comparison between the subsystem density distribution predicted by the wave function and the statistical properties of the single Bohm trajectory. In order to recover a probabilistic description from a single Bohm trajectory, one has necessarily to resort to the statistical sampling of the coordinates during their time evolution, like in ergodic theory of Classical Statistical Mechanics [Khinchin (1949)]. As long as such a sampling represents overall effects of system evolution, it is an equilibrium property which should in general depend on the constants of motion, that is the populations P determining the pilot wave function. The probability density on the generalised coordinates q extracted from the sampling of a single trajectory $Q(t)$ will be denoted as $w_{eq}(q)$, keeping implicit the reference to the parametric dependence on the population set to deal with a more compact notation. Broadly speaking, $w_{eq}(q)$ is defined in order to ensure that the following equation holds for any observable of the type $B(q)$:

$$\lim_{T\to+\infty} \frac{1}{T} \int_0^T \mathrm{d}t \; B\big(Q(t)\big) = \int \mathrm{d}q \; B(q) w_{eq}(q). \tag{3.28}$$

In other words, $w_{eq}(q)$ relates the time average of any observables $B(q)$ along a single Bohm trajectory $\overline{B\big(Q(t)\big)}$ and a space average on the configuration space. In a multicomponent system the probability density $w^S_{eq}(q_S)$ on the subsystem S describes the Bohm trajectory sampling of the subsystem coordinates and it is defined similarly to $w_{eq}(q)$. If the isolated system is large enough, $w^S_{eq}(q_S)$ can be compared with the quantum equilibrium density of the subsystem $p^S_{eq}(q_S)$, since $p^S(q_S, t)$ has negligible fluctuations. In other words, by examining a part of a much larger system, the quantum distribution can be described by $p^S_{eq}(q_S)$, that is a time independent function like the coordinate distribution $w^S_{eq}(q_S)$ obtained from a single Bohm trajectory and, therefore, a meaningful comparison between them can be done. This is the objective of the calculations in a model system reported in the next section.

3.2 Bohm trajectory in a multi-particle model system

In order to compare the single Bohm trajectory and the quantum distribution function, the dynamical behaviour of a model system of six confined planar rotors interacting through random potentials has been examined. The numerical calculations done for a typical situation clearly show that a correspondence exists between the Bohm coordinate distribution $w^S_{eq}(q_S)$ and the equilibrium quantum distribution $p^S_{eq}(q_S)$ for a rotor subsystem. In this section, after the presentation of the model system, we discuss the numerical methods employed for the calculation of the relevant properties and we illustrate the most relevant results.

3.2.1 The model system

We shall consider a system of $n = 6$ identical but distinguishable particles with mass m that move on a ring of constant radius R. Such a system is equivalent to n planar rotors described by the set of angles $q = (q_1, q_2, \ldots, q_n)$ with $0 \leq q_i < 2\pi$, each of them having an inertia momentum $I = mR^2$. A physical realisation of the system could be a set of methyl groups rotating about their $C - CH_3$ bonds. The Hilbert space $\mathcal{H}_i$ for the i-th rotor is the set of periodic functions of the angular coordinate q_i, whose Fourier representations can be generated by means of the following orthonormal basis set

$$\chi_j(q_i) = \frac{e^{\imath j q_i}}{\sqrt{2\pi}}, \tag{3.29}$$

with integer values for j index. The tensor product of the Hilbert spaces of each rotor, $\mathcal{H} = \mathcal{H}_1 \otimes \mathcal{H}_2 \otimes \ldots \otimes \mathcal{H}_n$, identifies the Hilbert space for the overall system. Such a model system will be described by means of the following Hamiltonian

$$\hat{H} = \hat{H}^{(0)} + \hat{V}^{(r)} = \sum_{i=1}^{n} \hat{H}_i^{(0)} + \hat{V}^{(r)}, \tag{3.30}$$

where $\hat{H}_i^{(0)}$ is the single particle Hamiltonian, while $\hat{V}^{(r)}$ is an interaction potential of random type. For the single particle Hamiltonian we use the model of a planar rotor confined by a cosine potential with minimum at $q_i = \pi$:

$$\hat{H}_i^{(0)} = -\frac{\hbar^2}{2I}\frac{\partial^2}{\partial q_i^2} + \frac{u}{2}(1 + \cos q_i), \tag{3.31}$$

the parameter $u \geq 0$ representing the energy barrier at $q_i = 0$. In the following the parameter $\hbar^2/2I$ will be employed as the energy unit. We intend to analyse

the quantum dynamics of the system in conditions of significant confinement of the rotors, and to this purpose we have selected the potential barrier as $u = 300(\hbar^2/2I)$.

The contribution $\hat{V}^{(r)}$ of the system Hamiltonian has the purpose of producing a dynamical coupling between rotors by means of random interactions typical of molecular systems. Moreover, it assures the rational independence of the Hamiltonian $\hat{H}$ eigenvalues, a property which does not hold in the presence of single particle Hamiltonians only. The modelling at the quantum level of random interactions and their effects is well developed starting from the Wigner distribution [Wigner (1967)] and including more general random matrix theories [Brody et al. (1981)]. In our rotors system we model it simply by introducing potential terms with a random profile. The coordinate representation of the potential $V^{(r)}$ has been parameterised as single particle contributions and interaction terms between pairs of rotors:

$$V^{(r)}(q_1, q_2, \ldots, q_n) = \sum_{i=1}^{n} V_i^{(r)}(q_i) + \frac{1}{2}\sum_{i,j=1}^{n}(1-\delta_{i,j})V_{i,j}^{(r)}(q_i - q_j). \tag{3.32}$$

Let us denote with $V(\theta)$ the periodic function representative of a single particle contribution, that is $V_i^{(r)}(q_i)$ for $q_i = \theta$, or of a two-particle interaction, that is $V_{i,j}^{(r)}(q_i - q_j)$ for $q_i - q_j = \theta$. By means of a gaussian random variable with null average and a given variance σ_V, a random profile is easily generated for its discretised values $V_k := V(\theta_k)$ at $(2L+1)$ equally spaced angles $\theta_k = 2\pi k/(2L+1)$ for $k = 0, 1, \ldots, 2L$. Standard algorithms can be employed to produce these random values of the function with statistical properties

$$\overline{V_k} = 0, \qquad \overline{V_k^2} = \sigma_V^2, \tag{3.33}$$

where the average is referred to different realisations of the same coefficient. In order to recover a continuous function $V(\theta)$ from these random coefficients, we resort to a truncated Fourier decomposition

$$V(\theta) = \sum_{l=-L}^{L} \tilde{V}_l e^{\imath l\theta}, \tag{3.34}$$

with its $(2L+1)$ components evaluated at the discretised angles

$$\tilde{V}_l = \frac{1}{2L+1}\sum_{k=0}^{2L} V_k e^{-\imath l\theta_k}. \tag{3.35}$$

Since an additive constant in the potential does not modify the quantum dynamical properties, a null value is attributed to the Fourier component $\tilde{V}_0$, this being

equivalent to the constraint of a null angular average for functions $V(\theta)$.

In conclusion, the previous procedure allows the generation of these random angular functions for each contribution of Eq. (3.32) on the basis of two parameters: the variance σ_V and the number $(2L+1)$ of discretised angles. The variance σ_V controls the strength of the random contribution $\hat{V}^{(r)}$ with respect to single particle Hamiltonians in Eq. (3.30). In the following calculations we shall use an unitary value of this variance in the adopted energy units, that is $\sigma_V = \hbar^2/2I$. This corresponds to random potentials with a strength much smaller than the confining potential with a barrier height $u = 300(\hbar^2/2I)$. In this way, the random potential contribution has nearly a perturbation effect so that eigenfunctions and eigenvalues of the full Hamiltonian Eq. (3.30) preserve the main features deriving from single rotor contributions. The other parameter L controls the size of the angular correlations in the potential, since it determines the distance between two adjacent discretised angles with uncorrelated values of the potential. In the calculations we shall use the value $L = 100$ because it produces an highly random potential. An angular dependence resembling that of a noisy signal is evident form Fig. 3.1 which displays the potential deriving from a particular realisation of the $(2L+1)$ coefficients V_k for $L = 100$. For each of the contributions of Eq. (3.32) an independent realisation of the random potential $V(\theta)$ is employed.

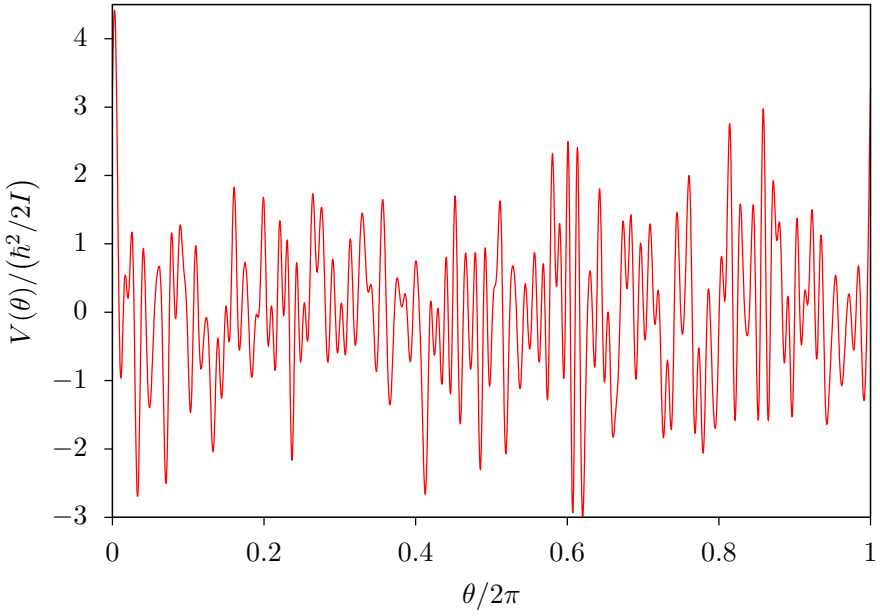

Figure 3.1: Random potential characterised by the parameters $\sigma_V = \hbar^2/2I$ and $L = 100$.

3.2.2 Numerical methods

Before to discuss the results for the quantum dynamics of the model system, we summarise in this section the numerical procedures employed in the calculations. They concern four main issues: i) the solutions for the single planar rotor Hamiltonian, ii) the eigenvalues and the stationary states for the system of interacting rotors, iii) the initial conditions and the time dependent wave function and related properties, iv) the Bohm trajectory.

The eigenfunctions of the single planar rotor Hamiltonian Eq. (3.31) are required because their tensorial products represent the most convenient basis for the numerical solution of the time independent Schröedinger Eq. (3.7) as long as the random potential $\hat{V}^{(r)}$ is weak. Let us denote the eigenvalue problem for the single rotor as

$$\hat{H}_i^{(0)}\varphi_m(q_i) = \epsilon_m\varphi_m(q_i), \tag{3.36}$$

with eigenvalues ordered from below, $\epsilon_m \leq \epsilon_{m+1}$, for $m = 0, 1, 2, \ldots$. Of course all the planar rotors have the same eigenvalues and eigenfunctions with the same functional form since they share the same Hamiltonian (see Eq. (3.31)). Even if the eigen-solutions of Eq. (3.36) can be identified with a particular class of Mathieu functions [Abramowitz and Stegun (1972)], we have preferred to obtain them by numerical diagonalisation of the matrix representation of Eq. (3.31) on the basis Eq. (3.29). In this way the eigenfunctions are specified as linear combinations of basis functions Eq. (3.29), and they allow a straightforward evaluation of the matrix elements due to the interaction potential Eq. (3.32) (see below). The matrix obtained from basis elements Eq. (3.29) with $|j| \leq 20$ has been diagonalised by employing the software routine *Armadillo*, a `C++` linear algebra library [Sanderson (2010)]. In Table 3.1 we have reported the lower energy eigenvalues, and in Fig. 3.2 the profiles of the corresponding squared eigenfunctions $|\varphi_m(q_i)|^2$ with the eigenvalues as offset together with the confining potential. In Table 3.1 we have also included the harmonic oscillator eigenvalues resulting from the parabolic approximation $u(1 + \cos q_i)/2 \simeq u(q_i - \pi)^2/4$ of the rotor potential, in order to attest the differences with respect to purely harmonic quantum dynamics. Indeed for increasing levels the difference between the two sets of eigen-energies clearly emerges. It should be mentioned that the numerical diagonalisation of the single rotor Hamiltonian supplies not only the eigenvalues ϵ_m, but also the eigenvectors, that is the coefficients for the expansion of the eigenfunctions $\varphi_m(q_i)$ on the basis of Eq. (3.29). When, in the following, operations on single rotor eigenfunctions $\varphi_m(q_i)$ are invoked,

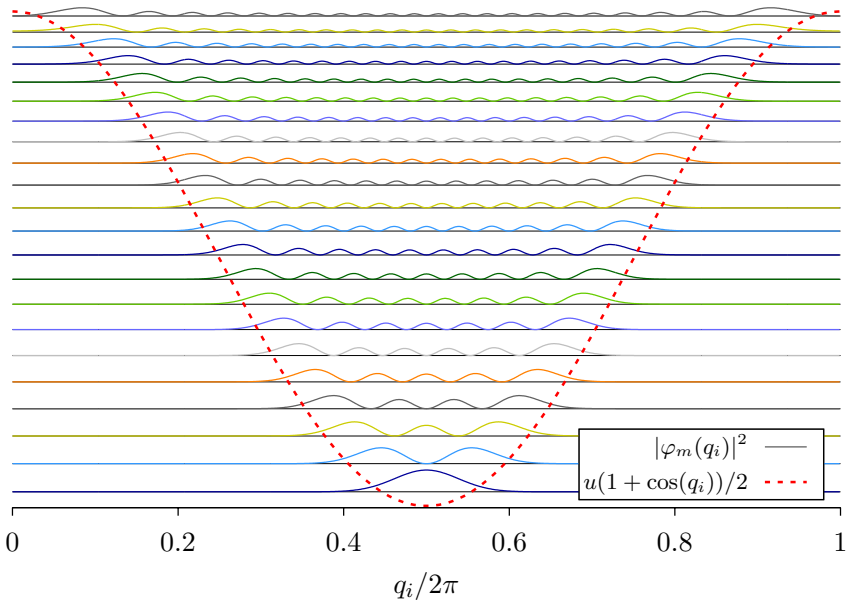

Figure 3.2: Squared modulus of eigenfunctions $\varphi_m(q_i)$ of the $H_i^{(0)}$ Hamiltonian for the single planar rotor, with $u = 300(\hbar^2/2I)$ as the intensity of the confining potential $u(1+\cos(q_i))/2$

implicitly we refer to operations on these linear combinations which can be easily encoded in computer programs.

Given the numerical solutions of Eq. (3.36), one can employ the following basis for the Hilbert space $\mathcal{H}$ of the overall system

$$|l\rangle = \bigotimes_{i=1}^{n} |\varphi_{l_i}\rangle \,, \tag{3.37}$$

where $l := (l_1, l_2, \cdots, l_n)$, and each index l_i identifies the eigenfunction $\varphi_m(q_i)$ of the corresponding i-th rotor with $m = l_i$. The basis elements $|l\rangle$ are eigenfunctions of the model system Hamiltonian in the absence of the random potential

$$\hat{H}^{(0)} |l\rangle = E_l^{(0)} |l\rangle \,, \qquad E_l^{(0)} = \sum_{i=1}^{n} \epsilon_{l_i}, \tag{3.38}$$

and they are conveniently ordered according to the corresponding energies $E_l^{(0)}$. As long as the random potential $\hat{V}^{(r)}$ acts like a perturbation, the diagonalisation of the full Hamiltonian is influenced mainly by the coupling between basis elements with nearby values of $E_l^{(0)}$, and this allows an efficient truncation of the Hamiltonian matrix representation. In practice, one considers all the basis elements with $E_l^{(0)}$ less than a given truncation energy cutoff $E_{tr}^{(0)}$. Then the matrix representation of

Table 3.1: Low energy eigenvalues ϵ_m of the single planar rotor Hamiltonian for the potential barrier $u = 300(\hbar^2/2I)$. The corresponding harmonic oscillator eigenvalues are reported between parentheses.

m	$\epsilon_m/(\hbar^2/2I)$
0	8.597 (8.660)
1	25.664 (25.981)
2	42.472 (43.301)
3	59.015 (60.622)
4	75.286 (77.942)
5	91.278 (95.263)
6	106.982 (112.583)
7	122.390 (129.904)
8	137.491 (147.224)
9	152.275 (164.545)

the full Hamiltonian is generated in order to perform the diagonalisation by means of the software *Armadillo*. The organisation of these energy levels in well separated multiplets is evident in analogy to the polyads describing molecular vibrations (see [Krasnoshchekov and Stepanov (2013); Herman and Perry (2013)] and references therein). Since in the harmonic approximation the oscillators for the confined rotors are degenerate, the polyad quantum number classifying the basis elements Eq. (3.37) is given as $P = \sum_{i=1}^{n} l_i$ with values $P = 0$ (ground state), $P = 1$ (6 states), $P = 2$ (21 states), and so on. As long the random potential $\hat{V}^{(r)}$ is weak, the corresponding Hamiltonian eigenfunctions $|E_k\rangle$ are substantially reproduced by linear combinations of basis elements with a given polyad quantum number P, with only perturbational contributions from the other polyads. Therefore the polyad quantum number can be used to classify also the eigenvalue multiplets, as done in Fig. 3.3.

The comparison in Fig. 3.3 of the numerical eigenvalues obtained with two values of parameter $E_{tr}^{(0)}$ allows one to evaluate the effects of matrix truncation. Notice that the chosen values of $E_{tr}^{(0)}$ leads to a complete inclusion of the selected polyads in the truncated matrix representation. The results with matrix representation for $E_{tr}^{(0)} = 154/(\hbar^2/2I)$ ($N = 924$), polyads from $P = 0$ to $P = 6$) will be employed as the reference for the calculation of time dependent properties of the model system. Their accuracy has been checked by comparison with the larger matrix obtained for $E_{tr}^{(0)} = 171/(\hbar^2/2I)$ which includes a further polyad. Such a matrix enlargement, besides introducing new eigenvalues (i.e., the $P = 7$ polyad), produces a change of about $0,04\%$ for the upper energy eigenvalues, and smaller variations for decreasing energy (see the insets of Fig. 3.3). Such a behaviour agrees with the perturbational

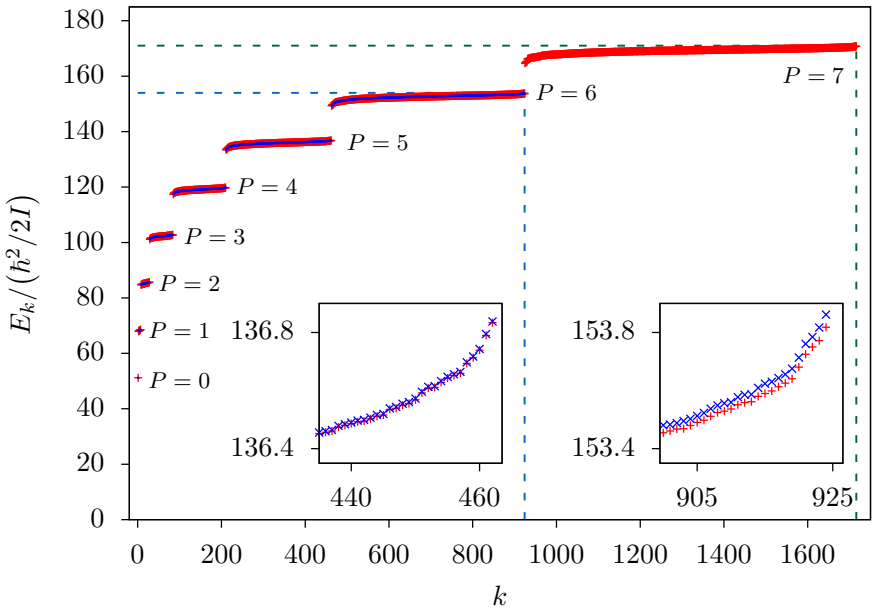

Figure 3.3: Numerical results of energy eigenstates E_k for two truncation parameters $E_{tr}^{(0)} = 154/(\hbar^2/2I)$ (blue crosses) and $E_{tr}^{(0)} = 171/(\hbar^2/2I)$ (red crosses). The states with comparable energy are labeled according to the polyad quantum number, from P=0 (ground state) to P=7. The last part of polyads $P = 5$ and $P = 6$ are magnified in the insets in order to show the effects of the truncation parameter.

contribution by the random potential $\hat{V}^{(r)}$: surely it has strong effects within a polyad in the presence of degenerate or nearly degenerate zero-order energies $E_l^{(0)}$, but it has weak effects on the coupling of states belonging to different polyads with well separated values of $E_l^{(0)}$. These informations allows us to conclude that with the truncation parameter $E_{tr}^{(0)} = 154(\hbar^2/2I)$ $(N = 924)$ we get numerical results with errors at most of $0,04\%$. As a matter of fact the accuracy of the data employed in the calculation of time dependent properties is much better, as long as we shall use an active space including up to $P = 5$ polyad whose eigenvalues deviate from those obtained with the larger matrix by $0,004\%$ at most. The final results of this computational task is the set of eigenvalues E_k and eigenstates $|E_k\rangle$, the latter specified as linear combinations of basis elements Eq. (3.37) through coefficients $\langle l|E_k\rangle$, for the time independent Schröedinger Eq. (3.7).

Once the eigenstates and the energy eigenvalues are obtained and the active space is identified on the basis of the cutoff energy E_{max}, the time dependent wave function has to be evaluated. Thus the initial quantum state has to be chosen according to the set of populations P and the set of initial phases $A(0)$ within the active space. Since the phases are homogeneously distributed [Fresch and Moro (2010a)], they are

simply selected at random within their domain. Also for the populations a random choice is performed but, in order to preserve their normalisation, by means of suitable set of auxiliary parameters homogeneously distributed in the $(0, 1]$ domain according to procedure discussed by Zyczkowski and Sommers (2001), Zyczkowski (1999) and Fresch and Moro (2011). Given these initial conditions, the wave function at an arbitrary time is specified as

$$|\Psi(t)\rangle = \sum_{k=1}^{N} \sqrt{P_k} e^{-\imath(A_k(0)+E_k t/\hbar)} |E_k\rangle , \tag{3.39}$$

where N is the dimension of the active space. For the calculation of the reduced density matrix, reference is made to the first planar rotor, $q_S = q_1$, so that its matrix elements on the basis of single rotor eigenfunctions Eq. (3.36) can be specified as

$$\begin{aligned}
&\sigma_{m,m'}(t) := \langle \varphi_m | \hat{\sigma}(t) | \varphi_{m'} \rangle \\
&= \sum_{l,l'} \left(\prod_{i=2}^{n} \delta_{l_i,l'_i} \right) \delta_{l_1,m} \delta_{l'_1,m'} \langle l | \Psi(t) \rangle \langle \Psi(t) | l' \rangle = \\
&= \sum_{k,k'} \sum_{l,l'} \left(\prod_{i=2}^{n} \delta_{l_i,l'_i} \right) \delta_{l_1,m} \delta_{l'_1,m'} \langle l | E_k \rangle \langle E_{k'} | l' \rangle \ \times \\
&\quad \times \sqrt{P_k P_{k'}} e^{-\imath[A_k(0) - A_{k'}(0) + (E_k - E_{k'})t/\hbar]}.
\end{aligned} \tag{3.40}$$

The same equation with the constraint $k = k'$ in the summations on the r.h.s. can be employed to evaluate the elements $\overline{\sigma}_{m,m'}$ of the equilibrium density matrix. Given the reduced density matrix, also the marginal quantum distribution of the subsystem (the first planar rotor) is recovered according to Eq. (3.26)

$$p^S(q_S, t) = \sum_{m,m'} \sigma_{m,m'}(t) \varphi^*_{m'}(q_S) \varphi_m(q_S), \tag{3.41}$$

and the equilibrium distribution as well by inserting the equilibrium density matrix elements

$$p^S_{eq}(q_S) = \sum_{m,m'} \overline{\sigma}_{m,m'} \varphi^*_{m'}(q_S) \varphi_m(q_S). \tag{3.42}$$

By specifying the eigenstates $|E_k\rangle$ in Eq. (3.39) as linear combinations of the basis functions Eq. (3.37), one gets for a given time the explicit dependence on the coordinates of the wave function, $\Psi(q, t)$, and of both the amplitude $R(q, t)$ and the phase $S(q, t)$ as well.

For the computation of the trajectory of the rotors, we adopted the Runge-

Kutta method [Press et al. (2007)] at the 4-th order to solve the Bohm equation of motion Eq. (2.5). We employed a time step $\Delta t = 0.01(4\pi I/\hbar)$ that assures a good approximation to the calculated trajectory from the point of view of its statistical properties. In particular we have evaluated the correlation function $G(t)$ of the rotor angle Q_S

$$G(\tau) := \frac{\overline{\Delta Q_S(t)\Delta Q_S(t+\tau)}}{\overline{\Delta Q_S^2(t)}}, \tag{3.43}$$

with $\Delta Q_S(t) = Q_S(t) - \overline{Q_S(t)}$, that we calculate from the discretised time average along the trajectory:

$$G(\tau) \simeq \frac{\sum_{j=0}^{M} \Delta Q_S(j\Delta t)\Delta Q_S(j\Delta t+\tau)}{\sum_{j=0}^{M} \Delta Q_S^2(j\Delta t)}, \tag{3.44}$$

where M is the number of sampling points that depends on the length of the examined trajectory.

Finally the distribution $w_{eq}^S(q_S)$ of the planar rotor coordinate along its trajectory has to be evaluated. In practice we have calculated its discretised counterpart by dividing the domain $0 \leq Q_S < 2\pi$ of the rotor angle into 10^4 equally spaced intervals. The probability density is recovered from the fraction of time spent by the rotor in each interval during its evolution. In order to check that the length of the trajectory is sufficient, we have verified that the resulting distribution is not significantly modified by a further evolution.

One might wonder whether the numerical procedure for the calculation of the Hamiltonian eigenvalues and eigenfunctions, which provides always approximate results, affects the behaviour of the computed trajectory. If this is the case, then in the comparison between the quantum distribution $p_{eq}^S(q_S)$ for the subsystem and the distribution $w_{eq}^S(q_S)$ on the Bohm coordinate, one should consider explicitly the influence of the errors introduced by the numerical diagonalisation. Let us denote with $E_k^{(app)}$ and $|E_k^{(app)}\rangle$ the approximate eigenvalues and eigenfunctions computed numerically. The computed wave function derives from the linear combinations of these approximate eigenfunctions, and it is a solution of the Schröedinger equation for the Hamiltonian

$$\hat{H}^{(app)} := \sum_{k=1}^{N} \left| E_k^{(app)} \right\rangle E_k^{(app)} \left\langle E_k^{(app)} \right| \tag{3.45}$$

instead of the assumed model Hamiltonian Eq. (3.30). Correspondingly the phase function $S(q,t)$ and the resulting Bohm trajectory is exact for the quantum problem

described by the Hamiltonian $\hat{H}^{(app)}$. In conclusion, the unavoidable errors introduced by the numerical diagonalisation are formally equivalent to a slight modification of the system Hamiltonian. Of course the Bohm trajectory is also affected by the numerical errors in the integration of the differential equation (2.5), but their effects can be easily controlled by checking that the coordinate distribution $w^S_{eq}(q_S)$, and the coordinate correlation function Eq. (3.43) as well, does not change by decreasing the integration time step.

3.2.3 Dynamical properties

The selected model system and its Hamiltonian with $u = 300(\hbar^2/2I)$ as the barrier of the confining potential, is compatible with different thermal states depending on the cut-off energy E_{max} of the RPSE. We have selected the value $E_{max} = 139(\hbar^2/2I)$ which corresponds to an active space of dimension $N = 462$ including the polyads from $P = 0$ to $P = 5$ and excluding the other polyads (see Fig. 3.3). With such a choice we deal with a state having a significant distribution between the ground state and the excited states of the single rotor, as witnessed by the subsystem reduced density matrix represented on the basis of single rotor eigenfunctions $\varphi_m(q_S)$ of Eq. (3.36). The equilibrium reduced density matrix calculated according to the methods illustrated in the previous section is nearly diagonal, and the diagonal components are reported in Table 3.2. The calculated off-diagonal elements $\overline{\sigma}_{m,m'}$ are less than $1/1000$ in magnitude with respect the associated diagonal elements $\overline{\sigma}_{m,m}$ and $\overline{\sigma}_{m',m'}$. The decrease of the diagonal elements $\overline{\sigma}_{m,m}$ with the single rotor energy ϵ_m (see Table 3.2) might suggest a canonical form $\overline{\sigma}_{m,m} \propto \exp(-\epsilon_m/k_BT)$ but this is not the case. In order to provide evidences about it, we have derived the hypothetical canonical thermal coefficient $1/k_BT = 0.0376(2I/\hbar^2)$ from the ratio $\overline{\sigma}_{1,1}/\overline{\sigma}_{0,0}$ and then the corresponding elements of the canonical density matrix, which are reported between parentheses in Table 3.2. The deviations with respect to the numerical values of $\overline{\sigma}_{m,m}$ clearly emerge, particularly for the upper energy elements, and this points out that the size of our model system (six interacting rotors) is not large enough to ensure the thermodynamic limit. On the other hand one can assert that the system resembles that of thermodynamic equilibrium.

As explained in the previous section, the instantaneous reduced density matrix allows the calculation of the time dependent quantum distribution $p^S(q_S, t)$ of the subsystem (the first planar rotor). The profiles of such a distribution are reported in Fig. 3.4 for a selected sample of times. As the reference for the visualisation of its

Table 3.2: Diagonal elements of the equilibrium reduced density matrix, with their canonical values reported between parentheses.

m	$\overline{\sigma}_{m,m}$
0	0.536 (0.475)
1	0.282 (0.250)
2	0.127 (0.133)
3	0.0431 (0.0712)
4	0.0122 (0.0386)
5	$5.15\ 10^{-4}$ (0.0211)
6	$3.61\ 10^{-7}$ (0.0117)

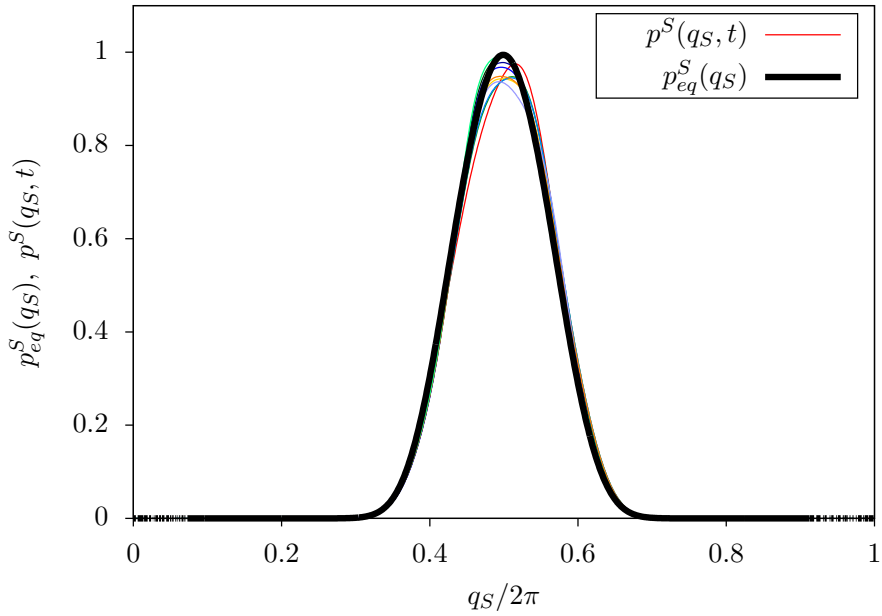

Figure 3.4: Equilibrium marginal density distribution $p^S_{eq}(q_S)$ (black thick line) and marginal density distributions $p^S(q_S,t)$ (coloured thin lines) at some selected times. The marginal distributions are referred to the first of the 6 planar rotors in our model system.

change with the time, in the same figure we have plotted also the equilibrium quantum distribution $p^S_{eq}(q_S)$ calculated according to equilibrium reduced density matrix $\overline{\sigma}_{m,m'}$. In Sec. 3.1 we have shown that in the thermodynamic limit, i.e., when the number of interacting components is large enough, the fluctuations of $p^S(q_S,t)$ become negligible and then $p^S_{eq}(q_S)$ would reproduce the quantum distribution function at all times. The data in Fig. 3.4 clearly show that this is not the case in our model system as long as time dependent deviations from $p^S_{eq}(q_S)$ are evident. On the other hand these deviations have a comparably low magnitude, so that the equilibrium distribution $p^S_{eq}(q_S)$ can be considered as representative, at least approximately, of the instantaneous quantum distribution $p^S(q_S,t)$.

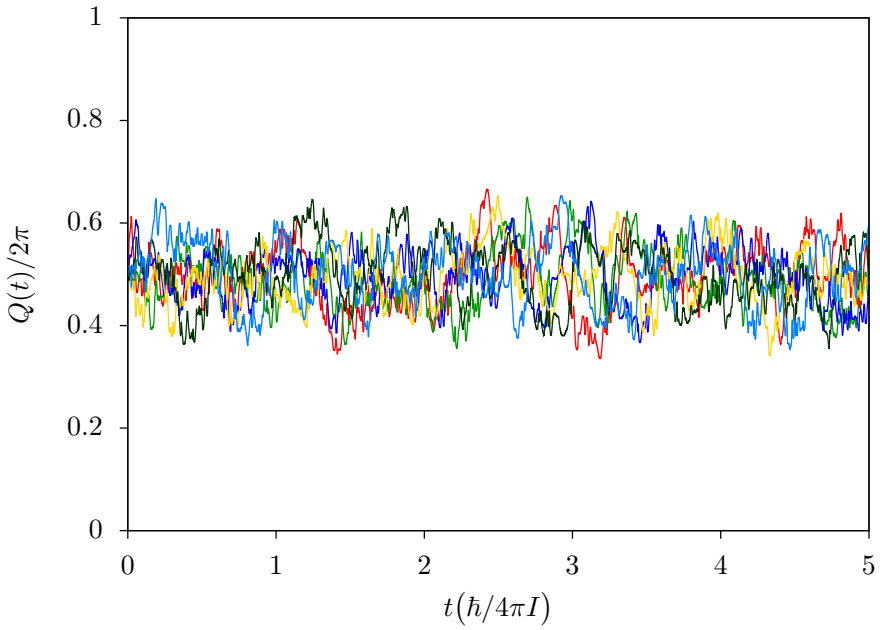

Figure 3.5: Time evolution of the Bohm coordinates (drawn with different colours) of the six planar rotors of the model system.

Having characterised the main quantum properties of the subsystem, we examine now the behaviour of the Bohm coordinates. By employing the procedure illustrated previously, time evolution of the angular coordinates $Q_i(t)$ of the six rotors have been computed according to Eq. (2.5) by choosing $Q_i(0) = \pi$ as initial conditions in correspondence of the bottom of the rotor confining potential. In Fig. 3.5 we have represented with different colours the time evolution of all the rotors coordinate within the time window $0 \leq t(\hbar/4\pi I) \leq 5$. Each rotor coordinate follows a strongly confined dynamics with limited excursions about the potential minimum. The time evolution of each rotor coordinate seems that of a fluctuating signal loosing correlation with time, somehow like in the brownian motion. To verify this feature, we have computed the correlation function $G(\tau)$ Eq. (3.43) which is displayed in Fig. 3.6. As expected on the basis of the behaviour of the trajectory, the correlation vanishes with a rather short correlation time of order $\tau_c(\hbar/4\pi I) \simeq 0.4$ supporting the analogy with brownian motion. It appears that the phase function $S(q,t)$ due to the wave function generates a fluctuating evolution of the Bohm coordinates, which leads to a fast loss of correlation.

If the Bohm coordinates Q_S of the subsystem is considered as a stochastic process, than its properties are naturally characterised by the correlation function Eq. (3.43) and its equilibrium distribution $w^S_{eq}(q_S)$. The expected confinement of the rotor

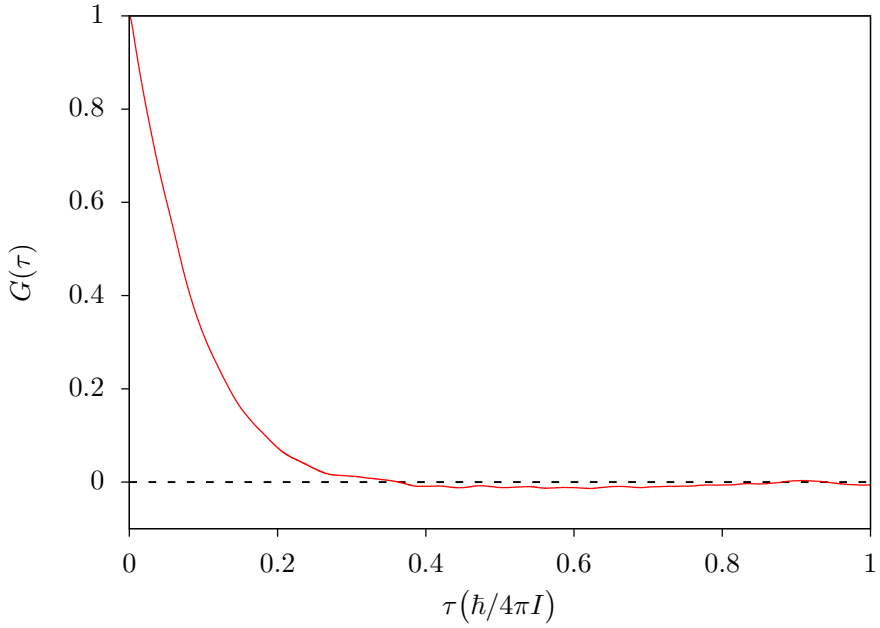

Figure 3.6: Correlation function $G(\tau)$ of the first planar rotor coordinate.

angle clearly emerges from such a distribution which is displayed in Fig. 3.7. In the same figure we have plotted also the equilibrium quantum distribution for the sake of comparison. The two equilibrium distributions, the one $p^S_{eq}(q_S)$ deriving from the evolution of the wave function, and the other $w^S_{eq}(q_S)$ calculated from a single Bohm trajectory, result to be very close

$$w^S_{eq}(q_S) \simeq p^S_{eq}(q_S). \tag{3.46}$$

Notice that the loss of correlation along the trajectory implies that the distribution $w^S_{eq}(q_S)$ is independent of the choice of the initial values $Q(0)$ of the Bohm coordinates.

It should be stressed that the correspondence of Eq. (3.46) cannot be considered as a general property for all quantum systems. Indeed one can use a single rotor system as a counterexample where Eq. (3.46) does not hold. If the same previous procedure is applied to an isolated confined rotor, with the same potential of our model system, by choosing an active space of dimension $N = 2$ in order do deal with a wave function with a nearly 50% probability of the ground state like for the reduced density matrix of Table 3.2, one obtains two very different equilibrium distributions like those displayed in Fig. 3.8. It should be mentioned that the asymmetry on the profile of $w_{eq}(q)$ derives from the difference of the randomly chosen

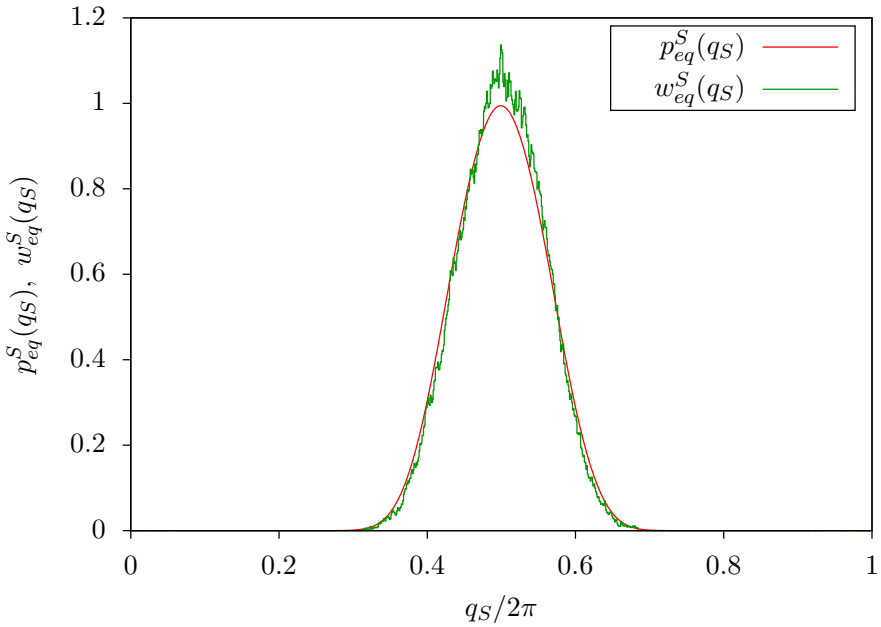

Figure 3.7: Equilibrium marginal quantum distribution $p^S_{eq}(q_S)$ and marginal density distribution $w^S_{eq}(q_S)$ of the Bohm coordinate for the first planar rotor.

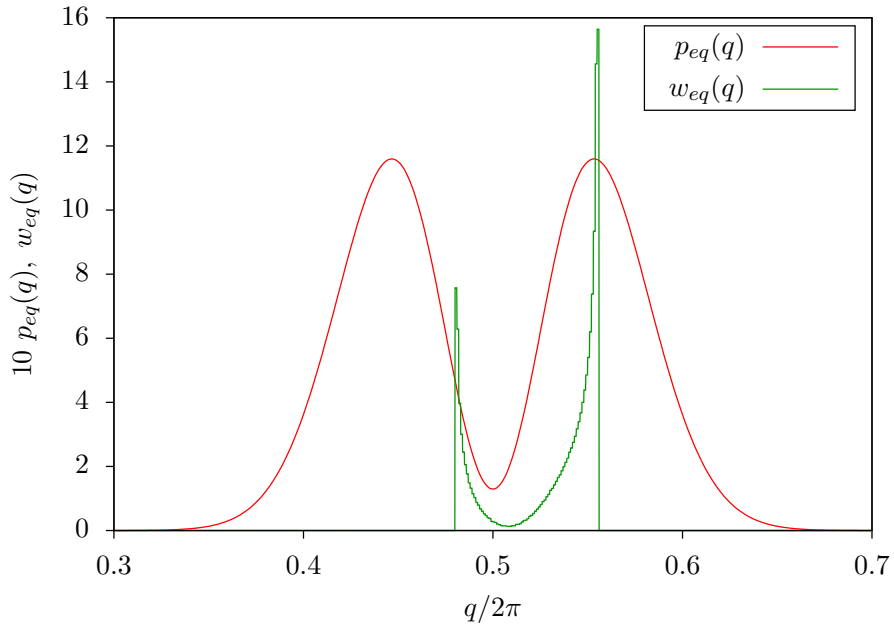

Figure 3.8: Quantum equilibrium distribution $p_{eq}(q)$ and the distribution $w_{eq}(q)$ of the Bohm coordinate for the model system with a single planar rotor.

populations of the two quantum states. At this stage one can conjecture that the correspondence Eq. (3.46) found in our model system is a consequence of the multi-particle interactions which are absent in the single rotor system. In Chap. 6 such a

correspondence is discussed rigorously and the reasons why Eq. (3.46) does not hold in the single rotor system emerge naturally.

Finally we emphasise that the correspondence (3.46) is not an accidental result of particular conditions employed for the calculation in our model system. As a matter of fact we have similar evidences of the correspondence from calculations in other conditions, for instance by using a confining potential with lower strength or even in the absence of the confining potential.

3.3 Bohm coordinates as Markov stochastic variables

As reported in the previous section, explicit calculations with a many body model system suggest that, even by considering Bohm theory at the level of single Bohm trajectory, a correspondence exists according to Eq. (3.46) between probability density determined by the wave function and the coordinate distribution derived from the trajectory. This is an important result since it allows a connection between the standard quantum theory and the description of system evolution through a single trajectory, without the need of the Bohm configurations ensemble and the corresponding swarm of trajectories. On the other hand, such a connection has a methodological role different from the Bohm ensemble. In particular we emphasise the following three features. i) It is a correspondence concerning the subsystem only, while the Bohm ensemble Eq. (2.11) deals with the overall isolated system. ii) Its validity has to be restricted to the case of negligible fluctuations on the quantum distribution Eq. (3.23) which then can be replaced by the equilibrium quantum distribution Eq. (3.24). Only in this case the quantum distribution becomes time independent and, therefore, it can be compared with Bohm coordinate distribution which, by definition, is time independent. iii) Such a correspondence in general is not exact, since there are evident counterexamples (Figure 3.8). The calculation results simply suggest that quantum distribution and Bohm trajectory coordinate distribution are close in suitable conditions. On the contrary the Bohm ensemble Eq. (2.11) is exactly verified once the third Bohm assumption Eq. (2.13) is introduced.

Besides these considerations, an important issue naturally arises: can the correspondence Eq. (3.46) find a support beyond the evidences resulting from calculations with specific model systems? In other words, can Eq. (3.46) be derived under particular conditions? A positive answer is found if the evolution of subsystem coordinate in the single Bohm trajectory follows a stationary Markov process for a stochastic variable [Gardiner (1986)]. A stationary Markov process is completely characterised

by the equilibrium distribution $w^S_{eq}(q_S)$ and the conditional probability distribution $w^S(q_{S,0}|q_S,\tau)$. The former is obtained from the sampling of subsystem coordinates $Q_S(t)$ along a single Bohm trajectory, as we have done in our model system. The latter requires the sampling of the correlation of coordinates $Q_S(t)$ and $Q_S(t+\tau)$ at two times separated by τ, and it should satisfy the constraint of correlation loss at long enough times:

$$\lim_{\tau\to+\infty} w^S(q_{S,0}|q_S,\tau) = w^S_{eq}(q_S). \tag{3.47}$$

The distributions characterising the Markov process observed in a single trajectory, can be used to describe also the probability density arising from an ensemble of trajectories. Let us denote with $\rho^S(q_S,t)$ the probability density on the coordinate for such an ensemble of trajectories. Given the initial distribution $\rho^S(q_S,0)$, the probability density at any time can be evaluated on the basis of the correlation function $w^S(q_{S,0}|q_S,\tau)$,

$$\rho^S(q_S,t) = \int \mathrm{d}q_{S,0}\ \rho^S(q_{S,0},0) w^S(q_{S,0}|q_S,t), \tag{3.48}$$

and, according to Eq. (3.47), it will relax to the equilibrium distribution $w^S_{eq}(q_S)$ at long enough times

$$\lim_{\tau\to+\infty} \rho^S(q_S,t) = w^S_{eq}(q_S). \tag{3.49}$$

Let us now recognise the conditions under which the distribution on the trajectories is stationary, that is $\rho^S(q_S,t)$ is time independent. Stationarity means that the equivalence in Eq. (3.49) must be verified at all times,

$$\rho^S(q_S,t) = w^S_{eq}(q_S), \tag{3.50}$$

and, therefore, the initial distribution $\rho^S(q_S,0) = w^S_{eq}(q_S)$ is the unique condition leading in Eq. (3.48) to a time independent distribution.

Let us apply these results to the ensemble of trajectories generated according to the third Bohm assumption, and with the further conditions: a) stationary quantum distribution for the subsystem, $p^S(q_S,t) = p^S_{eq}(q_S)$, b) stationary Markov process for subsystem coordinate in a Bohm trajectory. Then the subsystem probability density, according to the Bohm ensemble Eq. (2.11), is equivalent to the stationary quantum distribution

$$\rho^S(q_S,t) = p^S(q_S,t) = p^S_{eq}(q_S), \tag{3.51}$$

because of condition a). On the other hand, because of condition b), the same prob-

ability density can be computed according to Eq. (3.48) with $\rho^S(q_S, 0) = p^S_{eq}(q_S)$ as the initial distribution. However, such a probability density has only one stationary form specified by Eq. (3.50). One can conclude that, as long as the two conditions a) and b) are satisfied and, therefore, Eq. (3.50) and (3.51) are holding simultaneously, for the subsystem the quantum equilibrium distribution and the coordinate distribution in a Bohm trajectory are equivalent,

$$p^S_{eq}(q_S) = w^S_{eq}(q_S). \tag{3.52}$$

This is the important result of the previous analysis which, however, is conditioned by the validity of assumptions a) and b). In section 3.1 we have analysed the fluctuations of the quantum distribution for the subsystem, by showing that they vanish in the limit of an infinite size environment. This points out that in finite but large enough systems, condition a) is satisfied only approximately, and the same type of validity should be attributed to the equivalence Eq. (3.52). At this stage a specific analysis about the general validity of the description of subsystem coordinate as a Markov process is lacking even if, in analogy to classical brownian motion, one might conjecture that such a feature is determined by the coupling amongst many degrees of freedom. On the other hand the model results reported in the previous section suggest that for systems characterised by random interactions amongst its components, the subsystem evolution leads to distributions approximating Eq. (3.52).

3.4 Final remarks

We have considered the system of six confined planar rotors as a model to test the representation of quantum systems by the single Bohm trajectory. For the subsystem identified with one rotor, the others playing the role of the environment, we have found the following main results from the numerical solution of Bohm theory: i) the marginal quantum distribution derived from the wave function is nearly stationary, ii) the Bohm coordinates evolves like a randomly fluctuating signal with a clear loss of correlation with the time, iii) the rather close correspondence between the marginal quantum distribution and the distribution of the Bohm coordinates. We stress the interest of the last result in relation to the methodological status of Bohm theory. If a correspondence exists between the quantum distribution derived from the wave function and the distribution of the Bohm coordinates along a single trajectory, albeit at the level of the subsystem, then the ensemble of trajectories together with the postulate for their initial distribution is not mandatory to establish a connection

between standard quantum theory and the configuration of Bohm theory. A more direct picture of molecular systems would then be derived on the basis of a single realisation of both the quantum state (the wave function) and the configuration (the Bohm trajectory).

On the other hand, we emphasise that such a correspondence is presently an observation supported by the numerical results for a particular model system. The existence of conditions assuring the validity of the correspondences remains still an open issue. The hypothesis that the Bohm coordinates behaves as a Markov stochastic process has been used to justify the result, as shown in the previous section.

We would like also to comment on the implications of the near stationarity of the marginal quantum distribution for the subsystem, as shown in Fig. 3.4. This is strictly a consequence of the vanishing of fluctuations of the reduced density matrix in the thermodynamic limit as analysed by Fresch and Moro (2013). A direct relation exists also with the typicality analysed by Bartsch and Gemmer (2009) even if in their theory the effects of fluctuations in time are not separated from the distribution within the ensemble. At any rate, a static picture of the subsystem properties would be implied from these results, at odds with the opposite image of an ever fluctuating world as suggested by the Classical Mechanics. We think that Bohm theory, in the single trajectory approach, leads to a solution of these contradictory representations. Indeed, as in displayed in Fig. 3.5, the fluctuating evolution of the Bohm coordinates, very much like for a confined Brownian particle, results compatible with the nearly stationarity of the marginal quantum distribution.

Finally, we consider the results described in this chapter a numerical evidences that the single Bohm trajectory approach is a quantum method that justifies and explains the prediction of conventional Quantum Mechanics, at least for a subsystem interacting with the environment. For the sake of scientific investigation, we hypothesise that the single Bohm trajectory approach is the correct methodology for describing the behaviour of molecular systems and we will investigate the consequences of this assumption in next chapters. The final goal is the full characterisation of this approach and the identification of the the features of predicted molecular motions.

CHAPTER 4

Constants of motion

We have verified through a numerical simulation (see Chap. 3) that the predictions of conventional Quantum Mechanics and those of a single Bohm trajectory are compatible. In particular, if one is interested in the description of a subsystem interacting with the environment, that is the most common case in Chemistry, such a correspondence emerges naturally. The single Bohm trajectory corresponding to the coordinates of the subsystem samples the configuration space according to the square modulus of the wave function. Since we assumed that this method is the correct way for describing the molecular systems, we will investigate in detail its features and its predictions, for instance the case of vibrational motion of molecules during a vibrational transition in Chap. 5. In this chapter, we consider instead a more fundamental issue of the theory. Which are the constants of motion for the evolution of the system state (the set of configuration and wave function)?

In both Classical Mechanics and Quantum Mechanics, the solution of this problem is well known. For instance, in the framework of Classical Mechanics, the time evolution of an isolated system is characterised by constant values of the energy, total linear momentum and total angular momentum [Landau and Lifshitz (1976)]. Similarly, the expectation values of observables corresponding to operators that commute with the Hamiltonian operator are time independent [Cohen-Tannoudji et al. (1977a)]. Therefore, the expectation values of the Hamiltonian operator, total linear momentum operator and total angular momentum operator are conserved over time for an isolated system. We would like to recall that the relevance of the constants of motion, especially in Classical Mechanics, concerns the identification

of constraints that have to be satisfied during the whole time evolution of the system. It is particularly well known the representation of the classical motion on the manifold corresponding to the surface of constant energy that is a subspace of the phase space. A similar dimensional reduction can be performed for each constant of motion.

In the framework of Bohm theory, the problem of recognising the constants of motion arises when the focus shifts from a swarm of trajectories to a single trajectory. Indeed, the ensemble average (on the Bohm configurations ensemble) of every physical quantity is equal to the corresponding expectation value at any time. Consequently, the ensemble averages of the energy, total linear momentum, total angular momentum are constant during the time evolution. However, their value along a single Bohm trajectory is not time independent. Consider, for instance, that the quantum potential is explicitly time dependent. Therefore, by writing the energy of the system as the sum of kinetic energy, potential energy and quantum potential energy, its value is time dependent even if its ensemble average is instead in correspondence with the expectation value of the Hamiltonian operator. In other words, the single Bohm trajectory approach highlights the problem of identifying the constants of motion.

In this chapter we investigate this issue and we propose a self-consistent procedure for defining the constants of motion in the framework of the single Bohm trajectory approach. The basic idea is that of recovering the dynamical equations of Bohm theory (Bohm equation and Schrödinger equation) as a result of a variational problem, i.e., the variational formulation of Bohm theory. In general the variational problem is based on the identification of the stationary point of a suitably defined action functional. Then, by employing the Noether's theorem [Kosmann-Schwarzbach (2010)], one can recognise the constants of motion through the symmetries of the action functional. For the sake of completeness, we recall that in Classical Mechanics the time evolution of the system state can be defined either by solving the Hamilton equations (equations of motion or dynamical equations) or by calculating the stationary point of the action functional (principle of least action) [Arnol'd (1997)]. Albeit the two formulations are equivalent with regard to the dynamical equations, the variational formulation results to be more convenient for the identification of the constants of motion by employing the Noether's theorem. The Noether's theorem establishes a clear correspondence between the symmetries of the action functional and the conserved quantities [Giaquinta and Hildebrandt (1996a,b); Gelfand and Fomin (2000)]. For instance, the classical action function of isolated systems is sym-

metric with respect to time translation, space translation and space rotation. The corresponding constants of motion are respectively the energy, the total linear momentum and the total angular momentum. We mention that there could be further constants of motion that can not be inferred from the Noether's theorem [Lutzky (1979, 1978)]: they are determined by symmetries of the dynamical equations that do not correspond to symmetries of the action functional.

We propose to adopt the same procedure also in the framework of Bohm theory (in its single trajectory approach). Thus, some important issues arise. First of all, it has to be defined an action functional, whose "variables" are both the Bohm trajectory and the wave function. To the best of our knowledge, there is not a similar functional in the Mathematical Physics literature whose variables are both trajectory (time dependent Bohm configuration) and field (wave function). We would like to mention that an action functional whose stationary conditions include a formulation of Bohm equation has been proposed by Holland (2001a,b). However, this variational problem ensures that the formulation of the Bohm equations with a structure similar to the Newton law (see Eq. (2.7)) holds without specifying the time evolution of the wave function (that is known by hypothesis). Therefore, also trajectories that do not satisfy Bohm theory can be predicted depending on the initial conditions: the constraint between the configuration and the velocity is not considered directly. In our framework, the stationary conditions of the functional must be formally equivalent to both the Bohm equation (i.e., Eq. (2.6)) and the Schrödinger equation, in order to guarantee the full equivalence with Bohm theory. In particular, the independence of the Schrödinger equation with respect to the system configuration has to be assured. We tackle these issues in Sec. 4.1. Furthermore, the Noether's theorem has to be modified in order to be applicable to the action functional defined in Sec. 4.1. As a matter of fact, the action functional derived in Sec. 4.1 does not belong to the category of action functionals that are considered with the standard formulation of the Noether's theorem and this calls for a generalisation of a such a theorem which is presented in Sec. 4.2.

Once these issues have been overcome, we use our generalised Noether's theorem to recognise the constants of motion of the Bohm problem. We verify that the time independent expectation values are still conserved quantities also in this framework. Furthermore, we prove that there are no further constants of motion deriving from the single Bohm trajectory and corresponding to the symmetries of our action functional. We would like to emphasise that both the definition of functional and the generalisation of the Noether's theorem are rather technical issues. For this reason,

we present the derivations with the structure of theorems in order to highlight the main result in the statement and to move the details to the proof.

4.1 Variational formulation of Bohm theory

In this section we introudece a suitable functional $J[\bullet]$ of the Bohm trajectory $Q(t)$ and of the wave function $\Psi(q,t)$ in such a way that its stationary conditions are formally equivalent to the differential equations of Eq. (2.9) for the dynamical equations. In other words, the objective of our analysis is the identification of the action functional $J[\Psi, Q]$ such that the pair $\big(Q(t), \Psi(q,t)\big)$ that satisfies the condition

$$\mathrm{d}J[\Psi, Q] = 0, \tag{4.1}$$

is also solution of Eq. (2.9). For the sake of a simple nomenclature, we call hereafter the pair Bohm trajectory and wave function the variational variables, since they are the "variables" of the functional $J[\Psi, Q]$ and the unknown of the variational problem of Eq. (4.1) as well. In this regard, one can interpret the problem of determining the time dependence of configuration $Q(t)$ and wave function $\Psi(q,t)$ such that they satisfy the variational condition Eq. (4.1) as nothing more than a formalisation of solving Eq. (2.9) in terms of a variational problem. For this reason, we refer to the variational problem as the variational formulation of Bohm theory. Broadly speaking, we aim to define the counterpart of the principle of last action (Classical Mechanics) in the framework of Bohm theory: as the solution of Hamilton equations can be determined through the stationary point of the action functional, our purpose is of obtaining the trajectory $Q(t)$ and the wave function $\Psi(q,t)$ in terms of solution of Eq. (4.1).

It has to be emphasised that a variational formulation of conventional Quantum Mechanics leading to the Schrödinger equation has been already defined in the past [Kramer and Saraceno (1981)]. We mention a recent use of it that was aimed to model non linear terms of the Schrödinger equation for the final goal of describing solitons [Abbondandolo and Benci (2002); Benci et al. (2010)]. In the following we recall briefly the variational formulation of Quantum Mechanics, since also the variational formulation of Bohm theory must lead to the Schrödinger equation, besides the Bohm equation.

Let us denote the corresponding action functional as $J_0[R, S]$ with the variational variables specified by means of the polar representation of the wave function $\Psi(q,t)$ through its amplitude $R(q,t)$ and its phase $S(q,t)$. Similarly to what we have

done for specifying the Schrödiger equation as in Eq. (2.3), the wave function has been converted to its polar representation $\Psi(q,t) = R(q,t)e^{\imath S(q,t)/\hbar}$. According to Abbondandolo and Benci (2002), for a given time domain determined by the initial time t_0 and the final time t_1, $J_0[R,S]$ action functional is given as

$$J_0[R,S] = \int_{t_0}^{t_1} \mathrm{d}t \int_{\mathcal{C}} \mathrm{d}q \; \mathcal{L}_0(R, \nabla_k R, S_t, \nabla_k S, q)|_{R=R(q,t),S=S(q,t)} \tag{4.2}$$

with the following Lagrangian density

$$\mathcal{L}_0(R, \nabla_k R, S_t, \nabla_k S, q) = \sum_{k=1}^{n} \frac{\hbar^2}{2m_k} |\nabla_k R|^2 + \left(S_t + \sum_{k=1}^{n} \frac{|\nabla_k S|^2}{2m_k} + V(q) \right) R^2, \tag{4.3}$$

where the subscripts t in S_t denotes the partial derivatives of $S(q,t)$ with respect to the time, $S_t := \partial S(q,t)/\partial t$. This compact notation will be used hereafter. For avoiding undesired complications, we assume a configuration domain $\mathcal{C} = \mathbb{R}^n$ with n the number of degrees of freedom composing the quantum system. By imposing the stationarity condition, $\mathrm{d}J_0[R,S] = 0$, the Schrödinger equation in polar form, i.e., Eq. (2.3), is recovered. We do not prove explicitly that the condition $\mathrm{d}J_0[R,S] = 0$ is equivalent to Eq. (2.3), since it is a common exercise of calculus of variations (see Kramer and Saraceno (1981) and Abbondandolo and Benci (2002) for completeness).

Let us now consider the action functional $J[R,S,Q]$ appropriate for Bohm theory whose state evolution $\big(Q(t), \Psi(q,t)\big)$ is fully specified by Eq. (2.9). As a matter of fact it can be formulated by taking into account that i) it should include the action functional $J_0[R,S]$ leading to dynamical equations for the polar components of the wave function $\big(R(q,t), S(q,t)\big)$, and that ii) there should be a further component denoted as $J_1[S,Q]$ responsible for the evolution of the Bohm coordinates $Q(t)$

$$J[R,S,Q] = J_0[R,S] + \lambda J_1[S,Q]. \tag{4.4}$$

In the above equation, λ can be considered a strength parameter for the contribution of $J_1[S,Q]$ whose meaning will be discussed at the end of this section. By taking into account that $Q(t)$ is a trajectory, for the contribution $J_1[S,Q]$ one expects the action functional of Classical Mechanics with the Lagrangian:

$$\sum_{k=1}^{n} \frac{m_k |\dot{Q}_k(t)|^2}{2} - V(Q(t)) - U(Q(t),t), \tag{4.5}$$

where both the mechanical potential $V(q)$ and the quantum potential $U(q,t)$ of

Eq. (2.4) have to be included in the action functional $J_1[S,Q]$ for the Bohm trajectory. Notice that we use a compact notation also for the time derivative of the trajectory corresponding to the k-th degrees of freedom, i.e., $\dot{Q}_k(t) := \mathrm{d}Q_k(t)/\mathrm{d}t$. Inspired by the expected quantum Hamilton-Jacobi equation (2.3), the potential contributions can be specified according to the partial derivatives of the phase $S(q,t)$ and, therefore, one obtains the following trajectory component of the action functional

$$J_1[S,Q] = \int_{t_0}^{t_1} \mathrm{d}t \left\{ \sum_{k=1}^{n} \frac{m_k |\dot{Q}_k(t)|^2}{2} + S_t(Q(t),t) + \sum_{k=1}^{n} \frac{|\nabla_k S(Q(t),t)|^2}{2m_k} \right\}. \tag{4.6}$$

In the following, we will prove that if the set $\big(R(q,t), S(q,t), Q(t)\big)$ is a solution of the variational problem $\mathrm{d}J[R,S,Q] = 0$, with $J[R,S,Q]$ defined in Eq. (4.4), then it solves also the system of differential equations of Eq. (2.9). In other words, the solution of Eq. (2.9) is an extremal of the functional $J[R,S,Q]$. As anticipated previously, we present the formal derivation as a theorem in order to delineate the essential information in the statement and to leave the details in the proof.

Theorem 1. *Let $J[R,S,Q]$ be the functional defined on the set of functions $\big(R(q,t)$, $S(q,t)$, $Q(t)\big)$ that satisfies specific boundary conditions at t_0 and t_1 $\big(R(q,t_0) = R_0(q)$, $R(q,t_1) = R_1(q)$, $S(q,t_0) = S_0(q)$, $S(q,t_1) = S_1(q)$, $Q(t_0) = Q_0$, $Q(t_1) = Q_1\big)$. Then each extremal of $J[R,S,Q]$ solves the following system of differential equations (Euler-Lagrange equations):*

$$\begin{cases} \dfrac{\partial S(q,t)}{\partial t} + \displaystyle\sum_{k=1}^{n} \frac{|\nabla_k S(q,t)|^2}{2m_k} + V(q) - \sum_{k=1}^{n} \frac{\hbar^2}{2m_k} \frac{\nabla_k^2 R(q,t)}{R(q,t)} = 0 \\ \dfrac{\partial}{\partial t} R(q,t)^2 + \displaystyle\sum_{k=1}^{n} \nabla_k \left(R(q,t)^2 \frac{\nabla_k S(q,t)}{m_k} \right) = 0 \\ m_k \dot{Q}_k(t) = \nabla_k S(q,t)\big|_{q=Q(t)} \qquad \textit{with } k = 1,2,\ldots,n \\ m_k \ddot{Q}_k(t) = -\Big[\nabla_k \big(V(q) + U(q,t) \big) \Big]_{q=Q(t)} \quad \textit{with } k = 1,2,\ldots,n \end{cases} . \tag{4.7}$$

Proof. Let us denote with the set $\big(R(q,t), S(q,t), Q(t)\big)$ an extremal of the functional $J[R,S,Q]$ and with $\big(R(q,t)+r(q,t), S(q,t)+s(q,t), Q(t)+x(t)\big)$ the corresponding variation satisfying the boundary conditions $r(q,t_0) = r(q,t_1) = s(q,t_0) = s(q,t_1) = x(t_0) = x(t_1) = 0$. Furthermore, $R(q,t)$ and $r(q,t)$ as well should vanish at the boundaries of the configuration space $\mathcal{C}$ in order to ensure the integrability of the squared modulus of the wave function in its domain. By definition, the differential

variation of the function should vanish,

$$\mathrm{d}J[R,S,Q]=0, \tag{4.8}$$

for any admissible variations $r(q,t)$, $s(q,t)$, $x(t)=\big(x_1(t),x_2(t),\dots,x_n(t)\big)$. By calculating explicitly the differential variation of Eq. (4.8), one derives the following integral equation

$$\begin{aligned}&\int_{t_0}^{t_1}\mathrm{d}t\int_{\mathbb{R}^{3n}}\mathrm{d}q\,\left\{\sum_{k=1}^{n}\frac{\hbar^2}{m_k}\nabla_k R\nabla_k r+2\bigg(S_t+\sum_{k=1}^{n}\frac{|\nabla_k S|^2}{2m_k}+V\bigg)Rr+\right.\\&\left.+R^2\bigg(s_t+\sum_{k=1}^{n}\frac{\nabla_k S\nabla_k s}{m_k}\bigg)\right\}+\lambda\int_{t_0}^{t_1}\mathrm{d}t\bigg\{\sum_{k=1}^{n}m_k\dot{Q}_k\dot{x}_k+\\&+\sum_{j=1}^{n}\bigg[\nabla_j S_t+\sum_{k=0}^{n}\frac{\nabla_j|\nabla_k S|^2}{2m_k}\bigg]_{q=Q(t)}x_j+\bigg[s_t+\sum_{k=1}^{n}\frac{\nabla_k S}{m_k}\nabla_k s\bigg]_{q=Q(t)}\bigg\}=0,\end{aligned} \tag{4.9}$$

where we have omitted the functional dependence of the variational functions, e.g., $s(q,t)$ is substituted by s and so on, for the sake of a compact notation. Notice that the first and the second integral derive from the differential of the functional $J_0[R,S]$ and the functional $J_1[S,Q]$ respectively. From a suitable integration by part, one can separate the contributions of each variation $r(q,t)$, $s(q,t)$, $x(t)$ of the variational variables:

$$\begin{aligned}&\int_{t_0}^{t_1}\mathrm{d}t\int_{\mathcal{C}}\mathrm{d}q\,\bigg\{-\sum_{k=1}^{n}\frac{\hbar^2}{2m_k}\nabla_k^2 R+\bigg(S_t+\sum_{k=1}^{n}\frac{|\nabla_k S|^2}{2m_k}+V\bigg)R\bigg\}2r+\\&+\int_{t_0}^{t_1}\mathrm{d}t\bigg\{\lambda\sum_{k=1}^{n}\bigg[\bigg(\frac{\nabla_k S}{m_k}-\dot{Q}_k\bigg)\nabla_k s\bigg]_{q=Q(t)}-\int_{\mathcal{C}}\mathrm{d}q\,\bigg[\frac{\partial R^2}{\partial t}+\sum_{k=1}^{n}\nabla_k\bigg(R^2\frac{\nabla_k S_q}{m_k}\bigg)\bigg]s\bigg\}+\\&+\lambda\int_{t_0}^{t_1}\mathrm{d}t\,\sum_{k=1}^{n}\bigg\{-m_k\ddot{Q}_k+\bigg[\nabla_k S_t+\sum_{j=1}^{n}\frac{\nabla_k|\nabla_j S|^2}{2m_k}\bigg]_{q=Q(t)}\bigg\}x_k=0.\end{aligned} \tag{4.10}$$

Since $r(q,t)$, $s(q,t)$, $x(t)$ are independent, the fundamental lemma of calculus of variations ensures that the condition $\mathrm{d}J[R,S,Q]=0$ holds if and only if each integral of Eq. (4.10) vanishes independently. In other words, the condition of Eq. (4.10) is equivalent to the following three constrains:

$$\int_{t_0}^{t_1}\mathrm{d}t\int_{\mathcal{C}}\mathrm{d}q\,\bigg\{-\sum_{k=1}^{n}\frac{\hbar^2}{2m_k}\nabla_k^2 R+\bigg(S_t+\sum_{k=1}^{n}\frac{|\nabla_k S|^2}{2m_k}+V(q)\bigg)R\bigg\}2r=0, \tag{4.11}$$

$$\int_{t_0}^{t_1} \mathrm{d}t \left\{ \lambda \sum_{k=1}^{n} \left[\left(\frac{\nabla_k S}{m_k} - \dot{Q}_k \right) \nabla_k s \right]_{q=Q(t)} - \int_{\mathcal{C}} \mathrm{d}q \left[\frac{\partial R^2}{\partial t} + \sum_{k=1}^{n} \nabla_k \left(R^2 \frac{\nabla_k S_q}{m_k} \right) \right] s \right\} = 0, \tag{4.12}$$

$$\int_{t_0}^{t_1} \mathrm{d}t \ \sum_{k=1}^{n} \left\{ -m_k \ddot{Q}_k + \left[\nabla_k S_t + \sum_{j=1}^{n} \frac{\nabla_k |\nabla_j S|^2}{2m_k} \right]_{q=Q(t)} \right\} x_k = 0. \tag{4.13}$$

Let us consider Eq. (4.11) that has to hold for any admissible variation $r(q,t)$, i.e., any $r(q,t)$ that satisfies the boundary conditions. This implies that

$$-\sum_{k=1}^{n} \frac{\hbar^2}{2m_k} \nabla_k^2 R(q,t) + \left(S_t(q,t) + \frac{|\nabla_k S(q,t)|^2}{2m_k} + V(q) \right) R(q,t) = 0, \tag{4.14}$$

in all the space-time points of the integration domain, $\mathcal{D} = \{(q,t) \text{ with } q \in \mathcal{C},\ t \in [t_0, t_1]\}$, for the fundamental lemma of calculus of variation. On the other hand, Eq. (4.14) is precisely the quantum Hamilton-Jacobi equation corresponding to the first equation of Eq. (4.7).

Let us analyse the implications of the constraint of Eq. (4.12) which is specified as a time integral of two different contributions. The first one is proportional to the strength parameter λ and depends on the filed $S(q,t)$ and $s(q,t)$ evaluated only along the trajectory path, $q = Q(t)$. The second one is specified as an integral on all the configuration domain $\mathcal{C}$. The first contribution is further separated in the sum of terms that are proportional to the gradient $\nabla_k s(q,t)$ respectively and evaluated along the trajectory $Q(t)$, that is the set of points $(q,t) \in \mathcal{C}$ that belong to the subdomain $\mathcal{C}_Q = \left\{ \big(Q(t), t\big) \in \mathcal{C},\ \forall t \in [t_0, t_1] \right\}$. Since the integral must vanish for all the admissible variations $s(q,t)$, this must be true also for the subset of variations whose spatial derivative $\nabla_k s(q,t) = 0$ for all $(q,t) \in \mathcal{C}_Q$ and $\forall k$. Correspondingly, the first contribution vanishes and one has to consider only the second one which should vanish for any $s(q,t)$ of such a particular type of variations, leading to the following condition of stationarity

$$\frac{\partial R(q,t)^2}{\partial t} + \sum_{k=1}^{n} \nabla_k \left(R(q,t)^2 \frac{\nabla_k S_q(q,t)}{m_k} \right) = 0, \tag{4.15}$$

that is the second equation of Eq. (4.7). Notice that such an equation holds in all the points of $\mathcal{C}$, those of $\mathcal{C}_Q$ included. Indeed, the vanishing of the spatial derivatives $\nabla_k s(q,t)$ in $\mathcal{C}_Q$ does not require a corresponding vanishing of $s(q,t)$ at the same points, so that also in $\mathcal{C}_Q$ the square bracket term multiplying $s(q,t)$ must vanish. Then, one can take for granted the condition of Eq. (4.15) so that the second

contribution in Eq. (4.12) is lacking, and considers now the most general variation $s(q,t)$ with non vanishing gradient $\nabla_k s(q,t)$ in $\mathcal{C}_Q$. In order to ensure the validity of Eq. (4.12), the vanishing of the first contribution for any choice of the gradient $\nabla_k s(q,t)$ in $\mathcal{C}_Q$ has to be imposed, so deriving the third equation of Eq. (4.7):

$$m_k \dot{Q}_k(t) - \nabla_k S\big(Q(t),t\big) = 0, \qquad \text{with } k = 1,2,\ldots,n. \tag{4.16}$$

In order to visualise a simple exemplification of such a variation, let us consider a set of arbitrary functions $h_k : [t_0,t_1] \to \mathbb{R}$ such that $h_k(t_0) = h_k(t_1) = 0$ and the variation specified as $s(q,t) \equiv q_k h_k(t)$ leads to an arbitrary time dependent gradient $\nabla_k s(q,t) = h_k(t)$ (and $\nabla_j s(q,t) = 0$ if $j \neq k$). It is then clear that the term $\nabla_k S/m_k - \dot{Q}_k$ multipling $\nabla_k s$ must vanish for all integration times in agreement with Eq. (4.16).

Finally, we analyse Eq. (4.13). In order to ensure that the integral vanishes for every admissible variation $x(t)$, the following set of conditions for every k must hold

$$m\ddot{Q}_k(t) = \left[\nabla_k\left(S_t(q,t) + \sum_{j=1}^{n} \frac{|\nabla_j S(q,t)|^2}{2m_j}\right)\right]_{q=Q(t)} = -\left[\nabla_k\big(V(q)+U(q,t)\big)\right]_{q=Q(t)}, \tag{4.17}$$

where the last equality holds because of Eq. (4.14).

In this ways, it has been verified that if the set $\big(R(q,t),S(q,t),Q(t)\big)$ is a stationary point of $J[R,S,Q]$, then it is satisfies also the equations (4.14), (4.15), (4.16) and (4.17). □

Theorem 1 proves that the time evolution of the quantum state in the framework of the single Bohm trajectory $\big(Q(t),\Psi(q,t)\big)$ can be determined by solving the variational problem of Eq. (4.8), with the polar representation $\Psi(q,t) = R(q,t)e^{\imath S(q,t)/\hbar}$ of the wave function. In other words, we succeed in defining a variational formulation of Bohm theory by employing the action functional $J[R,S,Q] = J_0[R,S] + \lambda J_1[S,Q]$ having the Schrödinger component $J_0[R,S]$ of Eq. (4.2) and the trajectory component $J_1[S,Q]$ of Eq. (4.6).

At this stage we would like to emphasise three features of this variational formulation of Bohm theory. First of all, the time evolution of $\big(Q(t),\Psi(q,t)\big)$ is determined by a set of three differential equations if the wave function is converted to its polar form: the Bohm equation and the system of differential equations in Eq. (2.3). On the other hand, Theorem 1 establishes that the condition of Eq. (4.8) is equivalent to a system of four differential equations (see Eq. (4.7)). As a matter of fact, the

fourth equation in Eq. (4.7) does not provide any further conditions: once the trajectory $Q(t)$ satisfies Eq. (4.16), then Eq. (4.17) holds automatically because of the quantum Hamilton-Jacobi equation.

Secondly, the stationary condition of Eq. (4.8) leads to the correct time evolution equations Eq. (4.7) independently of the value of the strength parameter λ used in the definition of $J[R, S, Q]$ (see Eq. (4.4)), with the only limitation of a non vanishing value, $\lambda \neq 0$. In other words, the Euler-Lagrange equations of the functional $J[R, S, Q]$ are the set of the Euler-Lagrange equations corresponding to each functional J_0 and J_1 independently. Therefore each element of the one parameter family of functionals,

$$J_\lambda[R, S, Q] \equiv J_0[R, S] + \lambda J_1[S, Q] \tag{4.18}$$

where $\lambda \in \mathbb{R} \setminus \{0\}$, has the same extremal, that is the solution of Eq. (4.7). Notice that we add the subscript λ to the overall functional in order to stress the parametric dependence on λ. To the best of our knowledge, this feature is uncommon in variational problems and it induces an arbitrariness on the choice of the element of the family J_λ for describing a system according to Bohm theory. However, the arbitrariness of the parameter λ is the essential feature that ensures the independence of the wave function with respect to the Bohm trajectory in the variational framework: the same pair $\big(R(q,t), S(q,t)\big)$ which is extremal of $J_0[R, S]$, is also extremal of the overall functionals $J_\lambda[R, S, Q]$ independently of the values of λ. As matter of fact, a functional without these features does not conserve the Euler-Lagrange equations of the functional $J_0[R, S]$. Such unconventional feature of the action functional has consequences also for the identification of the constants of motion as we will describe in Sec. 4.2.

Finally, it should be stressed that the functional $J_1[S, Q]$ can be written in a full field theory format, analogous to the one of the functional $J_0[R, S]$ of Eq. (4.2), by specifying it as

$$J_1[S, Q] = \int_{t_0}^{t_1} \mathrm{d}t \int_{\mathcal{C}} \mathrm{d}q \; \delta(q - Q(t)) \; \mathcal{L}_1\big(\dot{Q}, S_t, \nabla_k S\big)\big|_{Q=Q(t), S=S(q,t)}, \tag{4.19}$$

where the Lagrangian density $\mathcal{L}_1\big(\dot{Q}, S_t, \nabla_k S\big)$ is recovered from Eq. (4.6) by specifying the action of the Dirac delta function:

$$\mathcal{L}_1\big(\dot{Q}, S_t, \nabla_k S\big) = \sum_{k=1}^{n} \frac{m_k |\dot{Q}_k|^2}{2} + S_t + \sum_{k=1}^{n} \frac{|\nabla_k S|^2}{2m_k}. \tag{4.20}$$

This notation will be convenient in Sec. 4.2 in order to simplify the derivation of the constants of motion through a suitable generalisation of the Noether's theorem.

4.2 Generalised Noether's theorem

As it has been recalled in the introduction of this chapter, the variational formulation of a dynamical system, e.g., of Classical Mechanics, Quantum Mechanics and Bohm theory, allows the identification of the constants of motion by employing the Noether's theorem [Giaquinta and Hildebrandt (1996a,b); Gelfand and Fomin (2000)]. The theorem correlates the symmetries of the action functional $J[\bullet]$ (also called Noether symmetries) to the conserved quantities which we denote as I. Even if there are constants of motion that do not correspond to Noether symmetries [Lutzky (1979, 1978)], the theorem has been extensively used in the framework of Classical Mechanics [Arnol'd (1997)] and Field Theory [Folland (2008)]. For this reason it is considered a common methodology and conserved quantities are often identified with their corresponding symmetries. For instance the energy, total linear momentum and total angular momentum of isolated systems are linked to the invariances of the action functional respectively under time translation, space translation and space rotation. In the following, we derive the constants of motion in the framework of Bohm theory through the use of the Noether's theorem. First of all, it has to be considered that some features of the functionals belonging to the family $J_\lambda[R, S, Q]$ do not allow us to use directly the standard formulation of the Noether's theorem. The definition of the functional $J_1[S, Q]$ includes partial derivatives of the variational variable $S(q, t)$ that depend on the variational variable $Q(t)$ through $S_t\big(Q(t), t\big)$ and $\nabla_k S\big(Q(t), t\big)$. This feature is not taken into account in the standard formulation of the Noether's theorem, and consequently the theorem has to be properly generalised. Then, we employ the modified version of the Noether's theorem for discussing the constants of motion corresponding to a particular set of transformations, such as time translation, space translation and space rotation, that leave the action functional unchanged in the case of isolated systems. Notice that each functional of the family $J_\lambda[R, S, Q]$ is symmetric with respect to time translation, whereas reasonable assumptions regarding the potential $V(q)$ have to be made in order to ensure that also the others two transformations leave the action functional unchanged.

However, one can anticipate some properties of the constants of motion before a formal generalisation of the Noether's theorem has been established. This can be done by taking into account that i) the functional $J_0[R, S]$ leads to the Schrödinger

equation independently of the Bohm equation and ii) the Euler-Lagrange equations are the same for every functional of the λ-dependent family $J_\lambda[R, S, Q]$. Therefore the conserved quantities determined by the wave function evolution have to be time independent also in the framework of Bohm theory since the wave function does not depend on the Bohm trajectory. The expectation values of operators that commute with the Hamiltonian operator are still time independent also in the framework of Bohm theory, and they are derived on the basis of the symmetries of the functional $J_0[R, S]$. Let us suppose now that these constants of motion correspond also to symmetries of the complete functional $J_\lambda[R, S, Q]$. This is the case if both the functionals $J_0[R, S]$ and $J_1[S, Q]$ are independently symmetric. In this way one identifies a first category of conserved quantities due to symmetries of both the functionals $J_0[R, S]$ and $J_1[S, Q]$.

In principle one might consider a second category of conserved quantities that could derive from transformations that do not modify only a particular functional $J_\lambda[R, S, Q]$ of the family for a given value of the parameter λ. In this case, the two functionals $J_0[R, S]$ and $J_1[S, Q]$ are not independently symmetric under these transformations. Then, the elements of this category are λ-dependent and they can not be identified as true constants of motion. Indeed, the dynamical equations (Eq. (4.7)) derived according to the variational problem are independent of the value of the strenght parameter λ, and therefore the conserved quantities during the time evolution of $\big(Q(t), \Psi(q, t)\big)$ can not be λ-dependent.

For this reason, we will investigate only transformations that leave both the functionals $J_0[R, S]$ and $J_1[S, Q]$ unchanged and the corresponding constants of motion. For each symmetry of $J_0[R, S]$ and $J_1[S, Q]$, one can define the conserved quantity I_0 that is specified by the time evolution of the wave function: it is a time independent expectation value. Furthermore, the quantity I_0 is recovered by applying the standard formulation of the Noether's theorem to the functional $J_0[R, S]$. Since such a procedure represents a standard application of the Noether's theorem, it is not reported in this thesis and it can be found in Giaquinta and Hildebrandt (1996a,b) and Gelfand and Fomin (2000).

The real challenge concerns the identification of the constants of motion I_1 resulting from the functional $J_1[S, Q]$. If they exist, one would get unconventional constants of motion specified on the basis of the system configuration $Q(t)$ along a Bohm trajectory. However, as we mentioned in advance, the Noether's theorem, in its standard formulation, can not be applied to the functional $J_1[S, Q]$. Therefore, we derive a generalised version of the theorem that takes into account also

the particular features of our functional. In this way, we propose a self-consistent methodology for the identification of the corresponding conserved quantities I_1.

Similarly to the standard derivation of the Noether's theorem, we consider an one parameter group of transformations

$$\begin{cases} \tilde{t} = \mathcal{V}_0(t;\epsilon) \\ \tilde{q}_k = \mathcal{V}_k(q,t;\epsilon) \text{ with } k = 1,2,\ldots,n \\ \tilde{S}\left(\tilde{q},\tilde{t}\right)\big|_{\tilde{q}=\mathcal{V},\ \tilde{t}=\mathcal{V}_0} = \mathscr{S}(q,t;\epsilon) \\ \tilde{Q}_k\left(\tilde{t}\right)\big|_{\tilde{t}=\mathcal{V}_0} = \mathcal{X}_k(t;\epsilon) \text{ with } k = 1,2,\ldots,n \end{cases} \tag{4.21}$$

that by hypothesis leaves $J_1[S,Q]$ unchanged. In Eq. (4.21) the functions $\mathcal{V}_0(t,\epsilon)$, $\mathcal{V}(q,t;\epsilon) = \left(\mathcal{V}_1,\mathcal{V}_2,\ldots,\mathcal{V}_n\right)$, $\mathscr{S}(q,t;\epsilon)$ and $\mathcal{X}(t;\epsilon) = \left(\mathcal{X}_1,\mathcal{X}_2,\ldots,\mathcal{X}_n\right)$ are the maps that represent the transformation. They depend smoothly on the parameter ϵ and they correspond to the identity transformation if $\epsilon = 0$. Notice that the functions $\mathcal{X}_k(t;\epsilon)$ do not depend on the variables q since they represent the transformation of a variational variable, the trajectory of the Bohm coordinates, that depends only on time. Furthermore, the infinitesimal generators of the above transformation are defined according to the following equations,

$$\begin{aligned} v_0(t) &= \left.\frac{\partial \mathcal{V}_0(t;\epsilon)}{\partial\epsilon}\right|_{\epsilon=0}, \qquad & v_k(q,t) &= \left.\frac{\partial \mathcal{V}_k(q,t;\epsilon)}{\partial\epsilon}\right|_{\epsilon=0}, \\ s(q,t) &= \left.\frac{\partial \mathscr{S}(q,t;\epsilon)}{\partial\epsilon}\right|_{\epsilon=0}, \qquad & x_k(t) &= \left.\frac{\partial \mathcal{X}_k(t;\epsilon)}{\partial\epsilon}\right|_{\epsilon=0}. \end{aligned} \tag{4.22}$$

Furthermore, we restrict the possible transformations by imposing the following constraint:

$$\sum_{k=1}^{n} \nabla_k v_k(q,t) = 0. \tag{4.23}$$

In this way, the infinitesimal generator $v(q,t) = (v_1, v_2, \ldots, v_n)$ is a solenoidal vector field that can not represent neither compression or expansion of the space of configurations. It should be emphasised that Eq. (4.23) holds for the common transformations, such as time translation, space translation and space rotation. Consequently, our method still represents an efficient and self-consistent way for investigating the problem of conservations during the Bohm dynamics.

Moreover, it has to be stressed that the infinitesimal generators of Eq. (4.22), $s(q,t)$ and $x(t)$, have not to be confused with the variations of Eq. (4.8), even if they are tagged with the same symbols. Since they are employed in a different framework and with different meanings, misunderstandings should be avoided.

Finally, our formulation of the Noether's theorem is proven in the following for transformations as those of Eq. (4.21) under the constraint of Eq. (4.23). We employ the functional of $J_1[S,Q]$ as specified in Eq. (4.19) in order to reduce as much as possible the differences between our procedure and the standard derivation of the Noether's theorem. In the statement of Theorem 2 and in the proof as well, for the sake of a concise notation, we omit the functional dependence of $\mathcal{L}_1$ and of its partial derivatives, which should conform to that of Eq. (4.19) and Eq. (4.20).

Theorem 2. *Let us suppose that the functional $J_1[S,Q]$ is invariant with respect to the one parameter group of transformations, which have infinitesimal generators $s(q,t)$, $x_k(q,t)$, $v_0(t)$ and $v_k(q,t)$ such that $\sum_k \nabla_k v_k = 0$. Then for every extremal $\big(S(q,t),Q(t)\big)$ of the functional $J_1[S,Q]$, the configurational integral I_1,*

$$I_1 = \int_{\mathcal{C}} \mathrm{d}q\ \delta(q-Q(t))\left[\mathcal{L}_1 v_0 + \frac{\partial \mathcal{L}_1}{\partial S_t}\overline{s} + \sum_{k=1}^{n}\frac{\partial \mathcal{L}_1}{\partial \dot{Q}_k}\overline{x}_k\right], \tag{4.24}$$

where

$$\overline{s} = s - S_t v_0 - \sum_{k=1}^{n}\nabla_k S\ v_k, \qquad\qquad \overline{x}_k = x_k - \dot{Q}_k v_0, \tag{4.25}$$

is time independent:

$$\frac{\mathrm{d}}{\mathrm{d}t} I_1 = 0. \tag{4.26}$$

Proof. By Proposition 2, the transformed functional $\tilde{J}_1\big[\tilde{S},\tilde{Q}\big]$ is independent of the parameter ϵ and therefore:

$$\left.\frac{\mathrm{d}\tilde{J}_1\big[\tilde{S},\tilde{Q}\big]}{\mathrm{d}\epsilon}\right|_{\epsilon=0} = 0. \tag{4.27}$$

By specifying the transformation according to Eq. (4.21) and repeating the mathematical manipulations of the standard proof of the Noehter's theorem, the functional derivative of Eq. (4.27) becomes

$$\begin{aligned}\left.\frac{\mathrm{d}\tilde{J}_1\big[\tilde{S},\tilde{Q}\big]}{\mathrm{d}\epsilon}\right|_{\epsilon=0} = \int_{t_0}^{t_1}\mathrm{d}t\int_{\mathcal{C}}\mathrm{d}q\ \delta(q-Q(t))\Bigg\{&\frac{\mathrm{d}}{\mathrm{d}t}\left[\mathcal{L}_1 v_0 + \frac{\partial \mathcal{L}_1}{\partial S_t}\overline{s} + \sum_{k=1}^{n}\frac{\partial \mathcal{L}_1}{\partial \dot{Q}_k}\overline{x}_k\right] + \\ &+ \sum_{k=1}^{n}\nabla_k\left[\mathcal{L}_1 v_k + \frac{\partial \mathcal{L}_1}{\partial \nabla_k S}\overline{s}\right] - \left[\frac{\mathrm{d}}{\mathrm{d}t}\frac{\partial \mathcal{L}_1}{\partial S_t}\overline{s} + \sum_{k=1}^{n}\nabla_k\frac{\partial \mathcal{L}_1}{\partial \nabla_k S}\overline{s} + \sum_{k=1}^{n}\frac{\mathrm{d}}{\mathrm{d}t}\frac{\partial \mathcal{L}}{\partial \dot{Q}_k}\overline{x}_k\right] + \\ &+ \sum_{k=1}^{n}\Big(\overline{x}_k + \dot{Q}_k v_0 - v_k\Big)\nabla_k \mathcal{L}_1\Bigg\}\end{aligned} \tag{4.28}$$

where the term in the third line derives from the derivative $\mathrm{d}/\mathrm{d}\epsilon$ of the Dirac delta function $\delta\big(\tilde{q}-\tilde{Q}(t)\big)$ and it is the main difference with respect to the standard procedure. For further elaboration, it is convenient to integrate by parts the time derivative according to the following relation

$$\begin{aligned}
&\int_{t_0}^{t_1}\mathrm{d}t\int_{\mathcal{C}}\mathrm{d}q\;\delta(q-Q(t))\left\{\frac{\mathrm{d}}{\mathrm{d}t}\left[\mathcal{L}_1 v_0+\frac{\partial\mathcal{L}_1}{\partial S_t}\overline{s}+\sum_{k=1}^{n}\frac{\partial\mathcal{L}_1}{\partial\dot{Q}_k}\overline{x}_k\right]\right\}=\\
&=\int_{t_0}^{t_1}\mathrm{d}t\int_{\mathcal{C}}\mathrm{d}q\;\frac{\mathrm{d}}{\mathrm{d}t}\left\{\delta(q-Q(t))\left[\mathcal{L}_1 v_0+\frac{\partial\mathcal{L}_1}{\partial S_t}\overline{s}+\sum_{k=1}^{n}\frac{\partial\mathcal{L}_1}{\partial\dot{Q}_k}\overline{x}_k\right]\right\}+\\
&-\int_{t_0}^{t_1}\mathrm{d}t\int_{\mathcal{C}}\mathrm{d}q\;\delta(q-Q(t))\left\{\sum_{k=1}^{n}\dot{Q}_k(t)\nabla_k\left[\mathcal{L}_1 v_0+\frac{\partial\mathcal{L}_1}{\partial S_t}\overline{s}\right]\right\}.
\end{aligned}\tag{4.29}$$

The restriction of the admissible transformations (Eq. (4.23)) allows one to verify the following relation

$$\sum_{k=1}^{n}\Big\{\nabla_k\big[\mathcal{L}_1 v_k\big]-v_k\nabla_k\mathcal{L}_1\Big\}=0.\tag{4.30}$$

Equation (4.30), together with the hypothesis that $\big(S(q,t),Q(t)\big)$ is an extremal of $J_1[S,Q]$ (i.e., $S(q,t)$ and $Q(t)$ satisfy the equations of (4.23)), and the q independence of v_0, leads the sum of i) the second integral in the r.h.s. of Eq. (4.29) and ii) the contributions to $\mathrm{d}\tilde{J}_1/\mathrm{d}\epsilon$ which are reported in the second and the third lines of Eq. (4.28) to the vanishing. The final result for the derivative of the functional is

$$\left.\frac{\mathrm{d}\tilde{J}_1\big[\tilde{S},\tilde{Q}\big]}{\mathrm{d}\epsilon}\right|_{\epsilon=0}=\int_{t_0}^{t_1}\mathrm{d}t\;\frac{\mathrm{d}}{\mathrm{d}t}\int_{\mathcal{C}}\mathrm{d}q\left\{\delta(q-Q(t))\left[\mathcal{L}_1 v_0+\frac{\partial\mathcal{L}_1}{\partial S_t}\overline{s}+\sum_{k=1}^{n}\frac{\partial\mathcal{L}_1}{\partial\dot{Q}_k}\overline{x}_k\right]\right\}.\tag{4.31}$$

Since by hypothesis, such a functional derivative should vanish for any arbitrary time interval, one verifies that the configurational integral I_1 of Eq. (4.24) is a constant of motion. □

Once the generalised formulation of the Noether's theorem has been proven, one can identify the conserved quantities in the framework of Bohm theory. The first step concerns the identification of the symmetries shared by $J_0[R,S]$ and $J_1[S,Q]$. Then by using the standard formulation of the Noether's theorem for fields like in the treatment of Benci (2009), one can recognise the constants of motion

$$I_0=\int_{\mathcal{C}}\mathrm{d}q\;\left\{\mathcal{L}_0 v_0+\frac{\partial\mathcal{L}_0}{\partial S_t}\overline{s}\right\}.\tag{4.32}$$

arising form $J_0[R,S]$. Finally, Theorem 2 allows the identification of the constants of motion corresponding to the evolution of the Bohm coordinates. By employing the definitions of $\mathcal{L}_1\big(\dot{Q},S_t,\nabla_k S\big)$, $\overline{s}(q,t)$ and $\overline{x}_k(t)$, the configuration integral of Eq. (4.24) can be evaluated, so recovering the following explicit form for the constants of motion:

$$I_1 = s(Q(t),t) + \sum_{k=1}^{n} m_k \dot{Q}(t)\Big(x_k(t) - v_k\big(Q(t),t\big)\Big). \tag{4.33}$$

At this stage we take into account some common transformations, i.e., time translation, space translation and space rotation, in order to discuss the corresponding conserved quantities. After a brief summary concerning the quantity I_0, simple considerations will allow us to recognise that no constants of motion correspond to the symmetries of our action functional as regards the evolution of the Bohm coordinates.

4.2.1 Constants of motion for isolated systems

In this subsection, we consider explicitly the constants of motion I_0 of Eq. (4.32) and I_1 of Eq. (4.33) for isolated systems. In particular we refer to the time translation, space translation and space rotation since they satisfy the constraint of Eq. (4.23). On the one hand, one can easily prove that both the functionals are left invariant with respect to time translation. On the other hand, $J_0[R,S]$ is invariant under space translation and rotation if the potential $V(q)$ has the same symmetries. As a matter of fact, molecular system are considered as an ensemble of particles whose interactions are described by a potential that depends only on the distance between the particles. In this case, space translations and rotations leave this kind of potential unchanged. It has to be emphasised that this in the natural condition of isolated systems.

As regards the wave function dynamics described according to the functional $J_0[R,S]$, it is well known that the expectation values of the Hamiltonian operator, total linear momentum operator, and total angular momentum operator are conserved. By using the definition of I_0 in Eq. (4.32) it can be formally verified that the constants of motion corresponding to the time translation, space translation, space rotation are specified by the following expectation values

$$\langle\Psi(t)|\hat{H}|\Psi(t)\rangle\,, \qquad \langle\Psi(t)|\hat{P}_\gamma|\Psi(t)\rangle\,, \qquad \langle\Psi(t)|\hat{L}_\gamma|\Psi(t)\rangle\,, \tag{4.34}$$

where $\hat{P}_\gamma$ and $\hat{L}_\gamma$ for $\gamma = (x, y, z)$ are the cartesian components of the total linear momentum operator and the total angular momentum operator respectively. Since the procedure for proving such a result is rather straightforward once each transformation is represented according to Eq. (4.21), it is not reported here. For more details, one could examine the the work of Benci (2009).

As regards the Bohm trajectory, the infinitesimal generators for these three transformations are characterised by the following conditions:

$$s\big(Q(t), t\big) = 0, \tag{4.35}$$

$$x_k(t) = v_k\big(Q(t), t\big), \tag{4.36}$$

for any time t. Equation (4.35) holds because we are not examining a transformation of the variational variable $S(q, t)$, but only of time and space. Furthermore, the infinitesimal generators x_k and v_k have to be the same because the Bohm coordinates must transform as the configuration space (Eq. (4.36)). Under these conditions, the constants of motion corresponding to the Bohm trajectory, that is I_1 of Eq. (4.33), vanish

$$I_1 = 0, \tag{4.37}$$

for any of the previously mentioned transformations.

This result implies that these important symmetries do not correspond to any constant of motion for the evolution of the Bohm coordinates, whereas they lead to the time independence of well defined expectation values as regards the wave function evolution.

4.3 Final remarks

In this chapter, we have investigated the constants of motion during the time evolution of a quantum system according to the single Bohm trajectory approach. To this aim, we have developed a variational formulation of Bohm theory and we have employed the Noether's theorem (both the standard formulation and a generalisation proven by us) in order to correlate the constants of motion to the symmetries of the system and of the action functional. It has to be emphasised that the existence of a variational formulation of Bohm theory was not known and we succeeded in defining the suitable action functional. Furthermore, we have verified that the time independent expectation values are still conserved quantities also in the framework of Bohm theory, since the wave function is independent of the Bohm trajectory. On

the other hand, no constants of motion are determined by the symmetries of our action functional associated to the Bohm coordinates. In conclusion, the Noether's theorem does not allow the identification of conserved quantities during the time evolution of the Bohm coordinates.

CHAPTER 5

Single molecule vibrations

Despite the undeniable advantage of Bohm theory to describe the molecular motion in a quantum framework, it is still little known in Chemistry. To the best of our knowledge, only few attempts of representing the electronic motion in atoms through quantum trajectories are reported in literature [Colijn and Vrscay (2004, 2002, 2003)], in addition to the studies of wave packet dynamics as models of reactivity pathways [Zhang (1999); Wyatt and Zhang (1996)]. Therefore, questions like "which is the motion of a molecule?" or "what is it happening to a molecule during a transition between two quantum states?" have not received any answer yet. One can easily predict the average motion by employing the configurations ensemble: since the average value of a coordinate at time t corresponding to a particular degree of freedom q_j is equal to its expectation value by Eq. (2.12) with $B(\hat{q}) = \hat{q}_j$, it can be computed by standard methods. However, this simple approach is too limited and does not exploit completely the potentialities of Bohm theory: it does not supply any kind of information about the behaviour of a molecule in a single system realisation, with a particular initial configuration. In other words, the characterisation of the molecular motion based on a single Bohm trajectory is totally absent in literature. Its importance lies on the common idea that the atomic components (nuclei) of molecules have precise spatial positions.

Therefore, the characterisation of the molecular motion with the single Bohm trajectory approach is extremely worthwhile in Chemistry because of the possibility to develop new paradigms about the molecular behaviour that do not rely on Classical Mechanics. Consider for example the molecular vibrations: by employing the model

of the harmonic oscillator, chemists are brought to explain the zero-point energy in terms of residual motion also at the temperature of the absolute zero. However, this interpretation is totally unjustified by Quantum Mechanics: the nuclei motion is indescribable in Quantum Mechanics since the time evolution of the nuclear positions is unpredictable. Only by using Classical Mechanics, that takes into account the instantaneous positions, the non-zero expectation values of the kinetic energy and the total energy can be interpreted as evidences of the underlying movement, i.e., the molecular vibration. However, the single Bohm trajectory approach allows a check of this interpretation in the framework of a pure quantum theory of motion.

For this purpose, the examination of the motion of a single isolated molecule can be useful. Even if the common chemical systems are composed of a number of molecules of the order of an Avogadro's number, the properties of single molecules or even single atoms predicted by Quantum Mechanics (through common *ab initio* calculations) have been widely employed to interpret, describe and predict the properties, including the reactivity, of complex chemical systems [Schatz and Ratner (2002); Jensen (2013); Szabo and Ostlund (2012)].

The same idea can be adopted for Bohm theory by investigating the molecular behaviour in simple cases of chemical interest, such as a single isolated molecule. In particular we examine the vibrational motion. If the vibrational degrees of freedom are well described by the corresponding ground state, the vibrational coordinates are unexpectedly at rest: all the nuclei are motionless (as it will be examined with more details in Sec. 5.1). It is obvious the great difference between this prediction and our image about the molecular behaviour. Nevertheless, the absence of molecular vibrations for a molecule in the ground state is exactly the Bohm prediction unlike what is expected by employing a classical interpretation of the zero-point energy: the idea of a residual motion due to the zero-point energy can be justified only in the framework of Classical Mechanics, by interpreting the non zero kinetic energy as the evidence of underlying moving particles. On the other hand, the ground state corresponds to the condition of a molecule at the temperature of the absolute zero, i.e., a "frozen" molecule, that can be easily imagined with static nuclei independently of the zero-point energy. In order to "defrost" the molecule, a vibrational transition induced by an external electric field can be employed. It can be shown that, once the molecule is excited, it vibrates and the vibration is conserved in time.

In this chapter the vibrational motion induced by an external field will be examined and described according to the single Bohm trajectory approach. This example has to be considered as the first attempt of describing the molecular motion, i.e., the

time dependence of the vibrational coordinates of a single molecule, in the framework of a quantum theory. In particular, we aim to supply an "incisive" representation of this phenomenon in order to push the boundaries of the quantum trajectory description by including the spectroscopic information. In other words, we would like to answer this question: what is happening to the molecular system throughout the experiment in terms of molecular motion? The focus of our attention will be on the nuclear motion for its importance concerning the reactivity of molecules: a reaction is the movement of some nuclei from a molecule to another by definition. First of all, we present the general methodology employed to correlate the features of an external field to the motion predicted according to Bohm theory in Sec. 5.1 and a simple example in Sec. 5.2. Secondly, the method will be used to describe the motion corresponding to the vibrational transition of diatomic and polyatomic molecules in terms of a single Bohm trajectory in Sec 5.3. In order to examine the motion of molecules some approximations have to be imposed. In particular, we employ a simplified representation of the eigenstates of the molecular Hamiltonian. For this reason, also the predicted motion will be a accurate representation of the real one, but it should conserve the main features according to the rationality of the approximations. Finally, it has to be emphasised that our methodology is not only helpful for describing the molecular motion, but also for highlighting some unexpected behaviours.

5.1 Perturbation approaches for the Bohm trajectory

It is well known that approximated methods, such as perturbation methods, were developed in the last century in order to describe the wave function dynamics when the quantum system is interacting with external fields. [Cohen-Tannoudji et al. (1977b)]. In the following, we present a quite straightforward way to transfer the effects of the external field from the wave function to the Bohm trajectory. We would like to emphasise that our approach is the first attempt of representing the molecular motion of perturbed quantum systems with Bohm theory.

The problem of describing the motion of a single molecule in terms of a Bohm trajectory and in the presence of an external field can be formulated as in the following. If the dynamics of the Bohm quantum state $\big(Q(t), \Psi(q,t)\big)$ induced by the zeroth-order Hamiltonian $\hat{H}^{(0)}$ (molecular Hamiltonian) is known, how does the trajectory change if the total Hamiltonian,

$$\hat{H} = \hat{H}^{(0)} + \lambda \hat{H}^{(1)}(t), \tag{5.1}$$

is the sum of two contributions $\hat{H}^{(0)}$ and $\hat{H}^{(1)}(t)$? The Hamiltonian $\hat{H}^{(1)}(t)$ is time dependent unlike the time independent zeroth-order one $\hat{H}^{(0)}$ and it describes formally the interaction with the external field. The parameter λ is usually set to unity, but it can be employed to define contributions of different orders due to the external Hamiltonian $\hat{H}^{(1)}(t)$ to the wave function.

Furthermore, we will focus on a chemically significant case: the dynamics of a system interacting with a sinusoidal resonant perturbation, i.e, an oscillating electric field, that is represented by the Hamiltonian operator

$$\hat{H}^{(1)}(t) = \hat{W}\sin(\omega t)\Theta(t), \tag{5.2}$$

where $\Theta(t)$ is the step function that ensures the introduction of the perturbation for $t > 0$; ω is the frequency of the external oscillanting field; $\hat{W}$ operator is specifying according to the dipole moment operator $\hat{\mu}$ multiplied by the amplitude of the electric field, $\hat{W} = -\hat{\mu}\mathcal{E}$. Usually the effect of this perturbation is interpreted as the transition between a pair of zeroth-order eigenstates having an energy difference ΔE satisfying the resonance constraint, $\Delta E = \omega\hbar$. Additionally, only the transition from the zeroth-order ground state $|\varphi_g\rangle$ $\left(\hat{H}^{(0)}|\varphi_g\rangle = E_g|\varphi_g\rangle\right)$ to a given k-th zeroth-order excited state $|\varphi_k\rangle$ $\left(\hat{H}^{(0)}|\varphi_k\rangle = E_k|\varphi_k\rangle\right)$ will be taken into account. Indeed, it is well known that the vibrational transitions of molecules can be reasonably described by including in the analysis only two states of the vibrational Hamiltonian: one can suppose that the vibrational degrees of freedom are in the ground state when the system is isolated and only the perturbation causes the transition to a precise excited state. The justification lies on the negligible populations of the excited states according to the Boltzmann distribution as long as the thermal energy is insufficient to populate them.

Our purpose consists in determining the coordinates evolution, that is the Bohm trajectory, by considering the effects due to the external perturbation on a system initially in the ground state. In this way, one can represent the motion of the molecule during an excitation process completely within a quantum framework, instead of describing the excitation process with Quantum Mechanics and the corresponding motion with Classical Mechanics (or suitable semiclassical approximation). The method developed by us is presented in this section by considering a generic transition from $|\varphi_g\rangle$ to $|\varphi_k\rangle$ of one-dimensional system, whereas the application to molecular systems will be investigated in Sec. 5.3.

We propose to express the Bohm velocity field, labeled with a compact notation

$$\Lambda_{\mathcal{C}}(q,t) := m^{-1}\nabla S(q,t), \tag{5.3}$$

by employing the wave function, or the corresponding corrections, determined through the standard perturbation methods once the system begins to interacts with the external field. Then, once the velocity field is known, the trajectory has to be computed by integrating the resulting Bohm equation. Notice that our idea consists in correcting the velocity field, and consequently the Bohm equation, instead of the trajectory directly. In this way, it is possible to exploit methodologies that are well known in literature, i.e., the perturbation methods, in order to solve the Schrödinger equation approximately. Once the wave function has been obtained, then the Bohm velocity field is immediately defined through Eq. (2.5). In particular two different approaches have been developed. The first one uses a perturbation method originally designed for the description of the spin dynamics in the presence of a static magnetic field and interacting with an oscillating perturbation [Pake (1950a,b)], e.g., an EPR or a NMR experiment. This method allows the calculation of the wave function over a long time domain by assuming that the magnitude of the external field is lower that the zeroth-order Hamiltonian. In this way also the velocity field is known over a long time window. The second strategy employs the standard perturbation method which finds many applications in Chemistry. Such a procedure leads to corrections of the wave function of the isolated system and of the velocity field as well. In practice, it becomes convenient only when the corrections of the lower order well represent the underlying dynamics. However, in this case one recovers an accurate representation of the dynamics only within a limited time interval: the width of the time window is strictly dependent of the number of correction terms considered. For this reason, the first approach is more advantageous since it does not restrict the examined time window. In the following, both these two methods are presented and their predictions are compared.

Long time perturbation approach. The first perturbation method solves the Schrödinger equation with the Hamiltonian of Eq. (5.1) and the external field of Eq. (5.2) by supposing that the initial wave function is the zeroth-order ground state $|\Psi(0)\rangle = |\varphi_g\rangle$ and the external field causes the resonance between two zeroth-order eigenstates only. In other words, it describes the dynamics of two levels in resonance because of the interaction acting as a perturbation. Consider for example a Morse oscillator and the condition $\omega = \omega_{1,g} = (E_1 - E_g)/\hbar$ where E_1 is the eigenen-

ergy of the first excited state. This constraint ensures that the perturbation causes only the transition from the ground state to the first excited state ($k = 1$). All the other pairs of zeroth-order eigenstates are characterised by energy separations $\omega_{k',k} \neq \omega_{1,g}$. Therefore, the wave function dynamics concerns the eigenstates $|\varphi_1\rangle$ and $|\varphi_g\rangle$ only. The same does not apply to the Harmonic oscillator: the frequency ω that induces the $k : 0 \to 1$ transition will induce also the transition $k : 1 \to 2$, once the first excited state is populated enough. Then it will induce also the $k : 2 \to 3$ when the second excited state is populated enough and so on. Since the effects of the perturbation involve more than two zeroth-order eigenstates, the approximate solution of the Schrödinger equation obtainable with this approach is not valid. On the other hand, the vibrational spectrum of molecules is anharmonic and the procedure can be safely employed. Therefore, by assuming that the constraint described above is satisfied, the resulting wave function of the system can be specified as

$$\Psi(q,t) = \sqrt{P_g(t)}e^{-\imath\omega_g t}\varphi_g(q) + \sqrt{P_k(t)}e^{-\imath\omega_k t}\varphi_k(q), \tag{5.4}$$

where $\big(\varphi_g(q), \varphi_k(q)\big)$ are the eigenfunctions of $\hat{H}^{(0)}$ involved in the transition and $\big(P_g(t), P_k(t)\big)$ are the populations of the zeroth-order ground state and of the k-th zeroth-order excited state respectively,

$$\sqrt{P_g(t)} = \cos\left(\frac{W_{k,g}}{2\hbar}t\right), \qquad \sqrt{P_k(t)} = \sin\left(\frac{W_{k,g}}{2\hbar}t\right), \tag{5.5}$$

with $W_{k,g} = \langle\varphi_k|\hat{W}|\varphi_g\rangle$. The time dependence of the populations in Eq. (5.5) is derived by means of the perturbation method summarised in Appendix A, where we take into account also the case of $\omega \simeq \omega_{k,g}$. It should be mentioned that the phenomenology does not change significantly if the resonance condition is not strictly satisfied. By examining Eq. (5.5), one can interpret the effects of the external field in terms of induced excitation and induced de-excitation. Indeed, the populations of the two states involved in the transition are characterised by an opposite dynamics: initially the population of ground state decreases while the population of excited state rises. Once the excited state is totally populated $P_k = 1$ ($P_g = 0$), the field induces the de-excitation: the population of ground state increases and the population of excited state is reduced. These two processes happen repeatedly as long as the system interacts with the oscillating field for $W_{k,g} \neq 0$, with the matrix element $W_{k,g}$ representing exactly the coupling strength between the system and the external field. In this regard, the assumption that the extern field represents a perturbation for the system means formally that $W_{k,g}/2\hbar \ll \omega_{k,g}$.

Furthermore, by substituting the wave function of Eq. (5.4) into the Bohm equation, Eq. (2.5), a well-defined velocity field is obtained over a long time interval:

$$\Lambda_{\mathcal{C}}(q,t) = \hbar m^{-1} \frac{\sqrt{P_g(t)P_k(t)}\sin(\omega_{k,g}t)\Big[\varphi_k\nabla\varphi_g - \varphi_g\nabla\varphi_k\Big]}{P_g(t)(\varphi_g)^2 + P_k(t)(\varphi_k)^2 + 2\sqrt{P_g(t)P_k(t)}\varphi_g\varphi_k\cos(\omega_{k,g}t)}\Bigg|_{q=Q(t)}. \tag{5.6}$$

In principle information about the motion could be inferred from Eq. (5.6) without solving it neither analytically nor numerically, but through a qualitative analysis. By neglecting the time dependence of the denominator of Eq. (5.6), one can suppose that the periodic time dependence of the sine factor of the velocity field produces an oscillating behaviour of the trajectory. Furthermore, one should take into account the time dependence of $\sqrt{P_g(t)P_k(t)}$ which will produce a modulation of the oscillations. In particular the amplitude vanishes when one of the pair of eigenstates is not populated ($P_g = 0$ or $P_k = 0$) and the system is motionless ($\Lambda_{\mathcal{C}}(q,t) = 0$). The resulting trajectory will not be a simple modulated oscillation because of the coordinate dependence of both the numerator and of the denominator. However, one expects that the exact motion does not differ too much from the previous picture.

The second approach for determining the Bohm trajectory under the influence of an external field is less direct than the previous one. Even if its predictions are limited over a short time interval, the calculation of the corrections to the Bohm velocity field requires a more complex elaboration. However, it has to be emphasised that this second approach can be extended also to a generic perturbation and a generic transition unlike the previous one that is limited to the resonance between two zeroth-order states.

Short time perturbation approach. We propose to express the Bohm velocity field, Eq. (5.3), as a series of corrections to the zeroth-order one $\Lambda^{(0)}_{\mathcal{C}}(q,t)$ corresponding to the Bohm equation in absence of an external field:

$$\Lambda_{\mathcal{C}}(q,t) = \Lambda^{(0)}_{\mathcal{C}}(q,t) + \sum_{p=1}^{+\infty} \lambda^p \Lambda^{(p)}_{\mathcal{C}}(q,t). \tag{5.7}$$

where p is the order of the correction and λ is the parameter of the expansion. In case of absence of the external field. The direct connection between the velocity field and the wave function through Eq. (2.5) allows a straightforward definition of each p-th order of correction of the velocity field. According to perturbative methods, the wave function for a system with the Hamiltonian operator of Eq. (5.1) is expressed

as a series of corrections to the zeroth-order one $\Psi^{(0)}(q,t)$,

$$\Psi(q,t) = \Psi^{(0)}(q,t) + \sum_{p=1}^{+\infty} \lambda^p \Psi^{(p)}(q,t), \tag{5.8}$$

where $\Psi^{(0)}(q,t) = \langle q| \exp(-\imath \hat{H}^{(0)} t/\hbar)|\Psi(0)\rangle$. The velocity field $\Lambda_{\mathcal{C}}(q,t)$ is defined through Eq. (2.5) by employing the wave function of Eq. (5.8) and the p-th correction order to the velocity field is equal to

$$\Lambda_{\mathcal{C}}^{(p)}(q,t) = \left. \frac{\partial^p \Lambda_{\mathcal{C}}(q,t)}{\partial \lambda^p} \right|_{\lambda=0}. \tag{5.9}$$

For a complete derivation of $\Psi^{(p)}(q,t)$ see for instance Cohen-Tannoudji et al. (1977b) or McQuarrie and Simon (1997).

If the magnitude of $\hat{H}^{(1)}$ is smaller than the magnitude of $\hat{H}^{(0)}$ and the focus is on the first steps of the time evolution, only few terms of the two series reported respectively in Eq. (5.7) and Eq. (5.8) are sufficient to represent accurately the dynamics. The zeroth-order $\Lambda_{\mathcal{C}}^{(0)}(q,t)$ and the first-order $\Lambda_{\mathcal{C}}^{(1)}(q,t)$ correction of the velocity field can be expressed by using the zeroth-order $\Psi^{(0)}(q,t)$ and the first-order $\Psi^{(1)}(q,t)$ correction of the wave function,

$$\Lambda_{\mathcal{C}}^{(0)}(q,t) = \hbar m^{-1} \mathrm{Im} \left\{ \frac{\Psi^{(0)*}(q,t) \nabla \Psi^{(0)}(q,t)}{|\Psi^{(0)}(q,t)|^2} \right\}, \tag{5.10}$$

$$\Lambda_{\mathcal{C}}^{(1)}(q,t) = \hbar m^{-1} \mathrm{Im} \left\{ \nabla \left[\frac{\Psi^{(1)}(q,t)}{\Psi^{(0)}(q,t)} \right] \right\}. \tag{5.11}$$

In this way the initial steps of the trajectory of the system in the presence of the external field $\hat{H}^{(1)}(t)$ is determined through integration of

$$\frac{\mathrm{d}}{\mathrm{d}t} Q(t) = \left[\Lambda_{\mathcal{C}}^{(0)}(q,t) + \Lambda_{\mathcal{C}}^{(1)}(q,t) \right]_{q=Q(t)} \tag{5.12}$$

Notice that the definitions of the velocity field corrections reported in Eq. (5.9) hold for every external Hamiltonian $\hat{H}^{(1)}(t)$ and every zero order wave function $\Psi^{(0)}(q,t)$ since $\Psi^{(p)}(q,t)$ is defined for every $\hat{H}^{(1)}(t)$ and $\Psi^{(0)}(q,t)$. However, as previously stated, our interest concerns the specific case of exciting a system initially in the ground state through the interaction with an oscillating electric field with a given frequency, such as the one of Eq. (5.2). In this case the motion is totally determined by the transition induced by the external field. By assuming that the

system is initially in the ground state, the zeroth-order wave function $\Psi^{(0)}(q,t) = \exp(-\imath E_g t/\hbar)\varphi_g(q)$ does not drive the particles: $\Lambda_{\mathcal{C}}^{(0)}(q,t) = 0$ since the eigenfunction of the a ground state is real function ($\varphi_g : \mathbb{R} \to \mathbb{R}$) and therefore the phase of the wave function is coordinate independent. In other words, the zeroth-order system is characterised by the absence of motion. The motion is induced only by the transition due to the interaction with the field. Formally this means that only $\Lambda_{\mathcal{C}}^{(1)}(q,t)$ is essential in order to determine the trajectory and it is equal to

$$\Lambda_{\mathcal{C}}^{(1)}(q,t) = -\frac{\hbar}{m}\sqrt{P_k(t)}\sin(\omega_{k,g}t)\frac{\mathrm{d}}{\mathrm{d}q}\frac{\varphi_k(q)}{\varphi_g(q)}, \tag{5.13}$$

where $P_k(t)$ is the first order population of the excited state,

$$\sqrt{P_k(t)} = \frac{W_{k,g}}{2\hbar}t = \frac{\langle\varphi_k|\hat{W}|\varphi_g\rangle}{2\hbar}t. \tag{5.14}$$

Notice that for this case, the first-order approximation of the wave function holds until $t \ll 2\hbar/W_{k,g}$: it is valid as long as the excited state is much less populated than the ground state ($\sqrt{P_k} \ll 1$). The velocity field $\Lambda_{\mathcal{C}}^{(1)}(q,t)$ of Eq. (5.13) has been obtained by substituting in Eq. (5.11) the wave function for the isolated system $\Psi^{(0)}(q,t) = \exp(-\imath E_g t/\hbar)\varphi_g$, and the result of the first order perturbation, $\Psi^{(1)}(q,t) = \sqrt{P_k(t)}\exp(-\imath E_k t/\hbar)\varphi_k$. In consequence of the absence of motion in the absence of the external field, $\Lambda_{\mathcal{C}}^{(0)}(q,t) = 0$, Eq. (5.12) can be simplified to

$$\frac{\mathrm{d}}{\mathrm{d}t}Q(t) = \Lambda_{\mathcal{C}}^{(1)}(q,t)\Big|_{q=Q(t)}. \tag{5.15}$$

Again information about the motion could be inferred from Eq. (5.15) and Eq. (5.13) through a qualitative analysis of the differential equation. For the same reasons previously explained, one can suppose that the sine factor in the velocity field corresponds to an oscillating motion. In parallel, the linear increase of $\sqrt{P_k(t)}$ in Eq. (5.15), usually interpreted as the excitation of the system, causes an almost linear increase of the amplitude of the oscillation. However, the motion should not be exactly an oscillation because of the coordinates dependence of the velocity field.

Finally, we would like to stress that this second approach can be derived directly from Eq. (5.6). First of all one can use an expansion of $\Lambda_{\mathcal{C}}(q,t)$ of Eq. (5.6) with respect to $\sqrt{P_k(t)}$ up to the first order. The justification is that $\sqrt{P_k(t)} \sim 0$ during the first steps of the dynamics. Then, the time dependence of $\sqrt{P_k(t)}$ can be further approximated according to Taylor series, $\sqrt{P_k(t)} \simeq W_{k,g}t/2\hbar$. In this way,

one can get Eq. (5.14) from Eq. (5.5) and Eq. (5.13) represents a special case of Eq. (5.6). The simplification $\sqrt{P_k(t)} \simeq W_{k,g}t/2\hbar$ is satisfactory for times such that $W_{k,g}t/2\hbar \ll 1$. Therefore, one can understand why the second approach describes the dynamics over a short time interval only.

Both the methodologies presented above are employed in Sec. 5.2 in order to describe the coordinate evolution of a simple quantum system, i.e., a Morse oscillator. First of all, we consider the predictions based on the second approach for short time interval. Then, the dynamics described by the more general approach over a long time window is examined and compared. The results obtained for the Morse model are then used also to describe successfully the case of molecular motion induced by a vibrational transition in Sec. 5.3 by employing, because of its greater generality, only the first perturbation approach.

5.2 Morse Oscillator

The Morse oscillator is a well known unidimensional quantum system [Morse (1929); Dahl and Springborg (1988)] characterised by the following zeroth-order Hamiltonian

$$\hat{H}^{(0)} = \frac{\hbar}{2m}\nabla^2 + D_e(1 - e^{-aq})^2, \tag{5.16}$$

where D_e and a are the parameters of the Morse potential that is reported in Fig. 5.1. The well depth defined with respect to the value of the potential in the limit of $q \to +\infty$ is represented by D_e and a corresponds to the "width" of the potential (smaller value of a means larger well of the potential). Since the Morse potential reproduces to a good approximation the internuclear potential of a diatomic molecule, the Morse eigenstates are a good model for the vibrational eigenstates of such a type of molecules (for example hydrogen chloride) and the corresponding Bohm coordinate $Q(t)$ can be interpreted as the internuclear distance, but this interpretation will be discussed in more detail in Sec. 5.3. For the purpose of this section the coordinate $Q(t)$ is simply the position of the Morse oscillator.

Let us consider the Morse oscillator with $D_e = 4.61$ eV, $a = 1.89 \cdot 10^{-4}$ Å^{-1} and $m = 0.98$ Da (the reasons of such a choice will be motivated in Subs. 5.3.1). The trajectory of the coordinate during a transition is determined by both the magnitude of the field and the system properties (such as the eigenvalues of $\hat{H}^{(0)}$ and the transition dipole moment). Suppose that the external field, with magnitude $\mathcal{E} = 3 \cdot 10^7$ V m^{-1}, causes the transition from the ground state to the first excited state ($\omega = \omega_{1,g}$) and that the transition dipole moment $\mu_{1,g}$ is equal to $6.7 \cdot 10^{-2}$ D

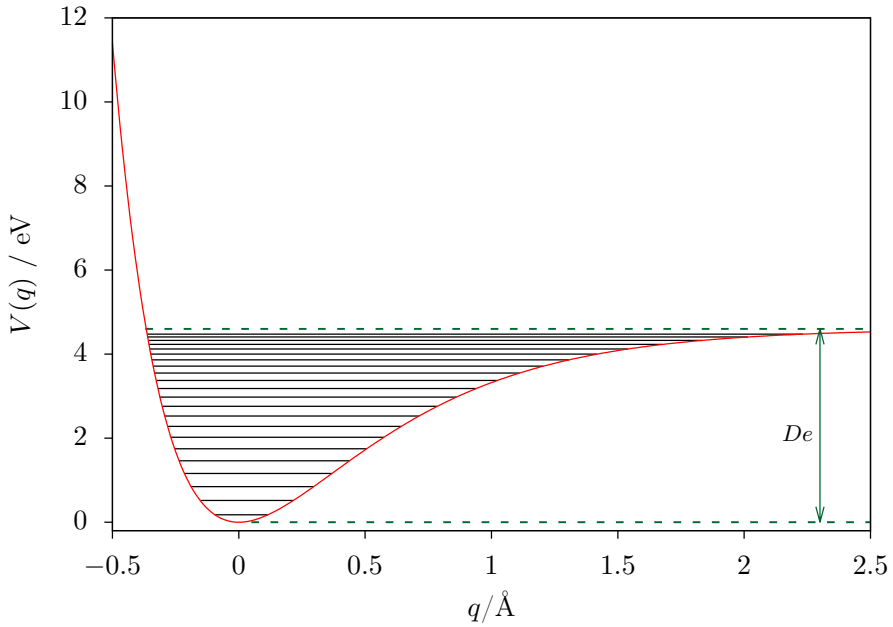

Figure 5.1: Morse potential characterised by the parameters $D_e = 4.61$ eV and $a = 1.89 \cdot 10^{-4}$ Å^{-1}. The black straight lines identifies the eigenvalues of each eigenstate with respect to the Morse potential.

(see Subs. 5.3.1 for the explanations of the choice of $\mu_{1,g}$). The magnitude of $\mathcal{E}$ is approximately the greatest one such that the interaction with the external field can be classified correctly as a perturbation ($W_{1,g}/2\hbar \ll \omega_{1,g}$).

Under the above specified conditions, the Bohm coordinate begins to move when the external field is activated and the corresponding trajectory $Q(t)$ is determined over a short time interval by integrating Eq. (5.15). The trajectory reported in Figure 5.2 is obtained under the assumption that the initial position $Q(0)$ is of the bottom of the Morse potential, $Q(0) = 0$ Å. The trajectory has been determined by numerically solving Eq. (5.15). We adopted the 4-th order Runge-Kutta algorithm in order to solve the approximate Bohm equation [Press et al. (2007)]. The main features of the trajectory can be observed in Fig. 5.2 and they are analogous to those inferred through the qualitative analysis of the differential equation: the coordinate oscillates with an amplitude that linearly increase in time. The frequency of the oscillation corresponds exactly to the resonance frequency $\omega_{1,g}$ that in this case is approximately equal to 0.57 fs^{-1}: every $t/\pi = 1/\omega = 1.75$ fs the coordinate $Q(t)$ inverts the direction of the motion. If the frequency ω of the external field does not satisfy exactly the resonance condition, only the amplitude of the oscillation is

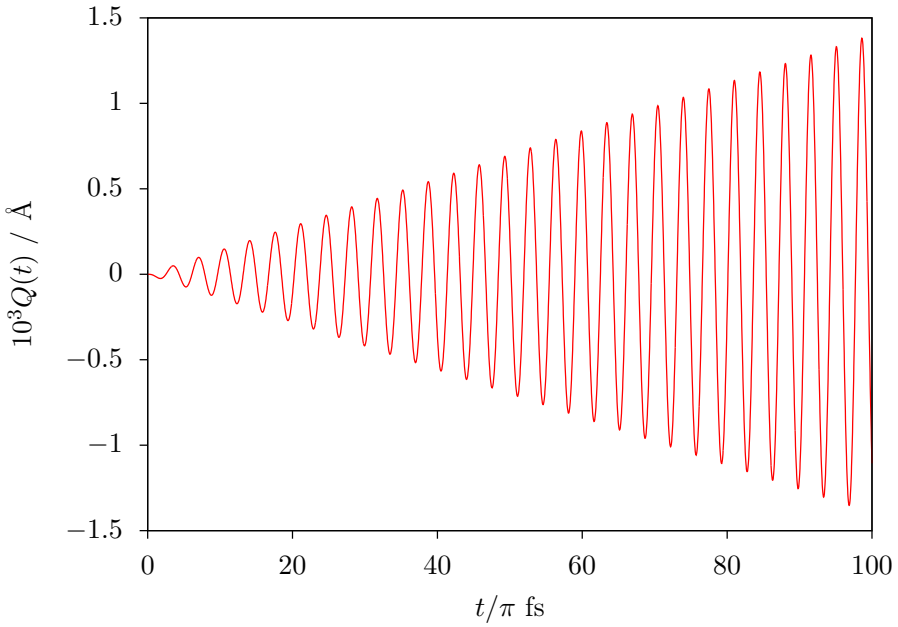

Figure 5.2: Time evolution over a short time interval of the Bohm coordinate corresponding to the Morse degree of freedom, during the transition between the ground and the first excited state. The trajectory has been determined by integrating Eq. (5.15).

influenced,

$$\sqrt{P_k(t)} = \frac{W_{k,g}}{2\hbar} \frac{\sin\left((\omega_{k,g} - \omega)t/2\right)}{(\omega_{k,g} - \omega)/2}, \tag{5.17}$$

but the motion conserves its own frequency $\omega_{1,g}$ that depends on the energy difference between the zeroth-order states involved in the transition (see for instance Cohen-Tannoudji et al. (1977b) for the explanation of Eq. (5.17)). Furthermore the different time dependence of $\sqrt{P_k(t)}$, described by Eq. (5.17) instead of Eq. (5.14), has no substantial effect on the motion: if ω is close to the resonance condition, $\sqrt{P_k(t)}$ evolution is characterised by a very small frequency and it is well approximated by a linear increase. Finally, notice that the configuration dependence of the first-order velocity field $\Lambda_{\mathcal{C}}^{(1)}(q,t)$ for the considered transition (Eq. (5.15)) does not influence significantly the motion over the time window examined in Fig. 5.2: the motion is fundamentally an oscillation. This kind of motion is representative of the dynamics until the population of the excited state is negligible with respect to the population of the ground state: $P_1 \ll P_0$. The time interval reported in Fig. 5.2 satisfies this restriction: at $t/\pi = 100$ fs the population of the first excited state can be determined by Eq. (5.14) and one can easily verify that $\sqrt{P_1} \simeq 1.6 \cdot 10^{-3}$.

The amplitude of the oscillation is conserved if the interaction with the external field is interrupted. As previously specified in the qualitative analysis of the ap-

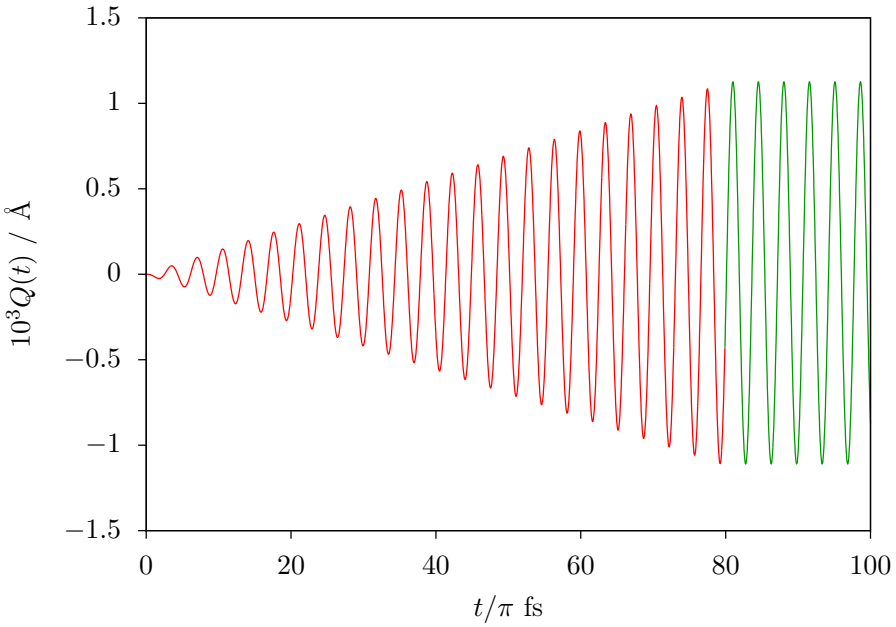

Figure 5.3: Time evolution over a short time interval of the Bohm coordinate corresponding to the Morse degree of freedom, during and after the perturbation. The red line represents the evolution in the presence of the field. The green line represents the evolution when the external field is switched off. The red section of the trajectory has been determined by integrating Eq. (5.15).

proximated Bohm equation, the amplitude increase corresponds to the population increase of the excited state. Therefore, when the irradiation is switched off, the populations of the two states involved in the transition do not change anymore and the Bohm coordinate oscillates with constant amplitude. Figure 5.3 shows the time evolution of the Morse oscillator previously considered in Fig. 5.2, but interrupting the interaction with the external field at $t/\pi = 80$ fs. Obviously, the system is isolated again once it does no more interact with the external field. This means that the Schrödinger equation and the Bohm equation can be solved exactly once the wave function and the configuration at moment of the interruption of the perturbation are known. Therefore, the green section of the trajectory reported in Fig. 5.2 has to be considered the correct trajectory and this kind of oscillation is conserved as long as the system Hamiltonian is provided only by $\hat{H}^{(0)}$. It has to be emphasised that a periodic motion, i.e., a nearly perfect oscillation, is unexpected by examining the Bohm equation, (see for example Eq. (5.6) for constant population for the absence of the field). Indeed, the structure of the Bohm equation does not lead to a simple explanation of this particular behaviour because of the coordinate dependence of the velocity. Therefore, it should be considered just as a "numerical" evidence.

In the time interval examined above the motion is confined around the initial

configuration. Even if the external field "defrosts" the Morse oscillator, its displacement is only about 0.002 Å to be compared with a width of a Morse potential such that of Fig. 5.1.

One can use the first perturbative method above described and summarised in Eq. (5.6) to determine the evolution of the Morse oscillator interacting with the external field over a long time window. Indeed the rational independence of the Morse eigenvalues ensures that a resonance frequencies between the possible pairs of eigenstates are different, so fulfilling the constraint for employing Eq. (5.6). The integration of Eq. (5.6) with $Q(0) = 0$ Å is displayed in Fig. 5.4 for a short time window, and in Fig. 5.5 for a longer time interval. By comparing qualitatively

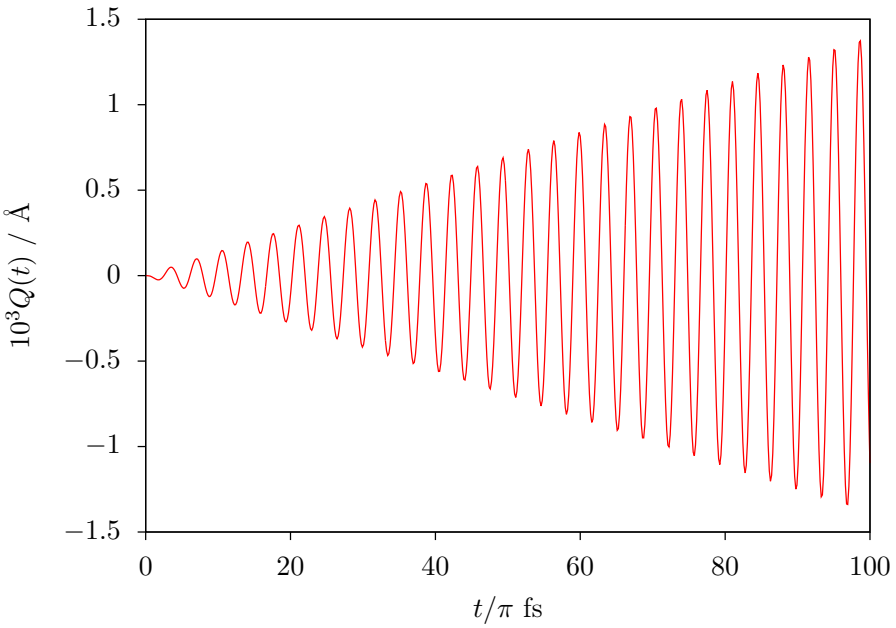

Figure 5.4: Time evolution over a short time interval of the Bohm coordinate corresponding to the Morse degree of freedom, during the transition between the ground and the first excited state. The trajectory has been determined by integrating Eq. (5.6).

Fig. 5.4 and Fig. 5.2, one can observe that the two perturbative methods supply the same picture of the motion for the fist steps of the dynamics: the Bohm coordinate oscillates with increasing amplitude. This result confirms the validity of Eq. (5.13) in order to describe the evolution of the system until $P_1 \ll P_g$. On the contrary, the behaviour over a long time interval (see Fig. 5.5) is an oscillation with amplitude modulated in time in accord with the qualitative analysis reported in Sec. 5.1. The profile of Fig. 5.5 is composed of many oscillations with a very short period in comparison of the displayed time window so that they can not be recognised in the figure. The amplitude changes approximately from 0 Å to 0.17 Å with a much

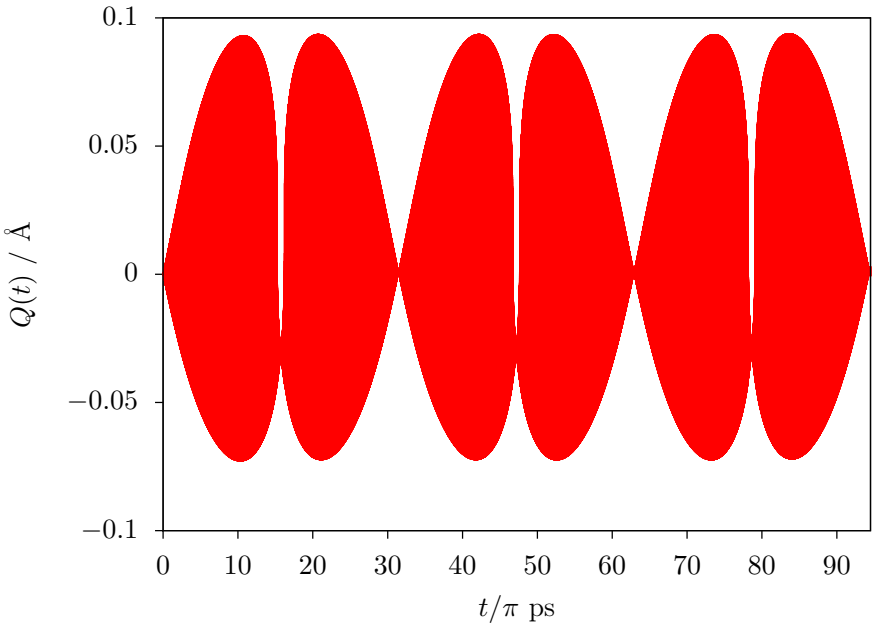

Figure 5.5: Time evolution over a long time interval of the Bohm coordinate corresponding to the Morse degree of freedom, during the transition between the ground and the first excited state. The trajectory has been determined by integrating Eq. (5.6).

larger displacement than the one previously discussed and shown in Fig. 5.2. As expected, the amplitude vanishes when only one eigenstate involved in the transition is populated. In other words, the coordinate is at rest when the wave function is a stationary state (either the ground state or the first excited state). This occurs when $W_{1,g}t/2\hbar = n\pi/2$ with $n \in \mathbb{N}$ according to Eq. (5.5). By taking into account the values of the transition dipole moment and of the field magnitude ($\mu_{1,g} = 6.7 \cdot 10^{-2}$ D, $\mathcal{E} = 3 \cdot 10^{7}$ V m^{-1}), one derives that the motion amplitude vanishes and the coordinate is at rest at $t/\pi \simeq 0$ ps ($P_g = 1$), 16 ps ($P_k = 1$), 32 ps ($P_g = 1$), 48 ps ($P_k = 1$), 64 ps ($P_g = 1$), 80 ps ($P_k = 1$), 96 ps ($P_g = 1$).

This behaviour appears unexpected according to the common interpretation of a vibrational transition. Moreover, it could seem unreasonable as long as the effect of an energy transfer is that of "freezing" the degree of freedom. Actually, it can be explained and it is not unreasonable even in the framework of Classical Mechanics. Let us consider a classic rigid rod pendulum. As a matter of fact, the pendulum is characterised by two different equilibrium configurations, i.e., the two vertical orientations, corresponding to different values of energy. One can think of pushing the pendulum from one equilibrium condition to the other and consequently of increasing its energy. Similarly, the Hamiltonian eigenstates represent the corresponding equilibrium conditions in the framework of Bohm theory (they can be interpreted

as mechanical equilibriums according to the comparison with the pendulum). The transition from the ground state to an excited state is simply the transition from one equilibrium to another. When the new equilibrium condition is reached, the system is again at rest.

On the other hand, the particle position changes in time when the wave function is a linear combination of different eigenstates. The features of the motion are determined by both intrinsic properties of the oscillator and the coupling between the system and the external field. The energy difference between the eigenstates involved in the transition establishes the frequency of inversion of the motion, whereas the coupling, described by the matrix element $W_{1,g} = \mu_{1,g}\mathcal{E}$, determines the time scale of the amplitude modulation. Another intrinsic feature is highlighted by the asymmetry of the motion with respect to the bottom of the Morse potential. The displacement is larger along the direction in which the potential slowly rises ($q > 0$ Å as displayed in Fig. 5.1) than the direction in which the potential soars ($q < 0$ Å as displayed in Fig. 5.1). This is caused by the asymmetry of the eigenfunctions $\varphi_g(q)$ and $\varphi_k(q)$ with a corresponding larger probability of finding the particle on the right side of the well.

When the interaction with the external field is interrupted, the populations do not change any more and the amplitude is conserved. The motion during the transition process and when the Morse oscillator is not interacting with the external field is shown in Fig. 5.6. By comparing Fig. 5.3 and Fig. 5.6, one can easily understand that the amplitude of the motion after the end of the perturbation is strongly dependent on the time of the switched off of the external field according to the values attained to the populations P_g and P_k. When the wave function is almost an eigenstate (either $P_g \ll P_k$ or $P_g \gg P_k$), the amplitude is very small. Conversely, a wide amplitude corresponds to almost equal values of the populations $P_g \simeq P_k$. In any case, the motion becomes nearly a stationary oscillation after the switched off of the perturbation. We would like to recall that this simple behaviour, i.e., a nearly perfect oscillation, can not be derived directly from the formal structure of the Bohm equation because of the spatial dependence of the velocity field: despite the complexity of the equation of motion the numerical calculation shows that the resulting trajectory is quite simple. One can reasonably think that the displacement of the coordinate is too much limited around the initial position to display the effects of the coordinate dependence of the velocity field. Because of the difficulties concerning the analytical investigation of the Bohm equation, we propose to consider this oscillating behaviour as an "numerical" evidence of the motion features.

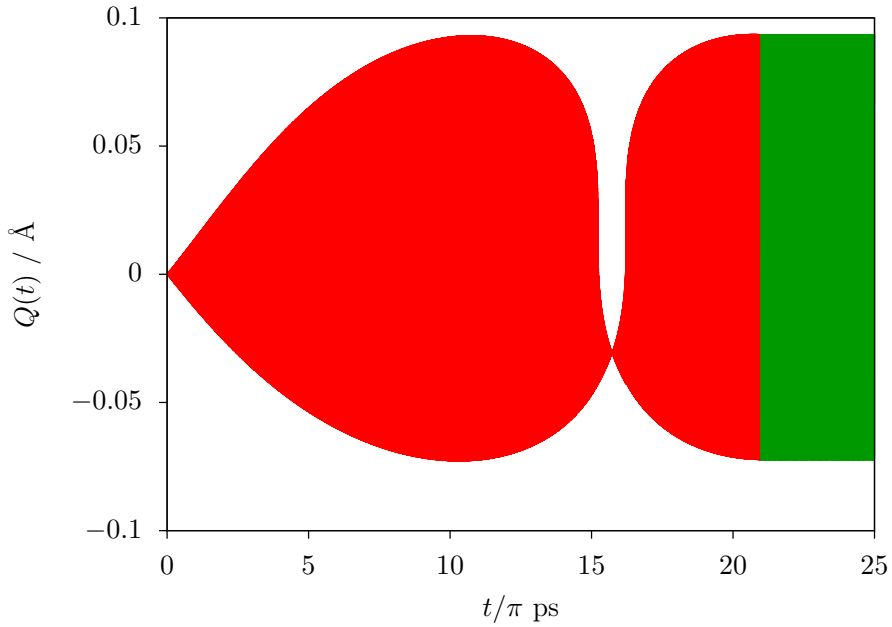

Figure 5.6: Time evolution over a long time interval of the Bohm coordinate corresponding to the Morse degree of freedom, during and after the perturbation. The red line represents the evolution when the system is interacting with the external field, while the green line represents the trajectory in the absence of the field. The red section of the trajectory has been determined by integrating Eq. (5.6).

It has to be emphasised that the all trajectories reported above describe the evolution of the Bohm coordinate from the bottom of the Morse potential, that means $Q(0) = 0$ Å. Different trajectories evolve from different initial configurations. For instance, Fig. 5.7 displays three trajectories that depart from the initial configurations $Q(0) = 0$ Å, $Q(0) = 0.5$ Å, $Q(0) = -0.5$ Å when the same Morse oscillator ($D_e = 4.61$ eV, $a = 1.89 \cdot 10^{-4}$ Å^{-1}) is excited from the ground to the first excited state. The red trajectory of Fig. 5.7 is the same of Fig. 5.5. In all cases, the dynamics is represented by an oscillation at the resonance frequency with modulated amplitude. However, it is evident that the trajectories initially at $Q(0) = \pm 0.5$ Å display some unexpected features. First of all, the trajectories do not pass through the bottom of the Morse potential. This phenomenon is totally at odds with Classical Mechanics in which case one expects the periodic displacement from the region of larger potential energy to lower potential energy and in particular to the potential minimum. However, it has to be recalled that in the case of Bohm trajectory the motion is driven by the wave function which acts as the pilot wave. Consequently the Bohm trajectory can be deeply different from the classical trajectory. Furthermore, the Bohm phenomenology can be explained by employing the quantum potential $U(q,t)$ defined in Eq. (2.4). As explained in Chap. 2, the Bohm trajectory is also

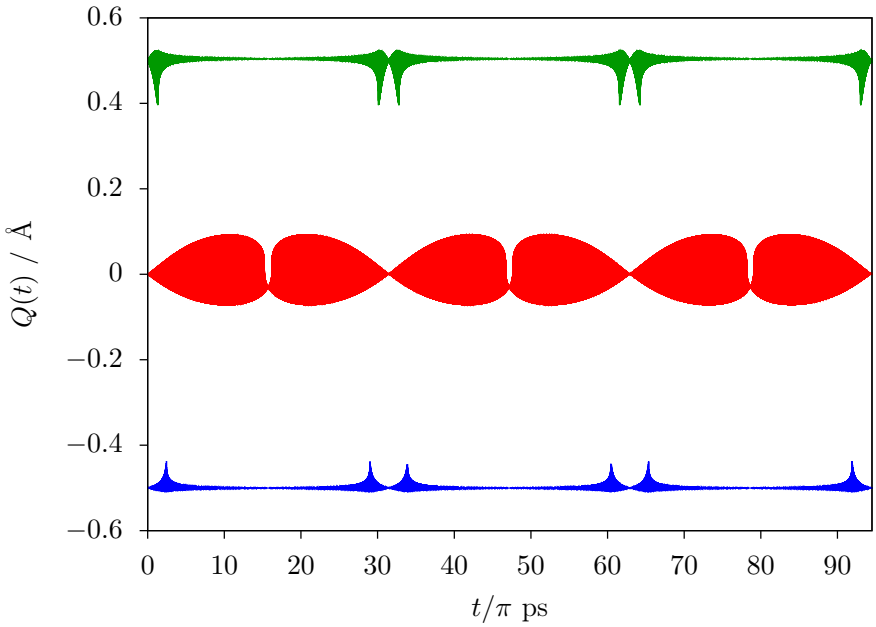

Figure 5.7: Time evolution over a long time interval of the Bohm coordinates corresponding to the Morse degree of freedom, during the transition between the ground and the first excited state. The trajectory has been determined by integrating Eq. (5.6) for three different initial configurations: $Q(0) = 0$ Å (red line), $Q(0) = 0.5$ Å (green line) and $Q(0) = -0.5$ Å (blue line).

solution of a pseudo Newton equation with a force deriving from the gradient of both the Morse potential and the quantum potential $U(q,t)$. Regarding the Morse oscillator system, one can suppose that the contribution of the quantum potential leads to an overall potential having further minima besides that of the Morse potential. This can explain the unconventional confinement of the trajectories of Fig. 5.7 with $Q(0) = \pm 0.5$ Å.

The amplitude modulation changes strongly depending on the initial configuration. In particular, it can be observed from Fig. 5.7 that the average amplitude of the trajectory started from the bottom of the potential is larger than the average amplitude of the two others. It is the configuration dependence of the velocity field $\Lambda_C(q,t)$ of Eq. (5.6) that causes this difference. Around the values of $q = \pm 0.5$ Å the magnitude of the eigenfunctions corresponding to the ground and the first excited state is small, since the Morse potential at those coordinates is greater than the energy of the two eigenstates (see Fig. 5.1). Therefore, the coordinate oscillates in a classically forbidden region and its displacement is limited around the initial configuration. One can suppose that those additional minima of the quantum potential have a shape such that the motion is strictly confined. Moreover, the quantum potential does not allow the escape of the particle from the classical forbidden region.

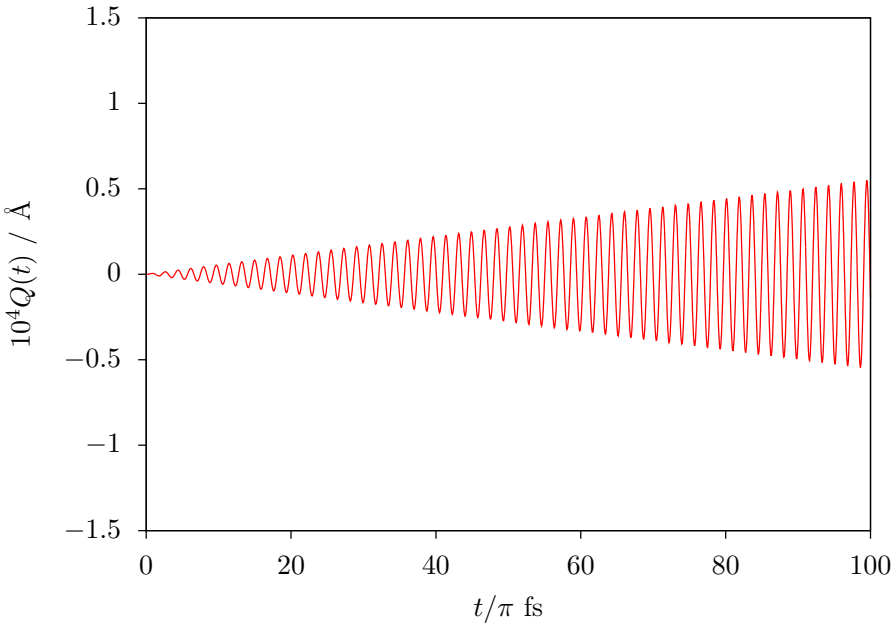

Figure 5.8: Time evolution over a short time interval of the Bohm coordinate corresponding to the Morse degree of freedom during the transition between the ground and the second excited state. The trajectory has been determined by integrating Eq. (5.6).

We would like to emphasise two features of the single Bohm trajectory approach. First of all, it allows the investigation of the evolution of the system for each possible initial configuration unlike the Bohm ensemble deriving from the sampling of $Q(0)$ according to the initial wave function. The evolution of a particular initial configuration, that is a particular system realisation, can be examined only in the framework of a single Bohm trajectory approach. Secondly, the single Bohm trajectory approach is not only suited to representing atomic motion in molecules, but it leads also to unexpected dynamical processes, like those displayed in Fig. 5.7.

Finally one can also investigate the case of a different transition. The same Morse oscillator system ($D_e = 4.61$ eV, $a = 1.89 \cdot 10^{-4}$ Å^{-1}) can be employed to study the transition from the ground to the second excited state by using an external oscillatory field with frequency $\omega = \omega_{2,g}$. In this case we assume that the transition dipole moment $\mu_{2,g}$ is $7.03 \cdot 10^{-3}$ D (see Subs. 5.3.1 for details). The trajectory for $Q(0) = 0$ Å is displayed over a short and over a long time interval in Fig. 5.8 and in Fig. 5.9 respectively. The main features of the motion are comparable to the previous cases: the coordinate oscillates at the resonance frequency, $\omega_{2,g} = 1.13$ fs^{-1}. The amplitude increase is still linear over a short time interval, but slower than the transition $g \to 1$ due to the different values of the transition dipole moments ($\mu_{2,g} = 7.03 \cdot 10^{-3}$ D, $\mu_{1,g} = 6.7 \cdot 10^{-2}$ D). Therefore, one obtains different

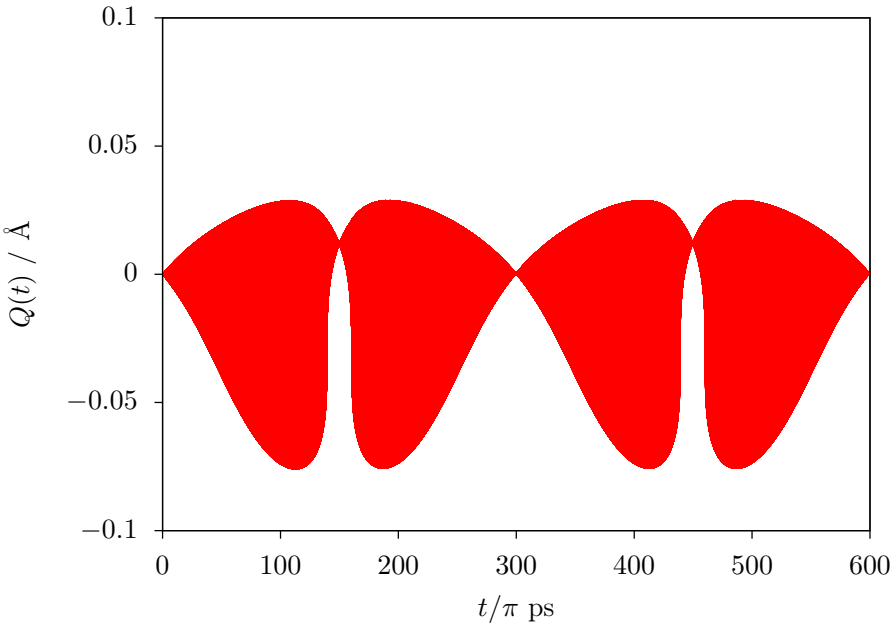

Figure 5.9: Time evolution over a long time interval of the Bohm coordinate corresponding to the Morse degree of freedom during the transition between the ground state and the second excited state. The trajectory has been determined by integrating Eq. (5.6).

periodicity and amplitude modulation of the oscillations. The transition dipole moment is lower than the previous case, $\mu_{2,g} < \mu_{1,g}$, and so the time necessary to populate the excited state is longer with smaller displacements. As it can be verified by observing Fig. 5.9, the amplitude vanishes and the coordinate is at rest for $t/\pi \simeq 0$ ps, 150 ps, 300 ps, 450 ps, 600 ps, that is when only one eigenstate only is populated. Notice that for this transition the displacement is larger along the direction in which the potential soars ($q < 0$ Å as displayed in Fig. 5.1) unlike the transition to the first excited state (see Fig. 5.5). This is due to the different profile of the eigenfunctions for the excited state in the two cases. Since the second excited eigenfunction has a nodal point of the right of well bottom, the motion is shifted on the left where the second eigenfunction determines an higher probability of observing the particle. Also this behaviour can not be recovered from Classical Mechanics and it requires the use of a quantum theory of motion in order to be predicted.

In conclusion we have illustrated the capabilities of our method to describe the motion of an one dimensional quantum system, a Morse oscillator, during a quantum transition. These results will be employed in the Sec. 5.3 in order to describe the vibrational transitions of molecules.

5.3 Molecular vibrational motion

In this section we employ our method to describe the motion of a single molecule during a vibrational transition. In our notation, the zeroth-order Hamiltonian $\hat{H}^{(0)}$ is the molecular Hamiltonian whereas the external field is the perturbation that acts on the vibrational degrees of freedom and induces the vibrational transition. Since the molecules are composed of many nuclei that interact reciprocally, it is reasonable to expect that the trajectory drawn by a particle, e.g., a nucleus, is strongly correlated to the evolution of the others. However, if one is not interested to the exact dynamics, but just to a good representation, then suitable approximations can be adopted in order to identify simple equations of motion that provide the main features of the dynamics. Then one can derive a representation of the molecular motion where each vibrational degrees of freedom is excited separately and the dynamics of the excited degree of freedom is independent of the others.

Some features of the description of molecular vibration in the framework of Quantum Mechanics are used also for determining the Bohm trajectory. Within the Born-Oppenheimer approximation, one identifies the internal potential dependent on the set of nuclear coordinates q_N in cartesian form. However, it turns out to be convenient to replace the cartesian coordinates of nuclei with the normal coordinates $\tilde{q}_N$ [Wilson et al. (1955)] as specified by the set of vibrational q_v, rotational q_r and translational q_t coordinates: $\tilde{q}_N = (q_v, q_r, q_t)$. The transformation is given by the linear relation:

$$q_N = q_{N,eq} + m^{-1/2} \Xi \, \tilde{q}_N \tag{5.18}$$

where $q_{N,eq}$ is the set of cartesian coordinates that corresponds to the equilibrium geometry and Ξ is an orthogonal matrix. For the purpose of this thesis, it is sufficient to know that $q_{N,eq}$ and Ξ depend on the nuclear effective potential arising from the electronic state and they can be computed by standard methods, already implemented in commercial softwares. The diagonal matrix $m^{-1/2}$ includes information about the nuclear masses; if the i-th element of q_N corresponds to one cartesian coordinate of the γ-th nucleus (with mass m_γ), then the i-th diagonal element of the matrix $m^{-1/2}$ is $1/\sqrt{m_\gamma}$. In this way the position of all the particles is identified by the generalised coordinate $\tilde{q} = (q_e, \tilde{q}_N) = (q_e, q_v, q_r, q_t)$. For the sake of completeness, we would like to recall that q_t is the set of three coordinates that identify the position of the molecular center of mass. Only two coordinates are included in q_r if the molecular is linear and they define the orientation of the molecule, otherwise the orientation has to be identified with three coordinates corresponding to the Eu-

ler angles. Finally, the number of vibrational coordinates for linear and non linear molecules is respectively of $3n_N - 5$ and $3n_N - 6$ (with n_N the number of nuclei).

The coordinate transformation of Eq. (5.18) is particularly suitable when one is interested in approximating the molecular eigenfunctions for values of the nuclear coordinates that are close to a minimum of the nuclear potential, i.e., the equilibrium geometry. The zeroth-order Hamiltonian $\hat{H}^{(0)}$ includes the kinetic operator of the nuclei and the effective potential for the given electronic state; we assume that it can be separated into the sum of vibrational, rotational and translation contributions, $\hat{H}^{(N)} = \hat{H}^{(v)} + \hat{H}^{(r)} + \hat{H}^{(t)}$. Correspondingly, $\hat{H}^{(0)}$ eigenfunctions can be factorised into the vibrational $\varphi_{k_v}(q_v)$, rotational $\varphi_{k_r}(q_r)$ and translational $\varphi_{k_t}(q_t)$ components,

$$\varphi_k(\tilde{q}_N) = \varphi_{k_v}(q_v)\varphi_{k_r}(q_r)\varphi_{k_t}(q_t), \tag{5.19}$$

where $k = (k_v, k_r, k_t)$ is the set of quantum numbers that tag the corresponding eigenfunctions (vibrational, rotational or translational). The parametric dependence of the rotational eigenfunctions on the the vibrational coordinates is neglected since we consider only small displacements around the equilibrium geometry. This is essential in order to ensure that $\varphi_k(\tilde{q})$ of Eq. (5.19) is eigenfunction of $\hat{H}^{(0)}$.

We assume that the molecule is initially in the vibrational $|\varphi_{g_v}\rangle$ ground state whereas the rotational and the translational state is a linear combination of different eigenstates labeled concisely as the roto-tanslational state $\left|\varphi^{(rt)}(0)\right\rangle$. Furthermore, we exclude the possibility of electronic transitions and we focus only on the nuclear dynamics. In this way the electronic degrees of freedom and the nuclear degrees of freedom are not entangled and a nuclear wave function can be defined in a consistent way. The zeroth-order nuclear wave function is $\Psi^{(0)}(\tilde{q}_N, t) = \exp(-\imath\hat{H}^{(N)}t/\hbar)\varphi_{g_v}(q_v)\varphi^{(rt)}(q_r, q_t, 0)$ by definition, and it is equal to

$$\Psi^{(0)}(\tilde{q}_N, t) = e^{-\imath\omega_{g_v}t}\varphi_{g_v}(q_v)\varphi^{(rt)}(q_r, q_t, t) \tag{5.20}$$

with $\omega_{g_v} = E_{g_v}/\hbar$ and E_{g_v} is the vibrational eigenvalue corresponding to the ground state $\hat{H}^{(v)}\varphi_{g_v} = E_{g_v}\varphi_{g_v}$. The roto-translational eigenfunction $\varphi^{(rt)}(q_r, q_t, t)$ is driven by the roto-translational Hamiltonian, $\hat{H}^{(rt)} = \hat{H}^{(r)} + \hat{H}^{(t)}$, and it has a non-trivial dependence on time as long as the initial state is not an eigenfunction of $\hat{H}^{(rt)}$. If the molecule interacts with a sinusoidal resonant perturbation whose frequency corresponds exactly to a vibrational frequency, e.g., the energy difference between the vibrational ground state and the k_v-th vibrational excited state, then the perturbed

wave function can be written as

$$\Psi(\tilde{q}_N, t) = \left[\sqrt{P_{g_v}(t)}e^{-\imath\omega_{g_v}t}\varphi_{g_v}(q_v) + \sqrt{P_{k_v}(t)}e^{-\imath\omega_{k_v}t}\varphi_{k_v}(q_v)\right]\varphi^{(rt)}(q_r, q_t, t). \quad (5.21)$$

The terms $\sqrt{P_{g_v}(t)}$ and $\sqrt{P_{k_v}(t)}$ represent the populations of the vibrational eigenstates involved in the transition. Notice that the roto-translation dynamics is not influenced by the perturbation that acting on the vibrational states. Therefore, the effects of the interaction with the external field are equivalent to produce a resonance between two vibrational states and the first approach proposed in Sec. 5.1 can be employed. By following the same procedure reported in Appendix A, one determines the time evolution of the vibrational populations, $P_{g_v}(t)$ and $P_{k_v}(t)$. As a matter of fact, a result like Eq. (5.5) is recovered because of the equivalence between the two cases:

$$\sqrt{P_g(t)} = \cos\left(\frac{W_{k_v,g_v}}{2\hbar}t\right), \qquad \sqrt{P_k(t)} = \sin\left(\frac{W_{k_v,g_v}}{2\hbar}t\right), \quad (5.22)$$

with $W_{k_v,g_v} = \langle\varphi_{k_v}|\,\hat{W}\,|\varphi_{g_v}\rangle$. In this way we can determine the evolution of the molecular wave function when an external field is producing a vibrational transition. Notice that it has been assumed that the operator $\hat{W}$ acts on the vibrational eigenstates only.

Let us now examining the Bohm equation for the set $Q_N(t)$ of the cartesian coordinates of all the nuclei at time t. Since the electrons are non entangled with the nuclei, the nuclear and the electronic trajectories are independent. The velocity of the nuclei $\dot{Q}_N(t)$ is defined through the Bohm equation Eq. (2.5) with the wave function of Eq. (5.21). This latter is function of the normal coordinates and then the velocity $\dot{Q}_N(t)$ has to be expressed explicitly using the coordinate transformation of Eq. (5.18):

$$\frac{\mathrm{d}}{\mathrm{d}t}Q_N(t) = m^{-1/2}\Xi\,\tilde{\nabla}S(\tilde{q}_N, t)\Big|_{\tilde{q}_N=\tilde{Q}_N(t)}, \quad (5.23)$$

with $\tilde{\nabla} = (\partial/\partial q_v, \partial/\partial q_r, \partial/\partial q_t)$ and $\tilde{Q}_N(t) = \big(Q_v(t), Q_r(t), Q_t(t)\big)$ is the set of the Bohm normal coordinates at time t, as derived according to Eq. (5.18) from the Bohm cartesian coordinates $Q_N(t)$.

The wave function of Eq. (5.21) ensures that the vibrational velocity, $\mathrm{d}Q_v(t)/\mathrm{d}t := \nabla_v S(\tilde{q}_N, t) = \partial S(\tilde{q}_N, t)/\partial q_v$, depends only on the vibrational coordinates $Q_v(t)$. This can be easily proven by inserting the wave function of Eq. (5.21) into the Bohm equation and by examining the vibrational components, i.e., $\nabla_v S(\tilde{q}_N)$: since

the roto-translational eigenfunctions are independent of the vibrational variables q_v by assumption, the vibrational velocity $\mathrm{d}Q_v(t)/\mathrm{d}t$ is given as

$$\frac{\mathrm{d}}{\mathrm{d}t}Q_v(t) = \hbar \frac{\sqrt{P_{g_v}(t)P_{k_v}(t)}\sin\left(\omega_{k_v,g_v}t\right)\left[\varphi_{k_v}\nabla_v\varphi_{g_v} - \varphi_{g_v}\nabla_v\varphi_{k_v}\right]}{P_{g_v}(t)\varphi_{g_v}^2 + P_{k_v}(t)\varphi_{k_v}^2 + 2\sqrt{P_{g_v}(t)P_{k_v}(t)}\varphi_{g_v}\varphi_{k_v}\cos\left(\omega_{k_v,g_v}t\right)}\Bigg|_{\tilde{q}_v=\tilde{Q}_v(t)}, \tag{5.24}$$

where $\omega_{k_v,g_v} = \omega_{k_v} - \omega_{g_v}$. Notice that in the above equation the mass matrix is not reported, since the standard procedure to define the normal coordinates supplies unitary mass for every vibrational degree of freedom [Wilson et al. (1955)]. Moreover, the above equation is a closed equation for of the vibrational coordinates. In other words, the time evolution of the vibrational coordinates can be computed independently of the others degrees of freedom and *vice versa*. Of course the resulting motion of each nucleus depends on both the vibrational and the roto-translational trajectories, since the rotational $\nabla_r S(\tilde{q}_N, t)$ and the translational $\nabla_r S(\tilde{q}_N, t)$ velocities do not vanish. However, our interest is on the effect of the vibrations on the nuclear motion. For this reason, the nuclear motion can be derived according to the transformation of Eq. (5.18) once the vibrational trajectory $Q_v(t)$ is known and by neglecting the contributions due to roto-translational motion.

We would like to emphasise that the result of a closed equation for a subset of the molecular coordinates such as Eq. (5.24) was anything but obvious: as already stressed, the non local nature of Bohm theory entangles the motion of different particles even if they do not interact. In this case we were able to simplify the problem by selecting an extremely specific situation. The eigenfunctions are factorised by transforming the cartesian coordinates in normal coordinates and it is assumed an excitation of the vibrational degrees of freedom only, otherwise a simultaneous excitation of both vibrational and roto-traslational states would correlate their motion. The investigation of this simple case is sufficient to highlight the main features of the vibrational motion and to develop an accurate representation. In particular we examine the details of the vibrational transition of diatomic and polyatomic molecules.

5.3.1 Diatomic molecules vibrations

For diatomic molecules, the natural vibrational coordinate q_v is the difference between the internuclear distance and the equilibrium bond length. We chose to consider an hydrogen chloride molecule HCl as the paradigm of this class of molecule. Our perturbation method is able to illustrate how the internuclear distance between

the hydrogen and the chlorine changes in time during a vibrational transition. Furthermore, the result for the Bohm coordinate $Q(t)$ previously reported in Fig. 5.2, Fig. 5.6, Fig. 5.7 represent exactly the evolution of the bond length around the equilibrium value, since the vibrational eigenfunctions of a diatomic molecule are well approximated by the Morse eigenfunctions. Indeed Eq. (5.24) is equivalent to Eq. (5.6) for a diatomic molecule with a monodimensional vibrational coordinate. The only constrains are the values for the Morse parameters (D_e and a) and the transition dipole moment ($\mu_{k,g}$). The parameters employed to compute the evolution of the Morse oscillator in Sec. 5.2 are exactly those of the hydrogen chloride [Herzberg (1963); Domcke and Mundel (1985); Benedict et al. (1957)]: $D_e = 4.61$ eV, $a = 1.89 \cdot 10^{-4}$ Å^{-1}, $\mu_{1,g} = 6.7 \cdot 10^{-2}$ D, $\mu_{2,g} = 7.03 \cdot 10^{-3}$ D. Therefore the dynamics of the Bohm coordinate $Q(t)$ reported in Figures 5.2 to 5.9 can be interpreted as the fluctuation of the hydrogen chloride bond distance around its equilibrium value of 1.27 Å. The condition $Q = 0$ Å corresponds to the assumption that the distance between hydrogen and chlorine is initially the equilibrium bond length.

It should be mentioned that a simpler model, like the Harmonic Oscillator, can be employed. For diatomic molecules, the aim is of understanding the changes in the vibrational motion due to the use of a rougher model than the Morse oscillator. This will be helpful in the next section where the description of polyatomic molecules is taken into account. As previously discussed, the spectral structure of the Harmonic Oscillator eigenvalues is not compatible with the perturbation method that allows the calculation of the equation of motion reported in Eq. (5.24): the resonance frequency between the ground state and the first excited state is also the resonance frequency between all the states whose quantum numbers differ for one unit and, therefore, the external field does not establish a resonance between two states only. Apparently, one can investigate only the coordinate evolution over a short time interval by employing the standard perturbation analysis, but this limits the range of applications. Nevertheless, one can use selectively the Harmonic Oscillator model: since in a real molecule the vibrational vibrational energies are rational independent, one can exploit only the Harmonic Oscillator eigenfunctions as a reasonable approximation for the real (e.g., Morse) vibrational eigenstates. Then, the equation of motion Eq. (5.6) can be solved by substituting the Morse eigenfunctions with the Harmonic Oscillator eigenfunctions, but by keeping the correct resonance frequency. For instance, Fig. 5.10 and Fig. 5.11 display the fluctuations of the HCl bond distance, under the harmonic approximation, over a short and over

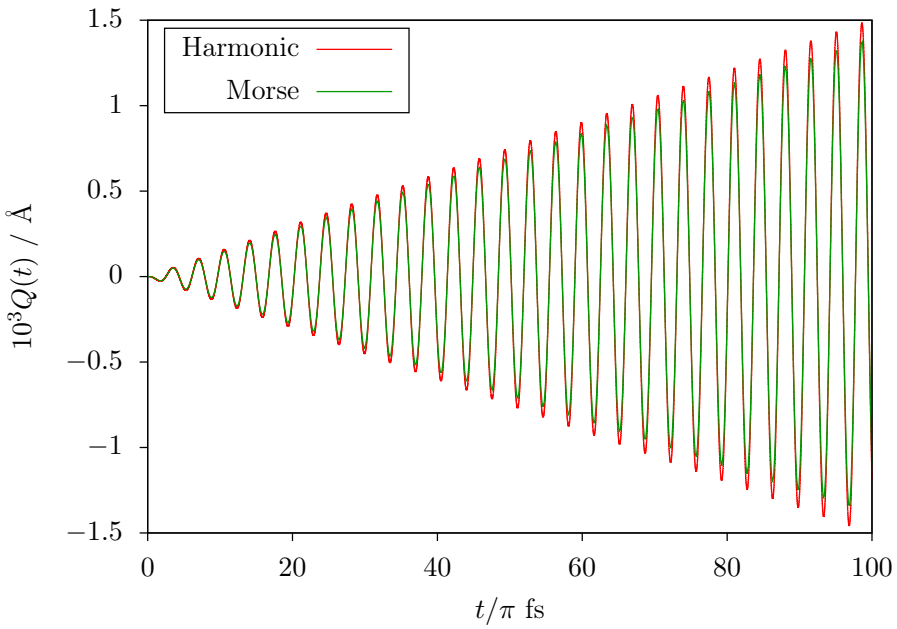

Figure 5.10: Time evolution over a short time interval of the Bohm coordinate corresponding to the HCl vibrational degree of freedom modelled with the Harmonic oscillator eigenfunctions (red line) and the Morse oscillator eigenfunctions (green line). During the displayed time window, the transition between the ground and the first excited state occurs.

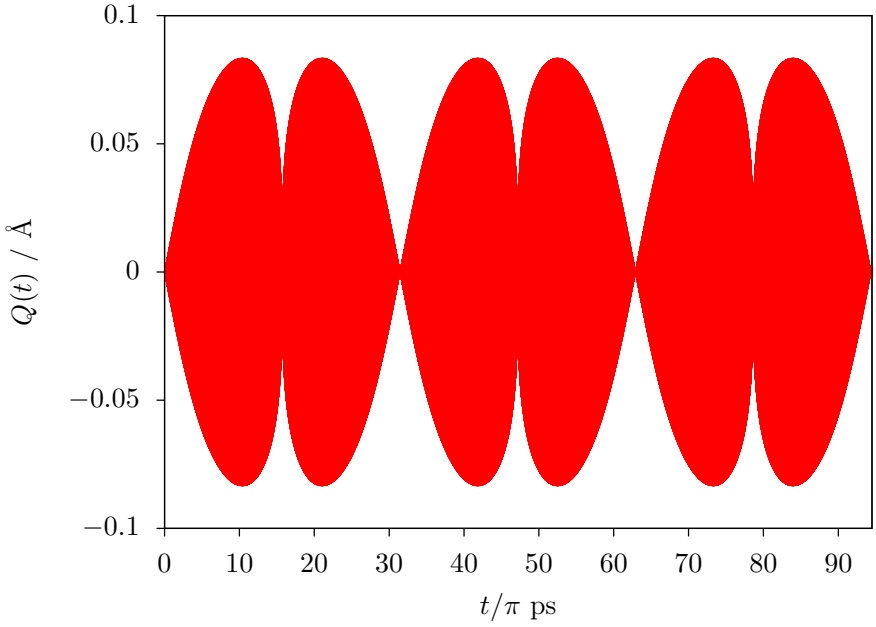

Figure 5.11: Time evolution over a long time interval of the Bohm coordinate corresponding to the HCl vibrational degree of freedom model with the Harmonic oscillator eigenfunctions. During the time window displayed, the transition between the ground and the first excited state occurs.

a long time window respectively. By observing Fig. 5.10 and comparing Fig. 5.11 with Fig. 5.5, one can verify that the main features of the motion are substantially not affected by the substitution of the eigenfunctions. The motion is an oscillation at the resonance frequency and with a modulated amplitude. The main differences concern the symmetry and the confinement of the movement. With the Harmonic Oscillator eigenfunctions, the motion results to be symmetric with respect to the potential minimum (notice the symmetry of the trajectory $Q(t)$ in Fig. 5.11 with respect to $Q = 0$ Å), unlike the Morse model where elongations of the bond length are preferred to the contractions (see Fig. 5.5). For the Harmonic oscillator the symmetry of the potential with respect to the elongation or contraction corresponds to a symmetric profile of the eigenfunctions and, therefore, also the molecular vibrations. Furthermore, the elongation of the harmonic oscillator is a bit longer than for the Morse oscillator (Fig. 5.10).

Finally, we would like to summarise the main features of the vibrational motion as derived from the application of our method to diatomic molecules. The vibrational motion of an isolated molecule induced by an external field on the ground state is essentially an oscillation at the resonance frequency. During the irradiation, that means during the energy exchange between the external field and the molecule, the amplitude of the oscillation is modulated by the coupling between the molecule and the field. The initial energy transfer causes the beginning of the molecular vibration and the increase of the amplitude of the oscillations. By using a fully classical model this amplitude should increase indefinitely; on the contrary, if the transition involves only two states, the molecule returns to be at rest when it is completely excited. This is a fully quantum behaviour which has no counterpart in Classical Mechanics. It can be interpreted as if a mechanical equilibrium is established whenever the wave function is an eigenstate of the Hamiltonian operator and the coordinate is then at rest. Furthermore, if the irradiation is interrupted, then the condition of isolation of the molecule is restored and it conserves the absorbed energy. Consequently, it vibrates continuously with an oscillation characterised by a constant amplitude.

Almost the same representation of the vibrational motion is recovered from the application of our method to polyatomic molecules as it is explained in the Subs. 5.3.2.

5.3.2 Polyatomic molecules vibrations

A polyatomic molecule is characterised by several vibrational degrees of freedom. Generally, each eigenfunction of the vibrational Hamiltonian depends on all the

vibrational coordinates. Therefore, Eq. (5.24) is equivalent to a set of $n_v = 3n_N - 6$ (or $n_v = 3n_N - 5$ if the molecule is linear) coupled differential equations and the velocity of each vibrational coordinate depends also on the positions of all the other vibrational degrees of freedom. In order to determine the vibrational motion either this set of differential equations has to be completely solved or some simplifications have to be taken into account in order to decrease the complexity of the problem. By employing some reasonable simplifications, an approximation of the motion would result, but hopefully preserving the main features of the vibrational dynamics.

For the purpose of supplying a good representation of the vibrations, the vibrational eigenfunctions can be conveniently simplified by employing their harmonic approximation. The nuclear potential can be well represented around the equilibrium geometry with the Harmonic potential and consequently each vibrational degree of freedom can be described as an independent Harmonic Oscillator. In the case of a molecule with n_v vibrational degrees of freedom, e.g., $n_v = 3$ for H_2O, the harmonic approximation separates the set q_v in monodimensional coordinates q_{v_i} (with $i = 1, 2, \ldots, n_v$) each corresponding to a different Harmonic Oscillator. Correspondingly the vibrational eigenfunctions are factorised into the product of independent eigenfunctions $\varphi_{k_{v_i}}(q_{v_i})$ each for any i-th Oscillator, as reported below for the ground state,

$$\varphi_{g_v}(q_v) = \prod_{i=1}^{n_v} \varphi_{g_{v_i}}(q_{v_i}). \tag{5.25}$$

The first vibrational excited state correspond to the excitation of a single Harmonic Oscillator. For instance, if the eigenfunction $\varphi_{k_v}(q_v)$ corresponds to the k_{v_j}-th excited state of the j-th Harmonic Oscillator, then it is equal to

$$\varphi_{k_v}(q_v) = \varphi_{k_{v_j}}(q_{v_j}) \prod_{i \neq j}^{n_v} \varphi_{g_{v_i}}(q_{v_i}). \tag{5.26}$$

This approximation of the zeroth-order Hamiltonian eigenstates leads to a simplified representation of the corresponding Bohm equation of motion.

Similarly to the case of vibrational, rotational and translational coordinates, the separation of the vibrational coordinates into a set of independent Harmonic oscillators corresponds to independent equations of motion for each oscillator if the degrees of freedom are separately excited. In this case the general equation of motion for the vibrational degrees of freedom interacting with an external field (Eq. (5.24)) can be simplified by substituting the generic φ_{g_v} and φ_{k_v} with their

harmonic counterparts Eq. (5.25) and Eq. (5.26):

$$\begin{cases} \dfrac{\mathrm{d}}{\mathrm{d}t}Q_{v_j} = \hbar \dfrac{\sqrt{P_{g_v}(t)P_{k_v}(t)}\sin\left(\omega_{k_{v_j},g_{v_j}}t\right)\left[\varphi_{k_{v_j}}\nabla_{v_j}\varphi_{g_{v_j}} - \varphi_{g_{v_j}}\nabla_{v_j}\varphi_{k_{v_j}}\right]}{P_{g_v}(t)\varphi^2_{g_{v_j}} + P_{k_v}(t)\varphi^2_{k_{v_j}} + 2\sqrt{P_{g_v}(t)P_{k_v}(t)}\varphi_{g_{v_j}}\varphi_{k_{v_j}}\cos\left(\omega_{k_{v_j},g_{v_j}}t\right)}\Bigg|_{\tilde{q}_{v_j}=\tilde{Q}_{v_j}(t)} \\ \dfrac{\mathrm{d}}{\mathrm{d}t}Q_{v_i} = 0 \quad \forall i \neq j \end{cases} . \tag{5.27}$$

Given the formal equivalence between the first equation reported above and the equation of motion for the bond distance of a diatomic molecule, one derives that the trajectory $Q_{v_j}(t)$ has the same main features of that displayed in Fig. 5.10 and Fig. 5.11 for diatomic molecule.

We would like to clarify two issues regarding the derivation of the above equation of motion for polyatomic molecules. First of all, the Harmonic approximation concerns only the vibrational eigenfunctions in such way that the Bohm equation for the coordinate of each degree of freedom is independent of the others. The transition frequencies can be determined either experimentally or computationally. It is obvious that this is a coarse grain method, but it is justifiable on the basis of the limited difference that can be observed for a diatomic molecule by substituting the Morse with the harmonic eigenfunctions (compare Fig. 5.5 and Fig. 5.11). Moreover, the accuracy of the approach should be sufficient if the transition involves the first few excited eigenstates as long as anharmonicity has a secondary role.

Secondly, the transformation from the normal modes to the cartesian coordinates is less obvious than for diatomic molecules. In particular, the matrix Ξ and the equilibrium geometry $q_{N,eq}$ of Eq. (5.18) has to be determined previously in order to transform the trajectory of the j-th vibrational coordinate into the trajectory of the cartesian coordinates corresponding to each atom. Even if the trajectory of the j-th vibrational degrees of freedom $Q_{v_j}(t)$ is substantially the same for every molecule, the resulting motion of the nuclei depends on the coordinate transformation formally described by the matrix Ξ. Moreover, one should take into account also the effects due to rotations and translations, but we neglect their effect in the following calculation in order to display only the feature of the vibrational motion.

As an example we consider the vibrations of H_2O molecule, that are the bending v_1, the symmetric stretching v_2 and the antisymmetric stretching v_3.

Equation (5.27) has to be solved in order to obtain the trajectories $Q_{v_1}(t)$, $Q_{v_2}(t)$ and $Q_{v_3}(t)$. To this end, one needs to know the resonance frequencies and the transition dipole moments. We computed the resonance frequencies by employing an

Hartree Fock method and 3-21G basis set. The calculations are run with *Gaussian09* [Frisch et al. (2009)]. Their values expressed in wavenumber are respectively 1799 cm^{-1}, 3813 cm^{-1} and 3946 cm^{-1}. The transition dipole moments for each transition are reported in literature [Shostak et al. (1991); Shostak and Muenter (1991)] and they are 0.126 D for the bending, 0.015 D for the symmetric stretching, and 0.015 D for the antisymmetric stretching. Also in this cases, we assume that the field magnitude is $\mathcal{E} = 3 \cdot 10^7$ V m^{-1} and that the molecule is initially in its equilibrium geometry $\tilde{Q}_N(0) = 0$. We adopted the 4-th order Runge-Kutta algorithm to solve the system of differential equations (5.27). Figure 5.12 displays the trajectory $Q_{v_2}(t)$ that represents the dynamics of the Harmonic Oscillator corresponding to the symmetric stretching. Over the time window examined the system is excited and

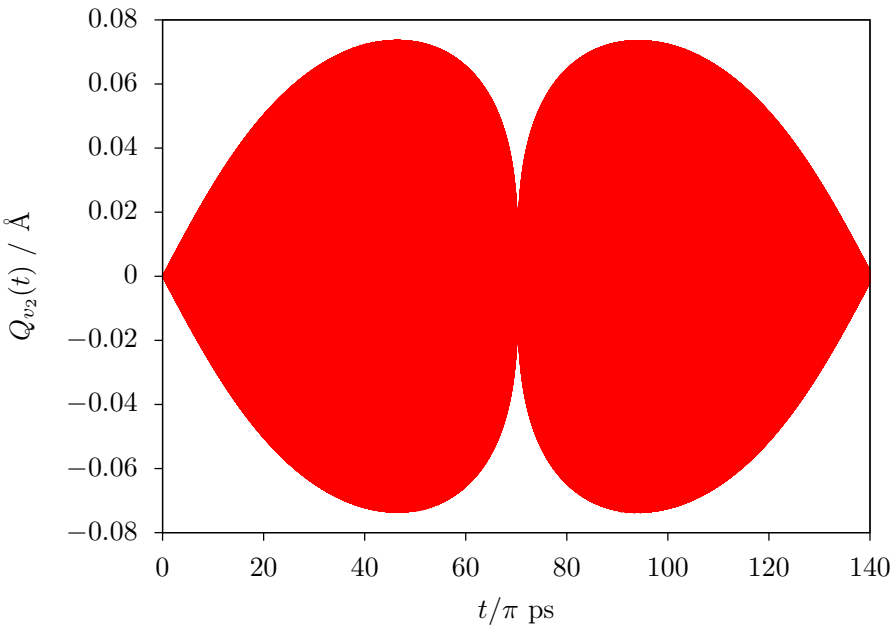

Figure 5.12: Time evolution over a long time interval of the Bohm coordinate corresponding to the symmetric stretching v_2 of H_2O. During the displayed time window, the transition of the v_2 vibrational degree of freedom between the ground and the first excited state occurs.

and then de-excited to the ground state. At $t/\pi \simeq 70$ ps the system is fully excited, P_1=1, and at $t/\pi \simeq 140$ ps it is in the ground state again. The time evolution of the coordinate $Q_{v_2}(t)$ keeps all the main features already observed and described for the change of the bond length of a diatomic molecule. It is an oscillation at the resonance frequency with a modulated amplitude. The behaviour of the other vibrational coordinates $Q_{v_1}(t)$ and $Q_{v_3}(t)$ has the same features examined in detail and the corresponding trajectories are not reported here.

Potentially more interesting, it is the corresponding nuclear motion. Knowing

Table 5.1: Equilibrium geometry of H_2O in the center of mass frame.

Atoms	x / Å	y / Å	z / Å
oxygen	0.0	0.0	0.0657
hydrogen	0.0	−0.7575	−0.5214
hydrogen	0.0	0.7575	−0.5214

the time evolution of the vibrational degrees of freedom, Eq. (5.18) allows the identification of the nuclear coordinates:

$$Q_N(t) = q_{N,eq} + m^{-1/2}\Xi\ \tilde{Q}_N(t) \tag{5.28}$$

where $Q_N(t)$ is the nuclear cartesian coordinates at time t whereas $\tilde{Q}_N(t)$ is the set of normal coordinates (vibrational, rotational and translational) at time t. Also the equilibrium geometry (Table 5.1) and the matrix Ξ have been determined through the HF/3-21G calculation. Since we neglect the effects of rotation and translation onto the nuclear motion, then each cartesian trajectory is equal to $Q_{v_2}(t)$ multiplied by one specific element of the matrix $m^{-1/2}\Xi$ and shifted by its equilibrium coordinate included in $q_{N,eq}$. For example, the motion of the two hydrogens projected onto the y axis is reported in Fig. 5.13. There it is displayed the dynamics over a short time interval during the excitation of the symmetric stretching v_2. It

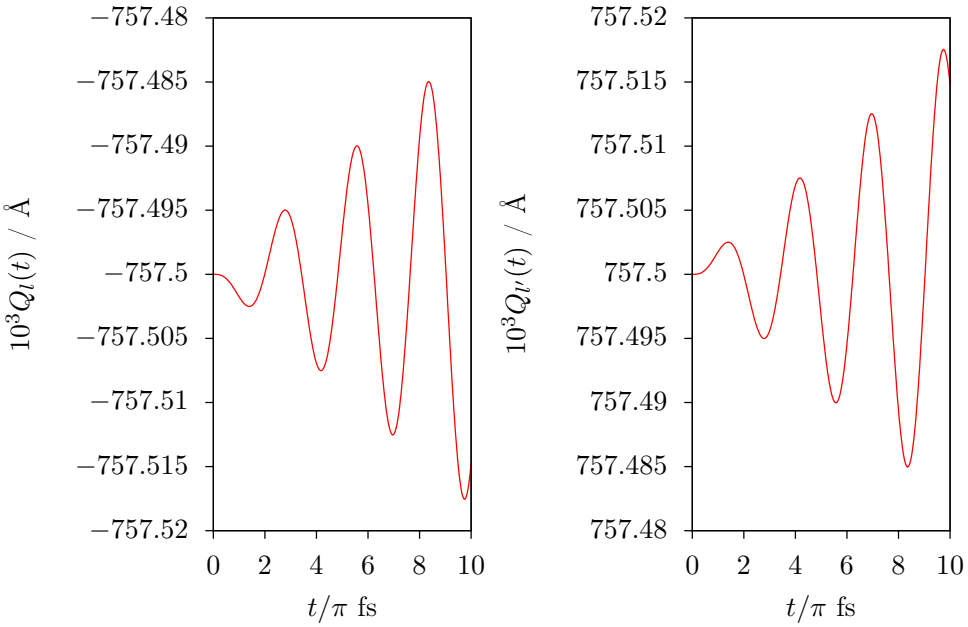

Figure 5.13: Bohm dynamics over a short time interval of the projection on the y axis of the first hydrogen coordinate $Q_l(t)$ and of the second hydrogen coordinate $Q_{l'}(t)$ during the symmetric stretching transition.

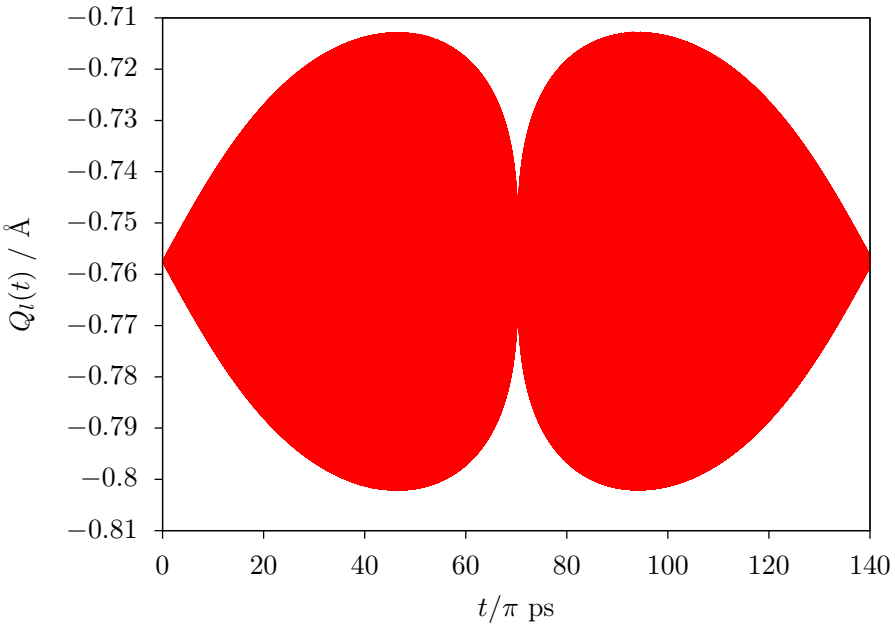

Figure 5.14: Time evolution over a long time interval of the Bohm coordinate $Q_l(t)$ corresponding to the y component of one hydrogen atom during the symmetric stretching transition.

can be seen that the motion is still an oscillation at the resonance frequency and with time dependent amplitude. Furthermore, both the hydrogen nuclei increase or decrease their distance from the center of mass simultaneously. In this way the nuclei describe a symmetric stretching. Over a long time scale the motion has again the same characteristics as in Fig. 5.14 for one of the two hydrogen atom. Similar consideration can be applied to the antisymmetric stretching, whose trajectory is dispalyed in Fig. 5.15. As expected, the distance between the center of mass and one hydrogen nucleus increases while the distance between the center of mass and the other hydrogen nucleus other decreases.

Finally, we would like to emphasise the similarity between the profile of the cartesian trajectory in Fig. 5.14 and the stretching in Fig. 5.12. This reveals that the main features of the vibrational motion of molecules, both diatomic and polyatomic, are substantialy the same: the motion of each coordinate is an oscillation at the resonance frequency and with a modulated amplitude.

5.4 Final remarks

In conclusion, we have been able to develop an approximate method that can describe the motion of molecules interacting with an oscillatory field in the framework of the single Bohm trajectory approach. In particular, we have been inspired by the

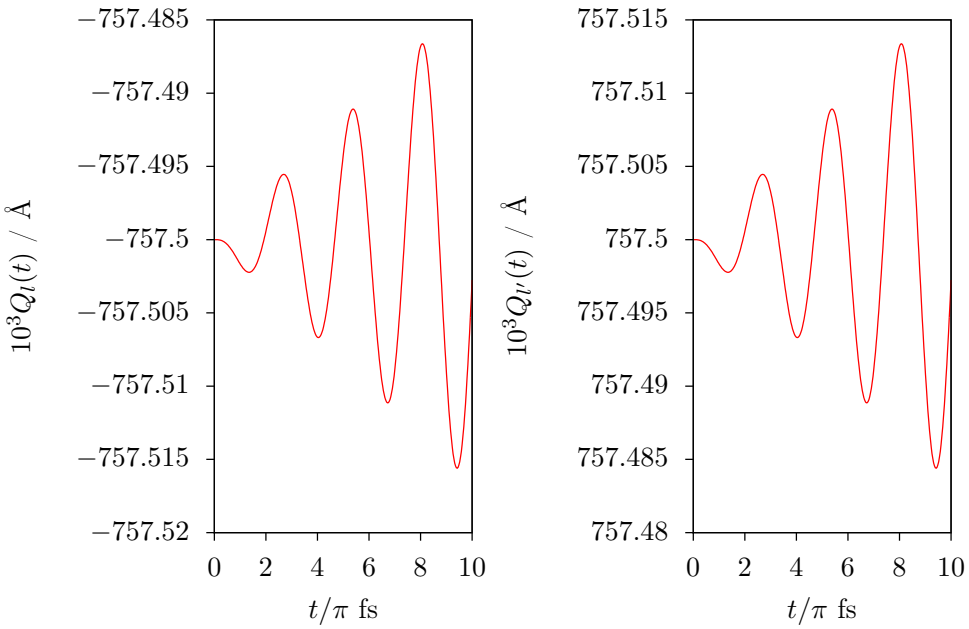

Figure 5.15: Bohm dynamics over a short time interval of the projection on the y axis of the first hydrogen coordinate $Q_l(t)$ and of the second hydrogen coordinate $Q_{l'}(t)$ during the antisymmetric stretching transition.

perturbation methods for solving the Schrödinger equation and we have proposed approximate Bohm equations that take into account the interaction with the external field (see Eq. (5.13) and Eq. (5.6)). Moreover, the method has been employed to describe the vibrations of isolated diatomic and polyatomic molecules, when an external radiation causes the transition from the ground to an excited vibrational state. The resulting motion is qualitatively an oscillation with modulated amplitude depending on the relative population of the states involved in the process. The advantage of this approach is its capability to supply a characterisation of the molecular motion within a full quantum framework. It has to be emphasised that the modulation of the oscillation is the main quantum feature: in Classical Mechanics a complete excitation of the system ($P_k = 1$) corresponds to a higher energy that qualitatively means a larger amplitude of the vibration. On the contrary, with the single Bohm trajectory approach, if the wave function is a stationary state then the system is motionless. The stationary states correspond to mechanical equilibrium conditions for the Bohm coordinates.

Part II

Statistical Mechanics of a single Bohm trajectory

CHAPTER 6

Typicality of a single Bohm trajectory

As it has been already mentioned several times, Bohm theory is a deterministic quantum theory such that the molecular motion can be exactly predicted by solving the Bohm and the Schrödinger equation once the initial conditions (initial configuration and initial wave function) are established. In particular, the configuration evolves by drawing continuous trajectory like in Classical Mechanics and defines univocally the spatial position of the particles at any time.

However, the computational efforts that are necessary for solving the equations of motion represent always limitations of any deterministic theory, not only of Bohm theory. In other words, even if the behaviour of a system is well described according to a particular theory, the difficulties for solving the dynamical equations can make the description impracticable. For instance, the dynamical evolution of a macroscopic volume of water composed of an Avogadro's number of molecules can not be computed even with Classical Molecular Dynamics simulations that are well known for the low computational cost of the corresponding algorithms (compared to the quantum chemistry methods): the huge number of variables characterising a macroscopic volume of water makes this system unmanageable. Moreover, the solutions of the dynamical equations can be unstable. Consider for example the Brownian motion when the system is described according to Classical Mechanics. Even if the equations of motion could be solved exactly for both the solvent molecules and the Brownian particle, negligible differences in the initial conditions correspond to completely different trajectories of the Brownian particle. Therefore, the round-off error of a computer is sufficient to produce completely different trajectories with

respect to the theoretical exact one. This behaviour emerges typically from the complex network of interactions between the solvent and the Brownian particle and it is rather common for systems composed of many molecules.

The same difficulties characterise also the Bohm theory. For instance, the exponential growth of the computational cost for solving the Schrödinger equation with the number of degrees of freedom is a well known fact that restricts significantly the dimension of the system that can be investigated. In parallel, the Bohm equation is strongly unstable even for small systems [Efthymiopoulos et al. (2007); Wu and Sprung (1999); de Alcantara Bonfim et al. (1998); Frisk (1997)]. Thus, the application of Bohm theory for describing chemical systems composed of many molecules is very computational demanding. In other words, the theoretical advantages of well representing molecules in a quantum framework seem to be in conflict with the strong practical limitations. Therefore, one may wonder if there is a way of overcoming the difficulties of the deterministic theory, but conserving some (at least) of its advantages at the same time.

The answer is affirmative and statistical methods can be developed for this purpose. For instance, Classical Statistical Mechanics succeeds in rationalising the general behaviour of portions of matter when the systematic description based on Classical Mechanics is completely powerless because of the insurmountable obstacle of solving the equations of motions [Khinchin (1949)]. The general idea consists in shifting the focus from a single state (the set of positions and momenta of all the particles in Classical Mechanics) to a density distribution on the space of all possible states (phase space) that evolves in time according to the Liouville's theorem [Schwabl and Brewer (2006)]. The density distribution describes the probability to observe the system in a particular state and it allows the calculation of the average values corresponding to physical properties at any time. In this way the details of the evolution of the system are neglected and the statistical properties emerge. Notice that the Liouville theorem has no a great relevance in itself as regards Classical Mechanics: it is of fundamental importance for inferring statistical methods. Conversely, its relevance in the framework of Bohm theory is not limited to the definition of stochastic equations (see Chap. 7), but it concerns also the correspondence between conventional Quantum Mechanics and Bohm theory.

Therefore, we propose to proceed similarly to Classical Mechanics also for Bohm theory: by defining a density distribution (or probability density) on the space of all possible states (that are all the possible pairs of configuration and wave function) and by determining the corresponding evolution by inferring the Bohm's counterpart

of the Liouville's theorem. We would like to emphasise that we are not giving up to the description of the molecular motion according to a single Bohm trajectory. The statistical characterisation is necessary in order to well represent the properties of a complex system composed of many molecules (that is perhaps the most common and interesting chemical system). In any case, the single Bohm trajectory approach has to be considered the basic description, whereas the corresponding statistical formulation is a necessary rough representation. Furthermore, the statistical predictions can be partial explained on the basis of the deterministic dynamics based on the single Bohm trajectory.

We aim to characterise statistically Bohm theory in order to highlight some specific properties of the corresponding dynamics that are hidden in the complexity of the deterministic description. In Chap. 7, we use statistical approaches for developing stochastic methods that can describe the molecular motion in the framework of Bohm theory also for complex chemical systems. In this chapter, we lay the foundations of this statistical method that is used in order to formally prove the existence of a correspondence between the predictions of the conventional Quantum Mechanics and those of the single Bohm trajectory approach. In more details, we define first of all the Bohm's counterpart of the Liouville's theorem in Sec. 6.1 and its formulation in the invariant subspaces Sec. 6.2. Secondly, we prove that the statistical description is strictly related to the deterministic one in Sec. 6.3. In particular, it can be demonstrated that the average of an observable on the equilibrium density distribution (that is the stationary solution of the Liouville equation) is equivalent to the time average of the same observable along a single trajectory for almost all possible initial states. The time average can be considered a typical value of the observable, since it is independently of the initial conditions. This property is usually related to the ergodicity: the evolution of a single state samples the dynamical space according to the equilibrium density distribution. Furthermore, the correspondence between the statistical description and the deterministic dynamics is sufficient to establish also a formal correspondence between the single Bohm trajectory approach and the conventional Quantum Mechanics (Sec. 6.4). In other words, the statistical representation, which is defined and characterised in this chapter, allows the formalisation of the correspondence highlighted in Chap. 3 and in particular in Fig. 3.7 through the numerical simulation. This formalisation has to be considered the main result reported in this chapter since it proves the existence of an equivalence (under some reasonable constraints) between the predictions of the conventional Quantum Mechanics and the single Bohm trajectory approach beyond the numerical observa-

tion of Sec. 3.2.3 and the *a priori* explanation of Sec. 3.3. In this way we support formally our proposal of describing molecular systems according to a single Bohm trajectory.

6.1 Liouville's theorem

In the framework of Classical Mechanics, the Liouville's theorem defines the evolution of a probability density on the space of all possible states (hereafter called dynamical space) for ensuring the conservation of the probability for a subset of possible states. The differential equation that describes the evolution of the probability density is called in literature Liouville equation. In order to develop the corresponding theorem for Bohm theory, first of all one has to identify the suitable dynamical space. Secondly, the dynamical equation for the probability density has to be inferred by imposing the conservation of the local probability. In the following, both these two steps are examined in detail.

It is well known that the dynamical space is the phase space in the framework of Classical Mechanics: it is the set of the possible positions and momenta of all the particles of the system. By analogy, the dynamical space in the framework of Bohm theory is the set of all possible pairs of configuration and wave function. Therefore, it can be identified with the cartesian product of the space of coordinates, i.e., the configuration space $\mathcal{C}$, and the Hilbert space $\mathcal{H}$:

$$\mathcal{C} \times \mathcal{H}. \tag{6.1}$$

Besides this simple consideration, an important issue arises: how can a probability density on this space be defined? The source of the issue is the mathematical deep difference between the configuration space and the Hilbert space. Broadly speaking, the configuration space is a set of points $\{q\}$ whereas the Hilbert space elements are functions $\{\psi(\bullet)\}$. Notice that we use a different notation for the component of a generic system state $\big(q, \psi(\bullet)\big)$ with respect to component of the actual system state $\big(Q(t), \Psi(q,t)\big)$ similarly to what we have already done for the wave function variable q and the specific coordinates at time t, $Q(t)$, in Sec. 2.1: from this point forward we employ capital letters, such as $Q(t)$ and $\Psi(q,t)$, to indicate the system state at time t and the corresponding lowercase symbols, such as q and $\psi(\bullet)$, to indicate respectively generic elements of the sets $\mathcal{C}$ and $\mathcal{H}$ independently of the actual conditions of the system. Moreover, the previous question has no obvious answer because of the difficulties regarding to the definition of a density distribution

on a space of function as the Hilbert space. However, by drawing inspiration from previous works concerning the statistics of quantum pure states [Goldstein et al. (2006); Fresch and Moro (2009, 2010a,b, 2011)], a suitable assumption can be made. Despite a Hilbert space is generally infinity dimensional, we suppose the system's wave function belongs to a finite dimensional Hilbert space in order to exploit its fundamental properties and simplifying the problem. We consider a N-dimensional Hilbert space $\mathcal{H}_N$, called active space, instead of a generic Hilbert space $\mathcal{H}$ and we represent a generic wave function $\psi(\bullet)$ belonging to $\mathcal{H}_N$ according to its components along the orthonormal basis set $\{\phi_k(q)\}$:

$$\psi(q) = \sum_{k=1}^{N} c_k \phi_k(q), \tag{6.2}$$

where each $c_k = \langle \phi_k | \psi \rangle$ is a complex number, $c_k \in \mathbb{C}$. Once the basis set $\{\phi_k(q)\}$ is established, each wave function $\psi(\bullet) \in \mathcal{H}_N$ can be univocally identified with a specific set of $2N$ real coefficients $c := \{\mathrm{Re}(c_k), \mathrm{Im}(c_k)\} \in \mathbb{R}^{2N}$ which is the representation of the wave function on the basis set $\{\phi_k(q)\}$. In this way each possible state in the framework of Bohm theory, $\big(q, \psi(\bullet)\big)$, can be identified with the variable z,

$$z := (q, c), \tag{6.3}$$

defined as the set of configuration and of the wave function expansion coefficients. The variable z has $n+2N$ components: q includes the n coordinates for each degree of freedom $q = (q_1, q_2, \ldots, q_n)$ whereas c includes the real and imaginary part of each of the N coefficients $c = \big(\mathrm{Re}(c_1), \mathrm{Im}(c_1), \ldots, \mathrm{Re}(c_N), \mathrm{Im}(c_N)\big)$. The corresponding dynamical space Ω_0 is the cartesian product of the configuration space $\mathcal{C}$ and of the coefficients' domain $\mathcal{D}$:

$$\Omega_0 = \mathcal{C} \times \mathcal{D}. \tag{6.4}$$

In this particular space Ω_0, that broadly speaking it is a set of points, a generic probability density $\varrho^{\Omega_0}(z,t)$ finds an obvious definition similar to that of a probability density in Classical Statistical Mechanics: it is an integrable function in Ω_0 with unitary normalisation [Schwabl and Brewer (2006)]. Furthermore, the actual system state $\big(Q(t), \Psi(q,t)\big)$ is well represented by

$$Z(t) := \big(Q(t), C(t)\big), \tag{6.5}$$

with $C(t) = \big\{\mathrm{Re}(C_k(t)), \mathrm{Im}(C_k(t))\big\}$ and $C_k(t) = \langle \phi_k | \Psi(t) \rangle$. Let us recall that with

our notation the capital letters, i.e., $Q(t)$ and $C(t)$, represent the actual system state whereas the lowercase symbols, i.e., q and c, symbolise the generic element of Ω_0. In this regard, the time evolution of $Z(t)$ can be described according to the velocity field $\Lambda_0(z)$,

$$\frac{\mathrm{d}}{\mathrm{d}t}Z(t) = \Lambda_0\big(Z(t)\big). \tag{6.6}$$

The velocity field $\Lambda_0(z)$ includes the Bohm equation for the coordinate of each degree of freedom in the first n components ($\Lambda_{0,j}$ with $j = 1, 2, \ldots, n$) and the representation of the Schrödinger equation on the basis set $\{\phi_k\}$ for the real and the imaginary part of each coefficient $C_k(t)$ respectively in the components $\Lambda_{0,n+2k-1}$ and $\Lambda_{0,n+2k}$ with $k = 1, 2, \ldots, N$. The explicit form of $\Lambda_0(z)$ is reported in the following for the sake of completeness:

$$\Lambda_{0,j}(q,c) = \frac{\hbar}{m_j}\mathrm{Im}\left\{\frac{\sum_{l,l'}^{N} c_l^* c_{l'} \phi_l^*(q)\nabla_j\phi_{l'}(q)}{\sum_{l,l'}^{N} c_l^* c_{l'}\phi_l^*(q)\phi_{l'}(q)}\right\}, \text{ with } j = 1, 2, \ldots, n, \tag{6.7}$$

$$\Lambda_{0,n+2k-1}(c) = -\frac{\imath}{2\hbar}\left\{\sum_{l=1}^{N}\langle\phi_k|\hat{H}|\phi_l\rangle\, c_l + \langle\phi_l|\hat{H}|\phi_k\rangle\, c_l^*\right\}, \text{ with } k = 1, 2, \ldots, N, \tag{6.8}$$

$$\Lambda_{0,n+2k}(c) = -\frac{1}{2\hbar}\left\{\sum_{l=1}^{N}\langle\phi_k|\hat{H}|\phi_l\rangle\, c_l - \langle\phi_l|\hat{H}|\phi_k\rangle\, c_l^*\right\}, \text{ with } k = 1, 2, \ldots, N. \tag{6.9}$$

Notice that Eq. (6.7) is the Bohm equation, Eq. (2.5), for the k-th degree of freedom with the wave function specified as a linear combination of the basis set elements $\{\phi_k(q)\}$. Equation (6.8) and Eq. (6.9) are respectively the dynamical equation for the real and imaginary part of the coefficient $C_k(t)$ obtained by representing the Schrödinger equation on the basis set $\{\phi_k(q)\}$. Furthermore, as the wave function evolution described according to the Schrödinger equation is completely independent of the configuration evolution (see for example Eq. (2.9)), also the time evolution of the set of coefficients described according to Eq. (6.8) and Eq. (6.9) is also independent of the coordinates evolution. In other words, the independence of the conventional quantum variables with respect to the Bohm variables is preserved also in the representation above defined as one can easily verify.

Once the dynamical space is well characterised, then the Liouville equation can be inferred by imposing the conservation of the local probability. The procedure for defining the Liouville equation from that constraint is precisely the Liouville's theorem and it is presented in the following in reference to Bohm theory.

Let $\varrho^{\Omega_0}(z, 0)$ be an arbitrary initial density probability on the space Ω_0 and $V(0) \subseteq \Omega_0$ be a subset of possible states in Ω_0. Then, the probability that the

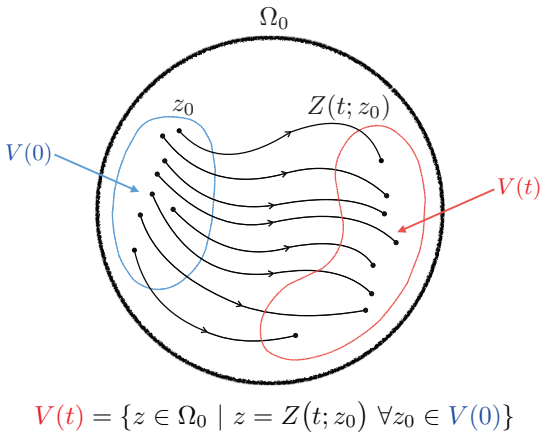

Figure 6.1: Graphical representation of the dynamical space Ω_0. The subset $V(t) \subseteq \Omega_0$ is the set of states that evolve from the subset $V(0) \subseteq \Omega_0$ along the curve $Z(t;z_0)$. In the figure, some elements of $V(0)$ are connected to the corresponding elements of $V(t)$ through hypothetical curves.

actual system state is initially one of the states belonging to $V(0)$ is specified as

$$\mathcal{M}\big(V(0)\big) := \int_{V(0)} \mathrm{d}z\ \varrho^{\Omega_0}(z,0). \tag{6.10}$$

In other words, $\mathcal{M}\big(V(0)\big)$ is the probability measure that the initial state of the system is one of the possible sets of configuration and wave function represented by the points $z \in V(0)$ according to the probability density $\varrho^{\Omega_0}(z,0)$. Since this probability is also called the "measure" of the set $V(0)$, it has been labeled with the symbol $\mathcal{M}\big(V(0)\big)$. Consider now each possible state of the system at time t whose corresponding initial state (at time $t = 0$) belongs to $V(0)$ through the deterministic evolution: by solving Eq. (6.6) one obtains the curve $Z(t;z_0)$ that maps each initial state z_0 into the corresponding state at time t, that is $z = Z(t;z_0)$. In our representation this curve maps the initial configuration and wave function (symbolised by z_0) to the configuration and wave function at time t (symbolised by z). In this way one can define another subset of possible states in Ω_0: $V(t) \subseteq \Omega_0$ is the subset of states that evolved from the states in $V(0)$ along the curves $Z(t,z_0)$ $\forall z_0 \in V(0)$. Formally it is defined in the next equation:

$$V(t) = \{z \in \Omega_0 \mid z = Z\big(t;z_0\big)\ \forall z_0 \in V(0)\}. \tag{6.11}$$

See Fig. 6.1 for a graphical representation of the definition of $V(t)$. One can recognise that $V(t)$ is nothing more than the evolution of the states initially belonging to $V(0)$. For this reason the probability that the initial state of the system is one of the states

in $V(0)$ and the probability that the state of the system at time t is one of the states in $V(t)$ have to be the same,

$$\mathcal{M}\big(V(0)\big) = \int_{V(0)} \mathrm{d}z \; \varrho^{\Omega_0}(z,0) = \int_{V(t)} \mathrm{d}z \; \varrho^{\Omega_0}(z,t) = \mathcal{M}\big(V(t)\big), \tag{6.12}$$

by ensuring the conservation of the local probability. This constraint defines univocally the evolution of the probability density $\varrho^{\Omega_0}(z,t)$ since it has to be valid for every pair of subsets $\big(V(0), V(t)\big)$ and for every time interval. This means that it defines the Liouville equation. The precise derivation of the Liouville equation from Eq. (6.12) is summarised in Appendix B, whereas here we report the final result:

$$\frac{\partial}{\partial t}\varrho^{\Omega_0}(z,t) + \nabla_z \cdot \Lambda_0(z)\varrho^{\Omega_0}(z,t) = 0, \tag{6.13}$$

where $\nabla_z = (\partial/\partial z_1, \ldots, \partial/\partial z_n, \partial/\partial z_{n+1}, \ldots, \partial/\partial z_{n+2N})$ and each partial derivative corresponds to a partial derivative either in terms of coordinates q or in terms of coefficients c according to the definition of z in Eq. (6.3). The first n components of ∇_z are the partial derivatives of the coordinates, while the remaining $2N$ are the partial derivatives of the real and imaginary part of each coefficient. In this way the Bohm's counterpart of the Liouville equation has been established.

At this stage one could employ the Liouville equation for studying the evolution of a generic probability density. However, our interest concerns mainly the correspondence between the description based on the single Bohm trajectory approach and that based on the statistical approach in order to establish also the correspondence with the predictions of the conventional Quantum Mechanics. For this purpose, Liouville equation can be further simplified by focusing on some suitable subspaces of Ω_0 called invariant parts or invariant manifold/subspaces [Hirsch et al. (1977)]. The invariant subspaces of Ω_0 are subspaces with the property that an arbitrary state belonging to one of this subspace remains inside it during the natural evolution. In other words, if z_0 belongs to an invariant, then all the points of curve $Z(t; z_0)$ belong to the same invariant. In the Sec. 6.2 we propose a suitable separation of the dynamical space in its invariant subspaces that facilitates the successive analyses.

6.2 Invariant subspaces

In the framework of deterministic theories, like Classical Mechanics or Bohm theory, the relevance of the invariant subspaces is related to the dimensional reduction associated to their identification [Khinchin (1949)]. For example, the energy

of isolated systems is conserved in Classical Mechanics. Consequently, if a system is characterised by a certain value of energy, then one can identify a subspace of the phase space (usually called surface of constant energy) whose states are characterised by that precise value of energy and all the points of the curve describing the state evolution belong to this subspace. In other words, the value of the energy represents a constraint that has to be satisfied during the time evolution and it formally implies the reduction of the number of the degrees of freedom. If other constraints are identified, then the number of degrees of freedom is further reduced.

The same idea can be employed also in the framework of Bohm theory. In this case there are three important advantages: the dimensional reduction, the identification of a suitable set of variables for describing the dynamics within the invariant subspaces and the simplification of the dynamical equations (in particular those representing the Schrödinger equation). By recalling that all the constants of motion in the framework of Bohm theory are related to the wave function dynamics (see Chap. 4), then the constraints identifying the invariants must concern the representation of the wave function in terms of its expansion coefficients c. Furthermore, we have already examined in Chap. 3 a representation of the wave function that highlights the constants of motion. Instead of representing the wave function on a generic basis set, one can use the eigenfunctions of the Hamiltonian operator, $\hat{H}\phi_k(q) = E_k\phi_k(q)$. In this way the coefficients $C_k(t) = \langle\phi_k|\Psi(t)\rangle$ can be specified in polar form,

$$C_k(t) = \sqrt{P_k}e^{-\imath A_k(t)}, \tag{6.14}$$

in terms of constant populations $\{P_k\}$ and time dependent phases $\{A_k(t)\}$. As already mentioned in Chap. 3, the wave function at a given time $\Psi(q,t)$ is conveniently specified through the set of $N-1$ populations $P = (P_1, P_2, \ldots, P_{N-1})$ (one population is determined by the normalisation condition, see Eq. (3.10)) and the N phases $A = \big(A_1(t), A_2(t), \ldots, A_N(t)\big)$. Therefore, the actual system state in the framework of Bohm theory can be represented with the set of configuration, phases and populations $\big(Q(t), A(t), P\big)$ instead of $Z(t)$ (Eq. (6.5)). In parallel, the set (q, α, P) replaces the variable z (Eq. (6.3)). Notice that we use capital letter for the populations set also without reference to the actual state in order to stress the time independence of these parameters. The whole dynamical space Ω_0 is then separated into different disjoint subspaces Ω_P each of then corresponding to a particular set of populations,

$$\Omega_0 = \bigcup_P \Omega_P, \tag{6.15}$$

for all the possible sets of populations. Since each element of the subspace Ω_P, that is each configuration and each wave function for a given set of populations, is fully specified in terms of coordinates and phases, we introduce the new variable

$$x := (q, \alpha). \tag{6.16}$$

Correspondingly, Ω_P is parameterised with respect to the populations and it corresponds to the cartesian product of the configuration space $\mathcal{C}$ and of the pahses' domain:

$$\Omega_P = \mathcal{C} \times [0, 2\pi)^N. \tag{6.17}$$

Notice that the domain of each phase variable is periodic between $[0, 2\pi)$ by definition. Furthermore, the evolution of the system state is completely described within the given subspace Ω_P and it can be represented by the time dependent variable

$$X(t) := \big(Q(t), A(t)\big) \in \Omega_P. \tag{6.18}$$

In other words, the sets Ω_P are the invariants of the dynamical space in the framework of Bohm theory. The subspaces Ω_P are the counterpart of the surfaces of constant energy in Classical Mechanics. The set of coordinates and phases identifies completely a particular configuration and a particular wave function once the invariant subspace has been selected, so determining a significant reduction of the dynamical variables. The state is univocally identified by z (Eq. (6.3)) that is the set of $n + 2N$ variables (coordinates q and coefficients c) in the whole dynamical space Ω_0, whereas it is univocally identified by x (Eq. (6.16)) that is the set of $n + N$ variables (coordinates q and phases α) in the invariant subspace Ω_P. Also the velocity field $\Lambda_P(x)$ describing the dynamical equation for $X(t)$,

$$\frac{\mathrm{d}}{\mathrm{d}t} X(t) = \Lambda_P\big(X(t)\big), \tag{6.19}$$

is simpler than $\Lambda_0(z)$ (see Eq. (6.7), (6.8), (6.9)):

$$\Lambda_{P,j}(q, \alpha) = \frac{\hbar}{m_k} \mathrm{Im} \left\{ \frac{\sum_{l,l'}^{N} \sqrt{P_l P_{l'}} e^{-\imath(\alpha_{l'} - \alpha_l)} \phi_l^*(q) \nabla_k \phi_{l'}(q)}{\sum_{l,l'}^{N} \sqrt{P_l P_{l'}} e^{-\imath(\alpha_{l'} - \alpha_l)} \phi_l^*(q) \phi_{l'}(q)} \right\} \quad \text{with } j = 1, 2, \ldots, n \tag{6.20}$$

$$\Lambda_{P,n+k} = E_k/\hbar \equiv \omega_k \qquad \text{with } k = 1, 2, \ldots, N \tag{6.21}$$

Equation (6.20) is equivalent to the Bohm equation, Eq. (2.5), for the k-th degree of freedom, once the wave function is expressed as a linear combination of the Hamiltonian operator eigenfunctions and its time dependence is replaced by the phases dependence. On the other hand, Eq. (6.21) is the representation of the Schrödinger equation in terms of phases, leading to their time dependence in the form $A_k(t) = A_k(0) + E_k t/\hbar$ for every k.

Because of the advantages that emerge by employing the invariants, i.e., the reduction of dynamical variables and the simple representation of the wave function evolution according to the phases, we focus on a single invariant subspace in the following: we describe the evolution of both the Bohm state and the corresponding probability density within a given invariant subspace instead of examining it in the complete dynamical space. In this way, we assume implicitly that the populations of the quantum system are known, since they determine univocally the invariant subspace. This is similar to the idea of knowing the energy of the system in Classical Mechanics. Like with the impossibility of determining the exact energy of classical systems, there are neither theoretical methods nor experimental techniques that allow a complete characterisation of the initial wave function and, consequently, also of the populations. However, we aim to investigate the molecular motion according to the Bohm coordinates and therefore we can suppose that the system populations are established as well as it is commonly postulated that the system energy is known in Classical Mechanics.

In this regard, the probability density $\varrho^{\Omega_P}(x,t)$ on Ω_P can be defined similarly to what we have already done for Ω_0, and it describes the probability that the system state at time t is the set of configuration and phases represented by the point $x \in \Omega_P$. By imposing the conservation of the local probability, the following Liouville equation can be derived for $\varrho^{\Omega_P}(x,t)$

$$\frac{\partial}{\partial t}\varrho^{\Omega_P}(x,t) + \nabla_x \cdot \Lambda_P(x)\varrho^{\Omega_P}(x,t) = 0, \tag{6.22}$$

where $\nabla_x = (\partial/\partial x_1, \ldots, \partial/\partial x_n, \partial/\partial x_{n+1}, \ldots, \partial/\partial x_{n+N})$ with each partial derivative corresponding to a partial derivative either of a coordinate q_k or of a phase α_k according to the definition of x in Eq. (6.16). The first n components of ∇_x are the partial derivatives of the coordinates while the remaining N ones are the partial derivatives of the phases. In order to prove that the the predictions of the deterministic evolution correspond to those of the statistical representation in Ω_P, the fundamental ingredient is provided by the equilibrium density distribution $\varrho_{eq}^{\Omega_P}(x)$,

that is the stationary solution of the Liouville equation

$$\nabla_x \cdot \Lambda_P(x)\varrho_{eq}^{\Omega_P}(x) = 0. \tag{6.23}$$

Indeed, the deterministic evolution of a particular initial state x_0 should sample the space Ω_P according to $\varrho_{eq}^{\Omega_P}(x)$ in ergodic conditions. However, a direct solution of the above equation is rather complicated in general. An easier strategy consists in guessing the solution and in verifying if it satisfies the constraint of Eq. (6.23). We were inspired by the works of A. Valentini [Valentini (1991a,b)], where he investigated the properties of the configuration space $\mathcal{C}$ in the framework of Bohm theory and its statistical features. In particular, Valentini recognised that the square modulus of the wave function satisfies the continuity equation emerging from the natural dynamics in the configuration space $\mathcal{C}$ and it represents consequently an invariant measure of the configuration space. By bearing in mind that the time dependence of the wave function is represented by the phases α in our formalism, we identify the stationary solution for each invariant subspace:

$$\varrho_{eq}^{\Omega_P}(x)\Big|_{x=(q,\alpha)} = \sum_{k,k'} \frac{\sqrt{P_k P_{k'}}}{(2\pi)^N} e^{-\imath(\alpha_{k'}-\alpha_k)} \phi_k^*(q)\phi_{k'}(q), \tag{6.24}$$

where $\{\phi_k(q)\}$ are the eigenfunctions of the Hamiltonian operator. One can recognise that the equilibrium density distribution $\varrho_{eq}^{\Omega_P}(x)$ of Ω_P is the square modulus of the wave function where the time dependence has been replaced by the phases dependence:

$$\varrho_{eq}^{\Omega_P}(q,\alpha)\big|_{\alpha=A(t)} = \frac{|\Psi(q,t)|^2}{(2\pi)^N} \tag{6.25}$$

with a suitable choice of the phases $A(t)$. Indeed, the condition of Eq. (6.23) can be rewritten as in the following by making explicit the partial derivatives,

$$\sum_{k=1}^{N} \frac{\partial}{\partial \alpha_k} \omega_k \varrho_{eq}^{\Omega_P}(q,\alpha) + \sum_{k=1}^{n} \frac{\partial}{\partial q_k} \Lambda_{P,k}(q,\alpha)\varrho_{eq}^{\Omega_P}(q,\alpha) = 0. \tag{6.26}$$

The above equation is satisfied by the equilibrium distribution of Eq. (6.24), because of its equivalence with the continuity equation solved by the square modulus of the wave function:

$$\frac{\partial}{\partial t}\big|\Psi(q,t)\big|^2 + \nabla \cdot \Lambda_{\mathcal{C}}(q,t)\big|\Psi(q,t)\big|^2 = 0, \tag{6.27}$$

where $\Lambda_{\mathcal{C}}(q,t)$ is the Bohm velocity field according to the notation defined in Chap. 5

(see Eq. (5.3)). The only difference between Eq. (6.26) and Eq. (6.27) is that the second one is expressed implicitly for a particular set of phases associated to the specific wave function at time t (that means a specific set of phases $A'(t)$ such that $|\Psi(q,t)|^2 \propto \varrho_{eq}^{\Omega_P}(q, A'(t))$) whereas the first one is its generalisation for each possible set of phases.

In the Sec. 6.3 we employ the equilibrium density distribution $\varrho_{eq}^{\Omega_P}(x)$ in order to establish the correspondence with the deterministic evolution. Moreover, we will show that this correspondence is also the starting point for explaining the predictions of the conventional Quantum Mechanics in terms of statistical properties of a single Bohm trajectory.

6.3 Ergodicity of the single Bohm trajectory

Despite the title of this section is "Ergodicity of the single Bohm trajectory", we have to admit that an ergodic theorem appears to be indemonstrable in the framework of Bohm theory exactly as it has been unprovable in the framework of Classical Mechanics. By ergodicity we mean that the evolution of the system state (the curve) samples the dynamical space according to the equilibrium density distribution supplied by the Liouville equation independently of the initial conditions. An obvious counterexample in Classical Mechanics is given by the nonexistence of a curve that can move from a invariant subspace of the phase space to another by definition of invariant subspace: a single curve can not sample the whole dynamical space. In the framework of Bohm theory, we have been less ambitious: we limited ourself by considering the dynamics and the evolution of the probability density inside an invariant subspace, Ω_P. However, it is not ensured that a subspace Ω_P can not be further divided in smaller invariant subspaces. This is for instance the case of $P_l = \delta_{l,k}$ for given k (that is the case of a stationary state) in the absence of degeneration, where the Bohm equation predicts that all the coordinates are at rest. Therefore, if the coordinates do not change in time there are no trajectories sampling the space Ω_P according to the distribution $\varrho_e^{\Omega_P} q(q,\alpha) = |\phi_k(q)|^2$ for every possible initial configuration $Q(0)$.

Nevertheless, we can prove that some predictions of the single Bohm trajectory approach and those of the statistical description are compatible under reasonable conditions. Let us consider a generic observable that depends on the coordinates $B(q)$ and its average on the space Ω_P according to the equilibrium density distribu-

tion (that hereafter we call equilibrium statistical average),

$$\mathbb{E}^{\Omega_P}_{eq}[B] := \int_{\Omega_P} \mathrm{d}q\mathrm{d}\alpha \; B(q)\varrho^{\Omega_P}_{eq}(x)\big|_{x=(q,\alpha)}. \tag{6.28}$$

Consider also a generic initial state $x_0 \in \Omega_P$ and the curve $X(t;x_0)$ which is the solution of Eq. (6.19) with x_0 as the initial condition. The corresponding Bohm trajectory is the projection of the curve $X(t;x_0)$ on the configuration space $\mathcal{C}$ and it is labeled $Q(t;x_0)$ in order to stress the dependence on the initial state x_0.[1] Then, the time average of $B(q)$ along the Bohm trajectory,

$$\overline{B}(x_0) := \lim_{T\to+\infty} \frac{1}{T}\int_0^T \mathrm{d}t \; B\big(Q(t;x_0)\big), \tag{6.29}$$

depends in general on the initial state x_0: different initial states correspond to different trajectories and to different time averages of the observable $B(q)$. Nonetheless, it can be proven that if the quantity $B\big(Q(t;x_0)\big)$ is characterised by a loss of correlation, the time average $\overline{B}(x_0)$ is equal to the equilibrium statistical average $\mathbb{E}^{\Omega_P}_{eq}[B]$,

$$\overline{B}(x_0) = \mathbb{E}^{\Omega_P}_{eq}[B], \tag{6.30}$$

for almost all the initial states $x_0 \in \Omega_P$ except for a set of null measure. This means that $\overline{B}(x_0)$ is the typical value of the observable $B(q)$: it is independent of the initial state x_0 of the system. In other words, the Bohm trajectories show typicality as regards the time averages of the observables, since they are statistically independent of the initial condition x_0. This is similar to the time averages of the expectation values that are statistically independent of the set of populations in the thermodynamic limit (see Chap. 3 and Eq. (3.19)). Before explaining better what can be really proven, let us describe the restrictions on the validity of Eq. (6.30).

First of all, Eq. (6.30) is valid for almost all the initial states. Therefore, we can not exclude the existence of a subset $\tilde{V} \subseteq \Omega_P$ of points x_0 such that $\overline{B}(x_0) \neq \mathbb{E}^{\Omega_P}_{eq}[B]$. However, the demonstration ensures that, such a subset $\tilde{V}$ has always a null measure: the probability that a randomly chosen point x_0 belongs to $\tilde{V}$ vanishes. This can be

[1] Notice the difference between the terms "curve" and "trajectory". The curve $X(t;x_0)$ is the function that maps a generic initial state x_0 to the state at time t according to the deterministic evolution. Each point of the curve represents a pair of configuration and wave function. Instead the trajectory $Q(t;x_0)$ describes only the evolution of the Bohm coordinates omitting the information about the wave function. Formally, the trajectory is the set of the first n elements of the curve $X(t;x_0)$ according to the definition of x in Eq. (6.16).

expressed formally with the following equation

$$\mathcal{M}(\tilde{V}) = \int_{\tilde{V}} \mathrm{d}x_0 \; \varrho_{eq}^{\Omega_P}(x_0) = 0. \tag{6.31}$$

In other words, there are some initial states in Ω_P that do not ensure the validity of Eq. (6.30), but the selection of one of those states as initial condition is statistically impossible. In order to grasp better the idea of a set of points of null measure, one can think about the probability of drawing a rational number $\mathbb{Z}$ from the set of real numbers $\mathbb{R}$. Despite there are infinite rational numbers inside $\mathbb{R}$, the probability of drawing a rational number is zero: the amount of real numbers is so much greater than the amount of rational numbers in $\mathbb{R}$, that it is impossible of getting a rational number with a random sampling. The same idea has to be adopted also for $\tilde{V}$ and Ω_P.

Secondly, Eq. (6.30) is valid if the quantity $B\big(Q(t;x_0)\big)$ is characterised by a loss of correlation. By defining the autocorrelation function of the observable $B(q)$ as

$$G_B(\tau) := \frac{1}{\sigma_B^2} \int_{\Omega_P} \mathrm{d}x_0 \; \varrho_{eq}^{\Omega_P}(x_0) \Delta B\big(Q(t+\tau;x_0)\big) \Delta B\big(Q(t;x_0)\big), \tag{6.32}$$

with $\sigma_B^2 = \mathbb{E}_{eq}^{\Omega_P}\big[(\Delta B)^2\big]$ and $\Delta B(q) = B(q) - \mathbb{E}_{eq}^{\Omega_P}[B]$, Eq. (6.30) holds if and only if

$$\lim_{\tau \to +\infty} G_B(\tau) = 0, \tag{6.33}$$

like in the evolution of $Q(t;x_0)$ according to a stationary Markov process, so recovering a correspondence also with the stochastic interpretation developed in Sec. 3.3. Despite the fact that Eq. (6.33) is the only assumption that has to be made, its validity can be just checked through the analysis of the exact dynamics: there are not considerations that can be made *a priori* in order to understand if a generic observable $B(q)$ is or is not characterised by a loss of correlation. On the other hands, it can be observed numerically that this condition is easily satisfied in the framework of Bohm theory for the significant instability of the Bohm equation that causes a chaotic motion [Efthymiopoulos et al. (2007); Wu and Sprung (1999); de Alcantara Bonfim et al. (1998); Frisk (1997)]. Indeed, also systems composed of few degrees of freedom (such as one or two degrees of freedom) show this specific behaviour even if the corresponding classical systems do not. According to these numerical evidences, one can reasonably expect that Eq. (6.33) is easily satisfied for observables of molecular systems, since they are composed of many particles. This is also the case of the simplest chemical system, i.e., one hydrogen atom, which

has six degrees of freedom (the coordinates of a nucleus and of an electron in the cartesian space). However, the condition of Eq. (6.33) is not satisfied in the single rotor system (with one degree of freedom) of Chap. 3 and therefore, the predictions of the single Bohm trajectory do not correspond to those of Quantum Mechanics (see Fig. 3.8).

Finally, it should be emphasised that Eq. (6.30) can be only justified, but not exactly proved. By assuming that the observable $B\big(Q(t;x_0)\big)$ is characterised by a loss of correlation, one can derive that the variance of the time average with respect to the statistical average vanishes:

$$\mathbb{E}_{eq}^{\Omega_P}\left[\Big(\overline{B}(x_0)-\mathbb{E}_{eq}^{\Omega_P}[B]\Big)^2\right]=0. \tag{6.34}$$

The detailed proof is reported in Appendix C. Equation (6.34) means that the deviations of the time average with respect to equilibrium average $\mathbb{E}_{eq}^{\Omega_P}[B]$ are statistically insignificant. It is exactly the statistical nature of such a result that does not ensure that all the initial states x_0 lead to the same time average $\overline{B}(x_0)$ of $\mathbb{E}_{eq}^{\Omega_P}[B]$: Eq. (6.34) is compatible with a set of points with null measure for which $\overline{B}(x_0)\neq\mathbb{E}_{eq}^{\Omega_P}[B]$. In other words, Eq. (6.30) is valid only in a statistical sense as specified by Eq. (6.34).

Beyond what can be mathematically proven, one can speculate about the implications of Eq. (6.34) and Eq. (6.30). In particular, if Eq. (6.30) holds for any observable $B(q)$, then almost all the possible curves $X(t;x_0)$ correspond to Bohm trajectories that sample equally the configuration space $\mathcal{C}$. This can be explained in terms of proof by contradiction. Consider a set of curves that do not satisfy such a condition. If the set of all the points belonging to these curves has a null measure then they can be neglected. Otherwise, there is a set of points x_0 of finite measure such that at least one observable does not satisfy Eq. (6.34) and this is in contradiction with initial hypothesis that Eq. (6.30) holds for any $B(q)$. Then one can define a probability density $w_{eq}(q)$ on the configuration space by considering the sampling produced by one curve (one single evolving state) in order to calculate the time average of the observable $B(q)$

$$\overline{B}(x_0)=\int_{\mathcal{C}}\mathrm{d}q\ B(q)w_{eq}(q). \tag{6.35}$$

Also the density distribution $w_{eq}(q)$ $\big($as $\overline{B}(x_0)\big)$ is a typical property of the Bohm dynamics that does not depend on the actual condition of the system. Through

Eq. (6.30) and the definition of $\mathbb{E}_{eq}^{\Omega_P}[B]$, one obtains

$$\int_{\mathcal{C}} \mathrm{d}q \; w_{eq}(q)B(q) = \overline{B}(x_0) = \int_{\mathcal{C}} \mathrm{d}q \; B(q) \int_{[0,2\pi)^N} \mathrm{d}\alpha \; \varrho_{eq}^{\Omega_P}(x)\big|_{x=(q,\alpha)}. \tag{6.36}$$

Finally the following relation is derived

$$w_{eq}(q) = \int_{[0,2\pi)^N} \mathrm{d}\alpha \; \varrho_{eq}^{\Omega_P}(q,\alpha), \tag{6.37}$$

by assuming that Eq. (6.30) holds for all possible observables $B(q)$. Equation (6.37) means that a single trajectory of the Bohm coordinates samples the configuration space according to the same marginal density distribution of $\varrho_{eq}^{\Omega_P}(q,\alpha)$. It should be stressed that a similar result was obtained in the analysis of the numerical experiment described in Chap. 3 by considering the distribution with respect to the subsystem coordinates only. The numerical observation of the Chap. 3 can be considered as an evidence, at least in that case, about the ergodicity due to loss of correlation.

In Sec. 6.4, we show explicitly that the previous considerations allow the definition of a formal correspondence between the evolution of a single Bohm trajectory and the conventional Quantum Mechanics. As it can be easily realised, the essential ingredient of such a correspondence is $\varrho_{eq}^{\Omega_P}(x)$.

6.4 Expectation values from a single Bohm trajectory

In this section it is shown how the expectation values of the standard Quantum Mechanics emerge from the statistical properties of a single Bohm trajectory. Let us introduce the marginal density distribution $\varrho_{eq}^{\mathcal{C}}(q)$ on the configuration space $\mathcal{C}$ by integrating the equilibrium distribution $\varrho_{eq}^{\Omega_P}(q,\alpha)$ on the phases variables. It can be easily verified that in the case of rational independence of the Hamiltonian eigenvalues (but similar conclusion can be derived also in more general conditions), the time average of the square modulus of the wave function (which can be specified according to the populations) is the same of $\varrho_{eq}^{\mathcal{C}}(q)$:

$$\varrho_{eq}^{\mathcal{C}}(q) = \sum_{k=1}^{N} P_k |\phi_k(q)|^2 = \lim_{T\to+\infty} \frac{1}{T} \int_0^T \mathrm{d}t \; |\Psi(q,t)|^2, \tag{6.38}$$

independently of the initial phases $A(0)$ of the wave function. The only constraint is that the populations of the wave function have to be the same of the invariant

subspace Ω_P of the dynamical space Ω_0. Once Eq. (6.38) is recognised, the statistical average $\mathbb{E}^{\Omega_P}_{eq}[B]$ can be specified by the time average of the corresponding expectation value of the operator $B(\hat{q})$:

$$\mathbb{E}^{\Omega_P}_{eq}[B] = \lim_{T\to+\infty} \frac{1}{T}\int_0^T \mathrm{d}t \ \langle\Psi(t)|B(\hat{q})|\Psi(t)\rangle \,. \tag{6.39}$$

Furthermore, on the basis of Eq. (6.30), the time average of the same quantity along the single Bohm trajectory is equivalent to the time average of the corresponding expectation value,

$$\lim_{T\to+\infty} \frac{1}{T}\int_0^T \mathrm{d}t \ B\big(Q(t;x_0)\big) = \overline{B}\big(x_0\big) = \mathbb{E}^{\Omega_P}_{eq}[B] = \lim_{T\to+\infty} \frac{1}{T}\int_0^T \mathrm{d}t \ \langle\Psi(t)|B(\hat{q})|\Psi(t)\rangle \,, \tag{6.40}$$

for almost all the initial states $x_0 \in \Omega_P$. In this way, a clear connection is established between the properties of a single Bohm trajectory and the expectation values. In this framework the time average along a single Bohm trajectory and the time average of the expectation value of a particular observable $B(q)$ become statistically equivalent.

The case of an observable (labeled b in Chap. 3) of a subsystem interacting with the environment is even more interesting. By recalling what was already explained in Chap. 3, i.e., that the expectation values corresponding to the subsystem quantities become time independent in the thermodynamic limit, then the time average of the expectation value is no more necessary. It can be proven that the time average along the single Bohm trajectory $\overline{b}(x_0)$ of the observable $b(q_S)$ (where q_S are the subsystem coordinates) is equivalent to the corresponding expectation value at any time:

$$\overline{b}(x_0) = \langle\Psi(t)|b(\hat{q}_S)|\Psi(t)\rangle = \lim_{T\to+\infty} \frac{1}{T}\int_0^T \mathrm{d}t \ \langle\Psi(t)|b(\hat{q}_S)|\Psi(t)\rangle \,. \tag{6.41}$$

In this way the correspondence between the statistical properties of a single Bohm trajectory and the expectation values is direct. In the case of a finite size system in proximity to the thermodynamic limit, one can reasonably expect that the expectation values are almost the same of their time averages with the above equation holding only approximately. In any case, it has to be emphasised that this result permits the interpretations of the expectation values of a subsystem (that is an open quantum system such as a single molecule interacting with the environment) in terms of average properties of an underlying dynamics according to the single Bohm trajectory approach. In other words, by supposing that the single Bohm tra-

jectory approach is the correct method for describing molecular systems, then the conventional expectation values can be described in terms of the time average of the corresponding observables along the trajectory. Furthermore, the condition of an open quantum system (a single molecule interacting with the other molecules) is the most common experimental condition and also the most investigated one. This is the reason that makes the correspondence of Eq. (6.41) for a generic subsystem extremely important in order to validate the single Bohm trajectory approach.

6.5 Complementary results

For the sake of completeness, we would like to emphasise two features of the previous derivations, that are not directly related to the main topic of this chapter.

First of all, Eq. (6.22) is formally equivalent to the Liouville equation in Classical Mechanics. The only differences concern of course the definition of the variables x and of the velocity field $\Lambda_P(x)$. Let us recall that in the Bohm framework x represents a generic quantum state $\big(q, \psi(\bullet)\big)$ in terms of coordinates and phases with established populations, whereas its counterpart is given by the set of the positions and momenta of all the particles in Classical Mechanics. Similarly, $\Lambda_P(x)$ represents the Bohm equation and the Schrödinger equation, and it has to be substituted with the Hamiltonian equations of motion when dealing with Classical Mechanics. Besides these differences, the two formulations of the Liouville equation are equivalent and this allows the definition of the Liouville operator,

$$\hat{L} := -\imath \nabla_x \cdot \Lambda_P(x) \tag{6.42}$$

also in the framework of Bohm theory. The imaginary unit $\imath$ ensures that the Liouville operator has some specific properties, e.g., the symmetrised Liouville operator is an hermitian operator, that will be useful in the Chap. 7 where we shall derive stochastic equations of motion for a subset of Bohm coordinates on the basis of the formal equivalence between the Liouville equation in Classical Mechanics and in the framework of Bohm theory, written as

$$\frac{\partial}{\partial t} \varrho^{\Omega_P}(x,t) + \imath \hat{L} \varrho^{\Omega_P}(x,t) = 0. \tag{6.43}$$

Secondly, it has to be clarified that our statistical characterisation is different from the Bohm ensemble previously invoked in Chap. 2 and Chap. 3. Bohm presumed that the wave function of the system was known and only the initial config-

uration is unknown. Moreover, the initial density distribution on the configuration space was set equal to the square modulus of the initial wave function by assumption. In our approach the probability density is defined on the space Ω_P that includes both the possible configurations and the possible wave functions conveniently parametrised in terms of phases. Our fundamental idea consists in developing a statistical formulation of the single Bohm trajectory approach in order to manage the cases where the computational cost for solving the dynamical equations is too high. Furthermore, it has been proven that the statistical predictions can be explained in terms of the behaviour of a single Bohm trajectory: we formalised the correspondence between the statistical description and the deterministic one (the single trajectory). However, the Bohm statistical ensemble can be obtained from our statistical method as a peculiar case by setting conveniently the initial condition and solving Eq. (6.22), since the Liouville equation is valid independently of the initial density distribution $\varrho^{\Omega_P}_{eq}(x)$. Therefore, the Bohm probability density on the configuration ensemble in our notation is the following particular solution of the Liouville equation,

$$\varrho^{\Omega_P}(x,t)\Big|_{x=(q,\alpha)} = \int \mathrm{d}q_0\mathrm{d}\alpha_0 \; |\Psi_0(q_0)|^2 \delta\big(q - Q(t;q_0,\alpha_0)\big)\delta\big((\alpha - A(t;\alpha_0)\big), \quad (6.44)$$

where $\Psi_0(q_0) = \langle q_0|\Psi_0\rangle$ is the initial wave function whereas $Q(t;q_0,\alpha_0)$ and $A(t;\alpha_0)$ are the components of the curve $X(t;x_0)$. Indeed by integrating the probability density of Eq. (6.44) on the phases variables, one obtains a probability density on the configuration space that is equivalent to the square modulus of the wave function $|\Psi(t)\rangle = \exp(-\imath\hat{H}t/\hbar)\,|\Psi_0\rangle$ in agreement to the Bohm ensemble:

$$\int_{[0,2\pi)} \mathrm{d}\alpha \; \varrho^{\Omega_P}(x,t)\Big|_{x=(q,\alpha)} = |\Psi(q,t)|^2. \quad (6.45)$$

We would like to stress that the Bohm ensemble is nothing more of a particular solution of our Liouville equation by conveniently setting the initial density distribution $\varrho^{\Omega_P}(x,0)$.

6.6 Final remarks

In this chapter we have investigated the statistical properties of a single Bohm trajectory. First of all, we have developed the Bohm's counterpart of the Liouville equation for describing the evolution of a generic density distribution. The stationary solution, i.e., the equilibrium probability density, has been employed to establish

a correspondence between the statistical description and the deterministic one. Furthermore, the statistical method is essential in order to explain some properties of the conventional Quantum Mechanics in terms of the properties of the single Bohm trajectory. In particular, one can prove that the time average of an expectation value is equivalent to the time average of the corresponding observable along a single Bohm trajectory under reasonable conditions (that is the loss of correlation). In the case of observables related to subsystem properties, e.g., a single molecule interacting with the environment, the expectation values become time independent in the thermodynamic limit. Therefore, they can be defined with the time average of the observable along a single Bohm trajectory. In other words, the expectation values can be interpreted as average properties corresponding to the deterministic evolution described in terms of the single Bohm trajectory.

It has to be emphasised that this last correspondence is particular significant since the molecular systems usually are composed of many molecules, but one is typically interested in the properties of a single molecule. Finally, this statistical method validates formally the description based on a single Bohm trajectory and it can be employed also for inferring quantum stochastic equations as it is examined in the Chap. 7.

CHAPTER 7

Emergence of Quantum Stochastic Behaviour

Classical Mechanics, conventional Quantum Mechanics and Bohm theory are limited by the computational cost of solving the dynamical equations (respectively Newton equation, Schrödinger equation and Bohm equation). For example, the problem of computing the exact trajectory of a Brownian particle in a macroscopic volume of water is an unfeasible task also in the framework of Classical Mechanics because of the huge number of variables: one should take into account the position and momentum of the Brownian particle as well as the positions and momenta of all the water molecules. This limitation is particularly relevant when the variables can be divided in two sets and only one set includes the interesting ("relevant") variables whereas the other includes the remaining ("irrelevant") variables. It can be understood that the position of the Brownian particle is more significant for characterising the Brownian motion than the positions and momenta of the water molecules. However, all the variables have to be taken into account for examining the deterministic evolution of the system because of the interactions between the system components. Similarly, the coordinates corresponding to each degree of freedom and the wave function (or the phases in the representation defined in Chap. 6) have to be well characterised for describing the evolution of a macroscopic quantum system in the framework of Bohm theory. Also in this case, one can be interested in the behaviour of a single molecule interacting with the solvent. For instance, when a conformational change is occurring, the motion of the solvent molecules is

less significant than the dynamics of the degrees of freedom that characterise the molecular conformation.

In this regard, it might be extremely useful the development of dynamical equations for the interesting variables that are autonomous, by approximating the effects due to the other variables. It is well known that Stochastic Methods can be employed for this purpose: they are currently standard procedure in the framework of Classical Mechanics and they are very shared by several fields of Chemical Physics [Gardiner (1986)]. Stochastic equations succeed in representing satisfactorily different kinds of dynamical processes by modelling the fluctuating effects due to the irrelevant variables. For example, the description of a chemical reaction can be successfully accomplished by examining the dynamics of the relevant concentrations of some components. The use of stochastic equations for these reactive processes is already a common approach [Gillespie (1992, 2007); Gillespie et al. (2013)]. It can be mentioned a recent attempt of representing a two-states kinetics that takes into account how the system is observed and the noise corresponding to the measure process [Prinz et al. (2014)]. Furthermore, stochastic methodologies are extremely powerful when one is interested in the conformational motion of macromolecules of biological interest, such as proteins. The domain motion is fundamental in determining the biological functions and the relaxation processes in spectroscopy experiments, e.g., NMR. Recent efforts aim to understand the correlation between the internal dynamics and the global motion of proteins [Ryabov and Fushman (2007); Wong et al. (2009); Ryabov et al. (2012)].

The same methodologies can be adopted also in the framework of Bohm theory: stochastic equations can substitute the deterministic ones (Bohm equation and Schrödinger equation). To this end, two approaches can be implemented. The first one consists in modelling the stochastic equations on the basis of some evidences and some expectations about the behaviour of the relevant variables. Consider for example the Bohm trajectories of the six interacting rotors described in Chap. 3. By observing Fig. 3.5, one can suppose that the Bohm trajectory of each rotor could be well represented as a diffusion process according to the Smoluchowski equation. However, the complexity of the dynamical equations (Bohm equation and Schrödinger equation) and the absence of a significant number of studies about Bohm dynamics makes this approach unfeasible. The second strategy is more systematic and allows a formal derivation of the stochastic equations by starting from the Liouville equation, which has been defined in the context of Bohm theory in Chap. 6. This second way is known in literature as Nakajima-Zwanzig projection

operator techniques [Zwanzig (2001); Nakajima (1958); Henderson (2012)].

In this chapter we adopt the projection operators to infer the stochastic equations for a reduced number of variables in the framework of Bohm theory and the general procedure is summarised in Sec. 7.1. The final goal is the definition of an approximate method for describing open quantum systems, for instance a single molecule interacting with its environment (the other molecules). The method should allow an extension of the conventional quantum description of a single molecule by including both the coordinates trajectories and the fluctuating effects due to the environment. At this stage a question without an obvious answer arises: which are the relevant variables that have to be included by the stochastic equations in order to ensure an accurate description of the corresponding dynamics? Whereas one can try to guess the relevant variables for a system represented with Classical Mechanics, the same conjecture is more difficult in the framework of Bohm theory for the reasons mentioned above, i.e., the absence of a relevant number of studies. Two different methods for two different sets of relevant variables are examined in this chapter (see Sec. 7.3 and Sec. 7.4). After the theoretical derivation of the corresponding stochastic equations, we compare their predictions with the behaviour emerging from the deterministic dynamics for different model systems (described in Sec. 7.2) in order to validate each methodology. In particular, the second stochastic approach, which is the most efficient, replaces the Bohm equation, determining the set of all the particle velocities according to the full wave function, with a stochastic equation that approximates the velocity of a subset of coordinates from the corresponding reduced density matrix. In this way one can represent the motion of an open quantum system, i.e., a single molecule interacting with the environment, according to a quantum theory of motion. Furthermore, this method can be suitable in order to examine reactive systems, as for example a conformational change of a molecule in solvent. Our approach could supply precise information about the time evolution of the molecular geometry by taking into account the molecular geometry itself and the fluctuating behaviour of the solvent. Additionally, it is a quantum method developed in the framework of a quantum theory without any reference to a description based on Classical Mechanics. In this way one can avoid "mixed" methods that rely on both Classical and Quantum Mechanics without a clear definition of the border between one description and the other.

7.1 Projection operator techniques

In this section we summarise briefly the projection operator procedure adopted (and firstly developed by Nakajima (1958) and Zwanzig (1960)) to infer the approximate stochastic equations from the differential equations, describing the deterministic dynamics. The stochastic equations determine the evolution of a subset of all the variables that define the system state. In other words, they characterise approximately the dynamics of open systems by employing only the set of the corresponding variables. It has to be emphasised that the same procedure can be employed in many contexts, e.g., both Bohm theory and Classical Mechanics, since it is rather general and unrelated to a specific framework. Therefore, we make comparisons between our derivation and the Brownian motion for some relevant cases, in order to set our procedure in a more conventional field.

The problem of describing the dynamics of a limited number of degrees of freedom for a quantum system composed of a huge number of molecules in the framework of Bohm theory can be formally formulated as in the following. Consider the suitable dynamical space and the dynamics of the actual system state. In the framework of Bohm theory the appropriate dynamical space is Ω_P, defined in Eq. (6.17), and the dynamics of the actual system state is described by the curve $X(t; x_0)$ solving Eq. (6.19) with initial condition x_0. Notice that we adopt the representation of the Bohm state as the set of configuration and phases in order to employ the formulation of the Liouville's theorem developed in Chap. 6. Assuming that the interesting dynamics is described by the relevant variables $X_R(t; x_0)$, then the projection operator techniques define stochastic equations that depend on the relevant variables x_R only.

The procedure, represented schematically in Fig. 7.1, consists in inferring the Fokker-Planck equation by employing the projection operator $\hat{\mathbb{P}}$, once the Liouville equation and the relevant variables are identified. It is well known that the Fokker-Planck equation replaces the Liouville equation for the distribution $\varrho^R(x_R, t)$ describing the probability that the relevant variables x_R take some specific values at time t. Furthermore, there is a formal correspondence between the Fokker-Planck equation and the Langevin equation if the fluctuating effects of the neglected variables are modelled as a white noise $\zeta(t)$ [Gardiner (1986)]. In other words, if the Fokker-Planck equation replaces the Liouville equation, then the Langevin equation can be interpreted as the replacement of the dynamical equation for the relevant variables. In the following we summarise the procedure that defines the Fokker-Planck

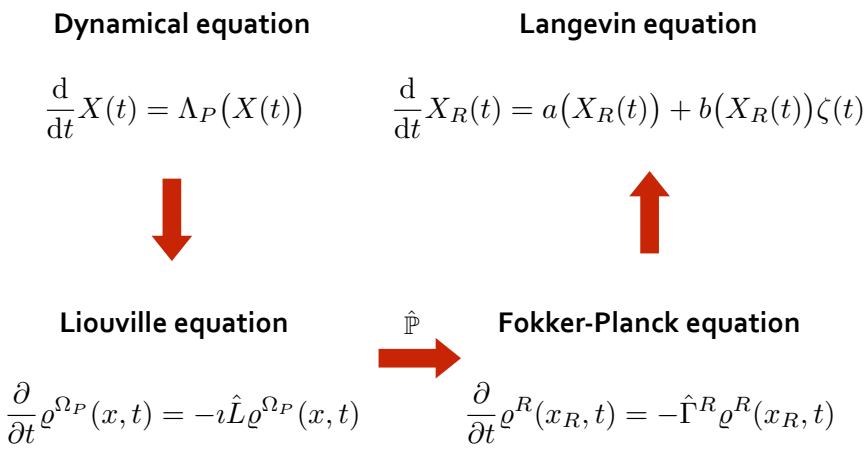

Figure 7.1: Schematic representation of the projection operator procedure for identifying the stochastic equations (Fokker-Planck and Langevin equation). The dynamical equation and the Liouville equation are defined in Chap. 6 (see Eq. (6.20), Eq. (6.21) and Eq. (6.42)). The Fokker-Planck operator is labelled $\hat{\Gamma}^R$ whereas $a\big(X_R(t)\big)$ and $b\big(X_R(t)\big)$ are the coefficients of the Langevin equation. The white noise is represented by $\zeta(t)$.

equation through those steps:

(i) the representation of the system states in terms of relevant x_R and irrelevant x_I variables;

(ii) the identification of the equilibrium density distribution $\varrho^R_{eq}(x_R)$ for the relevant variables;

(iii) the definition of the projection operator $\hat{\mathbb{P}}$;

(iv) the projection of the Liouville equation, for obtaining the corresponding Fokker-Planck equation.

These steps can be already found in the works of Zwanzig [Zwanzig (1960, 1964)], but they define an exact projected Liouville equation (see Eq. 7.7). The effects of the irrelevant variables are taken into account through the memory of the process involving the relevant variables. In order to obtain the corresponding Fokker-Planck equation (see Eq. (7.12)) the memory of the process has to be approximated and the specific simplifications are summarised in Appendix D.

First of all the relevant variables have to be recognised. The generic state of the quantum system, that is the set x of configuration and phases according to our representation, has to be separated in the set x_R of n_R relevant variables and the set x_I of n_I irrelevant variables,

$$x \longrightarrow x = (x_R, x_I). \tag{7.1}$$

The total number of variables $n_R + n_I$ has to be equal to $n + N$ (with n the number of the degrees of freedom and N the dimension of the Hilbert space) that is the dimension of the dynamical space Ω_P (Sec. 6.2). Furthermore, the transformation of Eq. (7.1) establishes also a separation of the dynamical space in two subspaces,

$$\Omega_P = \Omega_R \times \Omega_I, \tag{7.2}$$

such that $x_R \in \Omega_R$ and $x_I \in \Omega_I$. Broadly speaking, the projection operator techniques "project" the deterministic dynamics of the curve $X(t; x_0)$, belonging to the dynamical space Ω_P, onto the space Ω_R, i.e., the space of the relevant variables. The projection of the curve $X(t; x_0)$ onto Ω_R is represented by $X_R(t; x_0)$. The density distribution $\varrho^R(x_R, t)$ describes the probability that the relevant variables x_R in the space Ω_R take a certain value at time t. The stochastic equations are closed-form expressions into the space Ω_R. However, the choice of the relevant variables is anything but obvious in the framework of Bohm theory. For instance, if one is interested in examining the conformational dynamics of a specific molecule, then the coordinates that represent the molecular geometry belong almost certainly to the set x_R. But, do these coordinates complete the set x_R? Which are the other significant variables for describing the interesting phenomena? In the following of this chapter we propose two answers to these questions (Sec. 7.3 and Sec. 7.4), but for now let us assume to know the relevant set x_R: for the purpose of this section, one has just to bear in mind that x_R is a set of n_R relevant variables, $x_R = (x_{R,1}, x_{R,2}, \ldots, x_{R,n_R})$ and they are known.

The second step concerns the identification of the equilibrium density distribution $\varrho^R_{eq}(x_R)$ on the space Ω_R. In Chap. 6, $\varrho^{\Omega_P}_{eq}(x)$ on the space Ω_P has been recognised as the stationary solution of the Liouville equation through Eq. (6.23). By considering the transformation of Eq. (7.1) and the separation of the dynamical space according to Eq. (7.2), one can define the equilibrium density distribution $\varrho^R_{eq}(x_R)$ as the marginal distribution with respect to $\varrho^{\Omega_P}_{eq}(x)$. In other words, $\varrho^R_{eq}(x_R)$ is the equilibrium distribution $\varrho^{\Omega_P}_{eq}(x)$ integrated on the irrelevant variables,

$$\varrho^R_{eq}(x_R) := \int_{\Omega_I} \mathrm{d}x_I \; \varrho^{\Omega_P}_{eq}(x)\big|_{x=(x_R,x_I)}. \tag{7.3}$$

The time evolution of the relevant variables $X_R(t; x_0)$ should sample the space Ω_R according to the marginal density distribution $\varrho^R_{eq}(x_R)$, in the same way as the curve $X(t; x_0)$ should sample the dynamical space according to $\varrho^{\Omega_P}_{eq}(x)$ in the ergodic condition.

Once $\varrho_{eq}^{R}(x_R)$ is identified, the projection operator $\hat{\mathbb{P}}$ can be defined. Let $f(x)$ be a generic function of the whole set of variables. The following equation fully characterises the projection operator $\hat{\mathbb{P}}$ onto the subspace Ω_R:

$$\hat{\mathbb{P}}\left(\varrho_{eq}^{\Omega_P}(x)\right)^{1/2} f(x) = \left(\varrho_{eq}^{\Omega_P}(x)\right)^{1/2} \frac{\int_{\Omega_I} \mathrm{d}x_I \ \left[\varrho_{eq}^{\Omega_P}(x) f(x)\right]_{x=(x_R,x_I)}}{\varrho_{eq}^{R}(x_R)}. \tag{7.4}$$

The result of the projection is the average of the function $f(x)$ with respect to the irrelevant variables x_I weighted by the equilibrium density probability $\varrho_{eq}^{\Omega_P}(x)$ and multiplied by the term $\left(\varrho_{eq}^{\Omega_P}(x)\right)^{1/2}$. Since the purpose of the procedure is the definition of the Fokker-Planck equation through the projection the Liouville equation (see Fig. 7.2), the projection operator has to act on the probability density $\varrho^{\Omega_P}(x,t)$ as well as on the Liouville operator.

Therefore, it is convenient to employ the operator $\hat{\mathbb{P}}$ on the symmetrized Liouville equation instead of the original equation. In this way two main advantages arise. The first one is that the symmetrized Liouville operator $\hat{\tilde{L}}$ is a hermitian operator unlike $\hat{L}$. Secondly, the action of $\hat{\mathbb{P}}$ on the symmetrized probability density $\tilde{\varrho}^{\Omega_P}(x,t)$ is proportional to the probability density integrated on the irrelevant variables. For the sake of completeness, we recall that the symmetrized Liouville equation defines the evolution of the symmetrized probability density $\tilde{\varrho}^{\Omega_P}(x,t) := \left(\varrho_{eq}^{\Omega_P}(x)\right)^{-1/2} \varrho^{\Omega_P}(x,t)$,

$$\frac{\partial}{\partial t}\tilde{\varrho}^{\Omega_P}(x,t) + \imath\hat{\tilde{L}}\tilde{\varrho}^{\Omega_P}(x,t) = 0, \tag{7.5}$$

where $\hat{\tilde{L}} := \left(\varrho_{eq}^{\Omega_P}(x)\right)^{-1/2} \hat{L} \left(\varrho_{eq}^{\Omega_P}(x)\right)^{1/2}$. Indeed, it can be proven that if $\varrho^{\Omega_P}(x,t)$ satisfies the Liouville equation (Eq. (6.43)), then Eq. (7.5) holds for obvious reasons. Since the projection operator defined in Eq. (7.4) is linear and time independent, the symmetrized Liouville equation can be written as a pair of equations

$$\begin{cases} \dfrac{\partial}{\partial t}\hat{\mathbb{P}}\tilde{\varrho}^{\Omega_P}(x,t) + \imath\hat{\mathbb{P}}\hat{\tilde{L}}\left(\hat{\mathbb{P}} + \hat{\mathbb{Q}}\right)\tilde{\varrho}^{\Omega_P}(x,t) = 0 \\ \dfrac{\partial}{\partial t}\hat{\mathbb{Q}}\tilde{\varrho}^{\Omega_P}(x,t) + \imath\hat{\mathbb{Q}}\hat{\tilde{L}}\left(\hat{\mathbb{P}} + \hat{\mathbb{Q}}\right)\tilde{\varrho}^{\Omega_P}(x,t) = 0 \end{cases} \tag{7.6}$$

where $\hat{\mathbb{Q}}$ is the projection operator complementary to $\hat{\mathbb{P}}$, $\hat{\mathbb{Q}} := \hat{\mathbb{1}} - \hat{\mathbb{P}}$. The second equation in (7.6) can be solved formally for $\hat{\mathbb{Q}}\varrho^{\Omega_P}(x,t)$ and the solution can be substituted in the first equation in (7.6) (see Zwanzig (1964)). In this way an

equation for the projected probability density is obtained,

$$\frac{\partial}{\partial t}\tilde{\varrho}^{\mathbb{P}}(x,t) = -\imath\hat{\mathbb{P}}\hat{\tilde{L}}\tilde{\varrho}^{\mathbb{P}}(x,t) - \int_0^t \mathrm{d}\tau\ \hat{K}(\tau)\tilde{\varrho}^{\mathbb{P}}(x,t-\tau), \tag{7.7}$$

where $\tilde{\varrho}^{\mathbb{P}}(x,t)$ is a compact notation for the result of the action of the operator $\hat{\mathbb{P}}$ on the symmetrized probability density,

$$\tilde{\varrho}^{\mathbb{P}}(x,t) := \hat{\mathbb{P}}\tilde{\varrho}^{\Omega_P}(x,t), \tag{7.8}$$

and $\hat{K}(\tau)$ is the kernel operator defined as

$$\hat{K}(\tau) = \hat{\mathbb{P}}\hat{\tilde{L}}\hat{\mathbb{Q}}\ e^{-\imath\tau\hat{\mathbb{Q}}\hat{\tilde{L}}}\ \hat{\mathbb{Q}}\hat{\tilde{L}}\hat{\mathbb{P}}. \tag{7.9}$$

We would like to emphasise some features of Eq. (7.7). First of all, it is still an exact equation for the evolution of $\tilde{\varrho}^{\mathbb{P}}(x,t)$: no approximations have been adopted. The only assumption concerns the initial density distribution that is arbitrary and selected in such a way that $\hat{\mathbb{Q}}\varrho^{\Omega_P}(x,0) = 0$, since we are interested in the probability density of the relevant variables. The kernel operator $\hat{K}(\tau)$ includes the memory of the whole process in order to compensate for the loss of information due to the projection and to determine the time evolution of $\tilde{\varrho}^{\mathbb{P}}(x,t)$ exactly. Broadly speaking, the memory of the process substitutes the information neglected by projecting the Liouville equation. Despite the use of the projection operator, $\tilde{\varrho}^{\mathbb{P}}(x,t)$ is still function of all the variables, but it is proportional to the probability density $\varrho^{\Omega_P}(x,t)$ integrated on the irrelevant variables. By employing Eq. (7.4), it can be easily verified that

$$\hat{\mathbb{P}}\tilde{\varrho}^{\Omega_P}(x,t) = \frac{\left(\varrho^{\Omega_P}_{eq}(x)\right)^{1/2}}{\varrho^{R}_{eq}(x_R)} \int \mathrm{d}x_I\ \varrho^{\Omega_P}(x,t)\big|_{x=(x_R,x_I)}, \tag{7.10}$$

where the result of the integration is the marginal density distribution $\varrho^R(x_R,t)$ with respect to the irrelevant variables:

$$\varrho^R(x_R,t) := \int \mathrm{d}x_I\ \varrho^{\Omega_P}(x,t)\big|_{x=(x_R,x_I)}. \tag{7.11}$$

Finally Eq. (7.7) can be simplified in order to obtain a closed-form expression for $\varrho^R(x_R,t)$ that depends on the relevant variables only. The most common approximation leading to the Fokker-Planck equation concerns the memory of the process: it is usually assumed that the memory of $\hat{K}(\tau)$ extends over a short time interval.

In other words, the evolution of the relevant variables is a Markovian process by hypothesis. We summarise the essential steps for inferring the Fokker-Planck equation from Eq. (7.7) under the Markovian hypothesis in Appendix D, and in the following it is reported only the resulting Fokker-Planck equation:

$$\frac{\partial}{\partial t}\varrho^R(x_R,t) = -\left[\nabla_R\Lambda_R(x_R)\varrho^R(x_R,t) - \nabla_R\cdot\varrho^R_{eq}(x_R)\beta(x_R)\nabla_R\left(\varrho^R_{eq}(x_R)\right)^{-1}\varrho^R(x_R,t)\right], \tag{7.12}$$

where $\nabla_R = (\partial/\partial x_1, \partial/\partial x_2, \ldots, \partial/\partial x_{n_R})$, $\Lambda_R(x_R)$ is the averaged velocity field and $\beta(x_R)$ can be interpreted as the matrix of the diffusion coefficients similarly to the case of the diffusion of a Brownian particle in Classical Mechanics. The k-th element of the averaged velocity field $\Lambda_{R,k}(x_R)$ describes the deterministic evolution of the k-th relevant variable and it is equal to

$$\Lambda_{R,k}(x_R) = \frac{1}{\varrho^R_{eq}(x_R)}\int_{\Omega_I}\mathrm{d}x_I\ \left[\varrho^{\Omega_P}_{eq}(x)\Lambda_{P,k}(x)\right]_{x=(x_R,x_I)}. \tag{7.13}$$

As regards the matrix of diffusion coefficients, each element depends generally on the relevant variables according to their definition:

$$\beta_{k,k'}(x_R) = \int_0^{+\infty}\mathrm{d}\tau\frac{1}{\varrho^R_{eq}}\int_{\Omega_I}\mathrm{d}x_I\left[\left(\varrho^{\Omega_P}_{eq}\right)^{1/2}\Delta\Lambda_{P,k}\ e^{-\imath\tau\hat{\mathbb{Q}}\hat{\tilde{L}}}\ \Delta\Lambda_{P,k'}\left(\varrho^{\Omega_P}_{eq}\right)^{1/2}\right]_{x=(x_R,x_I)}, \tag{7.14}$$

with $\Delta\Lambda_{P,k}(x)$ the fluctuation of the k-th component of the velocity field with respect to its average value,

$$\Delta\Lambda_{P,k}(x) = \Lambda_{P,k}(x) - \Lambda_{R,k}(x_R). \tag{7.15}$$

However, it is usually assumed that each $\beta_{k,k'}(x_R)$ is a constant parameter, i.e., $\beta_{k,k'}(x_R) \simeq \beta_{k,k'}$. Notice that in Eq. (7.13), Eq. (7.14) and Eq. (7.15), the index k can assume the values $1, 2, \ldots, n_R$. Finally, the Fokker-Planck operator is

$$\hat{\Gamma}^R = \nabla_R\cdot\Lambda_R(x_R) - \nabla_R\cdot\varrho^R_{eq}(x_R)\beta\ \nabla_R\left(\varrho^R_{eq}(x_R)\right)^{-1} \tag{7.16}$$

and the corresponding Langevin equation (see Gardiner (1986)) is

$$\frac{\mathrm{d}}{\mathrm{d}t}X_R(t) = \Lambda_R\left(X_R(t)\right) + \beta\frac{\nabla_R\ \varrho^R_{eq}\left(X_R(t)\right)}{\varrho^R_{eq}\left(X_R(t)\right)} + (2\beta)^{1/2}\zeta(t), \tag{7.17}$$

where the averaged velocity field $\Lambda_{R,k}$ and the diffusive contribution $\beta\nabla_R\varrho^R_{eq}/\varrho^R_{eq}$ represent the deterministic dynamics, while the third term $(2\beta)^{1/2}\zeta(t)$ describes the fluctuating dynamics. The Fokker-Planck equation determines the evolution

of a generic initial density distribution of the relevant variables $\varrho^R(x_R, t)$ and the corresponding Langevin equation models the dynamics of $X_R(t; x_0)$. This is the general procedure which, however, leaves open the issue of the identification of the relevant variables that are essential to determine the ingredients of $\hat{\Gamma}^R$, i.e., $\Lambda_R(x_R)$, $\varrho^R_{eq}(x_R)$ and β; once they are established, then the stochastic equations (Fokker-Planck equation and Langevin equation) can be used to examine the properties of the relevant variables. In order to verify the accuracy of the stochastic method, its predictions have to be compared with the deterministic dynamics. In Sec. 7.2 we define a model system that is employed for the comparison of the deterministic predictions with the stochastic ones, for two different sets of relevant variables and system conditions.

7.2 Model system

In order to analyse the predictions of the stochastic equations for different sets of relevant variables, we consider an hypothetical quantum system whose deterministic dynamics can be calculated by solving the Bohm and the Schrödinger equations exactly. This system is composed of $n = 6$ interacting harmonic oscillators and it could represent n interacting vibrational degrees of freedom, such as the vibrational degree of freedom of n diatomic molecules. The set $q = (q_1, q_2, \ldots, q_n)$ includes the coordinate corresponding to each oscillator. By hypothesis, the first oscillator represents the open quantum system (or subsystem) of interest whose behaviour should be well described according to the stochastic method; the other oscillators play the role of the environment. Since this model system is rather similar to the system of n confined, randomly coupled, planar rotors examined in Chap. 3 (see the subsections 3.2.1 and 3.2.2), we characterise it on the one hand by briefly summarising the common features of the two models, particularly those regarding the numerical methodologies. On the other hand, we go into detail as regards their differences:

(i) each coordinate q_i is not periodic and the Hilbert space $\mathcal{H}_i$ for each oscillator can not be generated by means of the Fourier basis set;

(ii) we consider the possibility that the harmonic frequency of the subsystem could be different with respect to that of the oscillators composing the environment;

(iii) the interaction between the oscillators has been modelled with a random matrix [Wigner (1967); Brody et al. (1981)] instead of the random potential of

Eq. (3.32);

(iv) the initial conditions have been selected according to either the RPSE (Chap. 3) or an arbitrary non-equilibrium conditions.

If the stochastic method represents accurately both the equilibrium and the non-equilibrium case, then it could be used for describing and interpreting the molecular motion during a realistic spectroscopic experiment. Broadly speaking, the interaction with the external field establishes a condition of non-equilibrium, e.g., a vibrational or vibronic excitation; afterwards the system relaxes in order to restore the equilibrium conditions. With this new methodology, it is possible to improve the representation proposed in Chap. 5 and regarding the excitation of isolated molecules, by including also the effects of the environment.

Now, getting down to details, the model system is composed of $n = 6$ interacting harmonic oscillators. The Hilbert space for the whole system is the tensor product of the Hilbert space for each oscillator, $\mathcal{H} = \mathcal{H}_1 \otimes \mathcal{H}_2 \otimes \ldots \otimes \mathcal{H}_n$. Each element of the space $\mathcal{H}_i$ can be fully specified by means of the orthonormal basis functions

$$\varphi_{l_i}(q_i) = \frac{1}{\sqrt{2^{l_i} l_i!}} \left(\frac{m\omega_i}{\pi\hbar}\right)^{1/4} \mathrm{He}_{l_i}\left(\sqrt{\frac{m\omega_i}{\hbar}} q_i\right) e^{-\frac{m\omega_i q_i^2}{2\hbar}}, \tag{7.18}$$

with l_i an integer index that can take the values $l_i = 0, 1, 2, \ldots$, and $\mathrm{He}_{l_i}(\bullet)$ the l_i-th Hermite polynomial. Each function $\varphi_{l_i}(q_i)$ is the l_i-th eigenfunction of the harmonic Hamiltonian operator $\hat{H}_i^{(0)}$ for the i-th single oscillator with frequency ω_i, that is

$$\hat{H}_i^{(0)} = -\frac{\hbar^2}{2m}\frac{\partial^2}{\partial q_i^2} + \frac{1}{2} m\omega_i^2 q_i^2. \tag{7.19}$$

The eigenvalue ϵ_{l_i} corresponding to the eigenfunction of Eq. (7.18) is obviously $\epsilon_{l_i} = (l_i + 1/2)\hbar\omega_i$. The Hamiltonian of the whole system is

$$\hat{H} = \hat{H}^{(0)} + \lambda \hat{V}^{(r)} = \sum_{i=1}^{n} \hat{H}_i^{(0)} + \lambda \hat{V}^{(r)}, \tag{7.20}$$

where $\hat{V}^{(r)}$ represents the interaction between the oscillators and λ is a parameter that sets the magnitude of the interaction in order to ensure that it plays the role of a perturbation with respect to $\hat{H}^{(0)}$. The interaction $\hat{V}^{(r)}$ is modelled with a random matrix as it is described in the Subs. 7.2.1. Notice that the oscillators have the same mass, but their characteristic frequency ω_i can be different. This feature will be employed in order to test the flexibility of the stochastic methods for reproducing

accurately different deterministic dynamics.

Finally, we recall the classification of the first oscillator as the subsystem S of interest and the identification of the environment E with the other five oscillators. Therefore, the operator $\hat{H}_1$ is the subsystem Hamiltonian operator $\hat{H}_S = \hat{H}_1$ and its eigenvalues $\epsilon_{l_S} = \epsilon_{l_1}$ represent the energy of the corresponding eigenfunctions. Similarly, the environment Hamiltonian operator is $\hat{H}_E = \sum_{i=2}^{n} \hat{H}_i$, and its eigenvalues are $\epsilon_{l_E} = \sum_{i=2}^{n} \epsilon_{l_i}$ with $l_E = (l_2, l_3, \ldots, l_n)$. We study the time evolution of different initial conditions, i.e., a specific initial configuration $Q(0)$ and a specific initial wave function $\Psi(q, 0)$, by focusing on the properties of the subsystem. In all the cases which are examined in the following, the same frequency is taken into account for the oscillators composing the environment, $\omega_i = \omega_E \ \forall i = 2, 3, \ldots, n$, whereas the frequency of the first oscillator $\omega_1 = \omega_S$ is either equal or different with respect to ω_E depending on the investigated conditions.

7.2.1 Numerical methods

Similarly to the study in Chap. 3, numerical methods have been employed i) to determine the eigenstates of the full system Hamiltonian $\hat{H}$, ii) to establish the initial conditions, iii) to compute the Bohm trajectory. Furthermore, numerical solutions of the stochastic equations (deriving later in this chapter) are taken into account.

First of all, we identify the Hamiltonian eigenstates through the numerical diagonalization of $\hat{H}$ matrix representation. For this purpose, we consider the basis set $\{|l\rangle\}$ whose elements $|l\rangle$ are defined according to the equation

$$\hat{H}^{(0)} |l\rangle = E_l^{(0)} |l\rangle \,, \tag{7.21}$$

where $l = (l_1, l_2, \ldots, l_n)$ and

$$|l\rangle = \bigotimes_{i=1}^{n} |\varphi_{l_i}\rangle \,, \qquad\qquad E_l^{(0)} = \sum_{i=1}^{n} \epsilon_{l_i}. \tag{7.22}$$

We would like to recall that each function $\varphi_{l_i}(q_i)$ of Eq. (7.18) and each element $|\varphi_{l_i}\rangle$ of Eq. (7.22) are related as $\varphi_{l_i}(q_i) = \langle q_i | \varphi_{l_i} \rangle$ and the eigenstates $|l\rangle$ of $\hat{H}^{(0)}$ are conveniently ordered in such a way that the corresponding eigenenergies $E_l^{(0)}$ are sorted in ascending order. Moreover, we will refer to $E_l^{(0)}$ as both the eigenvalue of $\hat{H}^{(0)}$ corresponding to $|l\rangle$ and the energy of $|l\rangle$. Hereafter, it is assumed that all possible wave functions of the system belong to the finite dimensional subspace $\mathcal{H}'$ (the "computational" Hilbert space) of the whole Hilbert space $\mathcal{H} = \mathcal{H}_1 \otimes \mathcal{H}_2 \otimes$

$\ldots \otimes \mathcal{H}_n$. From a computational point of view this is necessary for employing the matrix representation of the operators. In this regards, we define $\mathcal{H}'$ as the Hilbert space generated by the basis set $\{|l\rangle\}$ that includes only the eigenstates of $\hat{H}^{(0)}$with eigenenergies $E_l^{(0)}$ smaller than the cutoff energy $E_{tr}^{(0)}$ of the truncation: $\mathcal{H}' := \left\{\bigoplus_l |l\rangle \text{ with } E_l^{(0)} < E_{tr}^{(0)}\right\}$. By representing the operators on the basis set $\{|l\rangle\}$, $\hat{H}^{(0)}$ is a diagonal matrix whose elements are the eigenvalues $\left\{E_l^{(0)}\right\}$, whereas the operator $\hat{V}^{(r)}$ has been modelled with a random matrix whose elements are gaussian distributed according to the following statistical constraints:

$$\overline{V_{i,j}} = 0, \qquad \overline{(V_{i,j})^2} = \frac{1}{2 - \delta_{i,j}}, \tag{7.23}$$

where $\delta_{i,j}$ is the Kronecker delta. Finally, the eigenstates $|E_k\rangle$ of $\hat{H}$ are identified by linear combinations of the basis set elements $|l\rangle$ according to the numerical diagonalization. It has to be emphasised that the use of a finite number of elements for the basis set is necessary for performing the numerical computation, but it can be justified as long as the random potential is a perturbation compared to $\hat{H}^{(0)}$. As already explained in Chap. 3, the diagonalization of the full Hamiltonian is influenced mainly by the coupling between basis elements with similar energies $E_l^{(0)}$, and this allows an efficient truncation of the Hamiltonian matrix representation. From a technical view point, the sampling of $\hat{V}^{(r)}$ elements and the diagonalization of the Hamiltonian have been performed by employing the software routine *Armadillo*, a `C++` linear algebra library [Sanderson (2010)]. The considerations about the effects of $E_{tr}^{(0)}$ different values are reported in Chap. 3 and not repeated here since they are essentially identical.

Secondly, the initial wave function $|\Psi(0)\rangle$ has to be established. In order to fulfil this objective, the RPSE procedure can be employed (see Sec. 3.1 for details). One can assume that the wave function belongs to an N-dimensional subspace of $\mathcal{H}'$, called active space,

$$\mathcal{H}_N := \left\{\bigoplus_{k=1}^{N} |E_k\rangle \text{ with } E_N < E_{max} < E_{N+1}\right\} \tag{7.24}$$

that is the subspace due to the eigenstates of $\hat{H}$ with eigenvalues smaller than the parameter E_{max}. By specifying the initial wave function $|\Psi(0)\rangle$ as a linear combination of the basis elements $|E_k\rangle$ belonging to the active space $\mathcal{H}_N$, the coefficients of the expansion can be expressed in terms of populations $(P_1, P_2, \ldots, P_N)$ and phases

$\big(A_1(0), A_2(0), \ldots, A_N(0)\big)$

$$|\Psi(0)\rangle = \sum_{k=1}^{N} \sqrt{P_k} e^{-\imath A_k(0)} |E_k\rangle \,. \tag{7.25}$$

The RPSE procedure samples randomly the $N-1$ independent populations, assuming that they are equally distributed on their domain. Furthermore, also the N independent phases are selected randomly from the uniformly distribution on their domain. The parameter E_{max} has to be smaller than $E_{tr}^{(0)}$ since it is reasonable to suppose that the effects of the basis set $\{|l\rangle\}$ truncation are more pronounced for the eigenstates $|E_k\rangle$ with higher energies. So E_{max} is selected small enough to make the truncation effects negligible (see the considerations about the effects due to different $E_{tr}^{(0)}$ values in Subs. 3.2.2). The RPSE selects a "typical" wave function as explained in Chap. 3: the expectation values are characterised by a pure fluctuating evolution about their typical values. Broadly speaking, the dynamics corresponding to a RPSE initial wave function is the equilibrium dynamics. The observation of a non-equilibrium dynamics would require the selection of a particular initial wave function.

We consider a specific initial conditions for analysing also the non-equilibrium dynamics: we examine an initially isolated subsystem that begins interacting with the environment at $t = 0$. At time $t < 0$ the subsystem is supposed to be unentangled with the environment with a factorised wave function of the whole system. For this reason, the initial wave function can be written as

$$|\Psi(0)\rangle = \big|\Psi^S(0)\big\rangle \otimes \big|\Psi^E(0)\big\rangle \,, \tag{7.26}$$

where $\big|\Psi^S(0)\big\rangle \in \mathcal{H}_S := \mathcal{H}_1$, $\big|\Psi^E(0)\big\rangle \in \mathcal{H}_E := \mathcal{H}_2 \otimes \mathcal{H}_3 \otimes \ldots \otimes \mathcal{H}_n$ and $\mathcal{H}_S$, $\mathcal{H}_E$ are respectively the Hilbert space of the subsystem and of the environment. Notice that the computational limitations demand that $|\Psi(0)\rangle$ belongs to the computational Hilbert space $\mathcal{H}' = \left\{\bigoplus_l |l\rangle \text{ with } E_l^{(0)} < E_{tr}^{(0)}\right\}$ and this requires for a suitable choice of $\big|\Psi^S(0)\big\rangle$ and $\big|\Psi^E(0)\big\rangle$ that it is made by employing the following procedure. Let us consider $|l\rangle$ of Eq. (7.22) and its factorisation according to the tensor product between the specific basis set elements $|l_S\rangle \in \mathcal{H}_S$ and $|l_E\rangle \in \mathcal{H}_E$:

$$|l\rangle = |l_S\rangle \otimes |l_E\rangle \,. \tag{7.27}$$

For the sake of completeness, we recall that $|l_S\rangle = |\varphi_{l_1}\rangle$ and $|l_E\rangle = \bigotimes_{i=2}^{n} |\varphi_{l_i}\rangle$ with $l_S = l_1$ and $l_E = (l_2, l_3, \ldots, l_n)$ in such a way that $l = (l_S, l_E)$. We specify the

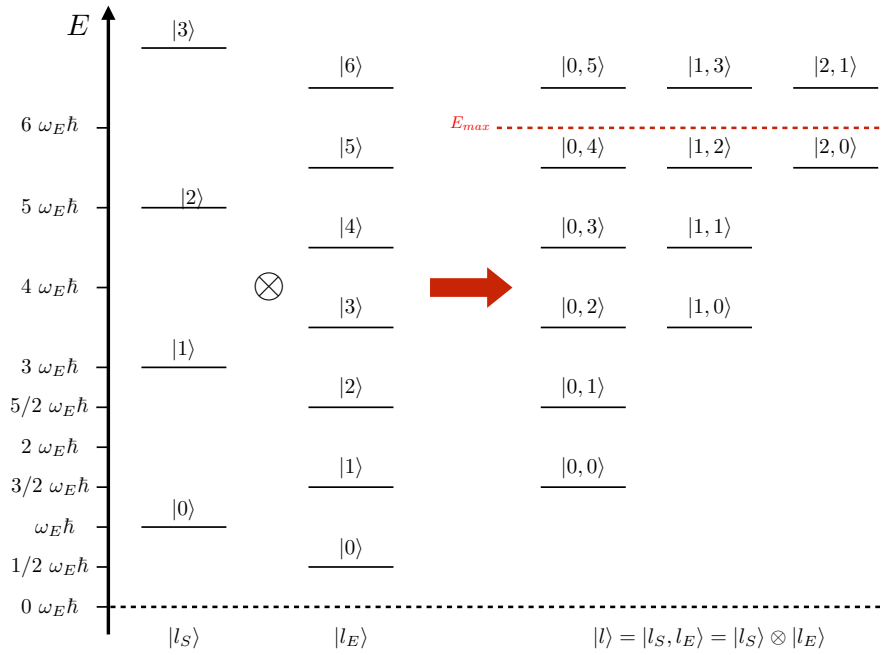

Figure 7.2: Representation of the basis set elements $|l_S\rangle$, $|l_E\rangle$ and $|l\rangle$ of the Hilbert spaces $\mathcal{H}_S$, $\mathcal{H}_E$ and $\mathcal{H}'$ ordered with respect to the corresponding eigenvalues in the case the system is composed of two oscillators. It has been assumed that $\omega_S = 2\omega_E$ and $E_{max} = 6\ \omega_E\hbar$.

subsystem initial wave function $\left|\Psi^S(0)\right\rangle$ and the environment initial wave function $\left|\Psi^E(0)\right\rangle$ according to the following equations,

$$\left|\Psi^S(0)\right\rangle = \sum_{l_S \in L_S} \sqrt{P^S_{l_S}}\,|l_S\rangle\,, \tag{7.28}$$

$$\left|\Psi^E(0)\right\rangle = \sum_{l_E \in L_E} \sqrt{P^E_{l_E}} e^{-\imath\chi_{l_E}}\,|l_E\rangle\,, \tag{7.29}$$

where L_S is an arbitrary set of l_S and L_E is the set of l_E, such that the eigenvalue $E^{(0)}_l$ of the Hamiltonian $\hat{H}^{(0)}$ corresponding to the eigenstate $|l\rangle = |l_S\rangle \otimes |l_E\rangle$ satisfies the inequality $E^{(0)}_l < E_{max}\ \forall l_S \in L_S$ and $\forall l_E \in L_E$.

Consider for example a system composed of two non interacting oscillators whose eigenstates are represented in Fig. 7.2. One oscillator is the interesting subsystem and the other is the environment. Their frequencies satisfy the equation $\omega_S = 2\omega_E$ by assumption. On the left hand side of Fig. 7.2 it is displayed how $|l_S\rangle$ and $|l_E\rangle$ are ordered with respect to their corresponding eigenenergies according to the equations $\hat{H}_S\,|l_S\rangle = \epsilon_{l_S}\,|l_S\rangle$ and $\hat{H}_E\,|l_E\rangle = \epsilon_{l_E}\,|l_E\rangle$. On the right hand side of Fig. 7.2 it is displayed how $|l\rangle = |l_S\rangle \otimes |l_E\rangle$ is distributed as a function of the energy $E^{(0)}_l = \epsilon_{l_S} + \epsilon_{l_E}$. If we assume that $L_S = (0, 1)$ and $E_{max} = 6\ \omega_E\hbar$, one can observe that the set L_E includes the l_E labels $(0, 1, 2)$. This can be verified with a simple reasoning.

Even if $E_l^{(0)} < E_{max}$ for $l_E = 3$ and $l_S = 0$, this is not true for $l_E = 3$ and $l_S = 1$. Since the definition of L_E imposes that $E_l^{(0)} < E_{max}$ $\forall l_S \in L_S$ and $\forall l_E \in L_E$, then $l_E = 3$ does not belong to L_E since there is a $l'_S \in L_S$ such that $E_{l'}^{(0)} > E_{max}$ with $l' = (l'_S, l_E)$.

With this approach the initial wave function is defined as a linear combination of some elements of the basis set $\{|l\rangle\}$ characterised by eigenvalues $E_l^{(0)}$ smaller than E_{max} instead of $E_{tr}^{(0)}$, which determines the computational truncation of the basis set. The use of E_{max} aims to get close to the limit that the initial wave function belongs to the active space $\mathcal{H}_N$ similarly to the RPSE sampling. Indeed, it is reasonably expected that the norm of the initial wave function component (Eq. (7.26), with $\left|\Psi^S(0)\right\rangle$ and $\left|\Psi^E(0)\right\rangle$ defined respectively in Eq. (7.28) and Eq. (7.29)), belonging to the active space, is greater then the norm of the component belonging to the complementary space as long as the interaction is a perturbation. However, we are aware that $|\Psi(0)\rangle$ can not belong exactly to $\mathcal{H}_N$; the above described method tries to mimic the condition of an initial wave function belonging to $\mathcal{H}_N$ as much as possible.

Then the problem of selecting $|\Psi(0)\rangle$ corresponds to the choice of the coefficients $\left\{P_{l_S}^S\right\}$, $\left\{P_{l_E}^E\right\}$, $\{\chi_{l_E}\}$. In order to ensure the normalisation of the wave function, the parameters $\left\{P_{l_S}^S\right\}$ and $\left\{P_{l_E}^E\right\}$ have to sum to one: $\sum_{l_S \in L_S} P_{l_S}^S = 1$ and $\sum_{l_E \in L_E} P_{l_E}^E = 1$; for the set $\{\chi_{l_E}\}$ there are no constraints. From a technical point of view, we select the parameters $\left\{P_{l_E}^E\right\}$ using the algorithm originally proposed for determining the RPSE populations [Fresch and Moro (2009)]: they are statistically sampled according to a uniform distribution and guaranteeing that the normalisation condition holds. Similarly, also the parameters $\{\chi_{l_E}\}$ have been randomly chosen inside the interval $[0 - 2\pi)$. The coefficients $\left\{P_{l_S}^S\right\}$ are instead picked arbitrarily in order to examine a particular phenomenology. Once the initial wave function has been established and written as a linear combination of the eigenstates $|E_k\rangle$ of $\hat{H}$, by using the numerical diagonalization, the solution of the Schrödinger equation is specified at an arbitrary time as in Eq. (3.39).

For solving numerically the Bohm equation and computing the deterministic Bohm trajectory of the oscillators, we adopted the Runge-Kutta method [Press et al. (2007)] at the 4-th order. This is fully equivalent to what we have done for determining the Bohm trajectory of the six rotors in Chap. 3.

As regards the numerical solution of the stochastic equations (Fokker-Planck and Langevin equation), we use common algorithms. For example, the Langevin equation can be solved by employing the Euler method [Press et al. (2007)] that is

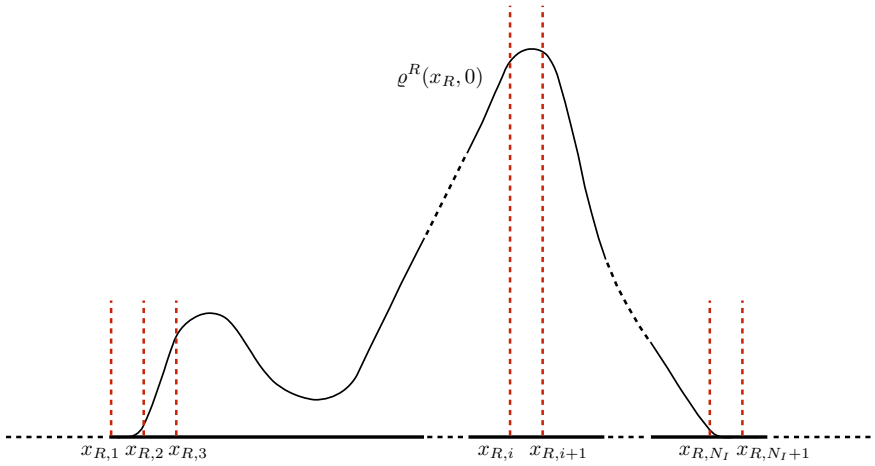

Figure 7.3: Hypothetical initial probability density $\varrho^R(x_R,0)$ on the space defined by the unidimensional relevant variables x_R. The probability density $\varrho^R(x_R,0)$ vanishes approximately outside the region between the endpoints $x_{R,1}$ and x_{R,N_I+1}. This region is further separated in N_I intervals whose endpoints are $x_{R,i}$ and $x_{R,i+1}$ for each i-th interval, with $i = 1, 2, \ldots, N_I$.

computationally less expensive than the Runge-Kutta method. Since the effects of the irrelevant variables are represented by a white noise in the Langevin equation, then the solution $X_R(t)$ can not be the exact projection of the deterministic dynamics on the relevant variables and one can use less accurate and less stable algorithm as the Euler method. In addition, for some cases we need to compute the average values predicted according to the Fokker-Planck equation. However, instead of solving directly this partial differential equation, we exploit the equivalence between the predictions of the Fokker-Planck equation and of a conveniently sampled swarm of Langevin trajectories [Gardiner (1986)]. Indeed one can determine the evolution of N_{tra} Langevin trajectories (through the Euler method) whose initial conditions $x_{R,0}$ are distributed according to the initial probability density on the relevant variables $\varrho^R(x_R,0)$. Then, each average property can be computed using the swarm of trajectories and it corresponds to the average property predicted by the Fokker-Planck in the limit of $N_{tra} \to +\infty$. The only numerical difficulty concerns the sampling of $x_{R,0}$ according to $\varrho^R(x_R,0)$. For accomplishing this task, one can implement a common Monte Carlo method, otherwise, if the space of the relevant variables is an unidimensional space, as it is in our case, we propose an alternative approach. Consider an initial density distribution $\varrho^R(x_R,0)$ as in Fig. 7.3; once the domain region where the density distribution does not vanish is identified, then this region has to be separated in N_I intervals with the same length. In Fig. 7.3 this region is delimited by the endpoints $x_{R,1}$, x_{R,N_I+1} and the extremes of the i-th interval are identified by $x_{R,i}$, $x_{R,i+1}$. The central point of each interval is the initial condition

of a number of Langevin equations proportional to the probability that the relevant variable belongs to that specific interval initially. In other words, the number of trajectories $N_{tra}(i)$ that depart from the central point of the i-th interval is defined by

$$N_{tra}(i) \simeq N_{tra} \int_{x_{R,i}}^{x_{R,i+1}} \mathrm{d}x_R \; \varrho^R(x_R, 0). \tag{7.30}$$

The above equation is not an exact equivalence since $N_{tra}(i)$ is the natural number closest to the value of the r.h.s. of Eq. (7.30). The choice of selecting the middle point of each interval as the initial condition of $N_{tra}(i)$ Langevin equation is reasonable as long as the length of the intervals is small compared to the length of the region $[x_{R,1} - x_{R,N_I+1}]$ and $\varrho^R(x_R, 0)$ changes negligibly inside each interval. Furthermore, the white noise ensures that different Langevin trajectories evolve from the same initial condition. In the limit of $N_{tra} \to +\infty$ and $N_I \to +\infty$, this approach should provide the same results as the Monte Carlo method. From a technical view point, the values of the parameters are set to $x_{R,1}/\sqrt{\hbar/m\omega_S} = -5$, $x_{R,N_I+1}/\sqrt{\hbar/m\omega_S} = 5$, $N_I = 100$, $N_{tra} = 10000$ for all the numerical simulations examined.

In the following, we analyse the predictions of the stochastic equations for the model system described above under different conditions and we compare the results with the deterministic behaviour.

7.3 Smoluchowski-Bohm equation

As already explained, we aim to describe the behaviour of an open quantum system (a subsystem of interest) with stochastic equations defined in the framework of Bohm theory. By bearing in mind the projection operator technique summarised in Sec. 7.1, the Fokker-Planck equation and the Langevin equation can be defined for a chosen set of relevant variables x_R. Of course, the coordinates q_S of the molecules composing the subsystem, or some of their degrees of freedom, belong to the set of relevant variables since our purpose is the description of their behaviour. This means that the coordinate $q_S = q_1$ of the first oscillator in our model system is one of the relevant variables. However, do these coordinates complete the set x_R? Should some coordinates of the environment or some phases be included too? To a first approximation, one can reasonably suppose that q_S is sufficient for well representing the dynamics of the subsystem with stochastic equations. Indeed, the trajectories of the six rotors of Chap. 3 (see Fig. 3.5) resemble a diffusion process that can be characterised according to the classical Smoluchowski equation [Gardiner (1986)]. This stochastic equation is well known to represent the dynamics of the coordinates

corresponding to relevant degrees of freedom, e.g., the coordinates of the center of mass of a Brownian particle. Therefore, we propose to classify the same variables as the relevant ones and to infer an analogous equation in the framework of Bohm theory that we call "Smoluchowski-Bohm" equation. Thus, the sets of relevant and irrelevant variables are defined as,

$$x_R = (q_S), \qquad x_I = (q_E, \alpha), \tag{7.31}$$

where α represents the wave function according to the formalism defined in Chap. 6. The coordinates of the molecules composing the environment are labeled q_E and with reference to the six oscillators $q_E = (q_2, q_3, \ldots, q_n)$. At this stage, the projection operators can be fruitfully employed to derive the following equilibrium density distribution and averaged velocity field,

$$\varrho^S_{eq}(q_S) = \sum_{l_S, l'_S} \overline{\sigma}_{l'_S, l_S} \varphi^*_{l_S}(q_S) \varphi_{l'_S}(q_S), \tag{7.32}$$

$$\Lambda_S(q_S) = \frac{\hbar}{m} \mathrm{Im} \left\{ \frac{\sum_{l_S, l'_S} \overline{\sigma}_{l'_S, l_S} \varphi^*_{l_S}(q_S) \nabla_S \, \varphi_{l'_S}(q_S)}{\varrho^S_{eq}(q_S)} \right\}, \tag{7.33}$$

that define the Fokker-Planck operator $\hat{\Gamma}^S$. We would like to emphasise some details concerning Eq. (7.32) and Eq. (7.33). They define the marginal equilibrium density distribution and the averaged velocity field by assuming that the subsystem of interest is the single oscillator of the model system, but their generalisation is straightforward. Secondly, the elements of $\{\varphi_{l_S}(q_S)\}$ are the eigenfunctions of the subsystem Hamiltonian $\hat{H}_S$, namely the eigenfunctions of the first harmonic oscillator: $\varphi_{l_S}(q_S) = \varphi_{l_1}(q_S) = \langle q_S | l_S \rangle$. The time average of the reduced density matrix element $\overline{\sigma}_{l'_S, l_S}$ in the representation of the basis set $\{\varphi_{l_S}\}$ is obtained by the integration on the α variables. Third, $\varrho^S_{eq}(q_S)$ is defined in Eq. (7.3) with $\varrho^{\Omega_P}_{eq}(x)$ of Eq. (6.24) and similarly $\Lambda_S(q_S)$ is defined in Eq. (7.13) with $\Lambda_{P,j}(x)$ of Eq. (6.20). In order to calculate the integrals on the irrelevant variables q_E involved in the definition of $\varrho^S_{eq}(q_S)$ and $\Lambda_S(q_S)$, it is convenient to write the eigenstates $|E_k\rangle$ of the Hamiltonian $\hat{H}$ (labeled $\phi_k(q)$ in Eq. (6.24) and Eq. (6.20)) as linear combinations of the basis set $\{|l\rangle\}$ elements through the numerical diagonalization $|E_k\rangle = \sum_l |l\rangle \langle l | E_k \rangle$. This leads to the factorisation of the function $\varphi_l(q) = \langle q | l \rangle$ as the product of a subsystem function and an environment function, $\varphi_l(q) = \varphi_{l_S}(q_S) \varphi_{l_E}(q_E)$. Finally, we tag the marginal equilibrium density distribution, the averaged velocity field and the Fokker-Planck operator with the label S instead of the generic R used in Eq. (7.3),

Eq. (7.13) and Eq. (7.16), for highlighting that the selected relevant variables are the coordinates of the subsystem S.

Despite Eq. (7.32) and Eq. (7.33) characterise completely the operator $\hat{\Gamma}^S$, other considerations can be invoked in order to further simplify the stochastic model. Indeed, the time average of the reduced density matrix is almost always equal to the canonical reduced density matrix for typicality [Goldstein et al. (2006); Fresch and Moro (2013)] (see also the statistics of quantum pure states in Sec. 3.1):

$$\overline{\hat{\sigma}} \simeq \frac{e^{-\hat{H}_S/k_BT}}{\mathrm{Tr}_S\left\{e^{-\hat{H}_S/k_BT}\right\}}, \tag{7.34}$$

where the thermodynamic limit has been considered. This means that its matrix representation on the basis set $\{\varphi_{l_S}(q_S)\}$ of the eigenfunctions of $\hat{H}_S$ is a diagonal matrix. By assuming that Eq. (7.34) holds, the averaged velocity field $\Lambda_S(q_S)$ vanishes since the eigenfunctions $\varphi_{l_S}(q_S)$ are real functions ($\varphi_{l_S}(q_S)$: $\mathbb{R} \to \mathbb{R}$). Consequently the Fokker-Planck operator is

$$\hat{\Gamma}^S = -\nabla_S \cdot \varrho^S_{eq}(q_S)\beta\ \nabla_S \left(\varrho^S_{eq}(q_S)\right)^{-1} \tag{7.35}$$

and the Langevin equation is

$$\frac{\mathrm{d}}{\mathrm{d}t}Q_S(t) = \beta\frac{\nabla_S\ \varrho^S_{eq}\left(Q_S(t)\right)}{\varrho^S_{eq}\left(Q_S(t)\right)} + \sqrt{2\beta}\zeta(t). \tag{7.36}$$

These two equations are formally equivalent to the classical Smoluchowski equation and the corresponding Langevin equation. All the quantum features of the motion are taken into account by the density distribution $\varrho^S_{eq}(q_S)$ that depends on the eigenfunctions of the subsystem Hamiltonian. For this reason, we refer to the Fokker-Planck equation with the operators $\hat{\Gamma}^S$ as the Smoluchowski-Bohm equation. In the following, we compare the predictions of Eq. (7.35) and Eq. (7.36) with those of the deterministic dynamics. In particular we consider two different cases. In the first case the system is already in equilibrium by sampling the wave function according to the RPSE statistical ensemble. In the second case, the subsystem is initially unentangled with the environment, which plays the role of a thermal bath warming the subsystem. Notice that the diffusion coefficient β has to be determined through the deterministic dynamics of $Q_S(t)$ interpreted as the result of an experimental observation. This approach is equivalent to that commonly employed in the framework of classical stochastic methods for recognising the value of the diffusion

Table 7.1: Diagonal elements of the equilibrium reduced density matrix $\overline{\sigma}_{l_S,l_S}$, with their canonical values reported between parentheses.

l_S	$\overline{\sigma}_{l_S,l_S}$
0	0.496 (0.456)
1	0.272 (0.250)
2	0.139 (0.137)
3	0.0618 (0.0749)
4	$0,0234$ (0.0410)
5	$6.71\ 10^{-3}$ (0.0224)
6	$1.14\ 10^{-3}$ (0.0123)
7	$6.50\ 10^{-7}$ ($6.73\ 10^{-3}$)

coefficient β.

7.3.1 Equilibrium dynamics

We consider six identical oscillators ($\omega_S = \omega_E$), coupled by a random potential with magnitude $\lambda = 0.001\ \omega_E\hbar$. The truncation energy is $E_{tr}^{(0)} = 10.5\ \omega_E\hbar$ and the cutoff energy is $E_{max} = 9.5\ \omega_E\hbar$. Therefore, the dimension of the computational Hilbert space is 1716 and the dimension of the active space is $N = 924$. By sampling the initial wave function according to the RPSE procedure, one can examine the deterministic wave function dynamics by solving the Schrödinger equation. The corresponding equilibrium reduced density matrix is almost diagonal ($\overline{\sigma}_{l_S,l'_S}/\overline{\sigma}_{l_S,l_S} < 1/100$) and the diagonal elements are reported in Table 7.1. Like with the model system of six interacting rotors, the decrease of the diagonal components $\overline{\sigma}_{l_S,l_S}$ with the subsystem energy (see Table 7.1) suggests a canonical form, i.e., $\overline{\sigma}_{l_S,l_S} \propto \exp(-\epsilon_{l_S}/k_BT)$, but this is not the case. Indeed, the hypothetical canonical coefficient $(1/k_BT)$ has been determined from the ratio $\overline{\sigma}_{0,0}/\overline{\sigma}_{1,1}$, and it is $1/k_BT = 0.602\ (\omega_S\hbar)^{-1}$. The corresponding elements of the canonical density are reported in Table. 7.1. Their deviations with respect to $\overline{\sigma}_{l_S,l_S}$ are evident: the model system is not large enough to reach the thermodynamic limit. However, it can be stated that the system resembles that of thermodynamic equilibrium, e.g., the reduced density matrix is a diagonal matrix.

The deterministic dynamics of the Bohm coordinates can be computed once the initial configuration is established. We assume that the initial positions of all the oscillators is the of bottom of the potential, $Q_i/\sqrt{\hbar/m\omega_i} = 0\ \forall i = 1, 2, \ldots, n$. The subsystem Bohm trajectory $Q_S(t)$ is displayed in Fig. 7.4. Similarly to the case of the system composed of six rotors, $Q_S(t)$ dynamics displays a fluctuating behaviour. In this case the trajectory is confined because of the harmonic potential as well as

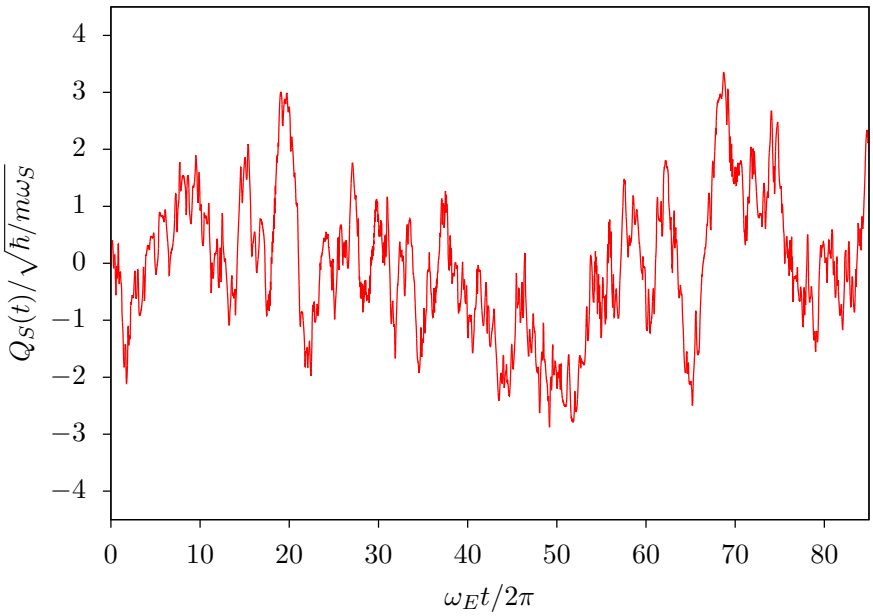

Figure 7.4: Deterministic time evolution of the Bohm coordinate of the first oscillator of the model system during the equilibrium dynamics (the initial wave function is sampled according to the RPSE statistics).

it was confined for the rotors by the cosine potential. In order to characterise the statistical properties of the trajectory $Q_S(t)$, the probability density $w^S_{eq}(q_S)$ and its autocorrelation function $G_{Q_S}(\tau)$ are analysed. We recall that the probability density $w^S_{eq}(q_S)$ is defined in such a way that the following equation holds for any observable of the type $b(q_S)$,

$$\lim_{T\to+\infty} \frac{1}{T}\int_0^T \mathrm{d}t\; b\left(Q_S(t)\right) = \int \mathrm{d}q\; b(q_S) w^S_{eq}(q_S). \tag{7.37}$$

The probability density $w^S_{eq}(q_S)$ and the autocorrelation function $G_{Q_S}(\tau)$ are shown in Fig. 7.5 and Fig. 7.6 respectively. Figure 7.5 clearly shows that the coordinate is distributed within a finite range and the probability of finding the particle outside is negligible. This confirms the hypothesis of a strongly confined motion based on the observation of the trajectory in Fig. 7.4. Furthermore, the fast loss of correlation (see Fig. 7.6) highlights the fluctuating character of the motion. These two features are similar to those already observed for the six rotor system in Chap. 3 and they can be reasonably interpreted as the evidences of a stationary Markov process as in Sec. 3.3. However, the stochastic theory presented in Sec. 7.1 is now available to represent this behaviour, in the effort to avoid the exact solution of the deterministic equations that are computationally too expensive for systems with a size larger than

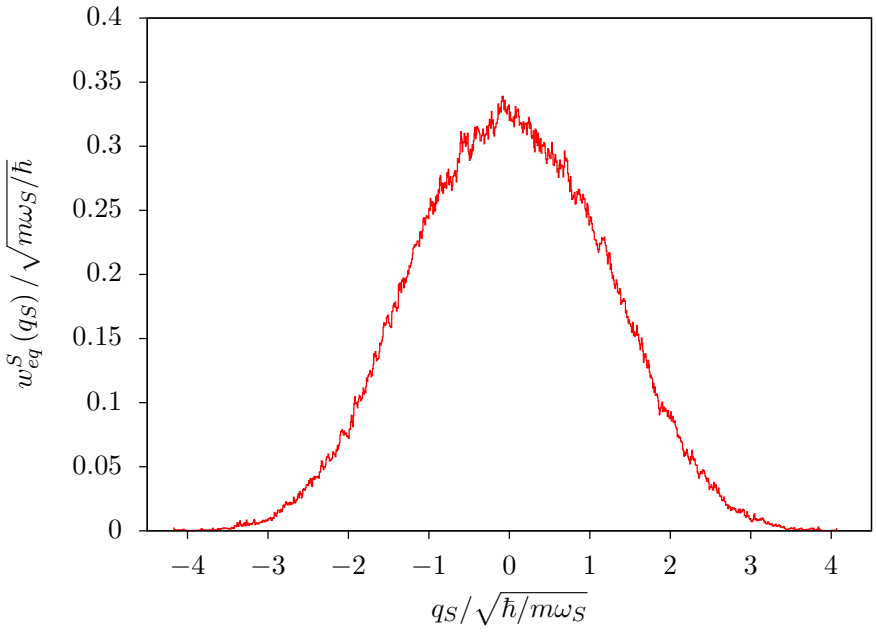

Figure 7.5: Marginal density distribution $w^S_{eq}(q_S)$ of the Bohm coordinate for the first oscillator. The distribution $w^S_{eq}(q_S)$ results from the sampling of the deterministic trajectory $Q_S(t)$ during the equilibrium dynamics.

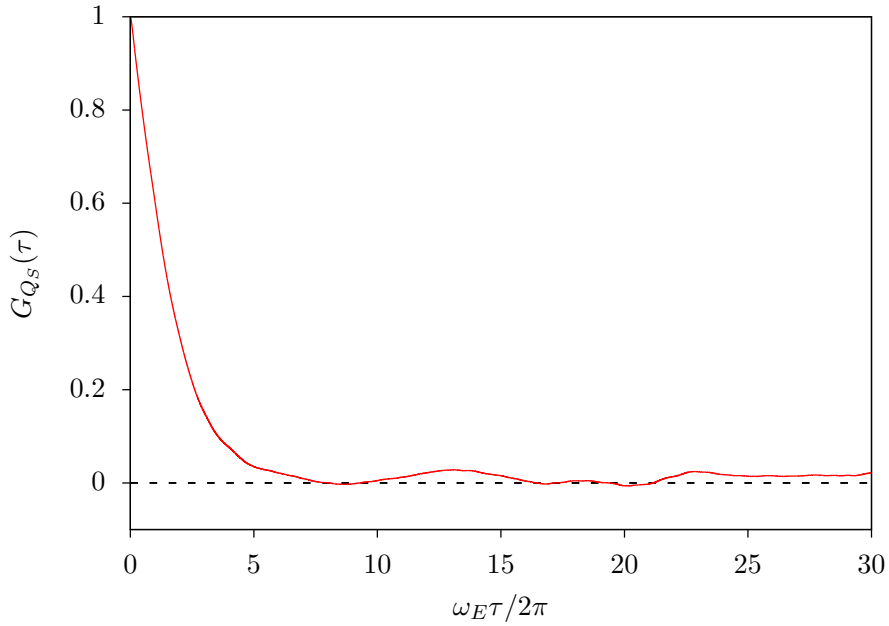

Figure 7.6: Correlation function $G_{Q_S}(\tau)$ of the first oscillator coordinate $Q_S(t)$ during the equilibrium dynamics.

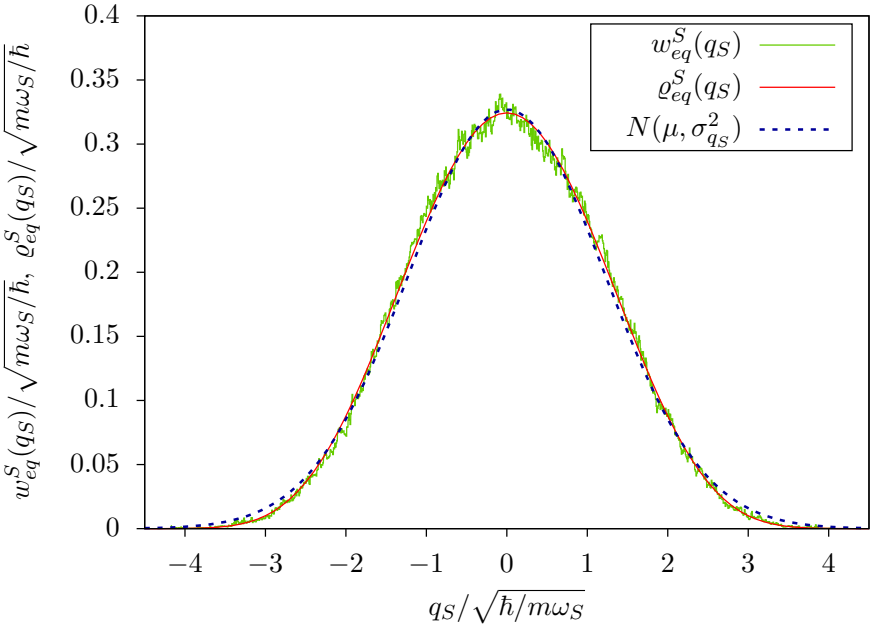

Figure 7.7: Marginal density distribution $w^S_{eq}(q_S)$ and equilibrium density distribution $\varrho^S_{eq}(q_S)$ of the Bohm coordinate of the first oscillator in the equilibrium experiment. They are compared with a gaussian distribution with average value $\mu = 0$ and variance $\sigma^2_{q_S} = 1.4884\ \hbar/m\omega_S$.

our model.

In order to use the Smoluchowski-Bohm equation the essential ingredient is the equilibrium density distribution $\varrho^S_{eq}(q_S)$ that can be exactly computed in the case of our model system. Moreover, it can be compared with the distribution $w^S_{eq}(q_S)$ obtained from the sampling of the Bohm trajectory and interpreted as the experimental observation. The two distributions $\varrho^S_{eq}(q_S)$, $w^S_{eq}(q_S)$ are shown in Fig. 7.7 together with a gaussian (normal) distribution $N(\mu, \sigma^2_{q_S})$, parametrised according to the average $\mu = 0$ and the variance $\sigma^2_{q_S} = 1.4884\frac{\hbar}{m\omega_S}$, of the Bohm coordinate Q_S. Notice that the equilibrium density distribution $\varrho^S_{eq}(q_S)$ is very close to $w^S_{eq}(q_S)$. This result is not surprising since $\varrho^S_{eq}(q_S)$ is formally equivalent to the distribution $p^S_{eq}(q_S)$ defined in Chap. 3 (compare Eq. (7.32) with Eq. (3.42)). Albeit they have been obtained from different type of analysis and for different purposes, but they are represented by the same function. In other words, the equilibrium density distribution $\varrho^S_{eq}(q_S)$ for the relevant variables q_S is equivalent to the time average of the wave function square modulus $|\Psi(q,t)|^2$ integrated on the degrees of freedom of the environment. In our representation of the Bohm state $(Q(t), \Psi(q,t))$ in terms of coordinates and phases $(Q(t), A(t))$, the average on the phases corresponds to the time average of the wave function. This can be considered as an additional evidence of the emergence of the conventional quantum properties, such as the equilibrium

distribution predicted according to the wave function, from the dynamics of a single Bohm trajectory. This issue has been already examined in detail in Chap. 3 and Chap. 6. For the purposes of this chapter, the important issue is the correspondence between the equilibrium distribution $\varrho^S_{eq}(q_S)$ of the stochastic theory and the statistical properties of the deterministic dynamics, i.e., $w^S_{eq}(q_S)$.

It should be stressed that the equilibrium probability density $\varrho^S_{eq}(q_S)$ can not be computed for a macroscopic system by evaluating the integral in Eq. (7.3). The problem can still be handled in two ways. The first consists in modelling the subsystem Hamiltonian $\hat{H}_S$, by computing the corresponding eigenfunctions and assuming that $\overline{\hat{\sigma}}$ satisfies the canonical condition of Eq. (7.34). The second strategy reproduces the profile of $w^S_{eq}(q_S)$ through the fitting with a suitable set of functions. Whereas the first approach can be very useful for the general case, the second one is suited to describe the single oscillator of our model because of the similarity between $\varrho^S_{eq}(q_S)$ and gaussian distribution properly parametrised (see Fig. 7.7). By assuming that the following equality holds

$$\varrho^S_{eq}(q_S) = \frac{e^{-q_S^2/2\sigma^2_{q_S}}}{\sqrt{2\pi}\sigma_{q_S}}, \tag{7.38}$$

with $\sigma^2_{q_S} = 1.4884\frac{\hbar}{m\omega_S}$, the characterisation of $Q_S(t)$ dynamics through the stochastic equations is further simplified. As long as the Smoluchowski-Bohm operator of Eq. (7.35) represents a Gaussian Markov process, an exponential function is recovered for the correlation function of the Bohm coordinate,

$$G_{Q_S}(\tau) := \frac{\int \mathrm{d}q_S \; q_S e^{-\tau\hat{\Gamma}^S} \varrho^S_{eq}(q_S) q_S}{\int \mathrm{d}q_S \; q_S^2 \; \varrho^S_{eq}(q_S)} = e^{-\frac{\beta}{\sigma^2_{q_S}}\tau}, \tag{7.39}$$

with a correlation time inversely proportional to the diffusion coefficient β. By comparing such a result with the computed correlation function displayed in Fig. 7.6, the diffusion coefficient can be fitted to the value $\beta = 0.1414\ 2\pi m/\hbar$. The effectiveness of such a fitting clearly emerges in the comparison done in Fig. 7.8 between the two correlation functions. The value of the diffusion coefficient β ($\beta = 0.1414\ 2\pi m/\hbar$) has been determined by trying different reasonable values in order to obtain the maximum possible agreement between the deterministic autocorrelation function and the one defined in Eq. (7.39).

A this point the Fokker-Planck operator is completely characterised according to the equilibrium density distribution $\varrho^S_{eq}(q_S)$ and the coefficient β. Consequently, also the Langevin equation is fully defined and the stochastic version of $Q_S(t)$ dynamics

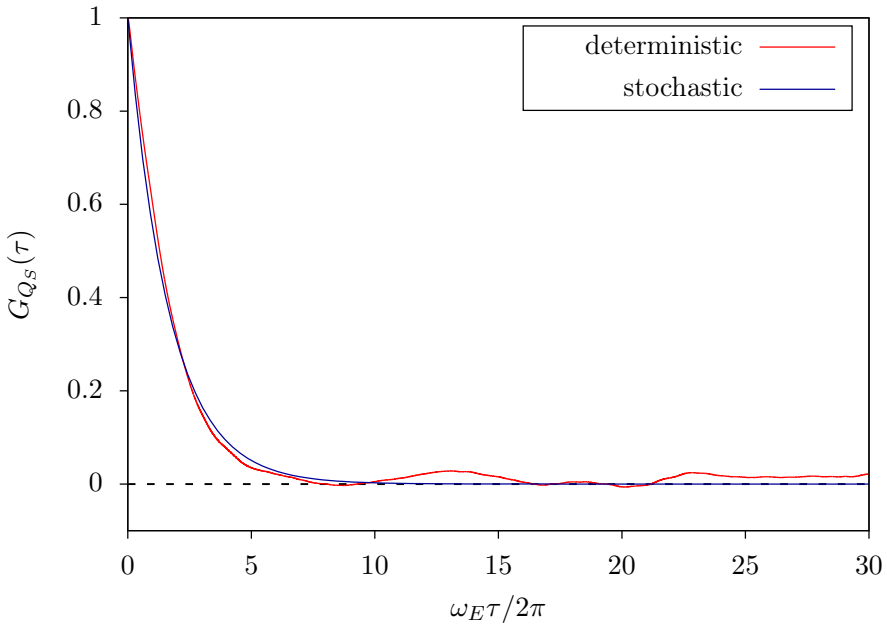

Figure 7.8: Correlation function $G_{Q_S}(\tau)$ of the first oscillator coordinate $Q_S(t)$ in the equilibrium experiment: comparison between the one obtained from the deterministic dynamics (red line) and the one obtained from the Gaussian Markov approximation (blue line) of the Smoluchowski-Bohm equation with $\beta = 0.1414\ 2\pi m/\hbar$ and $\sigma^2_{q_S} = 1.4884\ \hbar/m\omega_S$.

can be computed. In particular, if Eq. (7.38) holds, the following simple form of the Langevin equation can be employed:

$$\frac{\mathrm{d}}{\mathrm{d}t}Q_S(t) = -\frac{\beta}{\sigma^2_{q_S}}Q_S(t) + \sqrt{2\beta}\zeta(t). \tag{7.40}$$

By solving the above equation, the stochastic trajectory $Q_S(t)$ has been determined and it is shown in Fig. 7.9 together with the result of the deterministic calculation. Of course evident differences exist between the two kinds of trajectories. As a matter of fact, the stochastic methods (including the classical stochastic methods) can not supply the exact single trajectory since the environment effects are described as random forces (the white noise of Eq. (7.40)), but they reproduce correctly the statistical properties, like the loss of correlation or the sampling of the q_S space. By repeating the analyses also for the stochastic trajectory, one recovers the same distribution $w_{eq}(q_S)$ and the same correlation function $G_{Q_S}(\tau)$ obtained for the deterministic one. Moreover, the trajectory obtained by solving exactly the Bohm equation is strictly dependent on the initial conditions and it changes to a large extent with a slightly different initial position of the particles because of the chaotic nature of the motion. For this reason the knowledge of the exact trajectory has a

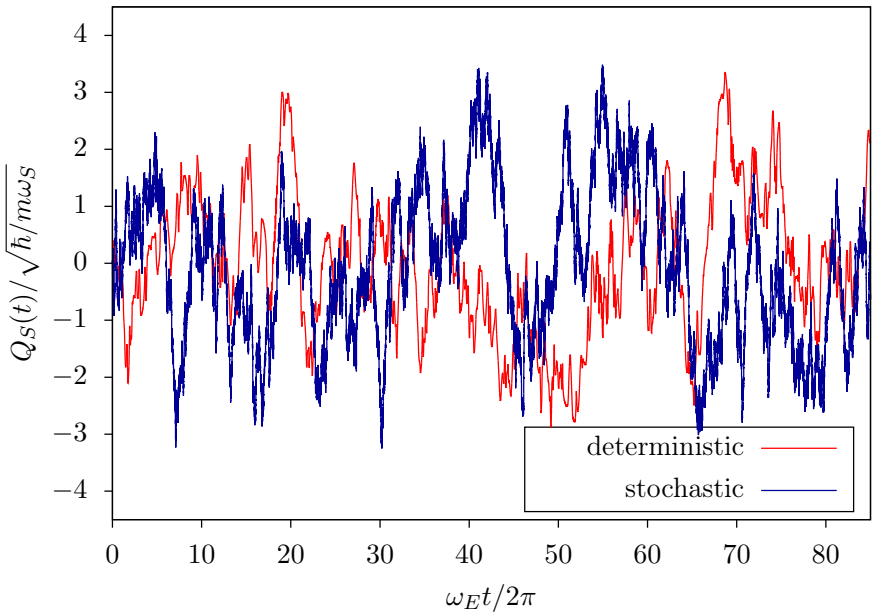

Figure 7.9: Time evolution of the Bohm coordinate of the first oscillator of the model system in the equilibrium experiment. One trajectory has been determined by solving exactly the Bohm equation (red line), whereas the other by solving the corresponding Langevin equation (blue line).

secondary role in opposition to the knowledge of its statistical properties.

In conclusion, the above proposed Smoluchowski-Bohm equation characterises accurately the equilibrium dynamics of a subsystem once the equilibrium density distribution $\varrho^S_{eq}(q_S)$ and the diffusion coefficient β have been established. As regards $\varrho^S_{eq}(q_S)$, one can model the subsystem Hamiltonian to determine it. On the contrary, the diffusion coefficient β has to be considered as a free parameter of the method and to be obtained from the analysis of the deterministic dynamics, similarly to what it is done for classical stochastic methods in the framework of Classical Mechanics.

In the next subsection, we examine the predictions of the stochastic equations for describing the dynamics in the case of non-equilibrium conditions.

7.3.2 Thermalisation dynamics

We consider the same system of six oscillators with $\omega_S = \omega_E$ characterised by the same values of the parameters, $\lambda = 0.001\ \omega_E\hbar$, $E^{(0)}_{tr} = 10.5\ \omega_E\hbar$, $E_{max} = 9.5\ \omega_E\hbar$, but with the initial wave function which is not sampled according to the RPSE statistic. As anticipated in Subs. 7.2.1, we examine the case of a subsystem initially unentangled with the environment. Whereas the coefficients $\left\{P^E_{l_E}\right\}$ and $\{\chi_{l_E}\}$ are randomly sampled, we select suitable coefficients $\left\{P^S_{l_S}\right\}$. In particular we assume

Table 7.2: Diagonal elements of the initial $\sigma_{l_S,l_S}(0)$ and of the equilibrium $\overline{\sigma}_{l_S,l_S}$ reduced density matrix. The canonical values are reported between parentheses.

l_S	$\sigma_{l_S,l_S}(0)$	$\overline{\sigma}_{l_S,l_S}$
0	0.5	0.523 (0.484)
1	0.5	0.271 (0.251)
2	0	0.128 (0.130)
3	0	0.0541 (0.0673)
4	0	0.0183 (0.0349)
5	0	$4.60\ 10^{-3}$ (0.0181)
6	0	$5.84\ 10^{-4}$ ($9.36\ 10^{-3}$)
7	0	$8.19\ 10^{-7}$ ($4.85\ 10^{-3}$)

that $L_S = (0, 1)$ and that the subsystem wave function is equally distributed between the ground and the first excited state:

$$P^S_{l_S} = 0.5 \qquad \forall l_S = 0, 1. \tag{7.41}$$

In order to rationalise the wave function dynamics and in particular the subsystem behaviour, one can compare the the diagonal elements of the initial reduced density matrix $\sigma_{l_S,l_S}(0)$ with those of the equilibrium reduced density matrix $\overline{\sigma}_{l_S,l_S}$. Their values are reported in Table 7.2. Subsystem states with $l_S > 2$ become populated after the interaction with the environment unlike in the initial state. One can suppose that the dynamics establishes an energy flux from the environment to the subsystem and consequently the excited eigenstates of the subsystem will be populated during the time evolution. This can be further visualised by examining Fig. 7.10, where the time evolution of the elements $\sigma_{0,0}(t)$, $\sigma_{1,1}(t)$ and $\sigma_{0,1}(t)$ is displayed. After such initial change, the element $\sigma_{0,0}$ becomes almost identical to its equilibrium value, while the element $\sigma_{1,1}$ decreases in time until to reach its equilibrium value $\overline{\sigma}_{1,1}$. This corresponds to increases the excited states populations and the warming of the subsystem, while the ground state population is approximately conserved. It should be recalled that in this process the trace of the reduced density matrix is conserved. On the other hand, the off-diagonal element $\sigma_{0,1}$ oscillates with angular frequency ω_S (coherent dynamics). The amplitude of its oscillation decreases because of the decoherence processes due to the interaction with the environment. For $\sigma_{0,1}$ as well as for all the other off-diagonal elements, the amplitude of the oscillation becomes negligible in equilibrium conditions leading with the time to a nearly diagonal reduced density matrix. One can observe that for $\omega_E t/2\pi > 25$ the elements of the reduced density matrix are almost time independent and equal

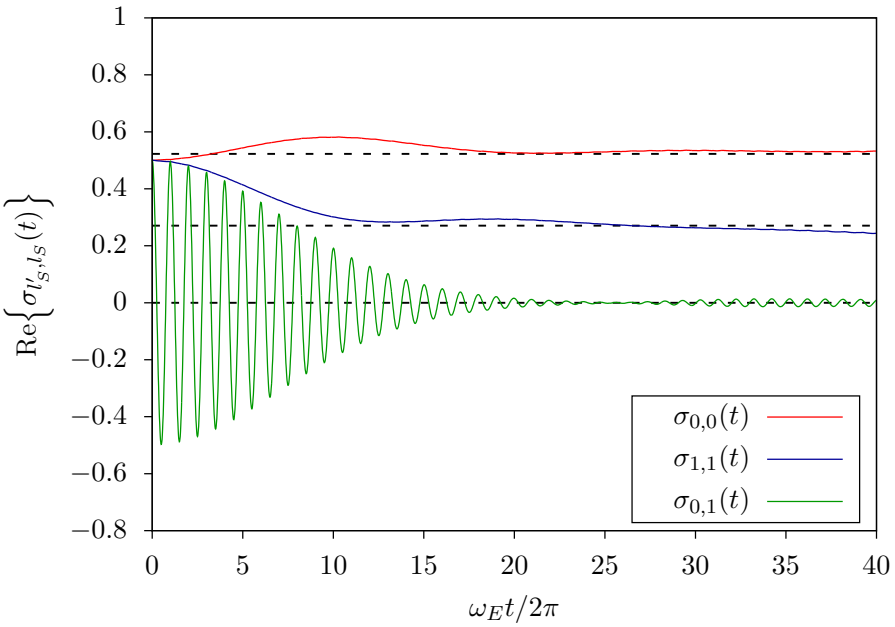

Figure 7.10: Deterministic time evolution of the reduced density matrix elements $\sigma_{0,0}$ (red line), $\sigma_{1,1}$ (blue line) and of the real part of $\sigma_{0,1}$ (green line) during the thermalisation dynamics. The black dashed lines represent the corresponding equilibrium values.

to their equilibrium values. In other words, for $\omega_E t/2\pi > 25$ the system has reached the equilibrium. However, the system is still not large enough to ensure the thermodynamic limit. By comparing the equilibrium and the canonical values of $\hat{\sigma}$ (where $1/k_B T = 0.658\ (\omega_S \hbar)^{-1}$ has been determined through the ratio $\overline{\sigma}_{0,0}/\overline{\sigma}_{1,1}$), it can be verified that the model system just resembles the thermodynamic equilibrium. We classify such a kind of dynamics as a thermalisation process that warms the subsystem through the increase of its energy: the excited states become populated.

The Bohm trajectory of the oscillator representing the subsystem of interest is shown in Fig. 7.11. The displayed time interval is shorter than in Fig. 7.4 in order to highlight a significant change of features in the time evolution of the Bohm coordinate corresponding to the subsystem. In particular, the motion is approximately an oscillation for $\omega_E t/2\pi < 15$: a distinctive frequency can be recognised from Fig. 7.11 in correspondence to the oscillator frequency ω_S. This type of behaviour is conserved until the the subsystem ground and first excited states are the main populated states. Once the equilibrium is established ($\omega_E t/2\pi > 25$) the trajectory is characterised by a fluctuating profile, similarly as the initial wave function was sampled according to the RPSE. For recognising this similarity between the two numerical experiments, one can compare the trajectory of Fig. 7.4 and the trajectory of Fig. 7.11 for $\omega_E t/2\pi > 25$. During the time interval between $\omega_E t/2\pi = 15$ and

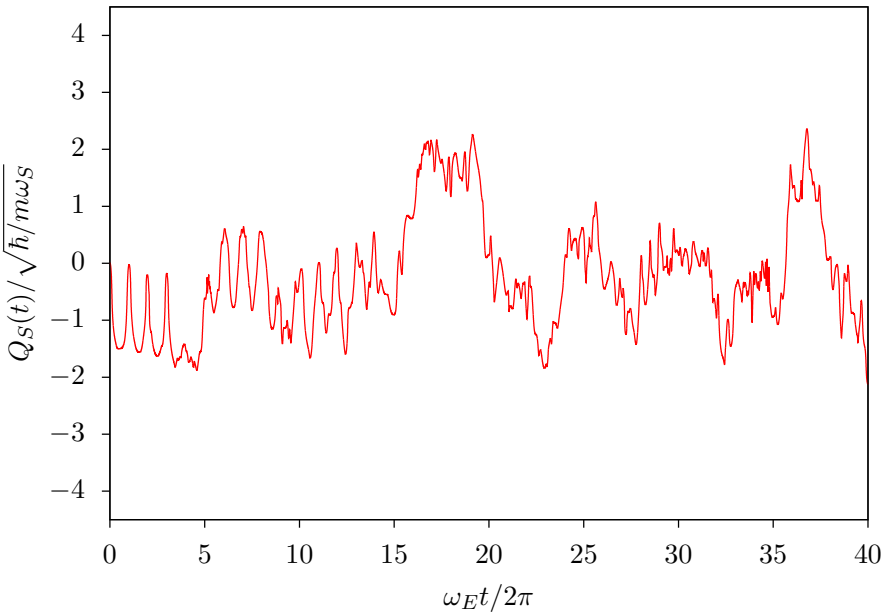

Figure 7.11: Deterministic time evolution of the Bohm coordinate of the first oscillator of the model system during the thermalisation dynamics (the initial wave function is factorised into the subsystem wave function and environment wave function).

$\omega_E t/2\pi = 25$, the motion is approximately a mixture of the two behaviours. The dynamics of the reduced density matrix of the subsystem is initially coherent because of the particular initial conditions where the ground state and the first excited state are equally populated (see Fig. 7.10). The corresponding Bohm trajectory is approximately an oscillation at the frequency of the coherence between the two subsystem states. On the other hand, when the reduced density matrix is almost the equilibrium density matrix ($\omega_E t/2\pi > 25$), then the Bohm coordinate fluctuates as in the previous case (equilibrium dynamics). For this reason, we use the term "coherent dynamics" also for the time evolution of the Bohm coordinate as regards the initial time evolution, while we call the second regime "fluctuating dynamics".

If the Bohm trajectory is analysed in terms of its equilibrium distribution $w^S_{eq}(q_S)$ and the autocorrelation function $G_{Q_S}(\tau)$ the results are comparable with those of the previous case (see Fig. 7.5 and Fig. 7.6). For this reason, they are not shown again, but they will be taken into account when examining the stochastic description.

In this case (thermalisation dynamics) also the analysis of the deterministic expectation values of subsystem observables, $b(t) = \langle\Psi(t)|\hat{b}|\Psi(t)\rangle$, is significant, unlike the previous numerical simulation. In equilibrium conditions the expectation values of the subsystem observables $b(t)$ are almost time independent because of the time independence of the reduced density matrix (see Eq. (3.21)). Conversely, the non-

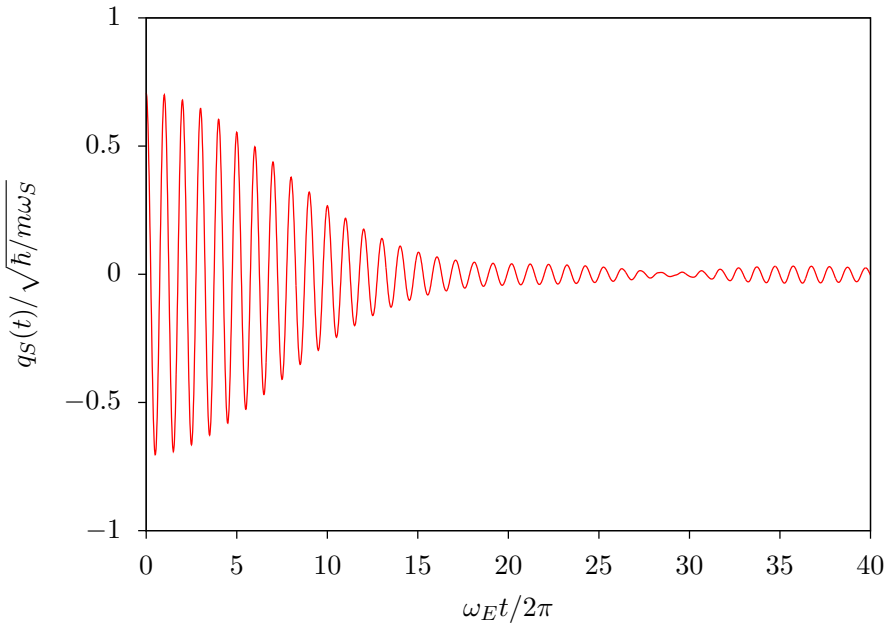

Figure 7.12: Deterministic time evolution of the expectation value for the subsystem coordinate during the thermalisation dynamics.

equilibrium dynamics is characterised by relaxation to the equilibrium value [Fresch and Moro (2013)]. One can suppose that the non-equilibrium dynamics of the expectation values should be represented according to the Fokker-Planck equation with a suitable choice of the initial distribution. This hypothesis might be reasonable since their equilibrium values, $b(t) \simeq \overline{b}$, have been already described in terms of the equilibrium average on the dynamical space according to $\varrho_{eq}^{\Omega_P}(x)$ (see Sec. 6.4 where we proved that $\mathbb{E}_{eq}^{\Omega_P}[b] = \overline{b} \simeq b(t)$). In particular we focus on the expectation value of the subsystem coordinate

$$q_S(t) = \langle \Psi(t)|\hat{q}_S|\Psi(t)\rangle = \mathrm{Tr}_S\left\{q_S\hat{\sigma}(t)\right\}, \tag{7.42}$$

that should evolve significantly in time until the equilibrium is reached. The complete time evolution of $q_S(t)$ from the deterministic dynamics is shown in Fig. 7.12 and resembles the time evolution of the element $\sigma_{0,1}(t)$ of the reduced density matrix (see Fig. 7.10). Similarly to the time evolution of the Bohm coordinate, also the dynamics of the expectation value $q_S(t)$ shows two different regime. For $\omega_E t/2\pi < 15$, the expectation value oscillates with ω_S frequency and the decrease of the amplitude of oscillations is the consequence of the reduced density matrix decoherence dynamics. For $\omega_E t/2\pi > 25$, the amplitude of the oscillation is negligible in consequence of the equilibrium dynamics. In this case, the deviations of the expectation value from

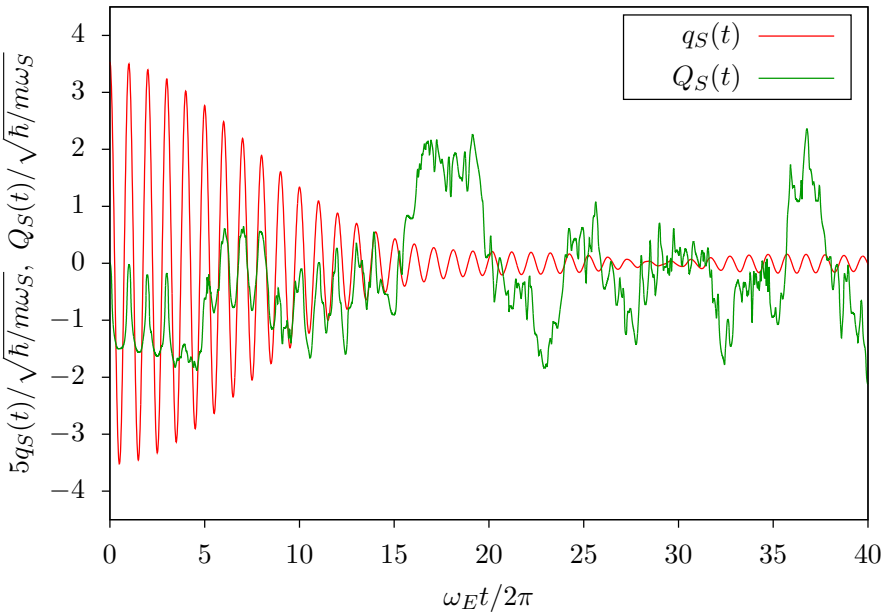

Figure 7.13: Deterministic time evolution of the expectation value $q_S(t)$ (red line) corresponding to the subsystem coordinate and of the subsystem Bohm coordinate $Q_S(t)$ (green line) during the thermalisation dynamics.

the equilibrium value do not vanish completely because of the limited dimension of the environment: the system resembles the thermodynamic limit. This behaviour of $q_S(t)$ is exactly the one expected according to the statistic of quantum pure states which has been summarised in Sec. 3.1.

Before the stochastic analysis, we would like to emphasise some differences between the Bohm trajectory $Q_S(t)$ for the subsystem and the corresponding expectation value $q_S(t)$ that are compared in Fig. 7.13. During the coherent regime, both the the trajectory and the expectation value are mainly characterised by an oscillating dynamics. The profile of the trajectory is less regular than the corresponding expectation value because of the fluctuating nature of the Bohm trajectories. However, the main feature is almost the same: an oscillation with ω_S frequency. On the other hand, the dynamics during the equilibrium regime is deeply different. Indeed, the expectation value is approximately time independent, whereas the Bohm trajectory shows a fluctuating dynamics as already discussed in Chap. 3. The transition between the two types of regimes is an excellent opportunity for highlighting their differences regarding the equilibrium dynamics. This is particularly important since it allows us to stress the impossibility of describing the equilibrium dynamics with the expectation values as long as they are almost time independent. The Bohm coordinates are the suitable tool to display the time evolution hidden in the nearly

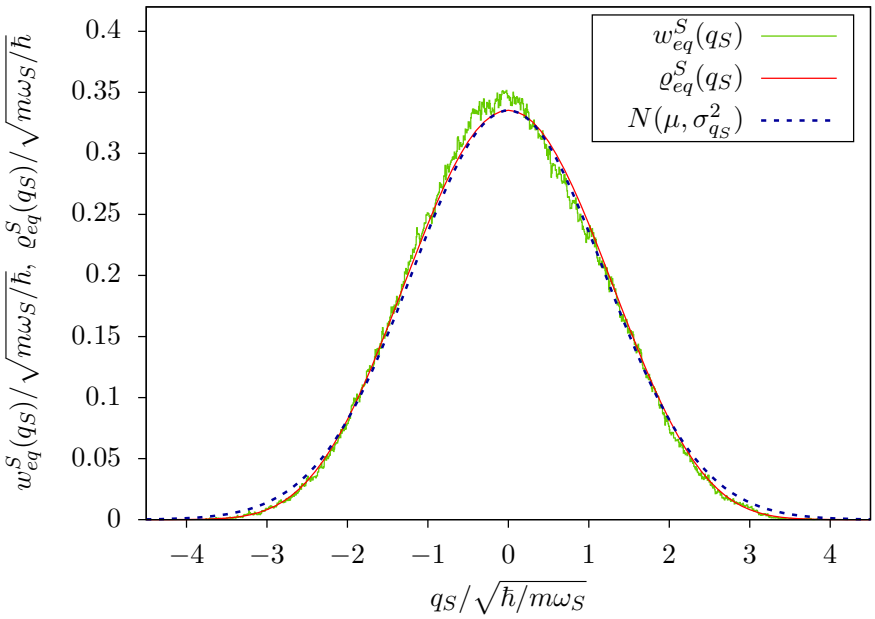

Figure 7.14: Marginal density distribution $w^S_{eq}(q_S)$ and equilibrium density distribution $\varrho^S_{eq}(q_S)$ of the Bohm coordinate of the first oscillator in the thermalisation experiment. They are compared with a gaussian distribution with average value $\mu = 0$ and variance $\sigma^2_{q_S} = 1.4161\ \hbar/m\omega_S$.

constant expectation values.

Once the deterministic dynamics has been completely examined, one can focus on the stochastic predictions. Similarly to the analyses of Subs. 7.3.1, we take into account the marginal equilibrium distribution $\varrho^S_{eq}(q_S)$ and the autocorrelation function $G_{Q_S}(t)$. The distribution $\varrho^S_{eq}(q_S)$ has been both exactly computed and approximated with a gaussian distribution with amplitude $\sigma^2_{q_S} = 1.4161\ \hbar/m\omega_S$. The comparison between $w^S_{eq}(q_S)$, $\varrho^S_{eq}(q_S)$ and the gaussian distribution are shown in Fig. 7.14. Also in this case the marginal equilibrium distribution $\varrho^S_{eq}(q_S)$ is compatible with the statistical properties of the deterministic dynamics $w^S_{eq}(q_S)$ and it can be approximated with a gaussian distribution: the differences between a gaussian function with $\sigma^2_{q_S} = 1.4161\ \hbar/m\omega_S$ and $\varrho^S_{eq}(q_S)$ are negligible. Consequently, we assume that Eq. (7.38) holds also in this case with $\sigma^2_{q_S} = 1.4161\ \hbar/m\omega_S$. Therefore, the autocorrelation function $G_{Q_S}(\tau)$ satisfies the equivalence of Eq. (7.39) and it is plotted in Fig. 7.15 with $\beta = 0.1345\ 2\pi m/\hbar$. The differences between the deterministic and the stochastic autocorrelation are not relevant since the main feature (the exponential decay) is well reproduced. Also in this case we select the value of the diffusion coefficient β by fitting the correlation function.

It should be noticed that $\varrho^S_{eq}(q_S)$ and β are slightly modified with respect to the equilibrium experiment (compare the values of the parameters $\sigma^2_{q_S}$ and β for the

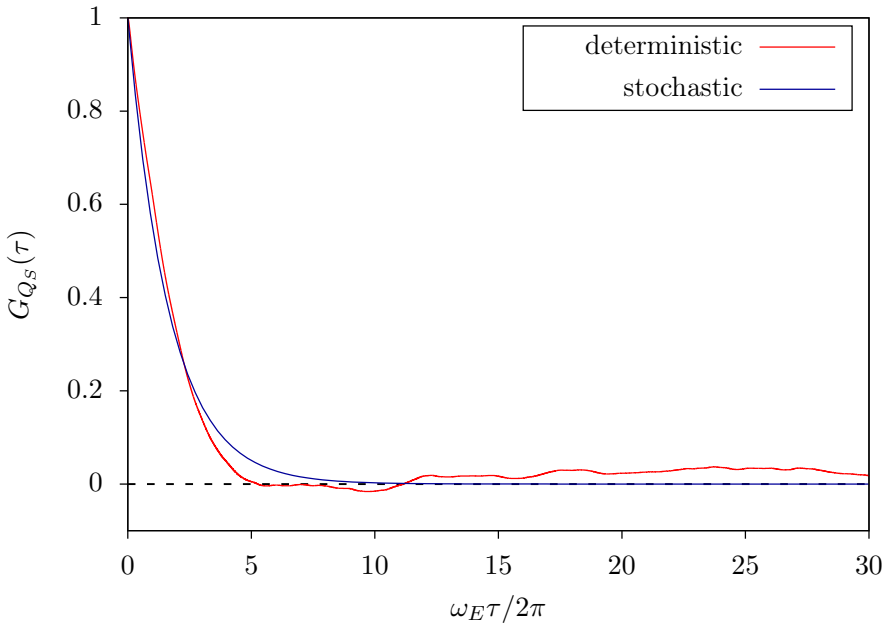

Figure 7.15: Correlation function $G_{Q_S}(\tau)$ of the first oscillator coordinate $Q_S(t)$ in the thermalisation experiment. One correlation function has been determined by analysing the deterministic dynamics (red line), whereas the other through Eq. (7.39) with $\beta = 0.1345\ 2\pi m/\hbar$ and $\sigma^2_{q_S} = 1.4161\ \hbar/m\omega_S$ (blue line).

two simulations). The differences can be attributed to the fact that the quantum dynamics is realised in different dynamical spaces. As a matter of fact, in the thermalisation experiment, the initial wave function $|\Psi(0)\rangle$ does not belong to the active space and the populations are not randomly sampled according to RPSE statistic. However, the statistical properties ($\varrho^S_{eq}(q_S)$ and β) appear to be resilient to the choice of deeply different initial wave functions, since they are almost conserved in the two experiments.

Independently of these considerations, one can compute the stochastic trajectory and the stochastic average value. As regards the stochastic Bohm trajectory, it has been computed by solving Eq. (7.40) with the correct value of the parameters $\sigma^S_{q_S}$, β and it is compared to the deterministic one in Fig. 7.16. The fluctuating behaviour ($\omega_E t/2\pi > 25$) is well reproduced, whereas the initial coherent dynamics is totally missing in the stochastic trajectory. This was expected since an oscillating motion in the framework of Classical Mechanics can not be recovered from the Smoluchowski equation; similarly, the Langevin equation corresponding to our Smoluchowski-Bohm equation can not predict the coherent motion of the Bohm trajectory. In other words, the Smoluchowski-Bohm equation describes only the fluctuating dynamics.

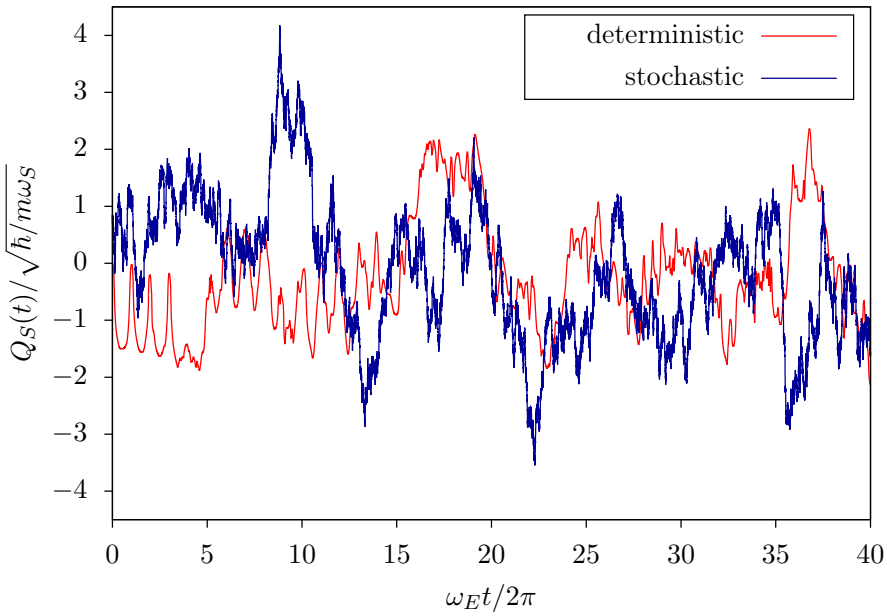

Figure 7.16: Time evolution of the Bohm coordinate of the first oscillator of the model system in the thermalisation experiment. One trajectory has been determined by solving exactly the Bohm equation (red line), whereas the other by solving the corresponding Langevin equation (blue line).

This can be further verified by comparing the expectation value $q_S(t)$ and the average value $\mathbb{E}^S[q_S](t)$ defined according to the formal solution of the Fokker-Planck equation,

$$\mathbb{E}^S[q_S](t) = \int \mathrm{d}q_S \; q_S \; e^{-t\hat{\Gamma}^S} \varrho^S(q_S, 0), \tag{7.43}$$

where $\varrho^S(q_S, 0)$ is a suitably chosen initial probability distribution on the relevant variable q_S. We select $\varrho^S(q_S, 0)$ according to the square modulus of the initial wave function integrated on the environment degrees of freedom,

$$\varrho^S(q_S, 0) := \int \mathrm{d}q_E \; |\Psi(q, 0)|^2 = \sum_{l_S, l'_S \in L_S} \sqrt{P^S_{l_S} P^S_{l'_S}} \varphi^*_{l_S}(q_S) \varphi_{l'_S}(q_S) \tag{7.44}$$

with $q = (q_S, q_E)$. The last equality in Eq. (7.44) holds because of our assumption regarding the initial wave function (see Eq. (7.26) and Eq. (7.28)). The profile of $\varrho^S(q_S, 0)$ is reported in Fig. 7.17. By solving numerically the Fokker-Planck equation with the initial condition of Eq. (7.44), one can determine the time dependence of the average value $\mathbb{E}^S[q_S](t)$. The result is shown in Fig. 7.18 and compared with the expectation value of the observable q_S as derived from the time dependent wave function. The deep differences between the two profiles are evident and highlight the

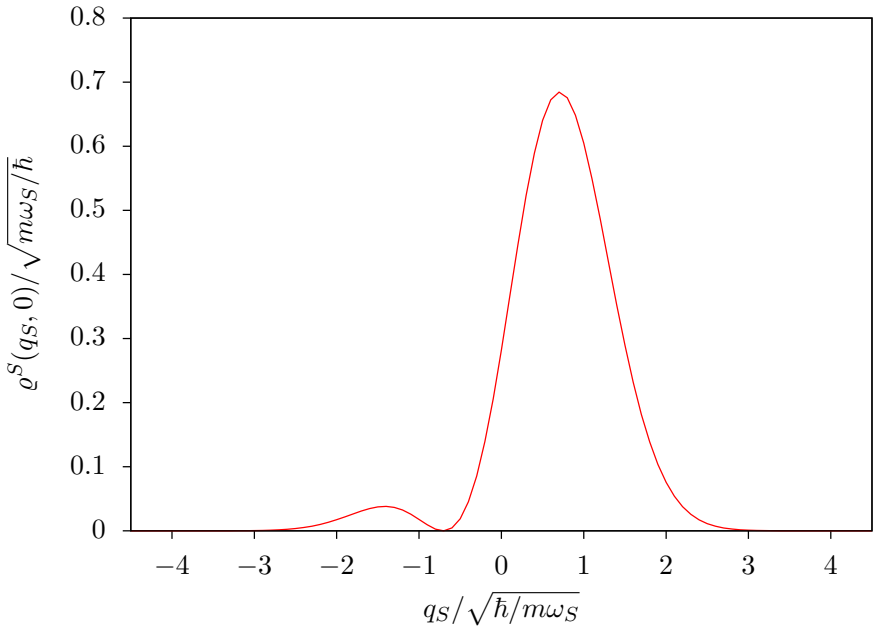

Figure 7.17: Initial probability distribution $\varrho^S(q_S, 0)$ of the coordinate of the first oscillator (the subsystem of interest) in the thermalisation experiment.

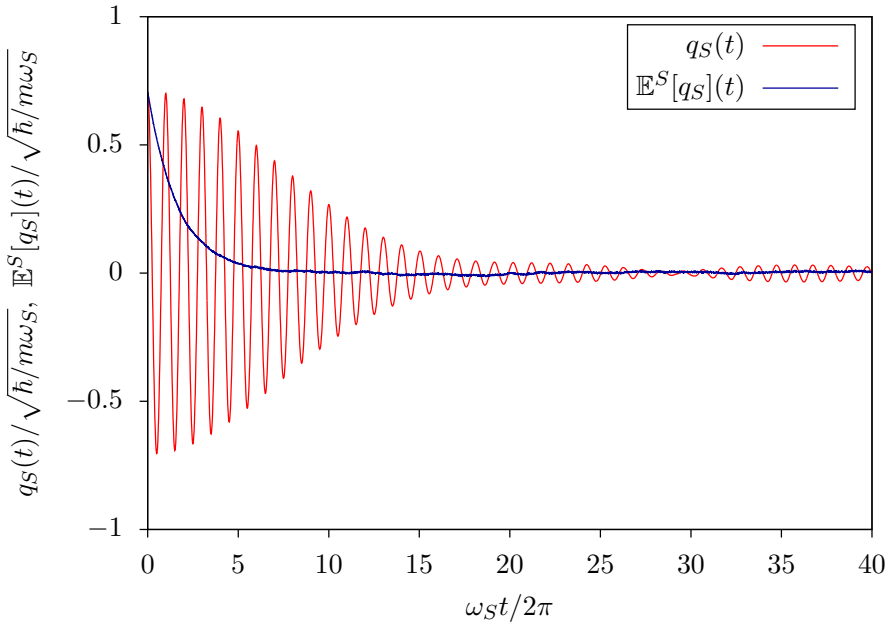

Figure 7.18: Time evolution of the expectation value corresponding to the subsystem coordinate in the thermalisation experiment. One profile has been determined through the exact solution of the Schrödinger equation (red line), whereas the other by numerically solving the Fokker-Planck equation (blue line).

incapability of the Smoluchowski-Bohm equation of describing the correct dynamics in non-equilibrium conditions.

In conclusion, the Smoluchowski-Bohm equation represents accurately the equilibrium dynamics like a purely fluctuating (diffusion) process. However, it fails to describe the non-equilibrium dynamics, since it does not predict the coherent (oscillations) process. This problem can not be solved by a better determination of the equilibrium probability density $\varrho_{eq}^{S}(q_S)$ or the diffusion coefficient β: it is an intrinsic feature of this stochastic equation. In the framework of classical stochastic methods, one can employ a different Fokker-Planck equation in order to characterise the oscillating dynamics, such as the Kramers-Klein equation. In the framework of Bohm theory a projection of the Liouville equation onto the space defined by the relevant variables q_S and the corresponding velocity is still insufficient. Therefore, we consider a completely different type of projection in the Sec. 7.4.

7.4 Bohm equation driven by reduced density matrix

In this section, we answer more precisely to the question that we have already introduced at the beginning of Sec. 7.3: which are the relevant variables? As we have examined in Sec. 7.3, the coordinates q_S of the molecule composing the subsystem belong necessarily to the set of relevant variables. As long as we aim to describe the dynamics of the Bohm coordinates $Q_S(t)$ corresponding to the subsystem degrees of freedom, the variables q_S have to belong to the relevant variables. However we have verified, through numerical simulations on the model system in different conditions, that q_S is insufficient for describing all possible phenomenologies. On the one hand, the equilibrium dynamics is well represented with the Smoluchowski-Bohm equation, but the coherent dynamics is far the possible behaviours that can be examined with this stochastic equation. On the other hand, the non-equilibrium dynamics is certainly the most interesting one from different points of view. For instance the experiments in Chemical Physics usually examine the response of a system to perturbations that moves the system out-of-equilibrium. Therefore, an efficient methodology has to take into account the out-of-equilibrium dynamics if it is intended to deal with realistic experiments. Furthermore, the chemical reactions are often represented as a dynamical processes from an equilibrium state to a different one, that passes through non-equilibrium states. For these reasons, we would like to improve our stochastic approach in order to represent also the non-equilibrium dynamics.

By bearing in mind this final goal, the set of relevant variables has to be modified. One can reasonably think that the coherent dynamics of the thermalisation process of Subs. 7.3.2 arises from the pilot role of the wave function and not from the environment dynamics. The hypothesis is that the environmental degrees of freedom influence randomly the motion of the subsystem coordinates in both the equilibrium and the thermalisation dynamics. Conversely, the phases dynamics representing the pilot role of $\Psi(q,t)$ should be at the origin of the initial oscillating behaviour due to the particular initial wave function in the thermalisation process. With this regard, the pilot role of the wave function, characterised by the phases, is exactly what the Smoluchowski-Bohm equation is not able to take into account. Therefore, the set of relevant and irrelevant variables are defined as in the next equations:

$$x_R = (q_S, \alpha), \qquad\qquad x_I = (q_E). \tag{7.45}$$

Unlike what we have previously done (see Eq. (7.31)), we include the phases in the set of relevant variables. In other words, the idea of averaging the effect of the phases dynamics on the subsystem motion appears to be too limited when one is interested in the relaxation towards the equilibrium. By using the set of relevant variables of Eq. (7.45), the projection operator procedure supplies the new equilibrium density distribution and the new averaged velocity field:

$$\varrho^L_{eq}(q_S,\alpha) = \frac{1}{(2\pi)^N}\sum_{l_S,l'_S}\sigma_{l'_S,l_S}(\alpha)\varphi^*_{l_S}(q_S)\varphi_{l'_S}(q_S), \tag{7.46}$$

$$\Lambda_{L,q_S}(q_S,\alpha) = \frac{\hbar}{m}\mathrm{Im}\left\{\frac{\sum_{l_S,l'_S}\sigma_{l'_S,l_S}(\alpha)\varphi^*_{l_S}(q_S)\nabla_S\varphi_{l'_S}(q_S)}{(2\pi)^N\varrho^S_{eq}(q_S,\alpha)}\right\}, \tag{7.47}$$

$$\Lambda_{L,\alpha_k}(q_S,\alpha) = E_k/\hbar = \omega_k \qquad \text{with } k = 1,2,\ldots,N, \tag{7.48}$$

where $\Lambda_{L,q_S}(q_S,\alpha)$ is the component of the averaged velocity field for the subsystem coordinates, whereas $\Lambda_{L,\alpha_k}(q_S,\alpha)$ is the component for the k-th phase and E_k is the k-th eigenvalue of the Hamiltonian operator $\hat{H}$ of the whole isolated system. Similarly to the previous case, $\{\varphi_{l_S}(q_S)\}$ is the set of the $\hat{H}_S$ eigenfunctions. By comparing Eq. (7.46) and Eq. (7.47) with Eq. (7.32) and Eq. (7.33) respectively, one can observe that the main difference regards the reduced density matrix. Only the time averaged elements of the reduced density matrix $\left\{\overline{\sigma}_{l'_S,l_S}\right\}$ are included in $\varrho^S_{eq}(q_S)$ of Eq. (7.32) and $\Lambda_S(q_S)$ of Eq. (7.33). On the other hand, the α-dependence of $\varrho^L_{eq}(q_S,\alpha)$ and $\Lambda_L(q_S,\alpha)$ is modulated by the reduced density matrix, $\sigma(\alpha)$. This should not be unexpected since the procedure for obtaining the above equilibrium

density distribution and averaged velocity field is the same as the one employed for defining Eq. (7.32) and Eq. (7.33) except for the integration on the phases.

We would like to emphasise two additional features of the above equations. First, the velocity field $\Lambda_{L,\alpha}(q_S, \alpha_k)$ is the same of the deterministic case (see Eq. (6.21)). Since the evolution equation of each phase is independent of the other and of the Bohm coordinates, it is conserved in the projection procedure. Second, the averaged velocity field for the subsystem Bohm coordinates depends on the phases that fully represent the dynamical information of the wave function in our formalism. In other words, the whole set of phases specifies the information included in the wave function for the isolated system, i.e., the subsystem and the environment together. However, only the information included in the reduced density matrix is essential for defining $\varrho^L_{eq}(q_S, \alpha)$ and $\Lambda_{L,q_S}(q_S, \alpha)$. Only the "local" representation of the wave function for the subsystem (open quantum system), that is the reduced density matrix, is necessary in order to determine the averaged velocity field for the subsystem coordinates. For this reason, we tag the equilibrium density distribution, the averaged velocity field and the Fokker-Planck operator with the label L instead of the generic R used in Eq. (7.3), Eq. (7.13) and Eq. (7.16). The purpose is that of highlighting the relevant information for describing the motion of the subsystem which is provided by the subsystem Hamiltonian eigenfunctions $\{\varphi_{l_S}(q_S)\}$, the reduced density matrix $\sigma(\alpha)$ and the subsystem coordinates q_S. Furthermore, when it is possible, we specify the α-dependence of each function, e.g., $\varrho^L_{eq}(q_S, \alpha)$ and $\Lambda_{L,q_S}(q_S, \alpha)$, by writing explicitly that it is modulated by the reduced density matrix, e.g., $\varrho^L_{eq}\big(q_s, \sigma(\alpha)\big)$ and $\Lambda_{L,q_S}\big(q_S, \sigma(\alpha)\big)$. For these reasons, we call the new Fokker-Planck equation as the "Bohm equation driven by reduced density matrix". The resulting Fokker-Planck operator $\hat{\Gamma}^L$ is

$$\hat{\Gamma}^L = \omega\nabla_\alpha + \nabla_S \cdot \Lambda_{L,q_S}\big(q_S, \sigma(\alpha)\big) - \nabla_S \cdot \varrho^L_{eq}\big(q_s, \sigma(\alpha)\big)\beta\ \nabla_S\big(\varrho^L_{eq}\big(q_s, \sigma(\alpha)\big)\big)^{-1} \quad (7.49)$$

so that the corresponding Langevin equations are given as

$$\begin{cases} \dfrac{\mathrm{d}}{\mathrm{d}t}Q_S(t) = \Lambda_{L,q_S}\big(Q_S(t), \sigma(A(t))\big) + \beta\dfrac{\nabla_S\ \varrho^S_{eq}\big(Q_S(t), \sigma(A(t))\big)}{\varrho^S_{eq}\big(Q_S(t), \sigma(A(t))\big)} + \sqrt{2\beta}\zeta(t) \\ \dfrac{\mathrm{d}}{\mathrm{d}t}A(t) = \omega \end{cases}, \quad (7.50)$$

where $\nabla_\alpha = (\partial/\partial\alpha_1, \partial/\partial\alpha_2, \ldots, \partial/\partial\alpha_N)$ and $\omega = (\omega_1, \omega_2, \ldots, \omega_N)$. In this way, a deterministic dynamics is derived for the phases, since the dissipative term of the Fokker-Planck operator $\Big(\nabla_S \cdot \varrho^L_{eq}\ \beta\ \nabla_S\big(\varrho^L_{eq}\big)^{-1}\Big)$ acts only on the subsystem coor-

dinates. As a matter of fact, the dynamical equation for the phases is still the deterministic one because of i) the independence of the Schrödinger equation with respect to the Bohm dynamics and ii) the inclusion of all the phases in the set of the relevant variables.

When the system is in equilibrium conditions, the reduced density matrix is almost always the same of the canonical reduced density matrix, $\hat{\sigma}(t) \simeq \overline{\hat{\sigma}} \propto e^{-\hat{H}_S/k_BT}$ (see Eq. (7.34)). This means that the α-dependence of σ is negligible, i.e., $\sigma(\alpha) \simeq \overline{\sigma}$. Correspondingly, the operator $\hat{\Gamma}^L$ becomes the same of the Smoluchowski-Bohm equation once a deterministic term for the phases is included:

$$\hat{\Gamma}^L \simeq \omega\nabla_\alpha + \hat{\Gamma}^S. \tag{7.51}$$

This can be verified by taking into account that the averaged velocity field vanishes, $\Lambda_{L,q_S}\big(q_S, \sigma(\alpha)\big) = 0$ and obviously $\varrho^L_{eq}(q_S, \sigma(\alpha)) \simeq \int \mathrm{d}\alpha\ \varrho^L_{eq}(q_S, \sigma(\alpha)) = \varrho^S_{eq}(q_S)$ when Eq. (7.34) is satisfied. In this way the coordinates dynamics is independent of the phases dynamics, and *vice versa*. Therefore, the equilibrium dynamics of the subsystem coordinates can be described according to the above equation as well as with the Smoluchowski-Bohm equation, since the same behaviour is recovered in both the cases. Thus, we can be sure that the stochastic Bohm equation driven by reduced density matrix represents correctly the equilibrium dynamics and we have now to investigate its capability of describing also the non-equilibrium dynamics. One can reasonably suppose that the correct representation of the coherent motion emerges from the averaged velocity field $\Lambda_{L,q_S}\big(q_S, \sigma(\alpha)\big)$ that vanishes in equilibrium conditions, whereas the dissipative term is mainly responsible of the fluctuating motion.

We consider particularly the interesting case with the following initial density distribution,

$$\varrho^L(q_S, \alpha, 0) = \delta(\alpha - \alpha_0)\varrho^S(q_S, 0). \tag{7.52}$$

It represents a complete knowledge of the initial phases, whereas the subsystem coordinates are distributed according to $\varrho^S(q_S, 0)$. By bearing in mind that $\hat{\Gamma}^L$ describes a deterministic evolution for of phases and defining $\hat{\Gamma}^S_{\sigma(\alpha)} := \hat{\Gamma}^L - \omega\nabla_\alpha$, it is possible to verify that the formal solution of the Fokker-Planck equation is

$$\varrho^L(q_S, \alpha, t) = \delta\big(\alpha - A(t; \alpha_0)\big)e^{-t\hat{\Gamma}^S_{\sigma(\alpha)}}\varrho^S(q_S, 0), \tag{7.53}$$

where $A(t; \alpha_0)$ is the evolution of the initial phases α_0 according to their deterministic dynamics (see Eq. (6.21)). This allows the definition of a closed-form expres-

sion for the marginal density distribution with respect to the phases, $\varrho^S(q_S,t) := \int \mathrm{d}\alpha\ \varrho^L(q_S,\alpha,t)$, whose time evolution is determined by the following Fokker-Planck operator

$$\hat{\Gamma}^S_{\sigma(t)} = \nabla_S \cdot \Lambda_{L,q_S}\big(q_S,\sigma(t)\big) - \nabla_S \cdot \varrho^L_{eq}\big(q_s,\sigma(t)\big)\beta\ \nabla_S\big(\varrho^L_{eq}\big(q_s,\sigma(t)\big)\big)^{-1} \tag{7.54}$$

that depends on the reduced density matrix parametrically, $\sigma(t) = \sigma\big(A(t;\alpha_0)\big)$. Once the time evolution of the reduced density matrix $\sigma(t)$ is known, then the time evolution of $\varrho^S(q_S,t)$ through the Fokker-Planck equation with $\hat{\Gamma}^S_{\sigma(t)}$ (Eq. (7.54)) and of $Q_S(t)$ through the corresponding Langevin equation are determined. Notice the differences between the Fokker-Planck operator $\hat{\Gamma}^S_{\sigma(t)}$ and $\hat{\Gamma}^S$ in Eq. (7.35): both the operators determine the time evolution of a probability density such as $\varrho^S(q_S,t)$ (that depends on q_S only), but $\hat{\Gamma}^S_{\sigma(t)}$ includes also the time evolution of the reduced density matrix as a parameter of the model. This is similar to the Bohm equation that establishes the velocity of all the particles once the wave function dynamics is known. The main difference is that a local information, i.e., the reduced density matrix, is necessary for our stochastic equations, whereas the total wave function is essential for the deterministic dynamics. It has to be stressed that this property is rather uncommon in the framework of the stochastic methods and it emerges from the independence of the wave function with respect to the Bohm trajectory.

The stochastic Bohm equation seems to have an evident disadvantage: the complete knowledge of the α-dependence of the reduced density matrix is required. This level of information can be reached by exactly solving the Schrödinger equation, that is unfeasible if one would like to describe macroscopic systems with our stochastic method. Nonetheless, we examine the predictions of this stochastic method by computing $\sigma(\alpha)$ for our model system (more details about the $\sigma(\alpha)$ calculation are reported in Sec. 3.2.2). On the other hand, the difficulties arising when dealing with macroscopic systems are discussed in more detail in Subs. 7.4.3; there we will explain that the subsystem dynamics can still be obtained from the Fokker-Planck operator $\hat{\Gamma}^S_{\sigma(t)}$ (Eq. (7.54)) by exploiting the information about the time evolution of the reduced density matrix $\sigma(t)$ to be determined through both models and experimental techniques.

7.4.1 Thermalisation dynamics

In this subsection, we employ Eq. (7.49) and Eq. (7.50) for representing the motion of the oscillator composing the subsystem in our model during the thermali-

sation process, whose deterministic dynamics has been presented in Subs. 7.3.2. On the one hand, we compute the equilibrium distribution $\varrho^L_{eq}\big(q_S, \sigma(\alpha)\big)$, since it can be neither determined with simple considerations as the Smoluchowski-Bohm equation nor suitably approximated with a common distribution like the Gaussian distribution. On the other hand, the diffusion coefficient has to be determined through an analysis of the deterministic dynamics. By observing Fig. 7.15, one can notice that the Smoluchowski-Bohm equation predicts accurately the loss of correlation with the diffusion coefficient $\beta = 0.1345\ 2\pi m/\hbar$. Given the equivalence between $\hat{\Gamma}^L$ and $\hat{\Gamma}^S$ in equilibrium conditions, Eq. (7.51), we use the same value of the diffusion coefficient as a first approximation.

At this stage, we solve the Langevin equation (7.50) with the appropriate initial condition $(Q_S(0), A(0))$. Furthermore, we determine also the average value $\mathbb{E}^L[q_S](t)$,

$$\mathbb{E}^L[q_S](t) := \int \mathrm{d}q_S \mathrm{d}\alpha\ q_S \varrho^L_{eq}(q_S, \alpha, t) \tag{7.55}$$

according to the solution of the Fokker-Planck equation with initial distribution

$$\varrho^L_{eq}(q_S, \alpha, 0) = \delta\left(\alpha - A(0)\right) \int \mathrm{d}q_E\ |\Psi(q, 0)|^2, \tag{7.56}$$

where $q = (q_S, q_E)$ and $\delta\left(\alpha - A(0)\right)$ is the Dirac delta function. Like in the analysis of Subs. 7.3.2, we assume that the coordinate of the oscillator representing the subsystem is initially distributed according to the subsystem initial wave function (see Eq. (7.44) and Fig. 7.17), whereas the phases dynamics is exactly known (they are distributed according to a Dirac delta function). Figures 7.19 and 7.20 show the stochastic trajectory $Q_S(t)$ compared to the deterministic one and the average value $\mathbb{E}^L[q_S](t)$ compared to the expectation value $q_S(t)$ respectively. The trajectories displayed in Fig. 7.19 are not perfectly overlapping, but as already recalled, the stochastic methodologies can not reproduce the exact single trajectory since the effects of the irrelevant variables are modelled in terms of white noise. Nevertheless, the stochastic trajectory conserves the main features of the deterministic one. For example, one can notice that the initial motion is roughly an oscillation at the resonance frequency of the oscillator, ω_S. The stochastic oscillation is more irregular than the deterministic, since the subsystem is initially isolated. The stochastic trajectory is immediately influenced by the random force, whereas the effects of the environment on the subsystem motion are weaker in the first steps of the dynamics because they are initially unentangled. However, both the coherent and the fluctuating regimes are correctly reproduced with our stochastic equation. As previously

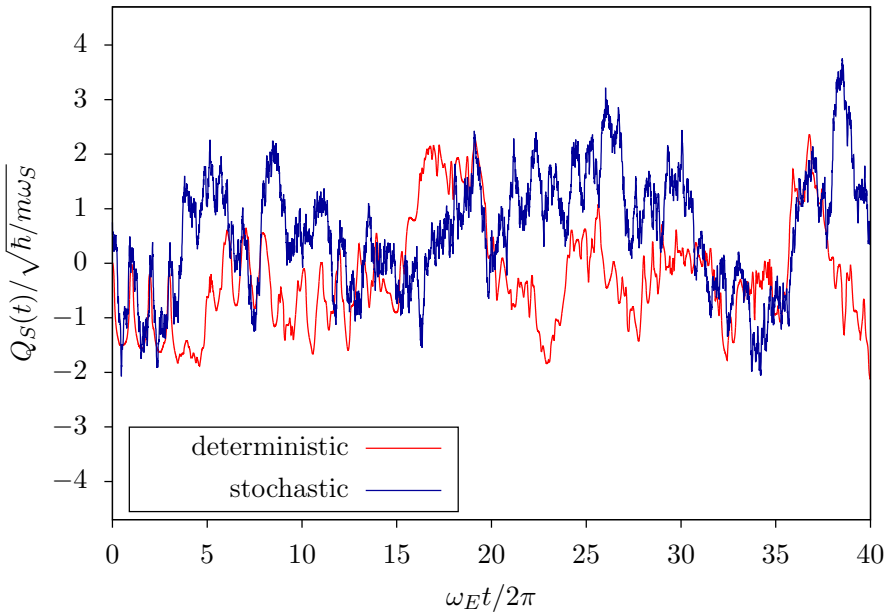

Figure 7.19: Time evolution of the Bohm coordinate of the first oscillator of the model system. One trajectory has been determined by solving exactly the Bohm equation (red line), whereas the other by solving the corresponding Langevin equation (blue line).

emphasised, the precise equivalence between the two trajectories can not be achieved because of the strongly chaotic character of the deterministic trajectory: the round off error is sufficient for computing completely different trajectories. Nevertheless, we would like to emphasise the qualitative similarity between the two trajectories that witnesses the accuracy of the stochastic equations in representing the main features of the deterministic motion.

The comparison between the average value and the expectation value is perhaps more impressive, since it is shown that they are nearly equivalent. The importance of this result is double. In the first place, it confirms the accuracy of the Langevin equation. Since the average value $\mathbb{E}^L[q_S](t)$ has been determined by averaging the observable q_S on a swarm of suitably distributed Langevin trajectories (see Subs. 7.2.1), one can recognise that the differences between the stochastic and the deterministic trajectory in Fig. 7.19 tend to vanish in average. In other words, these differences arise from the approximate modelling of the effects of the irrelevant variables, but our model is precise enough to preserve the main features of the deterministic behaviour, such as the average values. Secondly, this result confirms again the interpretation of the expectation values in terms of statistical properties emerging from the underlying deterministic dynamics of the Bohm theory as already pointed out in Chap. 6.

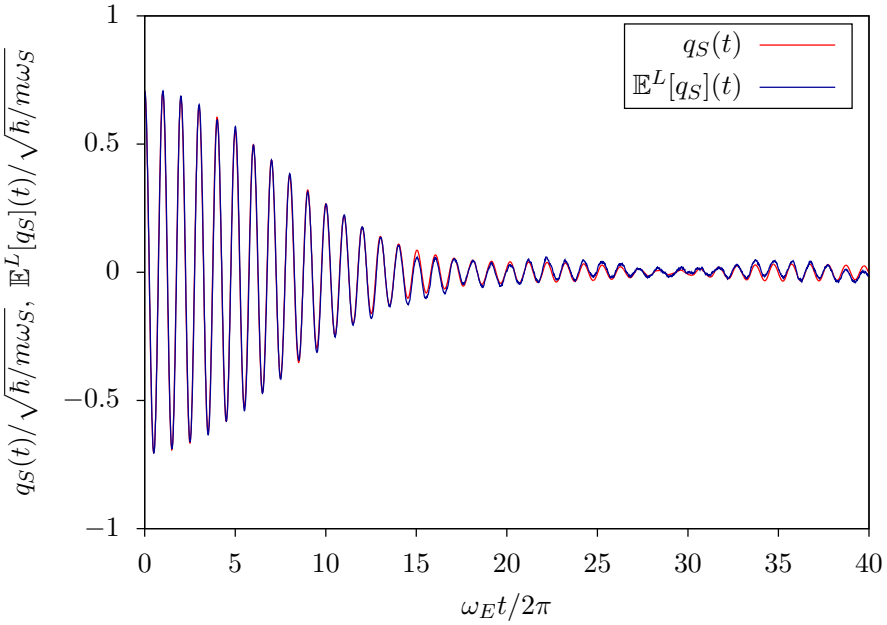

Figure 7.20: Time evolution of the expectation value corresponding to the subsystem coordinate. One profile has been determined through the exact solution of the Schrödinger equation (red line), whereas the other by numerically solving the Fokker-Planck equation (blue line).

On the basis of the results illustrated in Fig. 7.19 and in Fig. 7.20, it can be stated that the stochastic method of this section succeeds in well representing the out-of-equilibrium dynamics of our model system. In order to further verify the capabilities of this stochastic method, we will consider another case: the relaxation of the subsystem oscillator from the initial condition of equally populated ground and first excited states to the final equilibrium state with a large population of the ground state. In the following, we examine both the deterministic and the stochastic predictions for this case.

7.4.2 Relaxation dynamics

We consider again the model system of six interacting oscillators, when the initially partially excited subsystem relaxes because of the interaction with the environment. Then, in order to investigate this relaxation dynamics, it is necessary to couple the subsystem to a "cold" environment. For this purpose, it has been assumed that $\omega_S = 3\omega_E$. The parameters of the simulation are set to $\lambda = 0.001\ \omega_E\hbar$, $E_{tr}^{(0)} = 12.5\ \omega_E\hbar$ and $E_{max} = 11.5\ \omega_E\hbar$. Similarly to the thermalisation dynamics, the subsystem and the environment are initially unentangled. The subsystem wave function is equally separated between the ground state and the first excited state,

Table 7.3: Diagonal elements of the initial $\sigma_{l_S,l_S}(0)$ and of the equilibrium $\overline{\sigma}_{l_S,l_S}$ reduced density matrix. The canonical values are reported between parentheses.

l_S	$\sigma_{l_S,l_S}(0)$	$\overline{\sigma}_{l_S,l_S}$
0	0.5	0.893 (0.887)
1	0.5	0.102 (0.101)
2	0	4.15 10^{-3} (0.0116)

namely $L_S = (0, 1)$ with

$$P^S_{l_S} = 0.5 \qquad \forall l_S = 0, 1. \tag{7.57}$$

The coefficients $\left\{P^E_{l_E}\right\}$ and $\{\chi_{l_E}\}$ are randomly sampled.

Like with the thermalisation process, the subsystem dynamics due to the wave function evolution can be examined by considering the reduced density matrix. The diagonal elements values of the initial reduced density matrix $\sigma_{l_S,l_S}(0)$ and those $\overline{\sigma}_{l_S,l_S}$ of the equilibrium one are compared in Table 7.3. One can reasonably suppose that the quantum dynamics establishes an energy flux from the subsystem to the environment. Even if the two excited states of the oscillator are partially populated, one can observe that the subsystem is fundamentally de-excited when the system has reached the equilibrium: the main consequence of the dynamics is relaxation of the subsystem oscillator to the ground state. This can be further visualised by examining Fig. 7.21, where the time evolution of the elements $\sigma_{0,0}(t)$, $\sigma_{1,1}(t)$ and the real part of $\sigma_{0,1}(t)$ is displayed. During the first steps of the dynamics the element $\sigma_{0,0}(t)$ increases in time meanwhile $\sigma_{1,1}(t)$ decreases. This can be interpreted in terms of a de-excitation process. In parallel, the off-diagonal element $\sigma_{0,1}(t)$ oscillates at frequency ω_S (coherent dynamics) with a decreasing amplitude because of the interaction with the environment (decoherence dynamics). For $\omega_E t/2\pi > 20$ the system is in equilibrium and the displacements of the reduced density matrix elements from their equilibrium value tend to vanish. The residual time dependence of $\sigma_{0,1}(t)$ is caused by the limited dimension of the model system: it is not large enough to reach the thermodynamic limit. This can be further verified in Table 7.3 by comparing the equilibrium values of the reduced density matrix with those of the canonical density matrix where $1/k_BT = 2.17\ (\omega_S\hbar)^{-1}$ ($1/k_BT$ has been determined through the ratio $\overline{\sigma}_{0,0}/\overline{\sigma}_{1,1}$). The main features of the reduced density matrix dynamics highlight a relaxation process due to thermal interaction with the environment.

As regards the deterministic dynamics of this system, the Bohm trajectory for the subsystem coordinate is displayed in Fig. 7.22. Like with the thermalisation

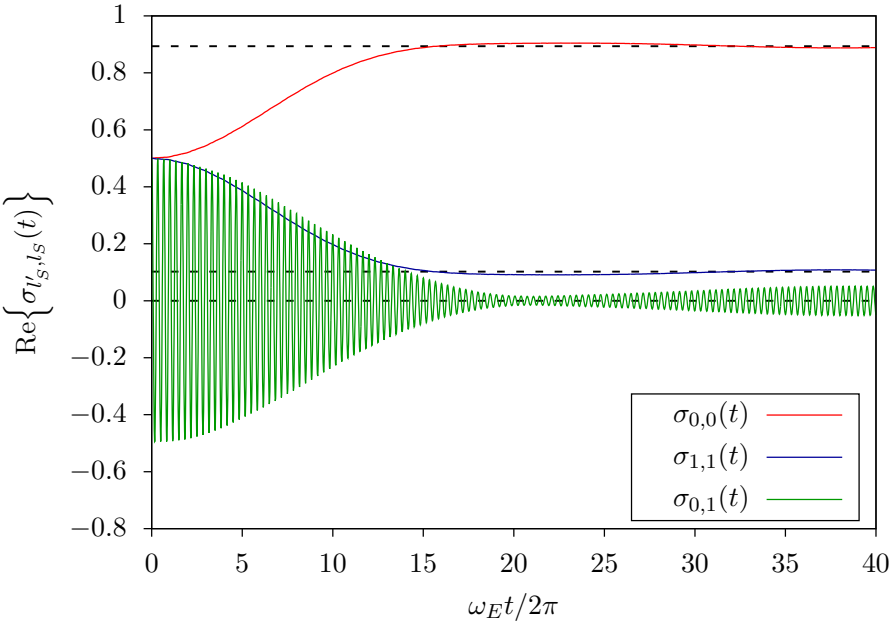

Figure 7.21: Deterministic time evolution of the reduced density matrix elements $\sigma_{0,0}$ (red line), $\sigma_{1,1}$ (blue line) and of the real part of $\sigma_{0,1}$ (green line) during the relaxation dynamics. The black dashed lines represent the corresponding equilibrium values.

process, the trajectory is characterised by two different behaviours. During the first steps of the dynamics, it is approximately an oscillation at the resonance frequency of the oscillator, $\omega_S = 3\omega_E$. Indeed, for $\omega_E t/2\pi < 10$, the periodicity of the motion is evident; for $\omega_E t/2\pi > 20$ the oscillating character is lost and the result is a fluctuating profile. In the intermediate time interval, the trajectory shows a behaviour that is neither a pure oscillation nor a pure fluctuation. Also in this case, we label the first steps of the time evolution, the out-of-equilibrium dynamics, as the coherent dynamics and fluctuating dynamics the time evolution in equilibrium conditions. The main features of this motion are similar to those of the Bohm trajectory in the thermalisation experiment.

One obvious difference between the two cases is the frequency of the oscillation with respect to the resonance frequency of the oscillators composing the environment: in this case $\omega_S = 3\omega_E$, whereas previously $\omega_S = \omega_E$. Another diversity emerges from the analysis of the trajectory in terms of its equilibrium density distribution $w^S_{eq}(q_S)$ that is shown in Fig. 7.23, where also the gaussian distribution with $\sigma^2_{q_S} = 0.6232\ \hbar/m\omega_S$ and the equilibrium density distribution $\varrho^S_{eq}(q_S)$ are displayed. By comparing Fig. 7.23 and Fig. 7.14, it can be noticed that the motion is confined more closely to the bottom of the harmonic potential during the relaxation dynamics than during the previous thermalisation experiment (see the different values of

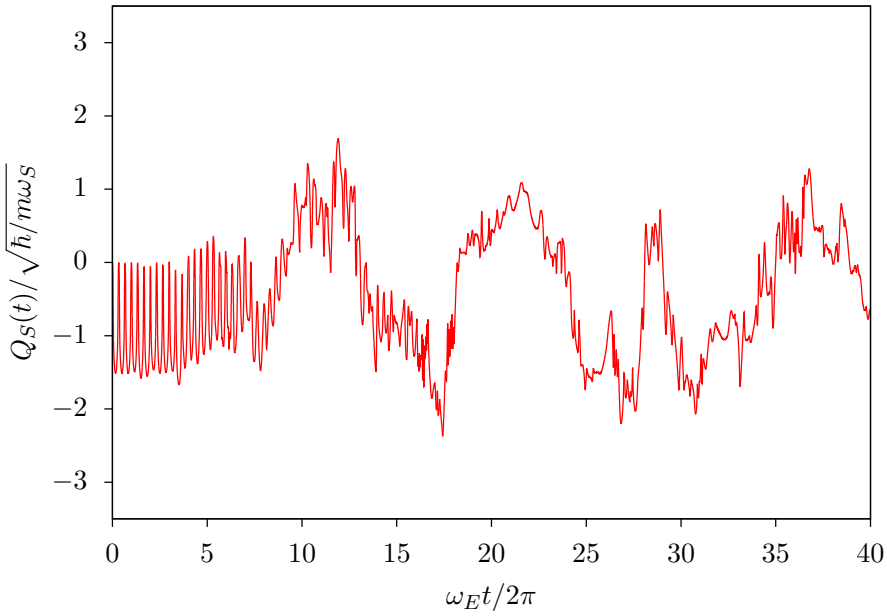

Figure 7.22: Deterministic time evolution of the Bohm coordinate of the first oscillator of the model system during the relaxation dynamics (the initial wave function is factorised into the subsystem wave function and environment wave function).

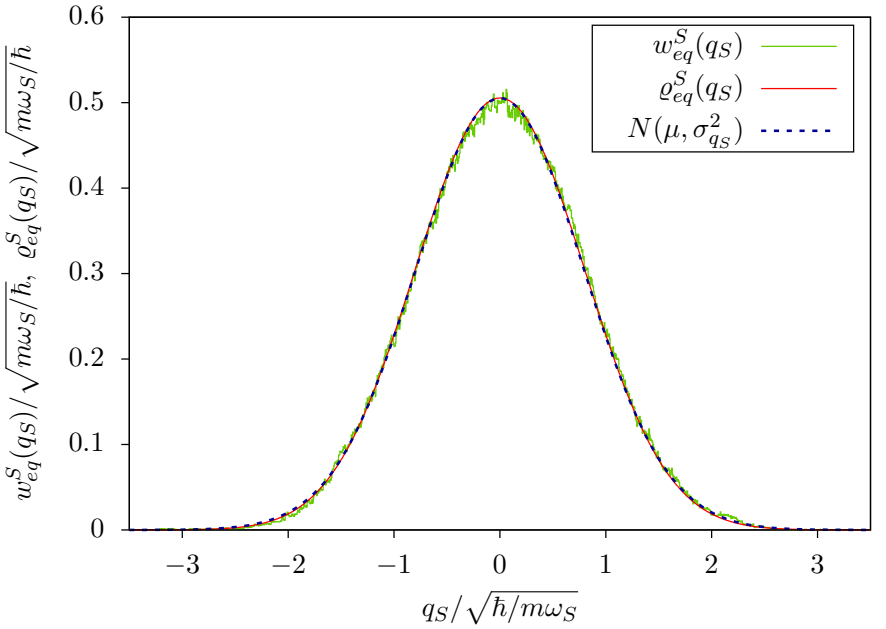

Figure 7.23: Marginal density distribution $w^S_{eq}(q_S)$ and equilibrium density distribution $\varrho^S_{eq}(q_S)$ of the Bohm coordinate of the first oscillator in the relaxation experiment. They are compared with a gaussian distribution with average value $\mu = 0$ and variance $\sigma^2_{q_S} = 0.6232\ \hbar/m\omega_S$.

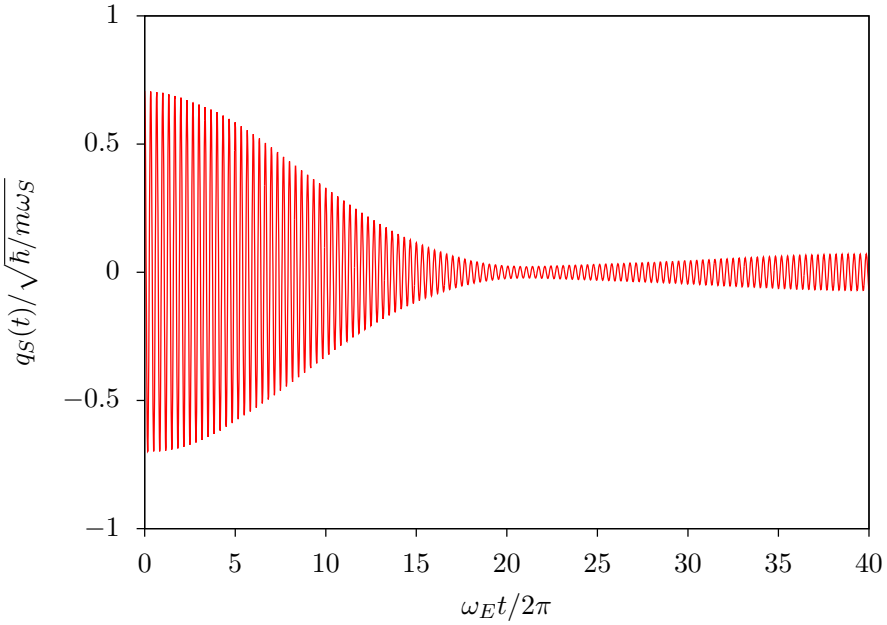

Figure 7.24: Deterministic time evolution of the expectation value corresponding to the subsystem coordinate during the relaxation dynamics.

$\sigma^2_{q_S}$). This is due to the different populations of the subsystem eigenstates. Once the thermalisation reaches the equilibrium, the first five states of the subsystem are effectively populated (see Table 7.2). This feature is absent in the relaxation process: only the ground and the first excited state are significantly populated once the equilibrium has been established. As matter of a fact, the ground and the first excited state correspond to an higher probability of finding the oscillator closer to the potential bottom than with the others excited states. Consequently, during the relaxation dynamics the Bohm trajectory is restricted within a smaller region than in the thermalisation case.

This different confinement is not evident if one examines the expectation value $q_S(t) = \langle\Psi(t)|\hat{q}_S|\Psi(t)\rangle$ instead of the Bohm trajectory. Indeed, by comparing Fig. 7.24, where $q_S(t)$ is shown for the relaxation process, and Fig. 7.12, one can notice that the amplitude of the oscillations is almost the same in both cases (thermalisation and relaxation). Of course, the two profiles differ in the frequency of the oscillation. It has to be emphasise that the vanishing amplitude of the oscillation around the average value in the fluctuating regime has a quite different origin in the thermalisation process with respect to the relaxation. In the first case, the reduced density matrix is almost the same of the canonical reduced density matrix; therefore, $\sigma(t)$ is approximately time independent and consequently also all

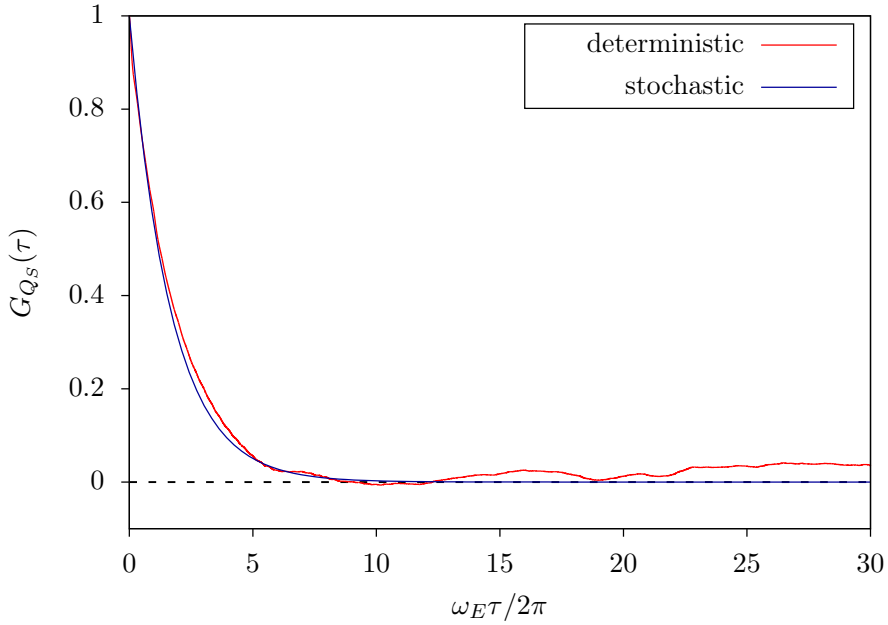

Figure 7.25: Correlation function $G_{Q_S}(\tau)$ of the first oscillator coordinate $Q_S(t)$ in the relaxation experiment. One correlation function has been determined by analysing the deterministic dynamics (red line), whereas the other through Eq. (7.39) with $\beta = 0.05292\ 2\pi m/\hbar$ and $\sigma^2_{q_S} = 0.6232\ \hbar/m\omega_S$ (blue line).

the subsystem expectation values are time independent. On the other hand, after the relaxation dynamics, the reduced density matrix represents a subsystem that is nearly in the ground state, i.e., almost in a stationary state, and this is the origin of the approximate absence of dynamics for the expectation values.

In order to compare this deterministic dynamics with the stochastic predictions, we have to select a value for the diffusion coefficient β. By bearing in mind that β was determined by modelling the autocorrelation function of the Bohm trajectory $G_{Q_S}(\tau)$ according to the Smoluchowski-Bohm equation for the thermalisation process, one can repeat the same approach in this numerical experiment. We employ the gaussian function to approximate the equilibrium distribution $\varrho^S_{eq}(q_S)$ (in this case $\sigma^2_{q_S} = 0.6232\ \hbar/m\omega_S$) and then we use Eq. (7.39) for modelling the autocorrelation. Once again, the idea is tuning the value of β in order to maximise the equivalence between the deterministic correlation function and the result of the stochastic model of Eq. (7.39) with $\sigma^2_{q_S} = 0.6232\ \hbar/m\omega_S$. Figure 7.25 shows the deterministic autocorrelation function and the stochastic one obtained through Eq. (7.39) with $\sigma^2_{q_S} = 0.6232\ \hbar/m\omega_S$ and $\beta = 0.0592\ 2\pi m/\hbar$.

Once the value of the diffusion coefficient has been identified, one can compute the stochastic trajectory $Q_S(t)$ and the average value of the observable q_S, i.e.,

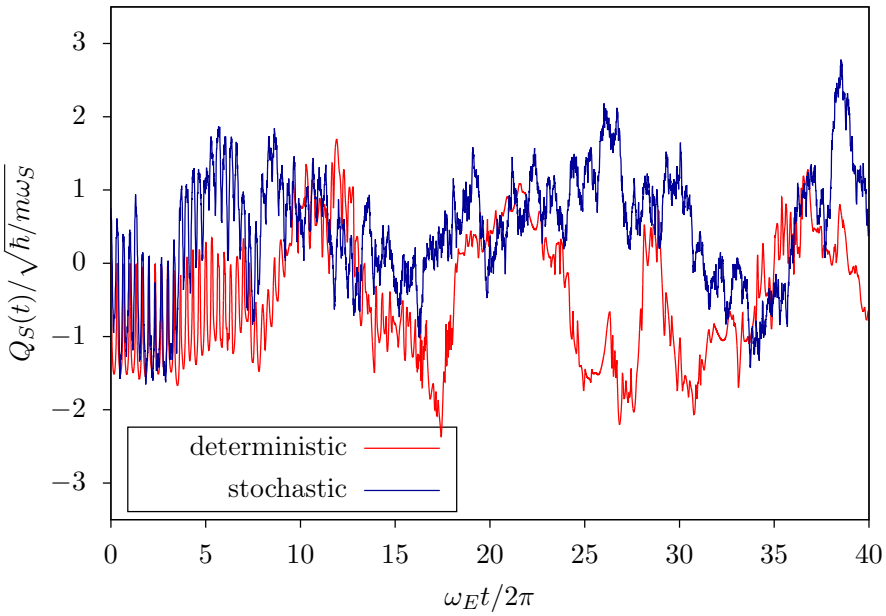

Figure 7.26: Time evolution of the Bohm coordinate of the first oscillator of the model system in the relaxation experiment. One trajectory has been determined by solving exactly the Bohm equation (red line), whereas the other by solving the corresponding Langevin equation (blue line).

$\mathbb{E}^L[q_S](t)$. We would like to recall that the equilibrium density distribution $\varrho^L_{eq}(q_S, \alpha)$ has been exactly determined since the α-dependence of the reduced density matrix must be known. Furthermore, the initial density distribution $\varrho^L(q_S, \alpha, 0)$ satisfies Eq. (7.56). The resulting $Q_S(t)$ and $\mathbb{E}^L[q_S](t)$ are displayed respectively in Fig. 7.26 and Fig. 7.27. Each stochastic profile is compared to its corresponding deterministic one: the stochastic $Q_S(t)$ with the deterministic $Q_S(t)$ and the average value $\mathbb{E}^L[q_S](t)$ with the expectation value $q_S(t)$. Also in this case the predictions of the stochastic approach are in agreement with the deterministic dynamics. Even if the deterministic and stochastic Bohm trajectories illustrated in Fig. 7.26 are not the same, the stochastic method is able to recognise the main features of the deterministic evolution, such as the initial coherent motion and afterwards the fluctuating motion. On the other hand, the average values $\mathbb{E}^L[q_S](t)$ and the expectation value $q_S(t)$ are perfectly overlapped in Fig. 7.27.

In this way, we have verified the validity of Eq. (7.49) and Eq. (7.50) for representing the quantum dynamics of a subsystem interacting with the environment. The only limitation seems to concern the knowledge of the reduced density matrix, but some strategies can be adopted in order to avoid such a difficulties as we illustrate briefly in the Sec 7.4.3.

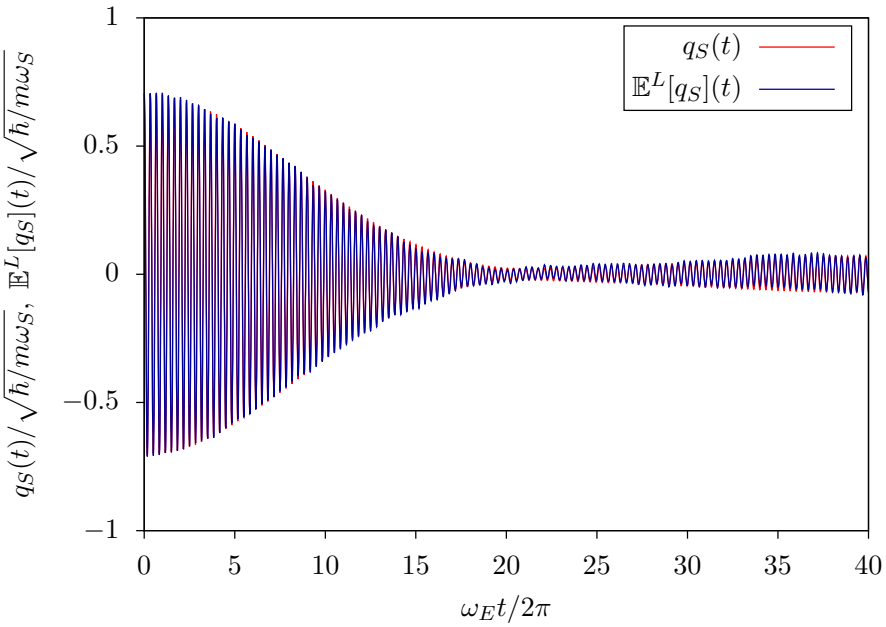

Figure 7.27: Time evolution of the expectation value corresponding to the subsystem coordinate in the relaxation experiment. One profile has been determined through the exact solution of the Schrödinger equation (red line), whereas the other by numerically solving the Fokker-Planck equation (blue line).

7.4.3 Beyond the exact reduced density matrix

The development of the stochastic equations in the framework of Bohm theory was aimed to avoid the computational limitations for describing the molecular motion of a subsystem interacting with the environment. The stochastic Bohm equation driven by reduced density matrix simplifies the problem of computing the Bohm trajectory, since the time evolution of the subsystem coordinates is defined according to the following Langevin equation:

$$\frac{\mathrm{d}}{\mathrm{d}t}Q_S(t) = \Lambda_{L,q_S}\big(Q_S(t),\sigma(A(t))\big) + \beta\frac{\nabla_S\ \varrho^S_{eq}\big(Q_S(t),\sigma(A(t))\big)}{\varrho^S_{eq}\big(Q_S(t),\sigma(A(t))\big)} + \sqrt{2\beta}\zeta(t). \quad (7.58)$$

The averaged velocity field $\Lambda_{R,q_S}\left(q_S,\sigma(\alpha)\right)$ and the equilibrium density distribution $\varrho^L_{eq}\left(q_S,\sigma(\alpha)\right)$ are fully specified according to the basis functions $\{\varphi_{l_S}(q_S)\}$ and the reduced density matrix $\hat{\sigma}$. For determining the subsystem eigenfunctions $\{\varphi_{l_S}(q_S)\}$, one can suitably model the subsystem Hamiltonian, $\hat{H}_S$. However, it has been supposed that the reduced density matrix is known. This means implicitly that the exact solution of the Schrödinger equation is known, since this is the only way to determine the α-dependence of the reduced density matrix. Of course, this is an impossible task when one is dealing with large or macroscopic system and this is

precisely the type of systems that we would like to represent with our stochastic method. Therefore, our method is apparently afflicted with the same computational limitations of the deterministic theory: we reduce the computational efforts for determining the Bohm trajectory for some interesting coordinates, but the bottle neck is still the Schrödinger equation.

On the other hand, the problem can be overcome. If one is interested in the coordinates dynamics, as we are, there are different models that describe the evolution of the reduced density matrix independently of exact solution of the Schrödinger equation. The idea consists in assuming that the phases dynamics is known, such as in Eq. (7.52). Then, one can investigate the time evolution of the subsystem (in terms of $\varrho^S(q_S,t)$ or $Q_S(t)$) by using the Fokker-Planck operator $\hat{\Gamma}^S_{\sigma(t)}$ of Eq. (7.54). This is convenient because $\hat{\Gamma}^S_{\sigma(t)}$ does not depend on the generic $\sigma(\alpha)$, but on the actual $\sigma(t)$ reduced density matrix that can be either modelled or partially determined through experimental techniques. For instance, different models have been developed to investigate the relaxation processes in open quantum systems mostly based on quantum master equations. The contributions of A. G. Redfield [Redfield (1957, 1965)] and G. Lindblad [Lindblad (1976); Gorini et al. (1976)] are particularly renowned in this field. Their approach consists in projecting [Nakajima (1958)] the whole dynamics of the wave function, represented in terms of the density matrix, onto the reduced density matrix with the assumption that the subsystem of interest is weakly coupled to the environment. Nowadays, these approximate equations for the reduced density matrix are rather common for describing the dynamics of open quantum systems [Breuer and Petruccione (2007)]. Furthermore, there are also experimental techniques that can supply some kind of evidences about the reduced density matrix dynamics. It can be mentioned that advanced 2D spectroscopy techniques, such as photon echo spectroscopy, provide suitable tools for investigating the reduced density matrix dynamics [Jonas (2003); Jeske et al. (2015); Hayes and Engel (2011)]. For example, by combining experimental and theoretical approaches, one can determine the reduced density matrix dynamics corresponding to some interesting vibrational degrees of freedom [Turner et al. (2011)]. Therefore, one can employ a not obvious property of our stochastic method: despite we include all the phases in the set of the relevant variables, only the information carried by the reduced density matrix is relevant for determining the stochastic dynamics of the subsystem coordinates. Theoretical methodologies or experimental techniques can be efficiently used to approximately determine the reduced density matrix.

Finally also the diffusion coefficient β can be determined without knowing the

deterministic dynamics as we have done in the previous examples. Indeed, if the reduced density matrix dynamics is determined in some way also the time dependence of all the expectation values is known. The diffusion coefficient β can be selected by tuning its value in order to ensure that the average of an observable $\mathbb{E}^L[b](t)$ is the same of the corresponding expectation value $b(t)$.

Our stochastic method allows the accomplishment of the original purpose: it is in an efficient method for representing the molecular motion of a subsystem within a quantum framework. What remains to be realised is just its application to a real molecular system.

7.5 Final remarks

In this chapter the problem of developing an efficient stochastic formulation of Bohm theory has been investigated. The original purpose was the definition of a quantum method able to describe accurately the molecular motion of a subsystem (such as a molecule of interest or even some relevant degrees of freedom) that is interacting with a macroscopic environment. We have introduced two different approaches. The Smoluchowski-Bohm equation represents the dynamics of the coordinates corresponding to the relevant degrees of freedom only. In equilibrium conditions, its predictions are in agreement with the full deterministic calculations. However, it is not able to characterise the non-equilibrium dynamics. On the other hand, the inclusion of the phases in the set of the relevant variables allows the definition of the stochastic Bohm equation driven by reduced density matrix that reproduces the correct behaviour in both the equilibrium and non-equilibrium conditions. Despite the inclusion of the whole set of phases amongst the relevant variables, only the reduced density matrix is essential to establish the coordinates time evolution of the subsystem. This feature is fundamental since it allows the use of both theoretical methods and experimental techniques to model the dynamics of the reduced density matrix. In this way, the stochastic equations describe the motion of the degrees of freedom corresponding to the reduced density matrix. The motion of molecule in very complex systems, such as in reactive systems, could be characterised in this way. Consider for instance a change of conformation induced by an external radiation. Our method has the potentiality of well representing the motion of this kind of processes if the dynamics of the reduced density matrix has been previously determined. The main advantage is the intrinsic quantum nature of the methodology, sharing with Classical Mechanics only the physical meaning of

the coordinates $Q_S(t)$, and without any arbitrary separation of the system into a quantum and a classical parts. The entire description can be done in the framework of a quantum theory suitably simplified in order to manage the huge number of variables of a macroscopic system.

Furthermore, the importance of the method is not only related to its capability of representing the molecular dynamics, but also to supply information that the conventional Quantum Mechanics can not provide. For example, how much time is it necessary in order to complete a reaction? Since no observable/operator corresponds to the time variable, then this question has no answer in the framework of Quantum Mechanics. On the contrary, Bohm theory is the natural framework in order to find an answer: by following the the nuclear movement one can determine the time length of the events. In this regard, our stochastic approach can extend the ensemble of information that can be determined with quantum theoretical methodologies.

CHAPTER 8

Conclusions

The development of quantum methods that characterise the molecular motions completely is essential in Chemistry. First of all, the idea of molecule is always related to a set of particles with a specific spatial position. Consider for example to draw a molecule. This operation sets implicitly the position of the particles composing the molecule, i.e., of the nuclei. Nevertheless, Quantum Mechanics, that is considered the best theory at our disposal to describe molecular systems, does not provide precise positions of the quantum particles, including the nuclei. The statistical predictions of Quantum Mechanics do not establish a formal map between the quantum formalism and our chemical representation of what a molecule is without ambiguities. This issue is not only related to the problem of representing molecules with a quantum theory, but it has important implications in the understanding of chemical reactions. For example, in an autoprotolysis process a proton is transferred from a water molecule to another. However, the position of the proton has to be known at any given time in order to examine the extent to which the reaction proceeds.

We have developed a quantum approach that characterises molecular systems as composed of particles and it does not break the quantum laws. In this regard, Bohm theory is the suitable quantum framework because i) it characterises quantum systems in terms of wave function and coordinates (positions) of all the particles ii) it gives exactly the same prediction as conventional Quantum Mechanics by exploiting an ensemble of all possible trajectories. Our contribution is aimed to represent accurately the molecular behaviour according to the single Bohm trajectory, i.e., a

quantum molecular trajectory. The most appealing feature of our approach concerns the possibility of examining the molecular motion with a quantum method that allows the emergence of unexpected phenomenology. For instance, the vibrational degrees of freedom turn out to be at rest if the molecule is in its vibrational ground state, whereas the amplitude of the vibration is deeply related to the "mixing" between ground and excited state during a vibrational transition. Common paradigms based on Classical Mechanics can not predict this specific behaviour that results from the pilot role of the wave function.

Furthermore, it has been proven that the statistical properties of a single Bohm trajectory establish a formal correspondence with conventional Quantum Mechanics. For instance, the expectation values are correlated to the time average of the corresponding quantities along a single trajectory. In this way, the predictions of Quantum Mechanics can be interpreted as the observed statistical properties of an underlying deterministic dynamics, the Bohm dynamics indeed. One may think that Quantum Mechanics characterises the surface of a more precise theory that appears as Quantum Mechanics, but that is "bigger on the inside". This theory is the Bohm theory formulated according to the idea that molecular systems are fully represented by a single trajectory.

The theoretical advantages of this approach are limited by the high computational cost of solving both the Schrödinger and the Bohm equation. Therefore, only small systems seem to be examinable according to the deterministic description. From this point of view the applicability of the single Bohm trajectory approach appears to be confined to the motion of a molecule in vacuum. On the other hand, the motion of a molecule (or even some relevant degrees of freedom like the vibrational coordinates) interacting with the environment (the other molecules) is the real problem of interest. Therefore, we have derived efficient *stochastic theories*, through projection operator technique; in this way also the motion of open quantum systems can be examined by taking into account the *quantum fluctuations* due to the quantum degrees of freedom (Bohm coordinates) of the environment.

In this regard, one could use our stochastic equations, in parallel to experimental data (e.g., 2D spectroscopy) for representing the motion of open quantum systems. An interesting application is certainly the analysis of reactive systems where transformations of chemical interest occur, such as conformational changes (as the photoisomerization of azobenzene) or proton transfers (as photoinduced tautomerization). Our stochastic method has all the potentialities to accomplish the goal of representing the molecular motion accurately along a *quantum molecular trajectory*.

APPENDIX A

Perturbation method for two levels system in resonance

The perturbation methods solve approximately the Schrödinger equation when the considered quantum system is not isolated, i.e., it is interacting with an external field. It is particularly interesting the case of a two levels system interacting with an oscillating external field: if the perturbation is weak enough, then the wave function can be determined over a long time interval with a good accuracy. In the following we present the procedure for the approximate solution of the Schödinger equation according to Cohen-Tannoudji et al. (1977a,b).

Let us assume that the system wave function belongs to a two dimensional Hilbert space with basis set composed of the two eigenstates $|\varphi_g\rangle$ and $|\varphi_k\rangle$ of a zeroth-order Hamiltonian operator $\hat{H}^{(0)}$ corresponding respectively to the eigenvalues $\omega_g\hbar$ and $\omega_k\hbar$. The Hamiltonian operator is the sum of the zeroth-order one and an oscillating contribution (the perturbation),

$$\hat{H} = \hat{H}^{(0)} + \hat{W}\sin(\omega t)\Theta(t), \tag{A.1}$$

where $\Theta(t)$ is the step function that ensures the introduction of the oscillating contribution for $t > 0$ and $\hat{W}$ operator is the dipole moment operator multiplied by the amplitude of the electric radiation. Then the wave function in the interaction picture can be expressed as follows

$$|\Psi(t)\rangle = c_g(t)e^{-\imath\omega_g t}\,|\varphi_g\rangle + c_k(t)e^{-\imath\omega_k t}\,|\varphi_k\rangle\,. \tag{A.2}$$

In this representation, solving the Schrödinger equation is equivalent to solve the following system of differential equations for the coefficients $c_g(t)$ and $c_k(t)$:

$$\begin{cases} \dfrac{\mathrm{d}}{\mathrm{d}t}c_g(t) = -\dfrac{1}{2\hbar}\left\{\left[e^{\imath\omega t} - e^{-\imath\omega t}\right]W_{g,g}\ c_g(t) + \left[e^{\imath(\omega-\omega_{k,g})t} - e^{-\imath(\omega+\omega_{k,g})t}\right]W_{g,k}\ c_k(t)\right\} \\ \dfrac{\mathrm{d}}{\mathrm{d}t}c_k(t) = -\dfrac{1}{2\hbar}\left\{\left[e^{\imath(\omega+\omega_{k,g})t} - e^{-\imath(\omega-\omega_{k,g})t}\right]W_{k,g}\ c_g(t) + \left[e^{\imath\omega t} - e^{-\imath\omega t}\right]W_{k,k}\ c_k(t)\right\} \end{cases}. \tag{A.3}$$

By examining Eq. (A.3) one can easily verify that the time evolution of one coefficient is strictly dependent on the other and the system of differential equations can not be easily solved. However, some useful considerations can be done in order to simplify the problem and to determine an approximate solution. First of all, certain coefficients $c_g(t)$ and $c_k(t)$ are proportional to $e^{\pm\imath(\omega-\omega_{k,g})t}$ that are constant in time when the perturbation satisfies the resonance condition: $\omega = \omega_{k,g}$. On the other hand $e^{\pm\imath\omega t}$ and $e^{\pm\imath(\omega+\omega_{k,g})t}$ oscillate in time. By assuming that the temporal variations of the coefficients $c_g(t)$ and $c_k(t)$ proportional to either $e^{\pm\imath\omega t}$ or $e^{\pm\imath(\omega+\omega_{k,g})t}$ is due principally to the exponential term, then the contribution of these terms in the integration of the differential equations is negligible. In other words, if both $c_g(t)$ and $c_k(t)$ do not change very much over a time interval of the order of $1/\omega_{k,g}$, then the integration of the exponential terms over a large number of periods is almost zero. Therefore, Eq. (A.3) can be simplified to the following system of differential equations:

$$\begin{cases} \dfrac{\mathrm{d}}{\mathrm{d}t}c_g(t) = -\dfrac{1}{2\hbar}W_{g,k}c_k(t) \\ \dfrac{\mathrm{d}}{\mathrm{d}t}c_k(t) = \dfrac{1}{2\hbar}W_{k,g}c_g(t) \end{cases}. \tag{A.4}$$

Differentiating one of the above two equations and substituting the result into the other equation, one obtains:

$$\frac{\mathrm{d}^2}{\mathrm{d}t^2}c_g(t) = -\frac{1}{4\hbar^2}|W_{k,g}|^2 c_g(t), \tag{A.5}$$

that is a closed equation for the coefficient $c_g(t)$. The above equation and the analogous for the coefficient $c_k(t)$ can be easily solved once the initial conditions are established. For instance, if the initial wave function is the eigenstate $|\varphi_g\rangle$, the initial conditions are

$$\begin{cases} c_g(0) = 1 \\ c_k(0) = 0 \end{cases}, \qquad \begin{cases} \dfrac{\mathrm{d}}{\mathrm{d}t}c_g(0) = 0 \\ \dfrac{\mathrm{d}}{\mathrm{d}t}c_k(0) = \dfrac{W_{k,g}}{2\hbar} \end{cases}, \tag{A.6}$$

where the second set of initial conditions has been determined through Eq. (A.4). In conclusion the solution of Eq. (A.3) is approximately

$$\begin{cases} c_g(t) = \cos\left(\dfrac{W_{k,g}}{2\hbar}t\right) \\ c_k(t) = \sin\left(\dfrac{W_{k,g}}{2\hbar}t\right) \end{cases} . \tag{A.7}$$

It has to be emphasised that the approximation adopted to solve Eq. (A.3), that is $c_g(t)$ and $c_k(t)$ not changing very much over a time interval of the order of $1/\omega_{k,g}$, is satisfied if $W_{k,g}/2\hbar \ll \omega_{k,g}$. In other words, it is satisfied if the perturbation is weak with respect to the zeroth-order Hamiltonian. Moreover, in case ω is close to $\omega_{k,g}$ but not strictly equal, the system of differential equations (Eq. (A.3)) is still soluble. By a employing comparable simplification, one obtains

$$c_k(t) = \sqrt{\frac{|W_{k,g}|^2}{|W_{k,g}|^2 + \hbar^2\left(\omega - \omega_{k,g}\right)^2}} \sin\left(\sqrt{\frac{|W_{k,g}|^2}{\hbar^2} + (\omega - \omega_{k,g})}\frac{t}{2}\right) . \tag{A.8}$$

Equation (A.8) is the equivalent to Eq. (A.7) for the coefficient $c_k(t)$, while $c_g(t)$ is determined through the condition of normalisation of the wave function: $c_g(t) = \sqrt{1 - |c_k(t)|^2}$. Notice that the excited state will be never totally populated if the resonance condition does not hold: Eq. (A.8) proves that $c_k(t)$ can not satisfy $c_k(t) = 1$ for every possible time t since $(\omega - \omega_{k,g}) \neq 0$.

APPENDIX B

Conservation of the local probability

The Liouville's theorem defines the differential equation that a density distribution has to fulfil in order to ensure the conservation of the local probability. We recall in the following the main steps that are necessary to translate this constraint about the probability conservation to a differential equation. We employ the notation used in Chap. 6 with regard to Bohm theory even if the procedure is totally general and it can be used also in different frameworks. For the sake of completeness, we repeat some considerations already reported in Chap. 6.

Consider a dynamical space Ω_0 (that is the set of all possible states) and the evolution of a specific initial state z_0 according to the dynamical equation

$$\frac{\mathrm{d}}{\mathrm{d}t} Z(t) = \Lambda_0\big(Z(t)\big). \tag{B.1}$$

The solution of the above equation with initial condition z_0 is the curve $Z(t; z_0)$: given an initial state z_0, the curve identifies the state of the system at time t. Notice that both the state $Z(t)$ and the velocity field $\Lambda_0(z)$ are composed of $n+2N$ elements (see Chap. 6). Consider also two subsets $V(t)$ and $V(0)$ of Ω_0 such that

$$V(t) = \{z \in \Omega_0 \mid z = Z\big(t; z_0\big) \ \forall z_0 \in V(0)\}. \tag{B.2}$$

The elements of the two subsets are related by the deterministic evolution: each element belonging to $V(t)$ is the state at time t resulting from the evolution of a particular initial condition represented by an element of $V(0)$ according to the deterministic evolution described by the curve $Z(t; z_0)$.

Once the probability $\mathcal{M}\big(V(0)\big)$, that the system state belongs to $V(0)$ initially, is defined, then the probability $\mathcal{M}\big(V(t)\big)$ that the state belongs to $V(t)$ at time t must be the same since the elements of $V(t)$ are the natural evolution of the states in $V(0)$. Broadly speaking, the probability has to be conserved along the curves. This condition takes the name of "conservation of the local probability" and means formally

$$\mathcal{M}\big(V(0)\big) = \int_{V(0)} \mathrm{d}z \; \varrho^{\Omega_0}(z,0) = \int_{V(t)} \mathrm{d}z \; \varrho^{\Omega_0}(z,t) = \mathcal{M}\big(V(t)\big), \tag{B.3}$$

for every arbitrary initial probability density $\varrho^{\Omega_0}(z,0)$. In other words, the probability $\mathcal{M}\big(V(t)\big)$ is time independent

$$\frac{\mathrm{d}}{\mathrm{d}t}\mathcal{M}\big(V(t)\big) = 0. \tag{B.4}$$

The differential equation that describes the evolution of a generic probability density (Liouville equation) can be inferred from Eq. (B.4). First of all, the time dependence of $\mathcal{M}\big(V(t)\big)$ has to be explicited and the change of variables $z = Z(t;z_0) \to z_0$ is particularly suitable for this purpose:

$$\mathcal{M}\big(V(t)\big) = \int_{V(0)} \mathrm{d}z_0 \; |J(t)| \varrho^{\Omega_0}\big(Z(t;z_0),t\big), \tag{B.5}$$

where $|J(t)|$ is the determinant of the Jacobian matrix with elements $J_{i,j}(t) = \partial Z_i(t;z_0)/\partial z_{0,j}$. By inspecting Eq. (B.5), one can notice that the time dependence of $\mathcal{M}\big(V(t)\big)$ is specified by the time dependence of the integrand unlike in Eq. (B.3) where also the domain of integration is time dependent. Secondly, the time derivative of each term of the integrand has to be taken into account in order to represent the condition of Eq. (B.4) as a constraint for the time evolution of the probability density $\varrho^{\Omega_0}(z,t)$. By the rule of differentiation of the determinant, one can prove that

$$\frac{\mathrm{d}}{\mathrm{d}t}|J(t)| = \sum_k \big|J^{(k)}(t)\big|, \tag{B.6}$$

where $J^{(k)}(t)$ is the Jacobian matrix whose elements of the k-th column are substituted by their time derivative: $J^{(k)}_{i,j}(t) = J_{i,j}(t)$ if $j \neq k$ and $J^{(k)}_{i,k}(t) = \frac{\partial}{\partial z_{0,k}}\mathrm{d}Z_i(t;z_0)/\mathrm{d}t$. Furthermore, each determinant in Eq. (B.6) can be written explicitly,

$$\frac{\mathrm{d}}{\mathrm{d}t}|J(t)| = \sum_{k,i}(-1)^{i+k} J^{(k)}_{i,k}\big|C_{i,k}(t)\big|. \tag{B.7}$$

Notice that $C_{i,k}(t)$ is the minor of the Jacobian matrix with respect to the i-th row and the k-th column. By taking into account Eq. (B.1) and the definition of $J^{(k)}_{i,j}$, one obtains

$$\frac{\mathrm{d}}{\mathrm{d}t}|J(t)| = \sum_{k,i,j}(-1)^{i+k}\frac{\partial\Lambda_{0,i}(z)}{\partial z_j}\bigg|_{z=Z(t;z_0)}\frac{\partial Z_j(t;z_0)}{\partial z_{0,k}}\big|C_{i,k}(t)\big| \tag{B.8}$$

$$= \sum_{i,j}(-1)^{i+j}\frac{\partial\Lambda_{0,i}(z)}{\partial z_j}\bigg|_{z=Z(t;z_0)}\sum_{k}(-1)^{j+k}\frac{\partial Z_j(t;z_0)}{\partial z_{0,k}}\big|C_{i,k}(t)\big|. \tag{B.9}$$

Except for the elementary rearrangement of the terms, the only difference between Eq. (B.8) and Eq. (B.9) is that we introduced the term $(-1)^{2j}$ in such a way that the sum over the k-th index can be easily calculated: it vanishes unless $j = i$. Indeed $\sum_k(-1)^{j+k}\frac{\partial Z_j(t;z_0)}{\partial z_{0,k}}\big|C_{i,k}(t)\big|$ is the determinant of a matrix with two equal rows if $j \neq i$ as one can easily verify by recognising that $\partial Z_j(t;z_0)/\partial z_{0,k} = J_{j,k}(t)$; instead, it is the determinant of the Jacobian matrix if $j = i$. Therefore,

$$\frac{\mathrm{d}}{\mathrm{d}t}|J(t)| = |J(t)|\nabla_z\Lambda_0(z)\bigg|_{z=Z(t;z_0)}, \tag{B.10}$$

where $\nabla_z = (\partial/\partial z_1, \ldots, \partial/\partial z_n, \partial/\partial z_{n+1}, \ldots, \partial/\partial z_{n+2N})$. As regards the probability density $\varrho^{\Omega_0}\big(Z(t;z_0),t\big)$, its total time derivative satisfies the following equation

$$\frac{\mathrm{d}}{\mathrm{d}t}\varrho^{\Omega_0}\big(Z(t;z_0),t\big) = \left[\Lambda_0\nabla_z\varrho^{\Omega_0}(z,t) + \frac{\partial\varrho^{\Omega_0}(z,t)}{\partial t}\right]_{z=Z(t;z_0)}. \tag{B.11}$$

All things considered, the time derivative of the probability $\mathcal{M}\big(V(t)\big)$ of Eq. (B.5) is

$$\frac{\mathrm{d}}{\mathrm{d}t}\mathcal{M}\big(V(t)\big) = \int_{V(0)}\mathrm{d}z_0\ |J(t)|\left[\varrho^{\Omega_0}(z,t)\nabla_z\Lambda_0(z)+\Lambda_0\nabla_z\varrho^{\Omega_0}(z,t)+\frac{\partial\varrho^{\Omega_0}(z,t)}{\partial t}\right]_{z=Z(t;z_0)}. \tag{B.12}$$

In order to ensure that the condition of Eq. (B.4) holds for every possible subspace $V(0) \subseteq \Omega_0$, the integrand term of Eq. (B.12) included in the square brackets must be zero. In other words, the probability density $\varrho^{\Omega_0}(z,t)$ has to satisfy the following differential equation

$$\frac{\partial\varrho^{\Omega_0}(z,t)}{\partial t} + \nabla_z\Lambda_0(z)\varrho^{\Omega_0}(z,t) = 0, \tag{B.13}$$

that is the Liouville equation. We would like to recall that the Liouville equa-

tion determines the time evolution of a generic initial density distribution: given the probability density at time zero $\varrho^{\Omega_0}(z,0)$, its evolution $\varrho^{\Omega_0}(z,t)$ is completely established by Eq. (B.13).

APPENDIX C

Ergodic observables

The idea of ergodicity is widely employed for explaining the predictions of Statistical Mechanics in terms of the underlying deterministic evolution [Khinchin (1949)]. Maybe the most common interpretation in the framework of Classical Statistical Mechanics is that a single trajectory describing the evolution of the system state (the set of positions and momenta of all the particles) samples the phase space according to the equilibrium density distribution (that is the stationary solution of the Liouville equation). Nevertheless, it is well known that such an idea of ergodicity is unprovable for a general system [Tolman (1938)] and moreover there are also some obvious counterexamples like the existence of invariant subsets. On the other hand, if one focuses on the dynamics of a reduced number of variables characterised by a loss of correlation, e.g., the position of one specific particle, then it can be proved that some predictions of the statistical approach correspond to those of the deterministic description. In this appendix, we recall the main steps that are necessary in order to demonstrate such an equivalence in the framework of the Bohm theory. In particular, by taking into account observables of the coordinates only, $B(q)$, one can verify the equivalence between the time average along a single trajectory and the statistical average. We examine the problem inside the invariant part Ω_P defined in Sec. 6.2, but the procedure can be easily extended also for the whole dynamical space Ω_0. The only restriction is the loss of correlation of $B(q)$ during the deterministic evolution.

Consider the invariant part Ω_P and the curve $X(t; x_0)$ that describes the evolution of the initial state x_0. The corresponding Bohm trajectory is the projection of

the curve $X(t;x_0)$ on the configuration space and it is labeled $Q(t;x_0)$ in order to emphasise its dependence on the initial conditions, namely coordinates and phases. By defining the time average along the single trajectory $\overline{B}(x_0)$ of the observable $B(q)$ that is function of the coordinates only,

$$\overline{B}(x_0) := \lim_{T\to+\infty} \frac{1}{T}\int_0^T \mathrm{d}t\ B\big(Q(t;x_0)\big), \tag{C.1}$$

and its equilibrium statistical average

$$\mathbb{E}_{eq}^{\Omega_P}[B] := \int_{\Omega_P} \mathrm{d}q\mathrm{d}\alpha\ B(q)\varrho_{eq}^{\Omega_P}(x)\big|_{x=(q,\alpha)}, \tag{C.2}$$

according to the equilibrium probability density $\varrho_{eq}^{\Omega_P}(x,t)$, one can prove that

$$\mathbb{E}_{eq}^{\Omega_P}\left[\left(\overline{B}(x_0) - \mathbb{E}_{eq}^{\Omega_P}[B]\right)^2\right] = 0, \tag{C.3}$$

if the quantity $B\big(Q(t;x_0)\big)$ is characterised by a loss of correlation (Eq. (6.33)). As already explained in Chap. 6, Eq. (C.3) means that the fluctuations of $\overline{B}(x_0)$ around $\mathbb{E}_{eq}^{\Omega_P}[B]$ are negligible. In other words, the two averages are equal for almost all the initial conditions $x_0 \in \Omega_P$ except for a set of null measure. The demonstration that Eq. (C.3) holds is reported here in the simplest possible way and for this reason we assume that $\mathbb{E}_{eq}^{\Omega_P}[B] = 0$ without loss of generality: if $\mathbb{E}_{eq}^{\Omega_P}[B] \neq 0$, the same procedure described in the following can be employed for the observable $\Delta B(q) = B(q) - \mathbb{E}_{eq}^{\Omega_P}[B]$. In this regard, the condition of Eq. (C.3) is equal to $\mathbb{E}_{eq}^{\Omega_P}\left[\left(\overline{B}(x_0)\right)^2\right] = 0$. The demonstration consists in writing $\mathbb{E}_{eq}^{\Omega_P}\left[\left(\overline{B}(x_0)\right)^2\right]$ as the sum of different terms that vanish simultaneously.

Let us consider $\mathbb{E}_{eq}^{\Omega_P}\left[\left(\overline{B}(x_0)\right)^2\right]$ by adding and subtracting the square of the quantity $\overline{B}^T(x_0) := (1/T)\int_0^T \mathrm{d}t\ B\big(Q(t;x_0)\big)$ to the integrand:

$$\mathbb{E}_{eq}^{\Omega_P}\left[\overline{B}^2\right] = \int_{\Omega_P} \mathrm{d}x_0\ \varrho_{eq}^{\Omega_P}\ \left(\overline{B}^2 - \left(\overline{B}^T\right)^2\right) + \int_{\Omega_P} \mathrm{d}x_0\ \varrho_{eq}^{\Omega_P}\ \left(\overline{B}^T\right)^2. \tag{C.4}$$

To deal with a compact notation, we keep implicit the x_0-dependence of $\varrho_{eq}^{\Omega_P}(x_0)$, $\overline{B}(x_0)$ and $\overline{B}^T(x_0)$. The above equation is valid for every value of the parameter T. In addition, the quantity $\overline{B}^T$ approaches the time average $\overline{B}$ for all $x_0 \in \Omega_P$ by increasing the value of T $\left(\text{notice that } \overline{B} = \lim_{T\to+\infty}\overline{B}^T\right)$. Therefore, one can realise that the first integral of Eq. (C.4) is negligible for some values of T, while the second integral can be written by employing the autocorrelation function in order to

exploit the property $\lim_{\tau\to+\infty} G_B(\tau) = 0$ and prove that also this integral vanishes in some limits. We can now analyse in detail each integral of Eq. (C.4).

As regards the first integral in Eq. (C.4), the integration domain can be usefully separated in two subdomains. In particular one can define $V_\epsilon(T)$ such that $V_\epsilon(T) = \left\{x_0 \in \Omega_P \text{ s.t. } \left|\overline{B}^2 - \left(\overline{B}^T\right)^2\right| < \epsilon\right\}$ with ϵ a positive real number arbitrarily small and $\overline{V}_\epsilon(T)$ the complementary subset, $\overline{V}_\epsilon(T) = \Omega_P \setminus V_\epsilon(T)$. The second integral in Eq. (C.4) can be expressed by using the correlation function $G_B(\tau)$:

$$\int_{\Omega_P} \mathrm{d}x_0 \; \varrho_{eq}^{\Omega_P} \left(\overline{B}^T\right)^2 = \frac{1}{T^2} \iint_0^T \mathrm{d}t_1 \mathrm{d}t_2 \int_{\Omega_P} \mathrm{d}x_0 \; \varrho_{eq}^{\Omega_P}(x_0) B\big(Q(t_1;x_0)\big) B\big(Q(t_2;x_0)\big) \tag{C.5}$$

$$= \frac{\sigma_B^2}{T^2} \iint_0^T \mathrm{d}t_1 \mathrm{d}t_2 \; G_B(t_2 - t_1) = \frac{2\sigma_B^2}{T^2} \int_0^T \mathrm{d}\tau \; (T-\tau) G_B(\tau), \tag{C.6}$$

where

$$G_B(t_2 - t_1) := \frac{1}{\sigma_B^2} \int_{\Omega_P} \mathrm{d}x_0 \; \varrho_{eq}^{\Omega_P}(x_0) B\big(Q(t_2;x_0)\big) B\big(Q(t_1;x_0)\big), \tag{C.7}$$

and $\sigma_B^2 = \mathbb{E}_{eq}^{\Omega_P}[B^2]$. Notice that the autocorrelation function of Eq. (C.7) depends only on the difference $t_1 - t_2$ and not on the absolute values (t_2, t_1) because of the conservation of the local probability ensured by $\varrho_{eq}^{\Omega_P}(x_0)$ obtained as the stationary solution of the Liouville equation. In other words, the autocorrelation function is invariant under time translation (since this properties is a well known feature of the correlation function, its proof is not reported in this thesis). In Eq. (C.6) the change of variables $(t_1, t_2) \to \big(\tau = (t_2 - t_1), t = t_2\big)$ has been adopted and the integral over the variable t has been solved. Furthermore, the integration domain of the variable τ can be separated: it can be defined the parameter a_ϵ in such a way that $G(\tau) < \epsilon$ for every $\tau > a_\epsilon$. The assumption that the observable $B(q)$ is characterised by a loss of correlation is necessary in order to ensure the existence of the parameter a_ϵ in agreement with the previous definition. For instance, if the correlation function oscillates periodically around zero, a τ' can be found such that $G_B(\tau) < \epsilon$ for values of τ around τ'. However, it does not exist an a_ϵ such that $G_B(\tau) < \epsilon$ for every $\tau > a_\epsilon$.

Therefore, one can verify that the absolute value of $\mathbb{E}_{eq}^{\Omega_P}\left[\overline{B}^2\right]$ satisfies the follow-

ing inequality

$$\left|\mathbb{E}_{eq}^{\Omega_P}\left[\overline{B}^2\right]\right| \leq \Bigg\{ \left| \int_{V_\epsilon(T)} \mathrm{d}x_0 \; \varrho_{eq}^{\Omega_P} \left(\overline{B}^2 - \left(\overline{B}^T\right)^2\right)\right| + \left| \int_{\overline{V_\epsilon}(T)} \mathrm{d}x_0 \; \varrho_{eq}^{\Omega_P} \left(\overline{B}^2 - \left(\overline{B}^T\right)^2\right)\right| + \frac{2\sigma_B^2}{T^2}\left| \int_0^{a_\epsilon} \mathrm{d}\tau \; (T-\tau) G_B(\tau)\right| + \frac{2\sigma_B^2}{T^2}\left| \int_{a_\epsilon}^{T} \mathrm{d}\tau \; (T-\tau) G_B(\tau)\right| \Bigg\}, \tag{C.8}$$

for every value of the parameters T and ϵ. At this stage, it has only to be verified that each integral of the above equation is negligible. Since T and ϵ are arbitrary parameters, then the limit of the absolute value of each integral on r.h.s of the above equation can be taken into account considering T and ϵ approaching respectively $+\infty$ and 0. In the first integral $\overline{B}^2 - \left(\overline{B}^T\right)^2 < \epsilon$ by definition of $V_\epsilon(T)$ and consequently the inequality

$$\left| \int_{V_\epsilon(T)} \mathrm{d}x_0 \; \varrho_{eq}^{\Omega_P} \left(\overline{B}^2 - \left(\overline{B}^T\right)^2\right)\right| \leq \epsilon \mathcal{M}_{eq}\big(V_\epsilon(T)\big) \tag{C.9}$$

holds, wiht $\mathcal{M}\big(V_\epsilon(T)\big)$ the equilibrium measure of the set $V_\epsilon(T)$ defined according to Eq. (6.10) and the equilibrium density distribution $\varrho_{eq}^{\Omega_P}(x)$. As $T \to +\infty$, $\mathcal{M}_{eq}\big(V_\epsilon(T)\big) \to 1$ because of the normalisation condition and the limit $\Omega_P = \lim_{T\to+\infty} V_\epsilon(T)$. As regards the second integral of Eq. (C.8), the quantity $B_M(T) := \max_{x_0\in\Omega_P}\left|\overline{B}^2 - \left(\overline{B}^T\right)^2\right|$ can be defined, a value of T can be chosen such that $\mathcal{M}_{eq}\big(\overline{V}_\epsilon(T)\big) < \epsilon$ and hence,

$$\left| \int_{\overline{V_\epsilon}(T)} \mathrm{d}x_0 \; \varrho_{eq}^{\Omega_P} \left(\overline{B}^2 - \left(\overline{B}^T\right)^2\right)\right| \leq \epsilon B_M(T). \tag{C.10}$$

Notice that it must exist a value of T such that $\mathcal{M}_{eq}\big(\overline{V}_\epsilon(T)\big) < \epsilon$ since $\overline{B}^T \to \overline{B}$ everywhere on the space Ω_P under the condition $T \to +\infty$, by definition of $\overline{B}^T$: the number of elements belonging to $\overline{V}_\epsilon(T)$ decreases by increasing the value of T and consequently also the corresponding measure $\mathcal{M}_{eq}\big(\overline{V}_\epsilon(T)\big)$. The third integral in Eq. (C.8) can be simplified by using the maximum value of the autocorrelation function, i.e., $G_B(0) = 1$, and by solving the integral. In particular, we employ the condition $2Ta_\epsilon - a_\epsilon^2 \simeq 2Ta_\epsilon$ which is valid if $T \gg a_\epsilon$. The result is

$$\frac{2\sigma_B^2}{T^2}\left| \int_0^{a_\epsilon} \mathrm{d}\tau \; (T-\tau) G_B(\tau)\right| \leq \frac{2\sigma_B^2 a}{T}. \tag{C.11}$$

Also the fourth integral in (C.8) can be overrated. In the integration domain, the autocorrelation function is always less than ϵ by definition of a_ϵ. We assume also that $(T-a_\epsilon)^2 \simeq T$ which is reasonable if $T \gg a_\epsilon$. Therefore, the following inequality is fulfilled

$$\frac{2\sigma_B^2}{T^2}\left|\int_{a_\epsilon}^{T} \mathrm{d}\tau\ (T-\tau)G_B(\tau)\right| \leq \epsilon\sigma_B^2. \tag{C.12}$$

Then in conclusion, the absolute value of the variance $\mathbb{E}_{eq}^{\Omega_P}\left[\overline{B}^2\right]$ satisfies the following inequality

$$\left|\mathbb{E}_{eq}^{\Omega_P}\left[\overline{B}^2\right]\right| \leq \epsilon\big(\mathcal{M}\big(V_\epsilon(T)\big) + B_M(T) + \sigma_B^2\big) + \frac{2\sigma_B^2 a}{T}. \tag{C.13}$$

Since the simplifications of Eq. (C.9), Eq. (C.10), Eq. (C.11) and Eq. (C.12) hold under the hypothesis of T sufficiently great and the parameters (T, ϵ) are completely arbitrary, one can consider the conditions $T \to +\infty$ and $\epsilon \to 0$ for $\left|\mathbb{E}_{eq}^{\Omega_P}\left[\overline{B}^2\right]\right|$ of Eq. (C.13). Under this conditions the r.h.s. of the above equation approaches zero and therefore

$$\mathbb{E}_{eq}^{\Omega_P}\left[\overline{B}^2\right] = 0, \tag{C.14}$$

for the reason that $\mathbb{E}_{eq}^{\Omega_P}\left[\overline{B}^2\right]$ is a positive real number that is less than or equal to zero for the constraint of Eq. (C.13) under the conditions $T \to +\infty$ and $\epsilon \to 0$. The above expression proves that the fluctuations of the time average $\overline{B}(x_0)$ around the statistical average $\mathbb{E}_{eq}^{\Omega_P}[B]$ are negligible. This means that the time average of the observable $B(q)$ along a single Bohm trajectory is equal to the corresponding statistical average $\mathbb{E}_{eq}^{\Omega_P}[B]$ for almost all the initial conditions. The observables characterised by this equivalence are called ergodic.

APPENDIX D

Projection operators

In this appendix, we focus on the mathematical steps that are necessary in order to simplify Eq. (7.7) and to define the corresponding Fokker-Planck equation, Eq. (7.12).

Consider the projected equation (7.7) that defines the exact time evolution of $\tilde{\varrho}^{\mathbb{P}}(x,t)$ since all the effects due to the history of the process are considered through the kernel operator $\hat{K}(\tau)$. This equation is reported also in the following for the sake of completeness,

$$\frac{\partial}{\partial t}\tilde{\varrho}^{\mathbb{P}}(x,t) = -\imath\hat{\mathbb{P}}\hat{\tilde{L}}\tilde{\varrho}^{\mathbb{P}}(x,t) - \int_0^t \mathrm{d}\tau\ \hat{K}(\tau)\tilde{\varrho}^{\mathbb{P}}(x,t-\tau), \tag{D.1}$$

with

$$\hat{K}(\tau) := \hat{\mathbb{P}}\hat{\tilde{L}}\hat{\mathbb{Q}}\ e^{-\imath\tau\hat{\mathbb{Q}}\hat{\tilde{L}}}\ \hat{\mathbb{Q}}\hat{\tilde{L}}, \tag{D.2}$$

$$\tilde{\varrho}^{\mathbb{P}}(x,t) := \hat{\mathbb{P}}\tilde{\varrho}^{\Omega_P}(x,t) = \frac{\left(\varrho_{eq}^{\Omega_P}(x)\right)^{1/2}}{\varrho_{eq}^{R}(x_R)}\varrho^{R}(x_R,t). \tag{D.3}$$

At this stage each addend in the r.h.s of Eq. (D.1) has to be examined in detail. The task of the procedure is the definition of a closed-form expression into the space Ω_R of the functions that depend on relevant variables. For this purpose, the second addend, that describes the memory effects of the stochastic process through the kernel operator $\hat{K}(\tau)$, will be approximated, whereas the first one will be written in terms of operators that act on the subspace Ω_R. In other words, the procedure consists in neglecting memory effects and in expressing suitably the operators $\hat{\mathbb{P}}\hat{\tilde{L}}$ (first addend

of Eq. (D.1)), $\hat{\mathbb{Q}}\hat{\tilde{L}}$ and $\hat{\mathbb{P}}\hat{\tilde{L}}\hat{\mathbb{Q}}$ both in the kernel operator.

First of all, we assume that the dynamical process involving the relevant variables is memoryless and this means that $\hat{K}(\tau)$ does not vanish only for small values of τ: $\hat{K}(\tau) \simeq 0$ for $\tau > \epsilon$ with ϵ a small number. In this regard, the following simplification is reasonable

$$\int_0^t \mathrm{d}\tau\ \hat{K}(\tau)\tilde{\varrho}^{\mathbb{P}}(x, t-\tau) \simeq \int_0^{+\infty} \mathrm{d}\tau\ \hat{K}(\tau)\tilde{\varrho}^{\mathbb{P}}(x,t), \tag{D.4}$$

since $t - \tau \simeq t$ and the integral on the interval $[t, +\infty)$ is negligible because of the hypothesis about the τ-dependence of the kernel operator.

As regards the first addend and in particular $\hat{\mathbb{P}}\hat{\tilde{L}}$, one can verify the validity of the equality

$$\hat{\mathbb{P}}\hat{\tilde{L}}\tilde{\varrho}^{\mathbb{P}}(x,t) = \hat{\mathbb{P}}\left(\varrho_{eq}^{\Omega_P}(x)\right)^{1/2} \hat{L}^{\dagger}\frac{\varrho^R(x_R,t)}{\varrho_{eq}^R(x_R)} \tag{D.5}$$

by employing both the adjoint operator of the Liouville operator and the property $\hat{\tilde{L}}\left(\varrho_{eq}^{\Omega_P}\right)^{1/2} = 0$. Furthermore, the operator $\hat{L}^{\dagger}$ can be separated into the sum of differential operators: some of them take the first derivative with respect to the relevant variables, and the others take the first derivative with respect to the irrelevant variables,

$$\hat{L}^{\dagger} = -\imath\Lambda_P \cdot \nabla_x = -\imath\left\{\sum_{x\in R}\Lambda_{P,k}\nabla_k + \sum_{x\in I}\Lambda_{P,k}\nabla_k\right\}, \tag{D.6}$$

where $k \in R$ ($k \in I$) tags the k-th variable that belongs (does not belong) to the set of relevant variables and the corresponding velocity field, $\Lambda_{P,k}(x)$. Since $\hat{L}^{\dagger}$ acts on functions that depend on the relevant variable only, the differential operators $\Lambda_{P,k}\nabla_k$ with $k \in I$ can be neglected without any approximation. Thus, by employing the definition of the projection operator (see Eq. (7.4)), one obtains the average velocity field of relevant variables

$$\Lambda_{R,k}(x_R) := \frac{1}{\varrho_{eq}^R(x_R)}\int_{\Omega_I}\mathrm{d}x_I\ \left[\varrho_{eq}^{\Omega_P}(x)\Lambda_{P,k}(x)\right]_{x=(x_R,x_I)} \tag{D.7}$$

and the first addend of Eq. (D.1) can be consequently written in the following concise way

$$\hat{\mathbb{P}}\hat{\tilde{L}}\tilde{\varrho}^{\mathbb{P}}(x,t) = -\imath\left(\varrho_{eq}^{\Omega_P}(x)\right)^{1/2}\Lambda_R \cdot \nabla_R\frac{\varrho^R(x_R,t)}{\varrho_{eq}^R(x_R)}, \tag{D.8}$$

where $\Lambda_R(x_R) = \{\Lambda_{R,k}(x_R)\}$ and $\nabla_R = \{\nabla_k\}$ for every $k \in R$.

As regards the second addend, and in particular the kernel operator, the analysis can be further separated for the operator $\hat{\mathbb{Q}}\hat{\tilde{L}}$ and for the operator $\hat{\mathbb{P}}\hat{\tilde{L}}\hat{\mathbb{Q}}$. First of all, the term $\hat{\mathbb{Q}}\hat{\tilde{L}}\tilde{\varrho}^{\Omega_P}(x,t)$ can be simplified by repeating the same procedure adopted

for $\hat{\mathbb{P}}\hat{\tilde{L}}\tilde{\varrho}^{\Omega_P}(x,t)$, since the operator $\hat{\mathbb{Q}}$ is defined as $\hat{\mathbb{Q}} = \hat{\mathbb{1}} - \hat{\mathbb{P}}$. The result is that

$$\hat{\mathbb{Q}}\hat{\tilde{L}}\tilde{\varrho}^{\mathbb{P}}(x,t) = -\imath \left(\varrho_{eq}^{\Omega_P}(x)\right)^{1/2} \Delta\Lambda_R \cdot \nabla_R \frac{\varrho^R(x_R,t)}{\varrho_{eq}^R(x_R)}, \tag{D.9}$$

where

$$\Delta\Lambda_{R,k}(x) = \Lambda_{P,k}(x) - \Lambda_{R,k}(x_R) \tag{D.10}$$

and $\Lambda_{P,k}(x)$, $\Lambda_{R,k}(x_R)$ are linked through Eq. (D.7).

Secondly, the analysis concerning the operator $\hat{\mathbb{P}}\hat{\tilde{L}}\hat{\mathbb{Q}}$ is less direct the previous ones. Consider the following integral written according to the Dirac notation,

$$\left\langle \left(\varrho_{eq}^{\Omega_P}\right)^{1/2} g \middle| \hat{\mathbb{P}}\hat{\tilde{L}}\hat{\mathbb{Q}} \middle| \left(\varrho_{eq}^{\Omega_P}\right)^{1/2} f \right\rangle := \int_{\Omega_P} \mathrm{d}x \ \left(\varrho_{eq}^{\Omega_P}(x)\right)^{1/2} g(x) \hat{\mathbb{P}}\hat{\tilde{L}}\hat{\mathbb{Q}} \left(\varrho_{eq}^{\Omega_P}(x)\right)^{1/2} f(x) \tag{D.11}$$

for every possible pair of functions $g(x)$ and $f(x)$. Since the operators $\hat{\mathbb{P}}$, $\hat{\mathbb{Q}}$ and $\hat{\tilde{L}}$ are self-adjoint operators, the above integral is equal to

$$\left\langle \hat{\mathbb{Q}}\hat{\tilde{L}}\hat{\mathbb{P}} \left(\varrho_{eq}^{\Omega_P}\right)^{1/2} g \middle| \left(\varrho_{eq}^{\Omega_P}\right)^{1/2} f \right\rangle. \tag{D.12}$$

The bra part of the integral can be expressed in a more useful way by recognising that the argument is analogous to the l.h.s. of Eq. (D.9). In other words, the features of $\tilde{\varrho}^{\mathbb{P}}$ that ensure the validity of Eq. (D.9) are the same of $\hat{\mathbb{P}} \left(\varrho_{eq}^{\Omega_P}\right)^{1/2} g$: they are functions of the relevant variables multiplied for $\left(\varrho_{eq}^{\Omega_P}(x)\right)^{1/2}$. Therefore, one can verify that equality between the integral of Eq. (D.12) and the next integral

$$\left\langle \left(\varrho_{eq}^{\Omega_P}\right)^{1/2} \left[-\imath\Delta\Lambda_R \cdot \nabla_R\right] \left(\varrho_{eq}^{\Omega_P}\right)^{-1/2} \hat{\mathbb{P}} \left(\varrho_{eq}^{\Omega_P}\right)^{1/2} g \middle| \left(\varrho_{eq}^{\Omega_P}\right)^{1/2} f \right\rangle, \tag{D.13}$$

holds. Then, one can write the above integral with the same bra and ket of Eq. (D.11) by employing the adjoints of the operators included in the bra. Since the above procedure holds for every pair of functions $f(x)$ and $g(x)$, the operator $\hat{\mathbb{P}}\hat{\tilde{L}}\hat{\mathbb{Q}}$ has to satisfy the following equation

$$\hat{\mathbb{P}}\hat{\tilde{L}}\hat{\mathbb{Q}} = -\imath\hat{\mathbb{P}} \left(\varrho_{eq}^{\Omega_P}(x)\right)^{-1/2} \nabla_R \cdot \Delta\Lambda_R \left(\varrho_{eq}^{\Omega_P}(x)\right)^{1/2}. \tag{D.14}$$

Once both the equivalences of Eq. (D.9) and of Eq. (D.14) are taken into accout,

the term $\hat{K}(\tau)\tilde{\varrho}^{\mathbb{P}}(x,t)$ can be written as

$$\hat{K}(\tau)\tilde{\varrho}^{\mathbb{P}}(x,t) = -\hat{\mathbb{P}}\left(\varrho_{eq}^{\Omega_P}\right)^{-1/2}\nabla_R\cdot\Delta\Lambda_R\left(\varrho_{eq}^{\Omega_P}\right)^{1/2}\ e^{-\imath\tau\hat{\mathbb{Q}}\hat{\tilde{L}}}\ \left(\varrho_{eq}^{\Omega_P}\right)^{1/2}\Delta\Lambda_R\cdot\nabla_R\frac{\varrho^R(x_R,t)}{\varrho_{eq}^R(x_R)}. \tag{D.15}$$

By performing the integration on the τ variable and using the projection operator $\hat{\mathbb{P}}$, one obtains

$$\int_0^{+\infty}\mathrm{d}\tau\ \hat{K}(\tau)\tilde{\varrho}^{\mathbb{P}}(x,t) = -\frac{\left(\varrho_{eq}^{\Omega_P}(x)\right)^{1/2}}{\varrho_{eq}^R(x_R)}\nabla_R\cdot\varrho_{eq}^R(x_R)\beta(x_R)\ \nabla_R\left(\varrho_{eq}^R(x_R)\right)^{-1}\varrho^R(x_R,t), \tag{D.16}$$

where the matrix of the diffusion coefficients is conveniently defined according to the following equation

$$\beta_{k,k'}(x_R) = \int_0^{+\infty}\mathrm{d}\tau\frac{1}{\varrho_{eq}^R(x_R)}\int_{\Omega_I}\mathrm{d}x_I\left[\left(\varrho_{eq}^{\Omega_P}\right)^{1/2}\Delta\Lambda_{P,k}\ e^{-\imath\tau\hat{\mathbb{Q}}\hat{\tilde{L}}}\ \Delta\Lambda_{P,k'}\left(\varrho_{eq}^{\Omega_P}\right)^{1/2}\right]_{x=(x_R,x_I)}, \tag{D.17}$$

with $k,k'\in R$.

Finally, the results of Eq. (D.8) and Eq. (D.16) can be merged in order to simplify the initial equation, that is Eq. (D.1) and the result is

$$\frac{\partial}{\partial t}\varrho^R(x_R,t) = -\left[\varrho_{eq}^R\Lambda_R\nabla_R\left(\varrho_{eq}^R\right)^{-1}\varrho^R(x_R,t) - \nabla_R\cdot\varrho_{eq}^R\beta\ \nabla_R\left(\varrho_{eq}^R\right)^{-1}\varrho^R(x_R,t)\right]. \tag{D.18}$$

The above equation is equivalent to Eq. (7.12) reported in Chap. 7. In order to prove this last step, one has to recognise that $\varrho_{eq}^R(x_R)$ satisfies

$$\nabla_R\Lambda_R(x_R)\varrho_{eq}^R(x_R) = 0. \tag{D.19}$$

This can be simply verified by integrating the Eq. (6.23) on the irrelevant variable x_I. Therefore,

$$\nabla_R\Lambda_R(x_R)\varrho_{eq}^R(x_R)f(x_R) = \varrho_{eq}^R(x_R)\Lambda_R(x_R)\nabla_R f(x_R) \tag{D.20}$$

for every $f(x_R)$. If one chooses $f(x_R) = \left(\varrho_{eq}^R(x_R)\right)^{-1}\varrho^R(x_R,t)$, then Eq. (D.20) establishes the equivalence between Eq. (D.18) and Eq. (7.12).

References

Abbondandolo, A. and Benci, V. (2002). Solitary waves and bohmian mechanics. *Proc. Natl. Acad. Sci.*, 99(24):15257–15261.

Abramowitz, M. and Stegun, I. (1972). *Handbook of Mathematical Functions*. Dover Publications.

Althorpe, S. C. and Clary, D. C. (2003). Quantum scattering calculations on chemical reactions. *Annu. Rev. Phys. Chem.*, 54(1):493–529. PMID: 12651964.

Arnol'd, V. (1997). *Mathematical Methods of Classical Mechanics*. Graduate Texts in Mathematics. Springer New York.

Askar, A. and Weiner, J. H. (1971). Wave packet dynamics on two-dimensional quadratic potential surfaces. *Am. J. Phys.*, 39(10):1230–1234.

Avanzini, F., Fresch, B., and Moro, G. J. (2016). Pilot-wave quantum theory with a single Bohm's trajectory. *Found. Phys.*, 46(5):575–605.

Balakrishnan, N., Kalyanaraman, C., and Sathyamurthy, N. (1997). Time-dependent quantum mechanical approach to reactive scattering and related processes. *Phys. Rep.*, 280(2):79 – 144.

Bartsch, C. and Gemmer, J. (2009). Dynamical typicality of quantum expectation values. *Phys. Rev. Lett.*, 102:110403.

Bell, J. S. (1982). On the impossible pilot wave. *Found. Phys.*, 12(10):989–999.

Benassi, E., Granucci, G., Persico, M., and Corni, S. (2015). Can azobenzene photoisomerize when chemisorbed on a gold surface? An analysis of steric effects based on nonadiabatic dynamics simulations. *J. Phys. Chem. C*, 119(11):5962–5974.

Benci, V. (2009). Hylomorphic solitons. *Milan Journal of Mathematics*, 77(1):271–332.

Benci, V., Ghimenti, M., and Micheletti, A. M. (2010). The nonlinear schroedinger equation: Solitons dynamics. *J. Differ. Equations*, 249(12):3312 – 3341.

Benedict, W. S., Herman, R., Moore, G. E., and Silverman, S. (1957). Infrared line and band strengths and dipole moment function in hcl and dcl. *J. Chem. Phys.*, 26(6):1671–1677.

Berezovsky, J., Mikkelsen, M. H., Stoltz, N. G., Coldren, L. A., and Awschalom, D. D. (2008). Picosecond coherent optical manipulation of a single electron spin in a quantum dot. *Science*, 320(5874):349–352.

Berndl, K., Dürr, D., Goldstein, S., Peruzzi, G., and Zanghì, N. (1995). On the global existence of bohmian mechanics. *Commun. Math. Phys.*, 173(3):647–673.

Biercuk, M. J., Uys, H., VanDevender, A. P., Shiga, N., Itano, W. M., and Bollinger, J. J. (2009). Optimized dynamical decoupling in a model quantum memory. *Nature*, 458(7241):996–1000.

Bohm, D. (1952a). A suggested interpretation of the quantum theory in terms of "hidden" variables. I. *Phys. Rev.*, 85:166–179.

Bohm, D. (1952b). A suggested interpretation of the quantum theory in terms of "hidden" variables. II. *Phys. Rev.*, 85:180–193.

Bohm, D. (1953). Proof that probability density approaches $|\psi|^2$ in causal interpretation of the quantum theory. *Phys. Rev.*, 89:458–466.

Braverman, B. and Simon, C. (2013). Proposal to observe the nonlocality of bohmian trajectories with entangled photons. *Phys. Rev. Lett.*, 110:060406.

Breuer, H. and Petruccione, F. (2007). *The Theory of Open Quantum Systems*. OUP Oxford.

Brody, T. A., Flores, J., French, J. B., Mello, P. A., Pandey, A., and Wong, S. S. M. (1981). Random-matrix physics: spectrum and strength fluctuations. *Rev. Mod. Phys.*, 53:385–479.

Cantatore, V., Granucci, G., Rousseau, G., Padula, G., and Persico, M. (2016). Photoisomerization of self-assembled monolayers of azobiphenyls: Simulations highlight the role of packing and defects. *J. Phys. Chem. Lett.*, 7(19):4027–4031.

Car, R. and Parrinello, M. (1985). Unified approach for molecular dynamics and density-functional theory. *Phys. Rev. Lett.*, 55:2471–2474.

Clary, D. C. (2016). Quantum dynamics in the smallest water droplet. *Science*, 351(6279):1267–1268.

Cohen-Tannoudji, C., Diu, B., and Laloë, F. (1977a). *Quantum mechanics*, volume I. Wiley.

Cohen-Tannoudji, C., Diu, B., and Laloë, F. (1977b). *Quantum mechanics*, volume II. Wiley.

Colijn, C. and Vrscay, E. (2002). Spin-dependent Bohm trajectories for hydrogen eigenstates. *Phys. Lett. A*, 300(4–5):334 – 340.

Colijn, C. and Vrscay, E. (2003). Spin-dependent Bohm trajectories associated with an electronic transition in hydrogen. *J. Phys. A*, 36(16):4689.

Colijn, C. and Vrscay, E. (2004). Quantum relaxation in hydrogen eigenstates and two-state transitions. *Phys. Lett. A*, 327(2–3):113 – 122.

Colin, S. and Struyve, W. (2010). Quantum non-equilibrium and relaxation to equilibrium for a class of de Broglie-Bohm-type theories. *New J. Phys.*, 12(4):043008.

Craig, I. R. and Manolopoulos, D. E. (2005). Chemical reaction rates from ring polymer molecular dynamics. *J. Chem. Phys.*, 122(8):084106.

Dahl, J. P. and Springborg, M. (1988). The morse oscillator in position space, momentum space, and phase space. *J. Chem. Phys.*, 88(7):4535–4547.

de Alcantara Bonfim, O. F., Florencio, J., and Sá Barreto, F. C. (1998). Quantum chaos in a double square well: An approach based on Bohm's view of quantum mechanics. *Phys. Rev. E*, 58:6851–6854.

de Broglie, L. (1928). *Electrons et Photons, Rapport au Ve Conseil Physique Solvay.* Gauhier-Villiars, Paris.

Domcke, W. and Mundel, C. (1985). Calculation of cross sections for vibrational excitation and dissociative attachment in hcl and dcl beyond the local-complex-potential approximation. *J. Phys. B*, 18(22):4491.

Dubrovin, B., Fomenko, A., and Novikov, S. (1991a). *Modern Geometry - Methods and Applications. Part I: The Geometry of Surfaces, Transformation Groups, and Fields.* Graduate Texts in Mathematics. Springer New York.

Dubrovin, B., Fomenko, A., and Novikov, S. (1991b). *Modern Geometry - Methods and Applications. Part II: The Geometry and Topology of Manifolds*. Graduate Texts in Mathematics. Springer New York.

Dubrovin, B., Fomenko, A., and Novikov, S. (1991c). *Modern Geometry - Methods and Applications. Part III: Introduction to Homology Theory*. Graduate Texts in Mathematics. Springer.

Dürr, D., Goldstein, S., and Zanghí, N. (1992). Quantum equilibrium and the origin of absolute uncertainty. *J. Stat. Phys.*, 67(5):843–907.

Dürr, D., Goldstein, S., and Zanghì, N. (2012). *Quantum Physics Without Quantum Philosophy*. Springer Berlin Heidelberg.

Efthymiopoulos, C., Kalapotharakos, C., and Contopoulos, G. (2007). Nodal points and the transition from ordered to chaotic bohmian trajectories. *J. Phys. A*, 40(43):12945.

Fang, C., Frontiera, R. R., Tran, R., and Mathies, R. A. (2009). Mapping GFP structure evolution during proton transfer with femtosecond raman spectroscopy. *Nature*, 462(7270):200–204.

Feynman, R., Leighton, R., and Sands, M. (1964). *The Feynman Lectures on Physics*. Number III in The Feynman Lectures on Physics. Addison-Wesley.

Figalli, A., Klein, C., Markowich, P., and Sparber, C. (2014). Wkb analysis of bohmian dynamics. *Comm. Pure Appl. Math.*, 67(4):581–620.

Folland, G. (2008). *Quantum Field Theory: A Tourist Guide for Mathematicians*. Mathematical surveys and monographs. American Mathematical Society.

Fresch, B. and Moro, G. J. (2009). Typicality in ensembles of quantum states: Monte Carlo sampling versus analytical approximations. *J. Phys. Chem. A*, 113(52):14502–14513.

Fresch, B. and Moro, G. J. (2010a). Emergence of equilibrium thermodynamic properties in quantum pure states. I. theory. *J. Chem. Phys.*, 133(3):034509.

Fresch, B. and Moro, G. J. (2010b). Emergence of equilibrium thermodynamic properties in quantum pure states. ii. analysis of a spin model system. *J. Chem. Phys.*, 133(3):034510.

Fresch, B. and Moro, G. J. (2011). Beyond quantum microcanonical statistics. *J. Chem. Phys.*, 134(5):054510.

Fresch, B. and Moro, J. G. (2013). Typical response of quantum pure states. *Eur. Phys. J. B.*, 86(5):1–13.

Frisch, M. J., Trucks, G. W., Schlegel, H. B., Scuseria, G. E., Robb, M. A., Cheeseman, J. R., Scalmani, G., Barone, V., Mennucci, B., Petersson, G. A., Nakatsuji, H., Caricato, M., Li, X., Hratchian, H. P., Izmaylov, A. F., Bloino, J., Zheng, G., Sonnenberg, J. L., Hada, M., Ehara, M., Toyota, K., Fukuda, R., Hasegawa, J., Ishida, M., Nakajima, T., Honda, Y., Kitao, O., Nakai, H., Vreven, T., Montgomery, Jr., J. A., Peralta, J. E., Ogliaro, F., Bearpark, M., Heyd, J. J., Brothers, E., Kudin, K. N., Staroverov, V. N., Kobayashi, R., Normand, J., Raghavachari, K., Rendell, A., Burant, J. C., Iyengar, S. S., Tomasi, J., Cossi, M., Rega, N., Millam, J. M., Klene, M., Knox, J. E., Cross, J. B., Bakken, V., Adamo, C., Jaramillo, J., Gomperts, R., Stratmann, R. E., Yazyev, O., Austin, A. J., Cammi, R., Pomelli, C., Ochterski, J. W., Martin, R. L., Morokuma, K., Zakrzewski, V. G., Voth, G. A., Salvador, P., Dannenberg, J. J., Dapprich, S., Daniels, A. D., Farkas, Ö., Foresman, J. B., Ortiz, J. V., Cioslowski, J., and Fox, D. J. (2009). Gaussian 09 Revision E.01.

Frisk, H. (1997). Properties of the trajectories in bohmian mechanics. *Phys. Lett. A*, 227(3–4):139 – 142.

Garashchuk, S., Dell'Angelo, D., and Rassolov, V. A. (2014). Dynamics in the quantum/classical limit based on selective use of the quantum potential. *J. Chem. Phys.*, 141(23):234107.

Garashchuk, S. and Rassolov, V. A. (2002). Semiclassical dynamics based on quantum trajectories. *Chem. Phys. Lett.*, 364(5–6):562 – 567.

Garashchuk, S. and Rassolov, V. A. (2004). Energy conserving approximations to the quantum potential: Dynamics with linearized quantum force. *J. Chem. Phys.*, 120(3):1181–1190.

Garashchuk, S. and Volkov, M. V. (2012). Incorporation of quantum effects for selected degrees of freedom into the trajectory-based dynamics using spatial domains. *J. Chem. Phys.*, 137(7):074115.

Gardiner, C. W. (1986). *Handbook of Stochastic Methods for Physics, Chemistry and the Natural Sciences*. Springer-Verlag, New York.

Gelfand, I. and Fomin, S. (2000). *Calculus of Variations*. Dover Books on Mathematics. Dover Publications.

Giaquinta, M. and Hildebrandt, S. (1996a). *Calculus of Variations I*. Grundlehren der mathematischen Wissenschaften. Springer.

Giaquinta, M. and Hildebrandt, S. (1996b). *Calculus of Variations II*. Calculus of Variations. Springer.

Gillespie, D. T. (1992). A rigorous derivation of the chemical master equation. *Physica A*, 188(1):404 – 425.

Gillespie, D. T. (2007). Stochastic simulation of chemical kinetics. *Annu. Rev. Phys. Chem.*, 58(1):35–55.

Gillespie, D. T., Hellander, A., and Petzold, L. R. (2013). Perspective: Stochastic algorithms for chemical kinetics. *J. Chem. Phys.*, 138(17):170901.

Goldstein, S., Lebowitz, J. L., Mastrodonato, C., Tumulka, R., and Zanghi, N. (2010). Approach to thermal equilibrium of macroscopic quantum systems. *Phys. Rev. E*, 81:011109.

Goldstein, S., Lebowitz, J. L., Tumulka, R., and Zanghì, N. (2006). Canonical typicality. *Phys. Rev. Lett.*, 96:050403.

Gorini, V., Kossakowski, A., and Sudarshan, E. C. G. (1976). Completely positive dynamical semigroups of N-level systems. *J. Math. Phys.*, 17(5):821–825.

Grotendorst, J. (2000). *Modern Methods and Algorithms of Quantum Chemistry*. NIC series. John-von-Neumann-Inst. for Computing.

Hayes, D. and Engel, G. S. (2011). Extracting the excitonic hamiltonian of the fenna-matthews-olson complex using three-dimensional third-order electronic spectroscopy. *Biophys J.*, 100(8):2043–2052.

Helgaker, T., Uggerud, E., and Jensen, H. J. A. (1990). Integration of the classical equations of motion on ab initio molecular potential energy surfaces using gradients and hessians: application to translational energy release upon fragmentation. *Chem. Phys. Lett.*, 173(2):145 – 150.

Henderson, D. (2012). *Physical Chemistry: An Advanced Treatise - Mathematical Methods*, volume XIB. Elsevier Science.

Herman, M. and Perry, D. S. (2013). Molecular spectroscopy and dynamics: a polyad-based perspective. *Phys. Chem. Chem. Phys.*, 15:9970–9993.

Herzberg, G. (1963). *Molecular Spectra and Molecular Structure*. Number III. D. Van Nostrand Company, INC.

Hirsch, M., Pugh, C., and Shub, M. (1977). *Invariant Manifolds*. Number No. 583 in Lecture Notes in Mathematics. Springer-Verlag.

Hoffmann, R. (1987). How chemistry and physics meet in the solid state. *Angew. Chem. Int. Ed. Engl.*, 26(9):846–878.

Holland, P. (2001a). Hamiltonian theory of wave and particle in quantum mechanics I. Liouville's theorem and the interpretation of the de Broglie-Bohm theory. *Il Nuovo Cimento B*, 116(9):1043–1069.

Holland, P. (2001b). Hamiltonian theory of wave and particle in quantum mechanics II: Hamilton-Jacobi theory and particle back-reaction. *Il Nuovo Cimento B*, 116(10):1143–1172.

Holland, P. R. (1995). *The Quantum Theory of Motion*. Cambridge University Press. Cambridge Books Online.

Huang, K. (1987). *Statistical mechanics*. Wiley.

Jensen, F. (2013). *Introduction to Computational Chemistry*. Wiley.

Jeske, J., Ing, D. J., Plenio, M. B., Huelga, S. F., and Cole, J. H. (2015). Bloch-redfield equations for modeling light-harvesting complexes. *J. Chem. Phys.*, 142(6):064104.

Jonas, D. M. (2003). Two-dimensional femtosecond spectroscopy. *Annu. Rev. Phys. Chem.*, 54(1):425–463.

Khinchin, A. (1949). *Mathematical Foundations of Statistical Mechanics*. Dover Books on Mathematics. Dover Publications.

Kosmann-Schwarzbach, Y. (2010). *The Noether Theorems: Invariance and Conservation Laws in the Twentieth Century*. Sources and Studies in the History of Mathematics and Physical Sciences. Springer New York.

Kramer, P. H. and Saraceno, M. (1981). *Geometry of the Time-dependent Variational Principle in Quantum Mechanics*. Springer.

Krasnoshchekov, S. V. and Stepanov, N. F. (2013). Polyad quantum numbers and multiple resonances in anharmonic vibrational studies of polyatomic molecules. *J. Chem. Phys.*, 139(18):184101.

Landau, L. D. and Lifshitz, E. M. (1976). *Mechanics*. Butterworth-Heinemann.

Lindblad, G. (1976). On the generators of quantum dynamical semigroups. *Commun. Math. Phys.*, 48(2):119–130.

Linden, N., Popescu, S., Short, A. J., and Winter, A. (2009). Quantum mechanical evolution towards thermal equilibrium. *Phys. Rev. E*, 79:061103.

Liu, W., Han, F., Smith, C., and Fang, C. (2012). Ultrafast conformational dynamics of pyranine during excited state proton transfer in aqueous solution revealed by femtosecond stimulated raman spectroscopy. *J. Phys. Chem. B*, 116(35):10535–10550.

Lopreore, C. L. and Wyatt, R. E. (1999). Quantum wave packet dynamics with trajectories. *Phys. Rev. Lett.*, 82:5190–5193.

Lutzky, M. (1978). Symmetry groups and conserved quantities for the harmonic oscillator. *J. Phys. A*, 11(2):249.

Lutzky, M. (1979). Non-invariance symmetries and constants of the motion. *Phys. Lett. A*, 72(2):86 – 88.

Madelung, E. (1927). Quantentheorie in hydrodynamischer form. *Zeitschrift für Physik*, 40(3):322–326.

Mahler, D. H., Rozema, L., Fisher, K., Vermeyden, L., Resch, K. J., Wiseman, H. M., and Steinberg, A. (2016). Experimental nonlocal and surreal bohmian trajectories. *Science Advances*, 2(2).

McQuarrie, D. and Simon, J. (1997). *Physical Chemistry: A Molecular Approach*. Physical Chemistry: A Molecular Approach. University Science Books.

Millam, J. M., Bakken, V., Chen, W., Hase, W. L., and Schlegel, H. B. (1999). Ab initio classical trajectories on the Born-Oppenheimer surface: Hessian-based integrators using fifth-order polynomial and rational function fits. *J. Chem. Phys.*, 111(9):3800–3805.

Morse, P. M. (1929). Diatomic molecules according to the wave mechanics. II. vibrational levels. *Phys. Rev.*, 34:57–64.

Nakajima, S. (1958). On quantum theory of transport phenomena: Steady diffusion. *Prog. Theor. Phys.*, 20(6):948–959.

Neumann, P., Mizuochi, N., Rempp, F., Hemmer, P., Watanabe, H., Yamasaki, S., Jacques, V., Gaebel, T., Jelezko, F., and Wrachtrup, J. (2008). Multipartite entanglement among single spins in diamond. *Science*, 320(5881):1326–1329.

Nielsen, M. and Chuang, I. (2010). *Quantum Computation and Quantum Information: 10th Anniversary Edition*. Cambridge University Press.

Norsen, T. (2013). The pilot-wave perspective on quantum scattering and tunneling. *Am. J. Phys.*, 81(4):258–266.

Pake, G. E. (1950a). Fundamentals of Nuclear Magnetic Resonance Absorption. I. *Am. J. Phys.*, 18(7):438–452.

Pake, G. E. (1950b). Fundamentals of Nuclear Magnetic Resonance Absorption. II. *Am. J. Phys.*, 18(8):473–486.

Petrone, A., Donati, G., Caruso, P., and Rega, N. (2014). Understanding THz and IR signals beneath time-resolved fluorescence from excited-state ab initio dynamics. *J. Am. Chem. Soc.*, 136(42):14866–14874.

Philbin, T. G. (2015). Derivation of quantum probabilities from deterministic evolution. *International Journal of Quantum Foundations*, 1(4):171–184.

Philippidis, C., Dewdney, C., and Hiley, B. J. (1979). Quantum interference and the quantum potential. *Il Nuovo Cimento B*, 52(1):15–28.

Popescu, S., Short, A. J., and Winter, A. (2006). Entanglement and the foundations of statistical mechanics. *Nat. Phys.*, 2(11):754–758.

Press, W. H., Teukolsky, S. A., Vetterling, W. T., and Flannery, B. P. (2007). *Numerical Recipes*. Cambridge University Press.

Prezhdo, O. V. and Brooksby, C. (2001). Quantum backreaction through the bohmian particle. *Phys. Rev. Lett.*, 86:3215–3219.

Prinz, J.-H., Chodera, J. D., and Noé, F. (2014). Spectral rate theory for two-state kinetics. *Phys. Rev. X*, 4:011020.

Rassolov, V. A. and Garashchuk, S. (2004). Bohmian dynamics on subspaces using linearized quantum force. *J. Chem. Phys.*, 120(15):6815–6825.

Rassolov, V. A. and Garashchuk, S. (2008). Computational complexity in quantum chemistry. *Chem. Phys. Lett.*, 464(4–6):262 – 264.

Raucci, U., Savarese, M., Adamo, C., Ciofini, I., and Rega, N. (2015). Intrinsic and dynamical reaction pathways of an excited state proton transfer. *J. Phys. Chem. B*, 119(6):2650–2657.

Redfield, A. (1957). On the theory of relaxation processes. *IBM J. Res. Devel.*, 1:19–31.

Redfield, A. (1965). The theory of relaxation processes. In Waugh, J. S., editor, *Advan. Magn. Reson*, volume 1 of *Advances in Magnetic and Optical Resonance*, pages 1 – 32. Academic Press.

Reimann, P. (2008). Foundation of statistical mechanics under experimentally realistic conditions. *Phys. Rev. Lett.*, 101:190403.

Richardson, J. O. and Althorpe, S. C. (2011). Ring-polymer instanton method for calculating tunneling splittings. *J. Chem. Phys.*, 134(5):054109.

Richardson, J. O., Althorpe, S. C., and Wales, D. J. (2011). Instanton calculations of tunneling splittings for water dimer and trimer. *J. Chem. Phys.*, 135(12):124109.

Richardson, J. O., Pérez, C., Lobsiger, S., Reid, A. A., Temelso, B., Shields, G. C., Kisiel, Z., Wales, D. J., Pate, B. H., and Althorpe, S. C. (2016). Concerted hydrogen-bond breaking by quantum tunneling in the water hexamer prism. *Science*, 351(6279):1310–1313.

Ryabov, Y., Clore, G. M., and Schwieters, C. D. (2012). Coupling between internal dynamics and rotational diffusion in the presence of exchange between discrete molecular conformations. *J. Chem. Phys.*, 136(3):034108.

Ryabov, Y. E. and Fushman, D. (2007). A model of interdomain mobility in a multidomain protein. *J. Am. Chem. Soc.*, 129(11):3315–3327.

Sanderson, C. (2010). Armadillo: An open source c++ linear algebra library for fast prototyping and computationally intensive experiments. *Technical Report, NICTA*.

Sawada, R., Sato, T., and Ishikawa, K. L. (2014). Analysis of strong-field enhanced ionization of molecules using bohmian trajectories. *Phys. Rev. A*, 90:023404.

Schatz, G. and Ratner, M. (2002). *Quantum Mechanics in Chemistry*. Dover Books on Chemistry. Dover Publications.

Schwabl, F. and Brewer, W. (2006). *Statistical Mechanics*. Advanced Texts in Physics. Springer Berlin Heidelberg.

Shannon, C. and Weaver, W. (1949). *The Mathematical Theory of Communication*. Number pt. 11 in Illini books. University of Illinois Press.

Shostak, S. L., Ebenstein, W. L., and Muenter, J. S. (1991). The dipole moment of water. I. dipole moments and hyperfine properties of h2o and hdo in the ground and excited vibrational states. *J. Chem. Phys.*, 94(9):5875–5882.

Shostak, S. L. and Muenter, J. S. (1991). The dipole moment of water. II. analysis of the vibrational dependence of the dipole moment in terms of a dipole moment function. *J. Chem. Phys.*, 94(9):5883–5890.

Shtanov, Y. V. (1997). Origin of quantum randomness in the pilot wave quantum mechanics.

Skouteris, D. (2016). Time-dependent calculations on systems of chemical interest: Dynamical and kinetic approaches. *Int. J. Quantum Chem.*, 116(22):1618–1622.

Skouteris, D., Lagana, A., Capecchi, G., and Werner, H.-J. (2004). Rotational and alignment effects in a multisurface wavepacket calculation for the $Cl + H_2$ reaction. *Phys. Chem. Chem. Phys.*, 6:5000–5006.

Suter, D. and Mahesh, T. S. (2008). Spins as qubits: Quantum information processing by nuclear magnetic resonance. *J. Chem. Phys.*, 128(5):052206.

Szabo, A. and Ostlund, N. (2012). *Modern Quantum Chemistry: Introduction to Advanced Electronic Structure Theory*. Dover Books on Chemistry. Dover Publications.

Tamura, H., Nanbu, S., Ishida, T., and Nakamura, H. (2006). Ab initio nonadiabatic quantum dynamics of cyclohexadiene/hexatriene ultrafast photoisomerization. *J. Chem. Phys.*, 124(8).

Teufel, S. and Tumulka, R. (2005). Simple proof for global existence of bohmian trajectories. *Commun. Math. Phys.*, 258(2):349–365.

Titov, E., Granucci, G., Götze, J. P., Persico, M., and Saalfrank, P. (2016). Dynamics of azobenzene dimer photoisomerization: Electronic and steric effects. *J. Phys. Chem. Lett.*, 7(18):3591–3596.

Tolman, R. (1938). *The Principles of Statistical Mechanics*. Dover Books on Physics. Dover Publications.

Towler, M. D., Russell, N. J., and Valentini, A. (2012). Time scales for dynamical relaxation to the Born rule. *Proc. R. Soc. A*, 468(2140):990–1013.

Tully, J. C. (1990). Molecular dynamics with electronic transitions. *J. Chem. Phys.*, 93(2):1061–1071.

Turner, D. B., Wilk, K. E., Curmi, P. M. G., and Scholes, G. D. (2011). Comparison of electronic and vibrational coherence measured by two-dimensional electronic spectroscopy. *J. Phys. Chem. Lett.*, 2(15):1904–1911.

Valentini, A. (1991a). Signal-locality, uncertainty, and the subquantum H-theorem. I. *Phys. Lett. A*, 156(1–2):5 – 11.

Valentini, A. (1991b). Signal-locality, uncertainty, and the subquantum H-theorem. II. *Phys. Lett. A*, 158(1–2):1 – 8.

Wang, Z. S., Darling, G. R., and Holloway, S. (2001). Dissociation dynamics from a de Broglie-Bohm perspective. *J. Chem. Phys.*, 115(22):10373–10381.

Weiner, J. H. and Askar, A. (1971). Particle method for the numerical solution of the time-dependent schrödinger equation. *J. Chem. Phys.*, 54(8):3534–3541.

Weiner, J. H. and Partom, Y. (1969). Quantum rate theory for solids. II. One-dimensional tunneling effects. *Phys. Rev.*, 187:1134–1146.

Wigner, E. P. (1967). Random matrices in physics. *SIAM Review*, 9(1):1–23.

Wilson, E., Decius, J., and Cross, P. (1955). *Molecular Vibrations: The Theory of Infrared and Raman Vibrational Spectra*. Dover Books on Chemistry Series. Dover Publications.

Wohlgemuth, M., Bonačić-Koutecký, V., and Mitrić, R. (2011). Time-dependent density functional theory excited state nonadiabatic dynamics combined with quantum mechanical/molecular mechanical approach: Photodynamics of indole in water. *J. Chem. Phys.*, 135(5):054105.

Wong, V., Case, D. A., and Szabo, A. (2009). Influence of the coupling of inter-domain and overall motions on NMR relaxation. *Proc. Natl. Acad. Sci. USA*, 106(27):11016–11021.

Wu, H. and Sprung, D. (1999). Quantum chaos in terms of Bohm trajectories. *Phys. Lett. A*, 261(3–4):150 – 157.

Wyatt, R. E. (1999a). Quantum wave packet dynamics with trajectories: Application to reactive scattering. *J. Chem. Phys.*, 111(10):4406–4413.

Wyatt, R. E. (1999b). Quantum wavepacket dynamics with trajectories: wavefunction synthesis along quantum paths. *Chem. Phys. Lett.*, 313(1–2):189 – 197.

Wyatt, R. E. (2005). *Quantum Dynamics with Trajectories - Introduction to Quantum Hydrodynamics*. Springer.

Wyatt, R. E. and Zhang, J., editors (1996). *Dynamics of Molecules and Chemical Reactions*.

Xie, W., Liu, L., Sun, Z., Guo, H., and Dawes, R. (2015). State-to-state reaction dynamics of $^{18}O+^{32}O_2$ studied by a time-dependent quantum wavepacket method. *J. Chem. Phys.*, 142(6).

Zhang, J. (1999). *Theory and Application of Quantum Molecular Dynamics*. World Scientific.

Zwanzig, R. (1960). Ensemble method in the theory of irreversibility. *J. Chem. Phys.*, 33(5):1338–1341.

Zwanzig, R. (1964). On the identity of three generalized master equations. *Physica*, 30(6):1109–1123.

Zwanzig, R. (2001). *Nonequilibrium Statistical Mechanics*. Oxford University Press.

Zyczkowski, K. (1999). Volume of the set of separable states. II. *Phys. Rev. A*, 60:3496–3507.

Zyczkowski, K. and Sommers, H.-J. (2001). Induced measures in the space of mixed quantum states. *J. Phys. A*, 34(35):7111.